Personalized Ambient Parameters Monitoring: Design and Implementing of a Wrist-Worn Prototype for Hazardous Gases and Sound Level Detection

For obtaining the academic title
Doctor Engineer (Dr.-Ing.)
At the Faculty of Computer Science and Electrical Engineering
University of Rostock
Prepared at the Center for Life Science Automation (celisca)

Submitted by:
Mostafa Haghi, born on April 12th 1986, in Iran
Rostock, Germany, 2019

CELISCA
Friedrich-Barnewitz-Str.8
18119 Rostock, Germany
Mail: info@celisca.de

https://doi.org/10.18453/rosdok_id00002537

This work was supported by the Ministry of Economics, Employment and Health of the Government of Mecklenburg-Vorpommern, Germany, under Project MV (TBI-V-1-127-VBW-044).

Reviewers:

1. Reviewer:
Prof. Dr. -Ing. habil. Kerstin Thurow
Institute of Automation
University of Rostock, Germany

2. Reviewer:
Prof. Dr. med. habil. Regina Stoll
Institute of Preventive Medicine
University Medicine Rostock, Germany

3. Reviewer:
Prof. Dr. Emil Jovanov
University of Alabama, Huntsville, USA

Date of Submission: 17.05.2019
Date of Defense: 01.10.2019

“To my parents”

Acknowledgement:

I would like to first express my honestly gratitude to my supervisors Prof. Dr.-Ing. habil. Kerstin Thurow and Prof. Dr.-Ing. Norbert Stoll for all the support and encouragement they gave me, during both the long months for the preparation of coming to the center, and also the time I spent at center for life science automation. Without their guidance and constant feedback this Ph.D. would not have been achievable.

I gratefully acknowledge the funding received towards my Ph.D. from the Ministry of Economics, Employment and Health of the Government of Mecklenburg-Vorpommern, Germany, under Project MV (TBI-V-1-127-VBW-044).

My sincere respect and gratitude to Dr. Ali Salehzadeh-Yazdi who is a true friend and always encouraged and motivated me to fight against difficulties and look forward.

Also, I would like to give a special thanks to Dr.-Ing. Sebastian Neubert for the inspiring discussions we had.

A very special thanks to Mr. Heiko Engelhardt for his patient and the collaboration in various aspects of assembling and implementation of the prototype.

I would like to appreciate all my colleagues at center for life science automation who were greatly supporting me to fulfill the requirements of my Ph.D. thesis. In particular, PD Dr.-Ing. habil. Heidi Fleischer, Dr.-Ing. Thomas Roddelkopf, Dr.-Ing. Steffen Junginger, Dipl.-Ing. André Geißler and Sybille Horn.

No word can describe my love to my parents. I would like to say thank you.

Table of Contents

List of Figures

List of Tables

List of Abbreviation

IoT	Internet of Things
M2M	Machine-to-Machine
PC	Personal Computer
WWHM	Wearable Wireless Health Monitoring
WBAN	Wireless Body Area Network
ECG	Electrocardiography
IOAQ	Indoor and Outdoor Air Quality
NO_2	Nitrogen Dioxide
CO	Carbon Monoxide
SO_2	Sulfur Dioxide
WHO	World Health Organization
VOC	Volatile Organic Compound
DoF	Degrees of Freedom
AURN	Automatic Urban and Rural Network
PM	Particulate Matter
IAQ	Indoor Air Quality
OAQ	Outdoor Air Quality
AQD	Air Quality Directive
O_3	Ozone
PAH	Polycyclic Aromatic Hydrocarbon
PPM	Parts Per Million
CVD	Cardiovascular Disease
SP	Sensor Platform
SAN	Sensor Area Network
BAN	Body Area Network
NC	Network Controller
LAN	Local Area Network
WAN	Wide Area Network
NBP	Narrow Bandpass
NDIR	Non-Dispersive Infrared Sensors
SPI	Serial Peripheral Interface
WEMS	Wearable Environmental Monitoring System
BLE	Bluetooth Low Energy
LPWAN	Low Power Wide-Area Network
LED	Light-Emitting Diode
EMG	Electromyography
WSN	Wireless Sensors Network
ADC	Analogue to Digital Converter
IIC	Inter-Integrated Circuit
CW	Clockwise
CCW	Counter Clockwise
SPL	Sound Pressure Level
OLED	Organic Light-Emitting Diode
OTA	Over-The-Air
DFU	Device Firmware Upgrade

1 INTRODUCTION

1.1 BACKGROUND

The development, infrastructure and the future of the Internet is depicting a world, consisting of heterogeneously connected devices that are going to extend the borders of the world by physical entities and virtual components [1], [2], [3]. The Internet of Things (IoT) is a new terminology that stepped into the world of science, as a concept that is supported with embedded technologies. IoT reflects a constructed network consisting of connected sets of anyone, anything, anytime, anyplace, and service [4].

It is expected that in the next generation of technologies, the IoT is a major player as a megatrend to influence the whole business spectrum and market and might be considered as the interconnection of uniquely identifiable smart objects and devices within today's Internet infrastructure with extended benefits. Benefits typically point out to the advanced connectivity of objects, systems and networks and goes beyond Machine-to-Machine (M2M) scenarios [4], [5]. The IoT supports and provides an appropriate solution to the wide range and categories of technologies, as a consequence, smart cities, traffic congestion, waste management, structural health, security, emergency services, logistics, retails, industrial control, and healthcare are applicable areas of IoT technologies [6], [7], [8], [9].

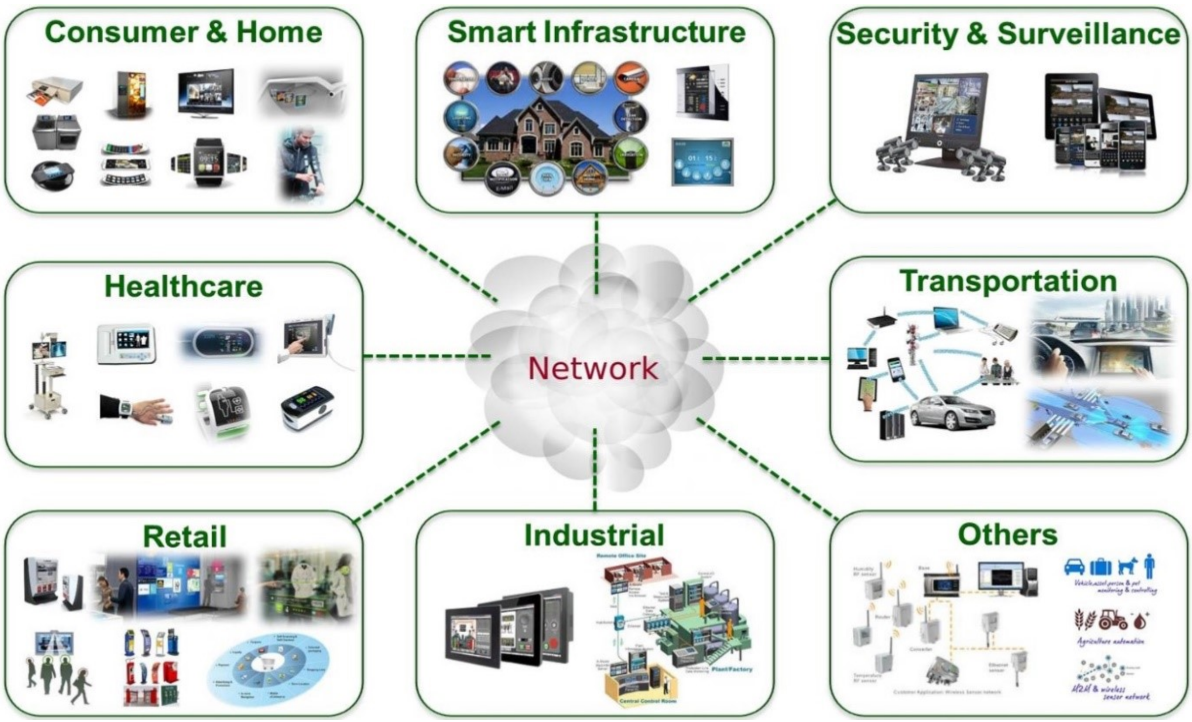

Fig. 1-1 Internet of things (IoT) [10].

Healthcare monitoring and in detail, self-health monitoring (personalized) that is a sub branch of preventive healthcare, environmental and motion tracking are positively affected by IoT. The IoT provides the possibility for individual status screening through wearable devices.
In the last decade, researchers in academic centers from one side, and industry from the other side, have paid much attention to this area of interest. The most relevant definition of wearable

electronics is the following: "…devices that can be worn or mated with human skin to continuously and closely monitor an individual's activities, without interrupting or limiting the user's motions." [11].

Table 1-1 Importance of wearable devices and Internet of Thing (IoT) in market.

	2013	2020 (expected)	Reference
IoT market	$ 1.3 trillion	$ 3.04 trillion	International data corporation (IDC)
Ready installed and connected base of IoT service	-	$ 30 billion	International data corporation (IDC)
Devices connected to the Internet	-	$ 50 billion	Cisco IBSG
Wearables to be connected to their networks	42 % of all wearable devices	-	Infonetics Research

Nowadays, wearable devices, systems and sensors are utilizing washable tiny micro-sensors seamlessly integrated into textiles, consumer electronics embedded in fashionable clothes [12], computerized watches, belt-worn personal computers (PCs) with a head mounted display [13], [14] or wearable glasses [15], [16]. These devices are worn in different mode of wearability and are designed for broadband operation [17]. Demands from the market are driving the field of wearable devices toward size minimization, secure data transmission and multi-parameter (measuring number of parameters) with comprehensive parameters in biosensors as well as fitness, medical data and environmental monitoring [18], [19], [20], [21].

Wearable wireless health monitoring (WWHM) systems, as one of the applications of IoT and wearable device, are becoming very attractive and efficient solutions in self-monitoring. In particular, screening of the noninvasive diagnosis of vital signs on the human health is widely applied [22], [23]. The application of the WWHM is not restricted to monitoring of the vital signs, but physiological and non-physiological parameters are included in the range of wearable sensors nodes [24].

Apart from the typical singular physiological sensor nodes and devices on heartbeat, blood pressure or perspiration and generally vital signs [25], which are broadly appeared in the market, especially during the recent years, the deployment and development of wireless body-worn sensor nodes might proceed to a helpful self-monitoring mechanism.

Typically, a WWHM may include several biosensors or non-biosensors which are monitoring and sampling data. To extend the solution to include more observable parameters, wireless body area network (WBAN) might be applied and these sensor nodes in large scale, construct a BAN [26] (see Fig. 1-2).

Data transmission from the WWHM system is performed due to two major reasons:

- Transmission of sensor data to on-body central processing node which is within BAN.

- Sending the sampled and measured data from the wearable device to a remote server/medical center monitoring for observation and permanent storage. This transmission can be implemented through a smartphone. This second data transfer is WBAN [27].

With advances in web-based platforms and smartphones in the recent years the collected data, obtained from the BAN, is directed to a hospital (e.g. nursing monitoring) or server through a smartphone as an intermediate hub and communication channel [28], [29].

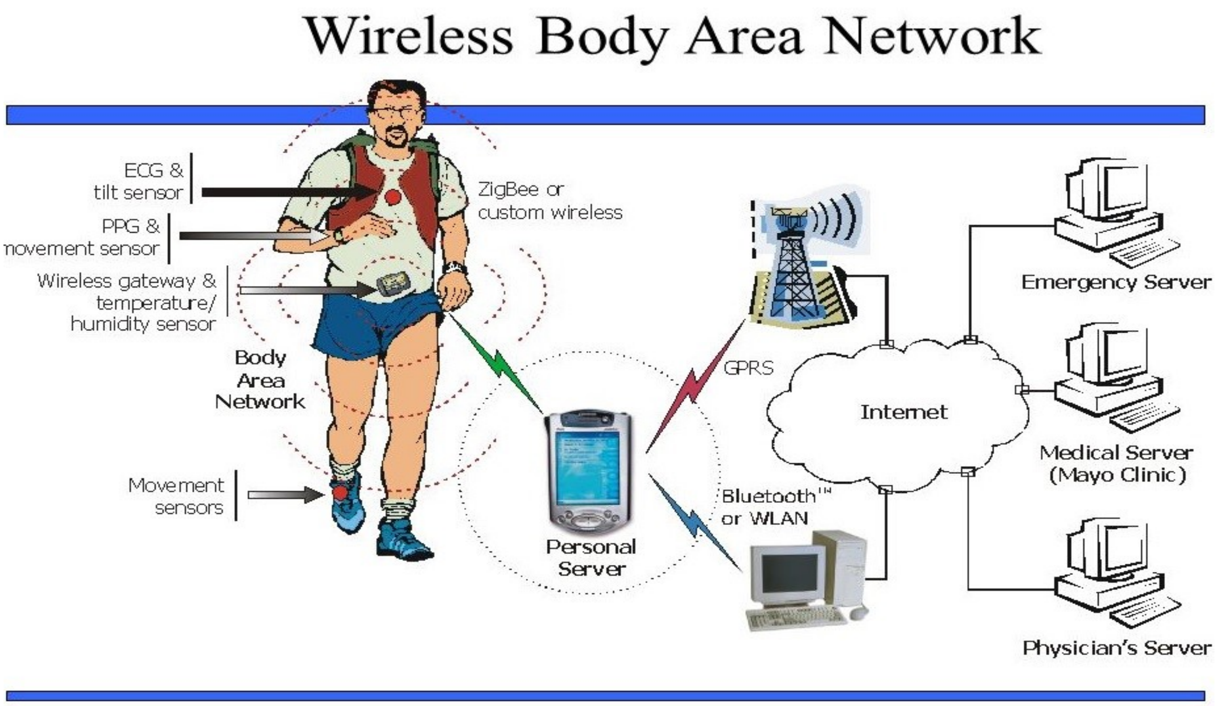

Fig. 1-2 Wireless area body network architecture including measuring parameters, intermediate hub and server [30, 15].

In general, used sensors in the BAN architecture are categorized in three major application monitoring:

- Physiological sensors:

  These sensors are used to measure the vital signs of an individual, such as body temperature, blood pressure or Electrocardiography (ECG); they might be internally or externally communicating.

- Bio-kinetic sensors:

  This group of sensors is often applied to human body movement, to measure individual activities during a period of time through accelerometer or angular rate of rotation.

- Ambient sensors:

  Additional information on temperature, humidity, pressure, light, sound level as well as air quality (IQ) are provided by these sensors. Furthermore, this information can be applied into physiological sensors during calibration process [31], [32].

1.2 GENERAL EFFECTIVE PARAMETERS ON HEALTH AND AMBIENT MONITORING

The monitoring of ambient conditions is a crucial part in occupational and preventive medicine. The ambient parameters are classified in the range of physical such as air pressure, humidity, temperature, sound level, light intensity, UV index and etc and chemical parameter (toxic and hazardous gases). The environmental elements adversely affect the human performance and health. The indoor and outdoor air quality (IOAQ) is determined by several elements (nitrogen dioxide (NO_2), carbon monoxide (CO), ozone (O_3), sulfur dioxide (SO_2) …) for evaluation, and creates higher degree of risk rather than some other environmental parameters. To evaluate the air quality, each location, environment and group of people (in particular, elderly and patients and children) have their own requirements, thus specific devices with the configuration, compatibility and adjustment capability are required in each case.

From the physical elements side, sound level assessment, attracts the attention from the medical prospective due to the long time irrecoverable side effects. The high sound level intensity exposure over long time, may cause cognitive disorders in children, sleep disorder, low sleep quality and ischemic heart disease.

With this emphasis, the major concentration of this thesis is physical and chemical ambient parameters (hazardous/toxic gases and sound level detection) monitoring. A better overview of healthcare is given by four major factors observation as the (see Fig. 1-3):

- Motion and activity
- **Environmental parameters**
- Relax and stress (physiological parameters and vital signs)
- Weight

Weight is a static indicator which does not requires a continuous monitoring.

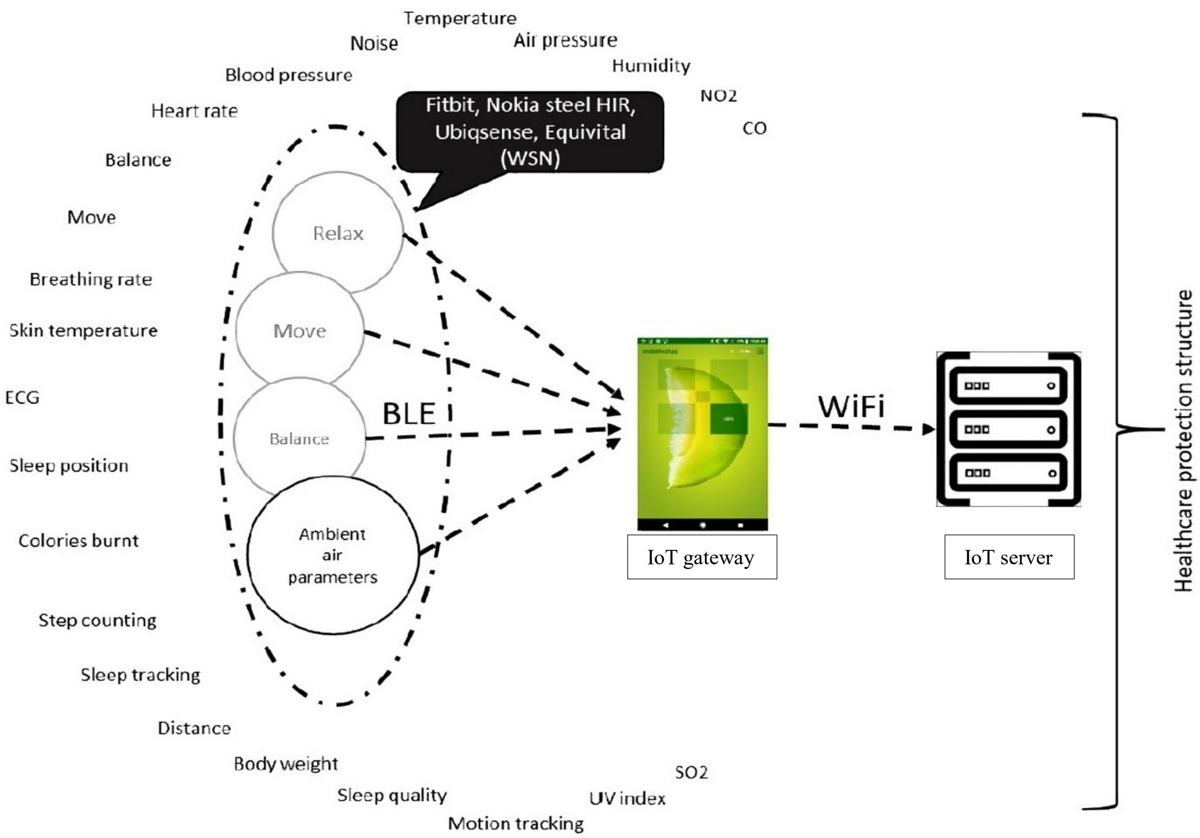

Fig. 1-3 Comprehensive monitoring of individual.

The main focus of this work is to design and implement a wearable prototype in an efficient way (hardware and software) to measure and evaluate the air ambient parameters. Nevertheless, the device is not restricted only to measuring these parameters. The potential motion tracking is provided too, therefore in the next two subsections, these indicators are briefly discussed.

1.2.1 Environmental Monitoring

Air pollutants adversely influence the human health in all regions of all over the world. However the latest statistics from the World Health Organization (WHO) indicates that 97% of cities with more than 100,000 inhabitants which are categorized in low and middle income, do not meet the air quality requirements released by WHO. Although the database shows 49% mismatch with the ideal thresholds in high income countries. However, in high-income countries, that percentage decreases to 49%. During last two years this database has been extended to cover 4300 cities in 108 countries (almost double). Extension of database and cities under measurement may leading to more precise investigation on health impact parameters and pollutants. As air quality declines, the risk of stroke, heart disease, lung cancer, and chronic and acute respiratory diseases, including asthma, increases for the people who live in them.
Ambient (outdoor air pollution) in both cities and rural areas was estimated to cause 4.2 million premature deaths worldwide in 2016 [33].

The ambient air pollutants are categorized into two general physical and chemical factors in the following two subsections.

1.2.1.1 Chemical Parameters (Air Quality-Gas concentration)

Air quality and human health Studies have proved that urban air pollution can affect human health (e.g. World Health Organization, 2000). At the first step to protect human health against air pollution, hazardous gases have to be identified for detection. Nitrogen dioxide/monoxide (NO_x) are identified as the most dangerous pollutants which long-time exposure in high gas concentration may lead to death. These pollutants can affect quality of life and mortality rates (Fig. 1.4) (e.g. World Health Organization, 2006). Both CO and NO_2 are known to be respiratory sensitizers (e.g. McConnell et al., 2010) with greater effect on those with existing respiratory or cardiovascular conditions (e.g. HEI, 2010) [53]. Another critical gas which adversely affects the human performance, is CO_2. Elevated indoor CO_2 levels are probably caused due to insufficient ventilation in occupied. Elevated CO_2 in air could lead to lack of concentration and consequently poor performance at work place as well as classroom or other similar places. Volatile Organic Compounds (VOCs) are widely used in industry as solvents or chemical intermediates. Unfortunately, they include various and wide range of gases and components that, if present in the atmosphere and human is exposed, may present a risk to health. Therefore, detection of VOCs at sub-Parts Per Million (PPM) levels is of paramount importance for human safety and thus critical for industrial hygiene in hazardous environments [53].

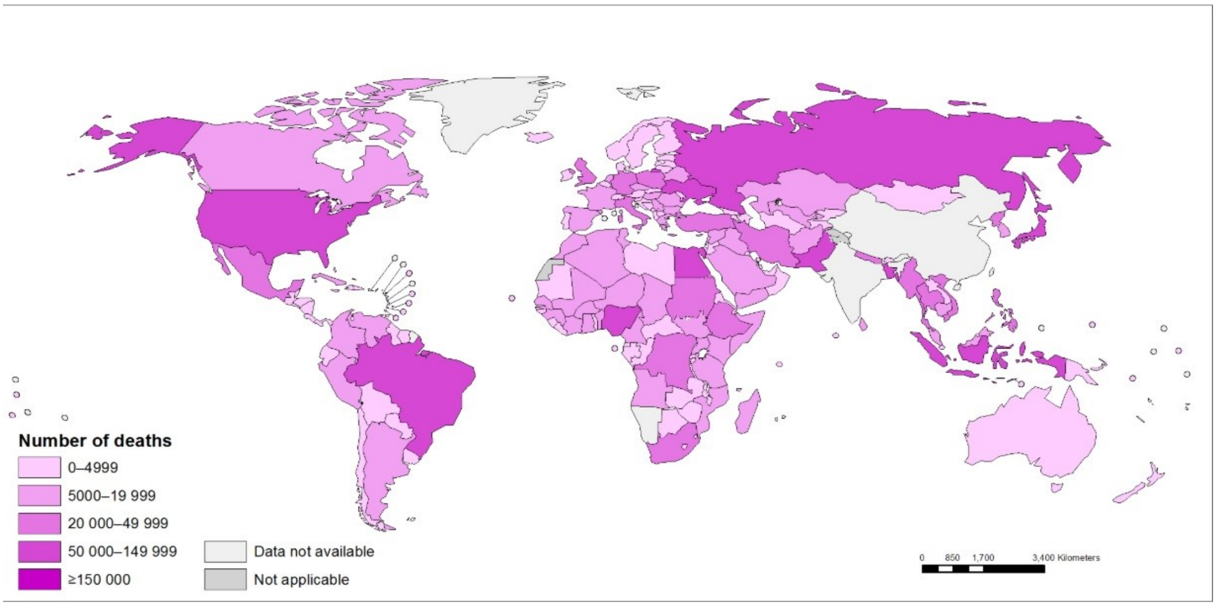

Fig. 1-4 Mortality from ambient air pollution [53].

1.2.1.2 Physical Parameters (Sound Level Measurement, Air Pressure, Humidity and Temperature)

Sound level detection (noise), temperature, humidity, and air pressure are the parameters which are taken into consideration to fulfill a full range of environmental observation. The focus of measurement in physical air parameter is on sound level as the part of evaluation. Exposing of high sound level for long-time may causes irrecoverable damages to health. This can be hearing loss, hearth diseases or even in some cases adversely impression of pregnant women and sleep disorder. However, the air ambient parameters including air pressure, air humidity and temperature are evaluated as well. As the chemical parameter evaluators (gas sensors) are influenced by the ambient conditions, these elements have to be considered too. In addition, ambient air parameters provide wider information from the area surrounding the wearable user.

1.2.2 Motion and Activity

Measuring of human movement (motion tracking) has many useful applications in sports, medical and other branches of studies. It is ranging from fall risk assessment, quantifying sports exercise, studying users' habits, and monitoring the elderly. Wearable trackers are becoming popular in two aspects increasingly, they can motivate the user during the daily workout for more exercise with providing activity measurement information in the combination of a smartphone without manual calculation [17] and also enable the wearer to become aware of daily undergone distance which is very useful. In particular, to observe an accurate motion of human body, three accelerometers, magnetometers, gyroscopes sensors are required to obtain data, each for a special purpose. These sensors can be used for human activity recognition in the ubiquitous computing domain either [18]. In most of cases the combination of these three sensors are led to 9 Degrees of Freedom (9 DoF).

In recent years, consumer electronics have employed a significant amount of semiconductor-based tracking system to allow user a different kind of interface control that uses body motion and gesture [19].

1.3 FRAMEWORK OF THIS WORK

In this study, we concentrate on the environmental parameters measurement and give a full range of observation. But the platform and solution are maintained extendable to other evaluation as well. With an eligible wearable device carried by individual multiple aims may be achieved:

- Environmental monitoring in preventive medicine healthcare system,
- Time efficiency in not often meeting a doctor to check up in tiny matters,
- Big data collection for further analysis.

To fulfill these requirements a sustainable health-care system presents a challenge to science and will be developed most effectively via the exploitation of information and communication technology. Self-monitoring based on multi-tasking device in cooperation with smartphone and web-based technologies, are necessary parts of this system. In recent years, efforts have led to significant improvements in health-care solutions. Self-monitoring and diagnostics are also possible through emergence of many smartphone apps for physiological status monitoring [2].

2 STATE OF THE ART

Air pollutants detection and monitoring is routinely performed in many spots and parts of the world such as Europe and North America. However, in some other areas of the world (less/not developed countries), information on air quality is either available rarely or completely non-existent. One of the most conventional ways of air quality monitoring in urban area, is stations providing information on density of gases in atmosphere. One of the largest air quality network monitoring currently exists in the UK with 132 sites (Defra, 2011). This Automatic Urban and Rural Network (AURN) routinely consists of several sensors to monitor gas-phase pollutants. These sites are operated by the UK Department for Environment Food and Rural Affairs (DEFRA). The UK AURN is designed primarily to monitor NO_2, NO_x, CO, O_3, SO_2 and particulate matter (PM10 and PM2.5)[1].

From the above short survey, the importance of the air quality monitoring is pretty obvious. The air pollution is not only harmful for elderly and patients but for all people who are exposed. Therefore, this area has received attention from the scientific community as well as commercial industries. During last decades many researches have been performed on this topic. Due to the importance of ambient parameters monitoring from one side and costly ambient stations which are also not available everywhere and high maintenance from the other side, the intention is toward personalized ambient parameters monitoring by using wearables. To implement and make a feasible wearable in this area of research to use, many factors such as quality of monitoring and reliability, resolution, prolonged monitoring, cost and wearability are of major concerns.

Systems based on wearable devices applied in health-monitoring, IOAQ, movement observation and etc. are becoming very popular and at the heart of just about every discussion related to the IoT and the full range of advantages of new capabilities pervasive connectivity can bring [3],[4]. Apart from a well-designed proposed structure of wearables, full range of observation for individual must be considered as well. To avoid wearing several devices, a wearable that can cover the most important parameters in environmental parameters monitoring, sounds essential (multi-parameters monitoring).

In this chapter, a brief overview on air pollutants including both hazardous gases and sound level measurement is given. The chapter is followed up with the most popular and applicable approaches in medical healthcare and ambient parameters monitoring. Then, it is continued with an introduction to the most recently commercial devices in the market and works from the scientific communities as well.

2.1 ENVIRONMENTAL PARAMETERS

Exceeding the ambient parameters thresholds, affect the human health, ecosystem and even agriculture directly. Environmental factors monitoring is attracting more attention where the rate of industrialization and urbanization is inflating, and the quality of environmental air is influenced [34], [35]. Sound level and air quality are two of the ambient elements which

[1] **PM_{10}** is particulate matter 10 micrometers or less in diameter, $PM_{2.5}$ is particulate matter 2.5 micrometers or less in diameter.

although are categorized in physical and chemical sections respectively, but human exposure could lead to irrecoverable damages.

2.1.1 Hazardous Gases

An investigation of the European community's information during these two years (2016 and 2017) exhibits that approximately one seventh of the this union (15 %) are exposed to air pollutants and beyond threshold sound level (noise) (EEA, 2016; EEA, 2017) [36]. It has been thirty years by now that researchers and different organizations involved in ambient pollutions topic, are notifying the indoor/outdoor air pollutants as a global risk that requires more attention [37], [38], [39], [40]. In table 2-1 and Fig. 2-1 the mortality attributable to air pollution by diseases is seen. These statistics indicate the importance of the ambient parameters monitoring on health of individuals.

Table 2-1 Mortality attributable to air pollution in 2015 by disease categories [41].

Region	Population, millions	Excess death (total thousands)	Death per 1000 person-years	COPD*	Cerebrovascular disease	Ischemic heart disease	Lung cancer
Africa	1184	5230	0.44	37	87	125	4
Asia	4516	3414	0.76	943	736	1074	254
Europe	597	373	0.62	50	66	203	31
Australia	31	3	0.10	1	0.4	1.5	0.2
North America	486	148	0.25	44	14	68	12
South America	498	94	0.19	15	17	42	3

*Statistical uncertainty is typically within ±30% of the mean, whereas total uncertainty can be larger. COPD=chronic obstructive pulmonary disease.

Although it is quite obvious to protect the people from the ambient air pollutants, but it is also very critical to recognize the source of pollutants. This can be helpful to avoid exposure. A close observation to the statistics in USA as the pioneering country in technology and India as one of the major countries in population, brings up significant results. This can be seen in Fig. 2-1.

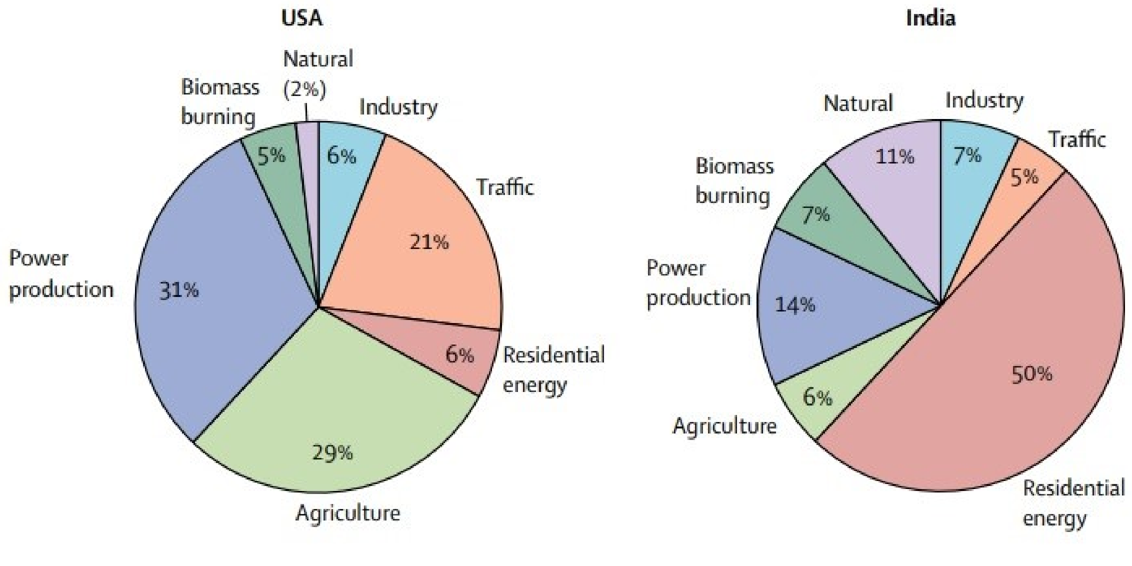

Fig. 2-1 YLLs from ambient air pollution by disease category Global YLLs in 2015 were estimated at 122 million. *LRI=lower respiratory tract infections. COPD=chronic obstructive pulmonary disease. YLL=years of life lost [41].

According to the different studies, people spend the majority of the time (up to 80% of the time) in indoor environments, whether it might be home, workplace, gym or some other closed places [42], [43]. Therefore, an Indoor Air Quality (IAQ) measurement is necessary as poor IAQ affects the health and this creates a higher risk especially for elderly and patients. In addition, poor air quality for working class people may affect the work performance adversely [44], [45], [46].
On the other hand, poor Outdoor Air Quality (OAQ) that consists of a wider range of pollutants measurement, causes serious issues for elderly, children and patients suffering from hearth diseases [47], [48], [49].

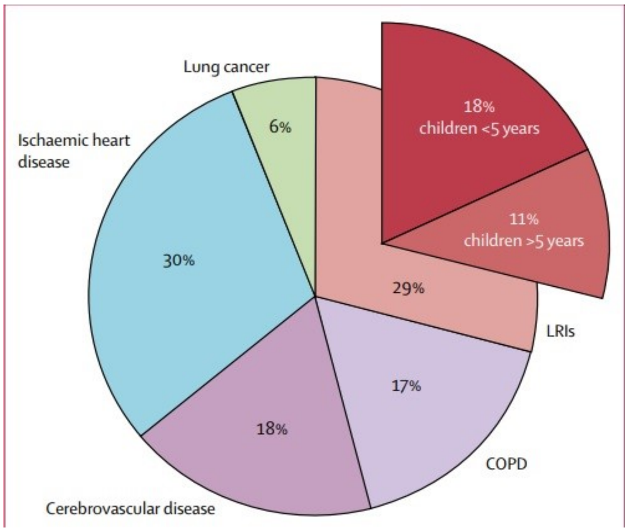

Fig. 2-2 Sources of mortality from air pollution Percentages are the proportions of the deaths attributable to ambient air pollution.

*Excess deaths attributable to air pollution in 2015 were estimated at 120000 (95% CI 81000–156000) in the USA and 967000 (753000–1 150000) in India. Natural refers to natural sources of air pollution, predominantly Aeolian dust [41].

To investigate all effective indicators on health and receive a realistic conclusion, it is obligatory to evaluate all major environmental players at the same time. Studies of the impact of multi exposure in self-monitoring via a convenient device, is a missing area of studies in noise and IOAQ.

According to statistics, the population of elderly is increasing especially in European countries, it was 841 million in 2013 worldwide and is expected to exceed 2 billion by 2050 [1]. This can cause a serious issue to the healthcare systems globally. To manage huge upcoming numbers of elderly people who need medical attention, higher budgets are required and more medical personnel has to be trained. Environmental parameters especially IOAQ is a problematic factor in elderly who are more vulnerable. As a consequence, policies and demands are changed to provide more efficient services. Patients, demand for long time, reliable and secure health monitoring. The tsunami of an old population in the close future although is important but not the only reason that make us to think of a more efficient methodology in healthcare mechanism and environmental parameters as one of the effective elements. Urbanization and industrialization in the last decades, bring larger part of population involved with industrial occupations.

Nowadays, use of low-cost gas sensors is compared to the reference methods defined in the Air Quality Directive (AQD) [54]. Using of low-cost gas sensors for monitoring of ambient air pollution demands particular sophisticated calibration [55] algorithms. This approach, in addition to reducing the air pollution monitoring costs also allows larger spatial coverage. The wider range of monitoring, is more applicable in remote areas where monitoring with traditional facilities is cumbersome [56]. However, the calibration and stability of low-cost sensors remain challenging [57], [58].

Discussion on indoor/outdoor air quality is an extensive topic with many elements. The target in this area is to detect and recognize the hazardous and toxic gases (active or reactive gases) in closed environment or outdoor, workplace or home. However, human exposure to these gases is critical and should be notified.

From one hand, SO_2, CO, lead (Pb) and benzene (C_6H_6) are some of the most famous pollutants. On the other hand, transportation facilities, industry, power plants, households, and agricultural activities as well are producing significant amounts of air pollutants (various sources). Combustion of biomass and solid fuels by households is an important source of directly emitted particulate matter (PM) and polycyclic aromatic hydrocarbons (PAHs) [50], [51]. Carbon dioxide, PM10 [52], ozone (O_3) [53], H_2S and NO_2 [51], and some other gases, are hazardous gases already in low concentrations of a few parts per million (ppm). Each of these indicators, is threatening the health. This is the reason a multi-sensor ubiquities device with the capability of operation in various situations is required. A device that independent of working condition and the environment gives the applicant the possibility of ease of use and wide range of parameters observation.

As an example, the degree of risk for CO in different concentration is presented. Information of this Table 2-2 is utilized for threshold determination of notification system in the next chapters.

Table 2-2 Carbon monoxide effect in various concentration (ppm) [54].

Concentration	Effect
0.1	Natural atmosphere level or clean air
50+	For a 50 ppm and higher CO is toxic for adults
70-75	Heart patients experience an increase in chest pain in this range. (HbCO 10%).
100	Headache, tiredness, dizziness, nausea is of signs of 100 ppm CO within 2 hrs of exposure. (Lewey & Drabkin)
200	Headache, nausea occur at this level. (NIOSH & OSHA)
400	life threatening within 3 hours
800	Healthy adults will have nausea, dizziness and convulsions within 45 minutes. Unconscious within 2 hours then death (determined in 1930)
1600	Headache, tachycardia, dizziness and nausea within 20 minutes

2.1.2 Sound Level (Noise)

The Nobel Prize Winner Robert Koch predicted in 1910 that “One day man will have to fight noise as fiercely as cholera and pest” [55].

High sound level (noise) is considered as a stressor as well [56]. Diverse effects of long-time exposure to above the standard threshold are not limited to hearing impairment but also connected with sleep quality, hypertension, and cardiovascular diseases [57, 58].

Noise annoyance created by long-time high noise exposure may cause cognitive disorders in children, sleep disorders, low sleep quality and ischemic heart disease. In general theory of stress described in [52], long term noise exposure hypothesis is taken into account as a source

cause in addition to other more known parameters such as, the autonomic nervous system, the endocrine system, and the homeostasis of the human body [59], [60], [61].
The negative effects of high noise exposure is not only limited to what was mentioned above. In [62], has been discussed that autonomic nervous system is also influenced adversely by the high sound exposure. This factor gets more serious when it is known that the autonomic nervous system regulates number of functions of the body including heart rate.
Sources of noise exposure can be different (see Fig. 2-3). As an example, transportation is of the most typical noise sources that is known as a stressor in daily lives, especially in urban area.

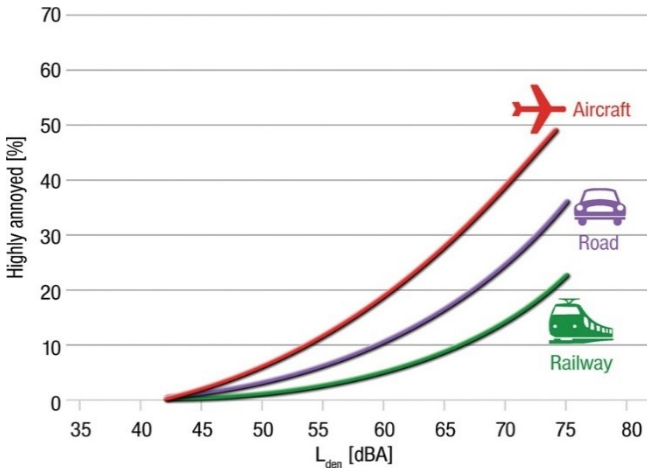

Fig. 2-3 The threshold for annoyance of noise exposure [63].

The numbers of evidences have supported that there is a correlation between noise exposure and wellbeing. Basner et al. [57] and Munzel et al. [64] provided a concise review of the effects of noise, including environmental noise, on health. In addition to causing sleep disturbance and psychological effects such as annoyance, noise is postulated to induce biological stress on the cardiovascular system, leading to changes in blood pressure and to cause hypertension [65].
Generated noise from railways and aircrafts also are well documented in this field. For example Croy et al. [66] demonstrated experimentally that night-time freight train noise and vibration can accelerate heart rate during sleep, which may in turn be linked to Cardiovascular Disease (CVD) (see Fig. 2-4).

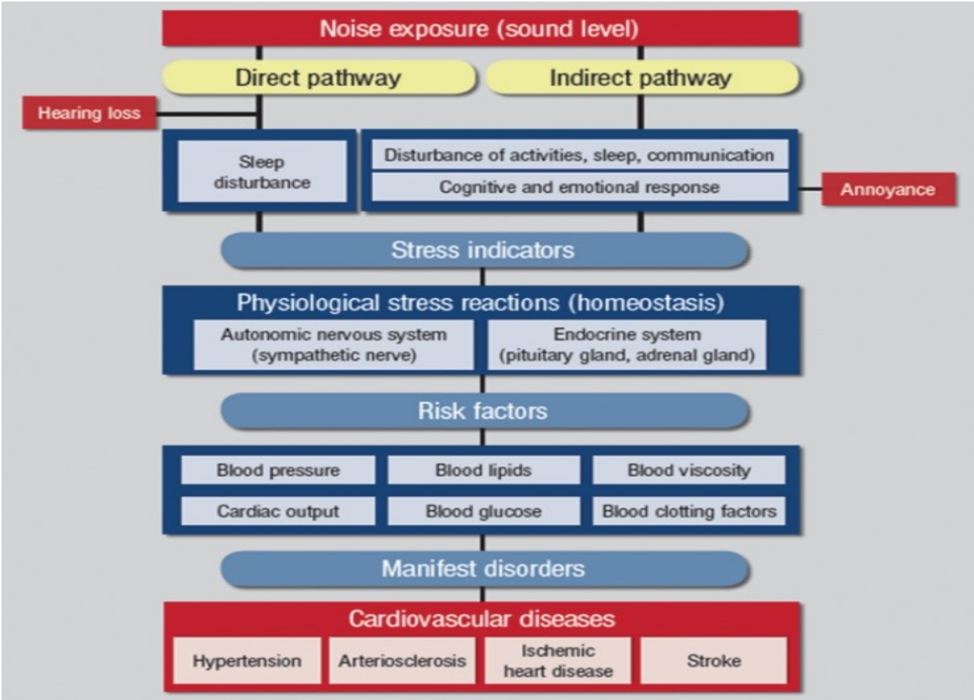

Fig. 2-4 The effects of long-time noise exposure on individual [58].

Generally, noise from any sources is disturbing and threatening the individual health. Long-time noise exposure of transportation or a laboratory machine may both create risks for the exponents. Thus, to protect the health, this noise exposure must be detected and at the second step the individual has to be noticed and protected.
However, some studies demonstrate that the long-time high noise exposure, causes health burden which leads to both medical and economic implications.
A study in the UK showed, that day-time noise levels of ≥ 55 dB have been estimated to cause an additional 542 cases of hypertension-related myocardial infarction, 788 cases of stroke, and 1,169 cases of dementia, with a cost valued at around £1.09 billion annually [67].

To conclude the results of some studies [67], [68], [69], [70] and [71] taken together, these data suggest that the exposure to sounds in the range between 55 and 60 dB, which would include large fractions of the population, may also contribute to the burden of disease.
To the best of our knowledge, the combination of sound level and comprehensive air quality evaluation is missing in the industry and researches and the lack is sensed.

2.2 MOTION TRACKERS

The concept of motion tracking is extensively applied in healthcare in terms of rehabilitation for disable patients and employee who do not have enough mobility. The motion tracking by accelerometer, magnetometer and gyroscope sensors provides 9 DoF, which multi sensor fusion approach [72], [73] produces a precise signal, applicable for fall detection [74] elderly group or even worker operators in industry, activity evaluation in sport [75], [76] [73], gesture recognition in art and music [77], [78]. Therefore, motion tracking measurement is utilized in broad range of fields and applications [79], [80], [81].

2.3 THE MOST FREQUENT AND POPULAR ARCHITECTURE

Measuring of several indicators either in ambient monitoring or healthcare requires a multi sensor platform with integrated sensor(s) or/and add on-sensors to collect the data from the different sensors each sampling and monitoring specific parameter.

In healthcare monitoring and biomedical trend, WBAN is widely used [82], [83], [84], [85], [86], [87], [88]. The WBAN usage is not restricted to the biomedical and vital sign measurement [88], [89].

In WBAN approach, different low-power, miniaturized, invasive or non-invasive, and lightweight sensor nodes (each might consist of one or more number of sensors) are used with capability of wireless communication. These sensors can communicate wired or wirelessly to the sensor platform. They are distributed on different locations of individual body or implemented even in tissue in a few centimeters.
In Fig. 2-5 a general overview of a typical WBAN system is depicted. Several miniature Sensor Platforms (SP) are integrated and located on the body. Each individual sensor might be wired to the main platform (hosted microcontroller) or integrated on the same platform. In such systems, communication and processing are consuming the majority of power, where the communication along the system is distributed in

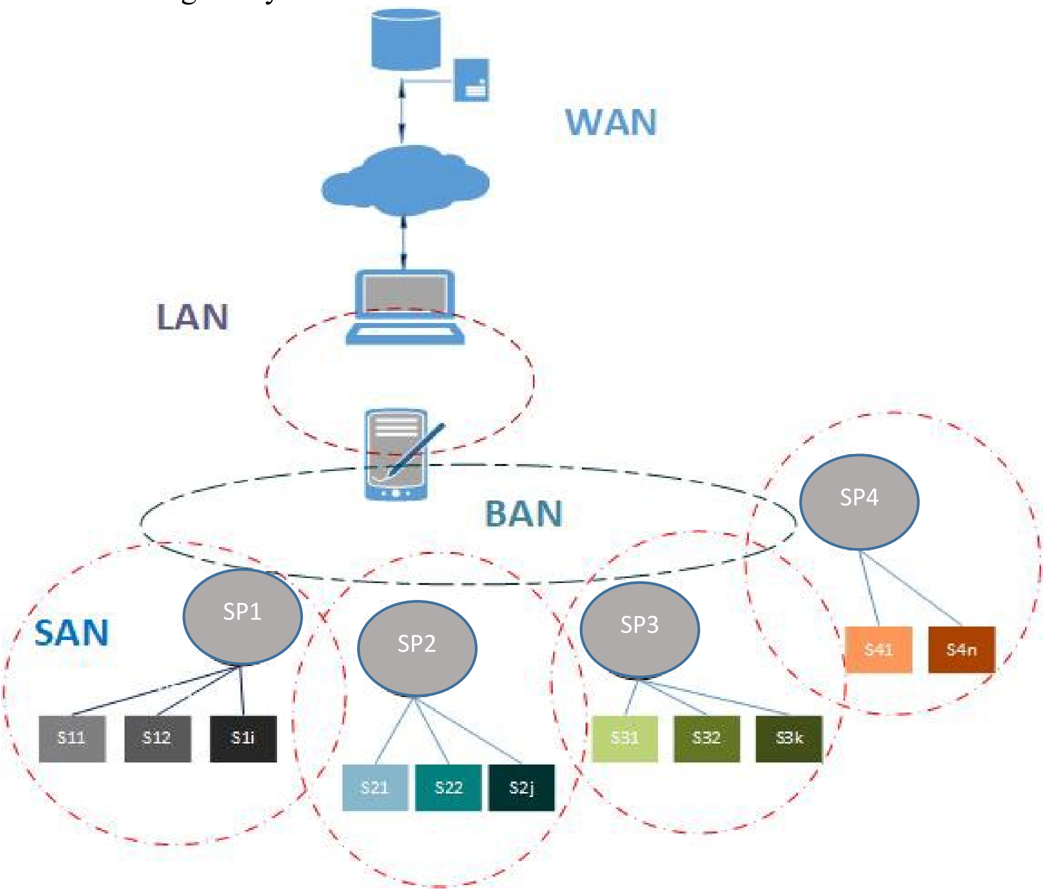

Fig. 2-5 Hierarchical multi-tier organization of ubiquitous WBAN systems.

-hierarchical level dissipating an order of magnitude of energy. Therefore, the preference is on-sensor processing when the system limitation allows.
The hierarchical levels of the WBAN is as the follows [15]:

- *Network Hierarchy*:

To describe the system architecture in details, the entire system is split into several subsystem, which each, forms a level and hierarchically are linked.
WBAN systems implement several levels of networks:

- *Sensor Area Network (SAN):*

SAN is the first layer and enables a direct communication with the user. In the SAN there is a central SP which sensor(s) can connect and send data through different methods of wired communications (SPI, I2C, 1-wire,) or even wireless.

- *Body Area Network (BAN)*:

BAN is in the second level of communication. When different SPs are integrated, these SPs send data to a Network Controller (NC) for monitoring by the user. The communication might be wired or wireless short-range communication (e.g. Bluetooth Low Energy (BLE)). An example of the NC is a smartphone.

- *Local Area Network (LAN)*:

LAN is established when integrated sensor platform (SPs) or BAN are intended to connect to a Home Server (HS).

- *Wide Area Network (WAN)*:

WAN is the last level of communication in the entire system when several monitoring systems are integrated and implemented through cellular network.

In WBAN approach, depending on the topology, each sensor node can directly link to the NC to complete the data transmission. In addition, a central processing node can be considered and all data from different nodes are merged there and consequently transferred to NC.

However, the deployment of BAN sensor nodes might be restricted by several technical concerns with respect to the positioning on-body. Form factor in terms of size and weight (leads to mode of wearability) is one of the fundamental issues. BAN as a wearable architecture has to be designed in the way to avoid user typical daily activities interference [90], [91], [92]. Prolonged monitoring is standing as the next critical factor [93]. Additional challenges are more often imposed. In particular, while short-range (Bluetooth, ZigBee ,…) and long-term communication channel establishment, deployment of the data transmission system imposes some more space to be worn [94], [95] (See Fig. 2-4).

2.3.1 WBAN Challenges and Restrictions

WBAN is an approach that is widely used to create networks of sensors, in physiological and vital sign measurement in particular. But, it is also encountering serious challenges, bottlenecks and restrictions (see Fig. 2-6).

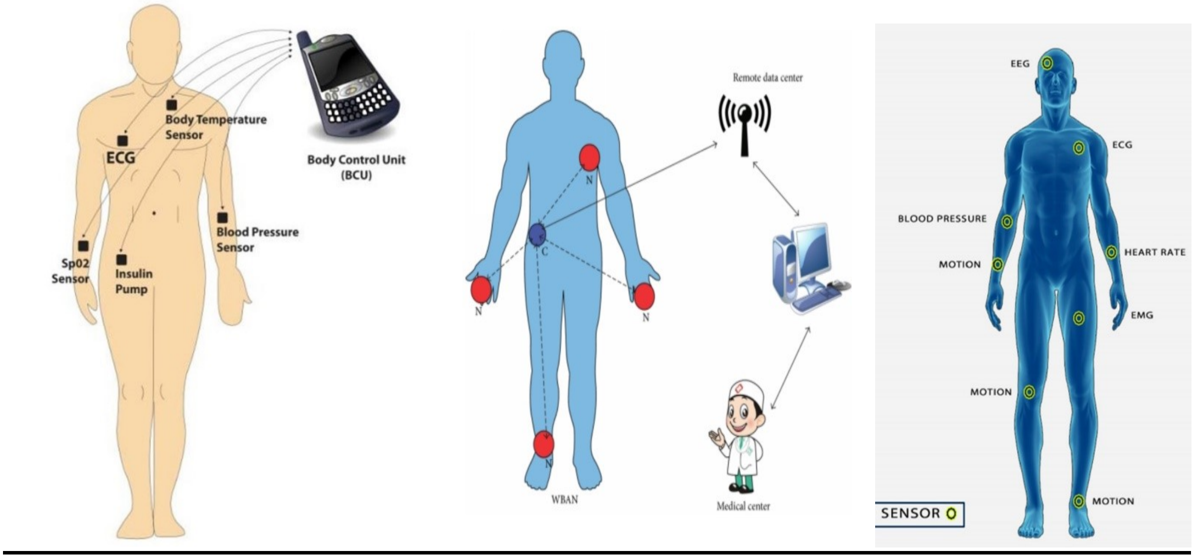

Fig. 2-6 WBAN network architecture in centralized processor node and direct communication mode [81].

- **Impact of the Radio Channel**
  Typically, in WBAN several sensors are engaged on-body or even in body (in healthcare). Therefore, a deep understanding of RF channel is required for system communication optimization. Any two sensor nodes communication channel establishment may interfere with the architecture performance [96]. For biomedical applications, where some sensors must be implemented in tissue, the channel characterization is presented in [97], and for different human tissue as well in [98].

- **Power Consumption**
  Continuous monitoring, several sensors operation, data packet transmission and real-time processing in a WBAN architecture limit the battery capacity and require frequent battery charging. Although efficient standard protocols (BLE, ZigBee, IEEE standards and …), sensor sampling rate, adequate gateway and packet efficiency in data transmission significantly reduce the power dissipation, battery life is still challenging for a prolonged screening [99].

- **Coexistence Issue**
  As is depicted in Fig. 2-7, if several WBANs, each consist of group of sensors are constructed close to each other, there is the possibility of coexistence and mitigation interference due to the same MAC protocol. In some WBAN coexistence, even if there are different MAC protocols, it might interfere with surrounding wireless networks with higher power data transmission as well [100].

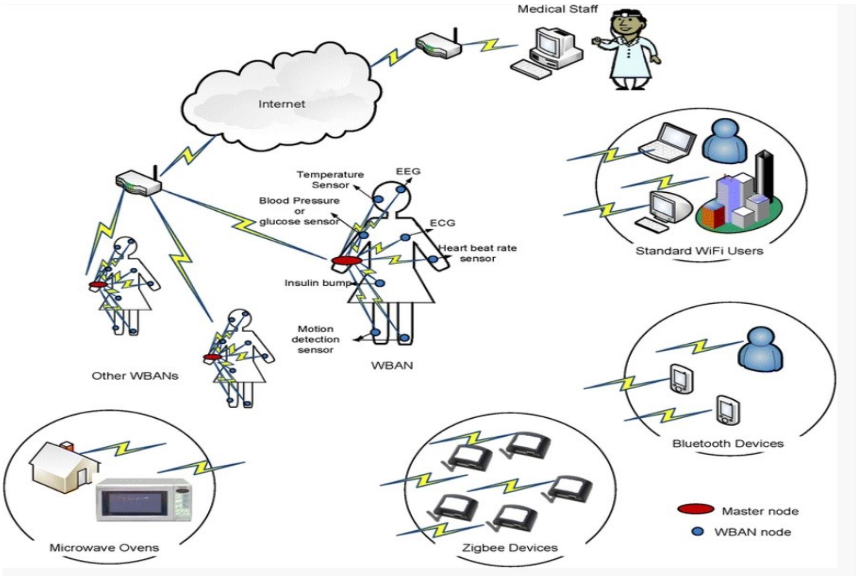

Fig. 2-7 Coexistence interference of several networks [85].

- **Form Factor**
  Either WBAN is applied by patients for physiological indicators monitoring or other purposes such as environmental monitoring and motion tracking, the wearable sensor nodes must be convenient and easy to carry (wear and forget). Furthermore, the node(s) do not have to interfere with daily activities of the wearer. To demonstrate such criteria, form factor definition is considered. The device form factor is the function of battery, size and weight of sensors. As a result to achieve a standard and convenient form factor, smaller and light-weighted sensors and components lead to a smaller sensor node construction and longer monitoring too [101], [102].

2.4 RECENT ADVANCES IN HEALTH AND AMBIENT MONITORING SYSTEM

Large number of wearable sensors in vital sign, environmental and motion tracking monitoring in quite different range of quality are already available in the market. As the emphasis of this work is on ambient parameters measurement, the major concentration of the literature survey is on wearables in ambient assessment, although the devices in vital signs and motion tracking as the part of healthcare measuring systems are mentioned as well.

2.4.1 Hazardous Gas Detectors

Toxic gases are measured by the gas detectors. These devices are already available in the market in portable wearable mode and mostly single-gas measuring. But what is important in this gas detector devices, is gas sensors from different and wide range of companies and manufacturers that will affect the form factor, accuracy, resolution response time and etc. which influence the performance of the device.

As the consequence here, both gas detector devices and gas sensors (as the fundamental means of devices) are briefly presented.

2.4.1.1 Sensors For Detecting Hazardous Gases

Based on the evaluation and validation of low-costs sensors [103], [104], [105], and identification of hazardous gases, the most important target pollutants which have to be detected are O_3, NO_x, CO and CO_2. The best performing sensors are the devices having rapid response time, high sensitivity, good repeatability and low power consumption. Many of these gas detectors are based on electrochemical, metal oxide and infrared methods. Electrochemical sensors were used in order to benefit from the different inherent cross-sensitivities of both types of sensors [106]. Many reputed manufacturers are activating in low-cost sensor area. Here it is paid attention to the most conventional environmental gas sensors which are available commercially in low cost.

2.4.1.1.1 CairClip

Cairclip is an integrated system that includes an ampere-metric sensor, a patented filter, dynamic air sampling and an electronic circuit [106]. This electronic circuit allows a direct real time display of the measured value and complete status with internal data logging. Reliability of the measurement is achieved by limiting the effect of humidity variations by using a dynamic air sampling system combined with a gas specific inlet filter to restrict the variation of humidity in order to reliability achievement. These devices often are used to measure the gas concentration between 2.5 to 10 ppm [107] (see Fig. 2-8.a).

2.4.1.1.2 Citytech

(Life Safety Germany GmbH, City Technology, Bonn, Germany) consist of 3 Electrodes ampere-metric sensors with organic electrolyte. O_3 (Model 3E1F [108]), NO_2 (Model NO_2 3E50 [109]) and NO (NO 3E100 [110]) sensors, from this company are available. There is an evaluation board of Citytech that converts the raw sensor signal voltage, with the possibility to vary the bias potential, using various load, feedback resistors and different levels of current amplification. The board was configured to give an output of 1V-100 nA with damping 10 [65]. Sensor ranges include electrochemical, pellistor (catalytic bead), infrared, PID and MMOS sensors for detecting oxygen, toxic gases, flammable gases and VOCs used in automotive, medical, emissions monitoring, industrial safety and hygiene applications (see Fig. 2-8.b).

2.4.1.1.3 Alphasense Sensors

By Sense Ltd (Essex, United Kingdom) is another company providing sensors in air quality measurement area. O_3 sensor (model O3B4 – 4 electrodes [111]) and NO_2 sensor (NO_2B4 – 4 electrodes [112]) from this company are examples of these sensors. The B4 type sensor is a 4 electrodes electrochemical sensor designed for nmol/mol gas levels as well as the normal working, reference and counter electrodes. In B4 sensors, the fourth electrode is used to correct the value when no current change is seen. In fact, this electrode is an auxiliary electrode. Each sensor gives two signals, one is for raw data and another is the background signal of the auxiliary electrode. This second signal value has to be subtracted from the value of the working electrode (raw response) (See Fig. 2-8.c).

Fig. 2-8 Gas sensors: a) Cairclip, b) Citytech, c) Alphasense d) SGX gas sensor [106,109,112,113].

2.4.1.1.4 SGX Sensor tech (Neuchâtel – Switzerland)

Two important sensors from this company are MICS 2710 for NO_2 [113] and MICS 4514 [114]. In the MICS 4514 sensor NO_2 and CO sensors are combined to detect these gases. Both of these sensors are operating based on Metal Oxide semiconductor sensors (MOS sensor). SGX provides a special evaluation kit which can directly solder and assemble sensors on it. Both, MICS 4514 and MICS 2710 have the capability of being assembled on the evaluation board. CO/HC, NO_2, NH_3 are of gases which are measured by this company products (see Fig. 2-8.d).

2.4.1.1.5 Figaro (Illinois –USA)

Comes with a variety of sensors. A low-cost gas sensor of this famous manufacturer is TGS 5042-A00 sensor. It consists of a battery like electrochemical sensor [115]. To bring TGS 5042-A00 into operation, current to voltage conversion is essential. This is done by evaluation modules COM5042 able to convert the sensor output current into a voltage. Figaro offers a wide range of gas sensor products for the detection of various gases, from explosive gases such as propane, toxic gases such as carbon monoxide, to air quality sensors for volatile organic compounds (VOCs) that are responsible for sick-house syndrome. Figaro offers a diverse portfolio of sensor technologies that can be matched to the unique requirements of each application [116] (see Fig. 2-9.a).

2.4.1.1.6 TCC ELT (Environment Leading Technology, South Korea)

For the detection of Carbon dioxide (CO_2), the module S-100 manufactured by this company is an option. It is categorized as a low cost sensor and is based on the NDIR (Non-Dispersive Infrared) technology [117] (see Fig. 2-9.b).

2.4.1.1.7 OEM Gascard®NG (Nano Generator)

Infrared gas sensor (0–1,000 mol) is manufactured by Edinburgh Sensors (Lancashire – UK). Dual wave length NDIR technology is the fundamental method of operation for this senor. It also works with automatic temperature and pressure corrections using real-time environmental condition measurements, these are used for calibration. This sensor is low power consumption. The CO_2 sensor uses an active sampling with a1 l/min pump [118] (See Fig. 2-9.c).

Fig. 2-9 Gas sensors: a) Figaro b) S-100 (TCC ELT) c) OEM) [117,118,119].

2.4.1.1.8 Spec (environmental indoor/outdoor gas sensors)

SPEC sensor are 3-lead electrochemical sensors that due to small size, low power consumption, fast response and high accuracy are especially designed for portable and wearable devices (See Fig. 2-10). SPEC sensors might be applied in wide range of usages from industry observation to safety monitoring due to high sensitivity. The size of these gas sensors makes to them well-suited for personalized environmental monitoring. CO, NO_2, O_3, SO_2, respiratory Irritants and IAQ sensors are available from this family [119].

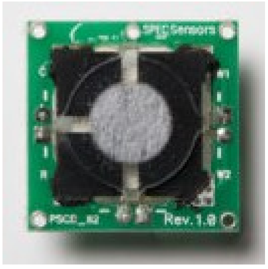

Fig. 2-10 Pinned Spec sensor[119].

2.4.1.1.9 Pyeros: NDIR gas sensor (Electro Optical Components Company)

The sensors from this company are provided in 1, 2 and 4 channels. In fact, the sensor operates based on the wavelength detection. The size, power consumption and accuracy of this detector, restrict its application to mostly portable devices. An NDIR gas sensor (nondispersive infrared sensors) is called nondispersive because the wavelength which passes through the sampling chamber is not pre-filtered. Instead a Narrow Bandpass (NBP) filter is used before the detector (See Fig. 2-11).

The NDIR system needs a broadband IR source. This source can be steady state for thermopiles but needs to be pulsed for pyroelectric and lead selenide detectors.

The target gas will absorb more IR energy as the gas concentration increases. This means that as the gas concentration increases the signal from the detector will decrease. However, gas detection according to the wavelength is influenced by the environmental parameters [120].

Fig. 2-11 Two channel NDIR gas sensor [120].

2.4.1.1.10 Summary

Size, design reusability, availability, power consumption, response time, recovery time, resolution, sensor sensitivity, ease of calibration, cost and long lifetime are of crucial requirements in gas sensors application and wearable design. Depending on the gas sensor application, each of these criteria may get a higher weight.
To summarize this subchapter, five most important of gas sensor families are compared from the different and critical aspects in Table 2-1.

Table 2-1 Sensor selection, criteria, features and requirements.

Features	Spec	Figaro (Rounded)	SGX	Cambridge CMOS	PyreOS (Rounded)
Size(mm)	15*15*3	14.7*49.8	5*7*1.55	2.7 * 4.0 * 0.6	20*20
Weight (g)	1-2	12	NA	NA	NA
Power consum. (mW)	0.01	38	30-81	<1.2	NA
Operation mode (V/A)	A	V	V	V	V
Output signal	A	A	A	D	A
Output ext. comp.	yes	yes	yes	no	yes
Products	CO, NO_2 SO_2, H_2S, O_3	CO, NH_3,CH_4,O_2	NO_2,CO	IAQ	CO_2,CO, SO_2,NO
Channel	1	2	1,2,3	1	1,2,4
Technology	Elec. Ch.	Elec. Ch.	(MEMS)	(CMOS)	Wave length IR
Package	SMD	Pins	SMD	SMD	TO
Response time (sec)	< 15	15	dependent	on condition	dependent
Wear ability	yes	On cond.	yes	yes	on cond.
Reusability	yes	no	perhaps	perhaps	no

2.4.1.2 Gas Sensor Detector Devices

Here the recent gas detector devices are presented. Both single-gas and multi-gas detectors are included in this part. In each, the advantages and disadvantages of each one are discussed briefly.

2.4.1.2.1 Digital Gas Detector with Wi-Fi Data Transmission

A multi-sensor gas detector is presented in [121]. This digital device is based on Serial Peripheral Interface (SPI) between microcontroller and sensors and equipped with WiFi antenna for data transmission. As the authors have described the tool, it is compatible with all types of sensors (electrochemical, metal oxide, thermos catalytic and optical), and is based on Attiny84-20MU microcontroller. All sensors are generating the digital output through an external circuit conversion. Data are sending to most frequent used such as smartphone or laptop. CO and O_2 are the gases that are measured by this digital platform. The authors have presented the results of 10 ppm for CO and up to 19% for the O_2.

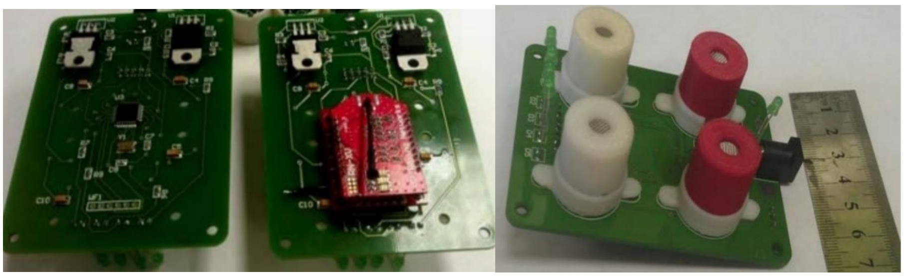

Fig. 2-12 Digital gas detector with Wi-Fi data transmission [121].

The first point to pay attention is, the Wi-Fi usage in data transmission. This significantly reduces the application of the device in portable mode, where internet WiFi is not accessible everywhere, and on the other hand, the device is not logging data through external memory nor through a display in real time observation. As a result, in the lack of internet this device is not useable any longer.

As in the Fig. 2-12 is depicted the device is using a voltage regulator and conversion. The supply voltage is 12 V which make this device a stationary monitoring device for air quality. A personal wearable monitoring more often is operating in less than 3.3 V with a coin cell or Li-ion battery. Lack of notification system is a weakness of this prototype as well.

2.4.1.2.2 Wireless Combustible Gas Sensor System attached on the Cloth

A wireless sensor system for monitoring of working conditions in term of temperature and combustible gas leakage is introduced by Spirjakin et al. in [24]. This wearable device is attached to uniform and monitor the environment. The major feature of the device is stated as the activation of the sensor node when the RF signal is available. The device is remotely controlled to switch from different blocks of power consumption and sensor data sampling at the frequency of 866 MHz. Data transmission is ZigBee based in response to the RF signal activation. The notification system is equipped with buzzer and lighting alarm.

A lithium-polymer battery with a nominal voltage of 3.6 V and a capacity of 250 mAh has been used for the power source of the system.

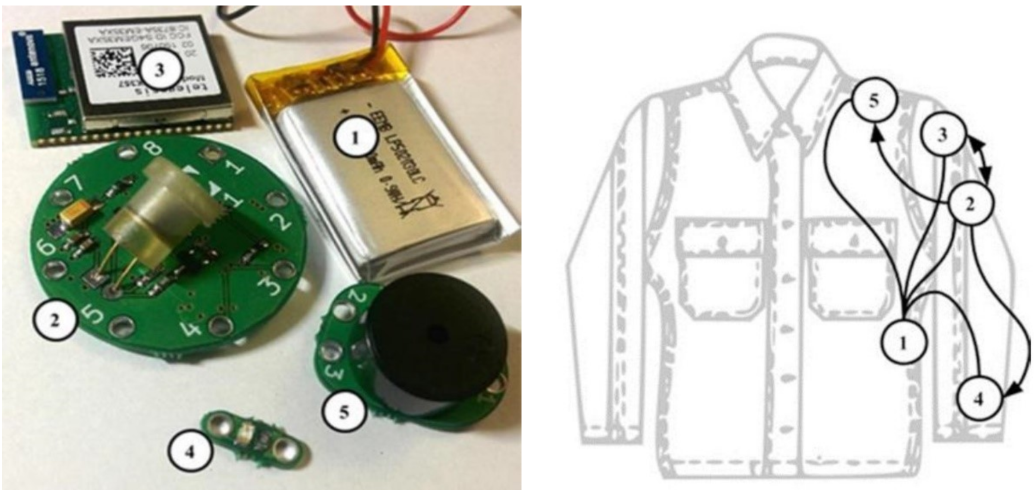

Fig. 2-13 Wireless sensor system, power source (1), sensor module (2), transceiver (3), light indicator (4) buzzer (5) [24].

Depicted Fig. 2.13, exhibited that different parts of the sensor system must be connected wired. This may significantly reduce the maneuverability of the wearer during typical daily activity. The second point to mention is that, this sensor system is attached to the uniform, therefore it is expected to remove and connected the components daily which is not convenient and might lead to permanent damage of the system. At the end, the main weakness of this device is single tasking operation which is applied only to gas monitoring.

2.4.1.2.3 Wearable Environmental Monitoring System (WEMS)

Jain et al. introduced a wearable environmental monitoring system (WEMS) [122] (See Fig. 2-14). In this platform OAQ for SO_2, NO_2 and O_3, in addition to UV radiation, humidity and temperature is evaluated. It utilizes a display for data monitoring and transmitting the data through BLE to a smartphone. WEMS is wrist-worn. The platform is based on MSP430 TI dual processor with M4 and maximum rate of the frequency is 168 MHz. WEMS consumes 6.5 mAh in standby mode and 98 mAh in watch display mode, this power consumption in sensing mode is 250 mAh.

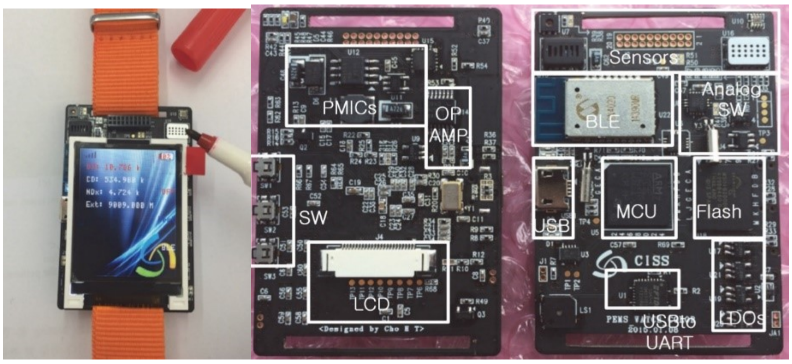

Fig. 2-14 WEMS device [122].

WEMS is a device with advantages of data transferring, data monitoring and multi-tasking. There are some technical points that bring serious concerns on this wearable sensor node.

The device is based on metal oxide gas sensor, which provides high power consumption and low accuracy. In gas sensor evaluation the recovery time is defined as: the minimum required time for the sensor for preparation for the next measurement. This means the time that is necessary to sensor recover from non-zero ppm concentration to zero concentration. This time for metal oxide sensors and typically SGX sensors in this work is quite high.

The next is, power consumption, as has been pointed out by the author, 250 mAh rate of energy harvesting, cause running out the battery in some cases, in 1 hour (depend on battery capacity). Using larger capacity demands larger battery, which results in larger size of sensor node. The second solution is lower sampling rate for power saving. In this case between each two sampling there is a big gap which does not reflect a real environmental monitoring.

2.4.1.2.4 Single-parameter Gas Monitoring (BW)

BW gas alert is a well-known company, which provides the gas detectors in the wide range of toxic and hazardous gases for single and multi-sensor gas detection [123], [124]. These devices are waist-worn and potable. The accuracy of the BW gas detectors is in 0.1 ppm concentration that make them usable as calibrator as well. One more advantage is the notification system that is using both vibrator motor and beeper in risky status (See Fig. 2-15).

Fig. 2-15 Wearable gas detector from BW gas alert [124].

In spite of many advantages and precisely measurement, BW gas alert sensor are suffering from data transmission to a second party such as smartphone or web-based station nor logging data on an external memory. The data must be observed only instantly by the individual.

2.4.1.2.5 TIDA-00056 Portable Gas Sensor Platform with BLE (TI)

Texas instrument company (TI) has launched a small, portable and low-power wireless gas sensor detector that is presented in [125]. This detector is running on CR2032 coin cell battery, and data transmission channel is established on BLE. The range of detected gases by the TIDA-00056 are Carbon monoxide, oxygen, ammonia, fluorine, chlorine dioxide. This portable sensor is supporting two and three lead electrochemical sensor and is compatible with iOS operating system (See Fig. 2-16).

Fig. 2-16 TIDA-00056 gas sensor platform with BLE [125].

TIDA-00056 provides the selectivity of the gas sensor, although it is limited to the number of sensors but still there is the possibility of the selection, this also might result in power saving, but TI does not provide more details in sensor selection, switching and requirements. BLE data transmission is an advantage which bring the device on low energy consumption. TIDA-00056 is not wearable and more often is portable and might operate as a small station in air quality monitoring. The data are transited to iOS smartphone or tablet but the serious concern is on data logging while the BLE is disconnected. Data are lost when BLE is disconnected. The next serious anxiety is the price of TIDA-00056 is 599 $ [125]. The notification system in the abnormal status has not been considered in the design. As a consequence, the user is not provided with warning alarm and the evaluation of must be monitored regularly via smartphone.

2.4.1.2.6 Physical Ambient Detector Box From Bosch

A ambient sensor device is presented by Bosch in [126]. The sensor node is provided as a portable box node, physical indicators such as humidity, temperature, light intensity, sound level and in chemical elements Volatile Organic Compounds (VOC) for indoor air quality monitoring is measured. The device is compatible with iOS through BLE (See Fig. 2-17).

Fig. 2-17 Ambient sensor monitoring [126].

In spite of comprehensive ambient monitoring, the tool does not do an investigation in OAQ. Furthermore, additional development and extension on the device is not possible.

2.4.1.2.7 W-air: A Personal Air Pollutant Monitoring

W-air prototype is an ambient air monitoring wrist-worn for evaluation of CO_2 and O_3. This prototype is monitoring two pollutants. It can be worn in different mode of wristband, back pack attachment and wait-worn. The major concentration of this work is heavy concentration on calibration of low-cost gas sensors. The applied gas sensor is based on metal-oxide technology. The data acquisition is implemented in predefined sampling rates and data are transmitted to a smartphone. High quality of calibration and re-calibration by means of neural network approach are serious advantages of this prototype [127].

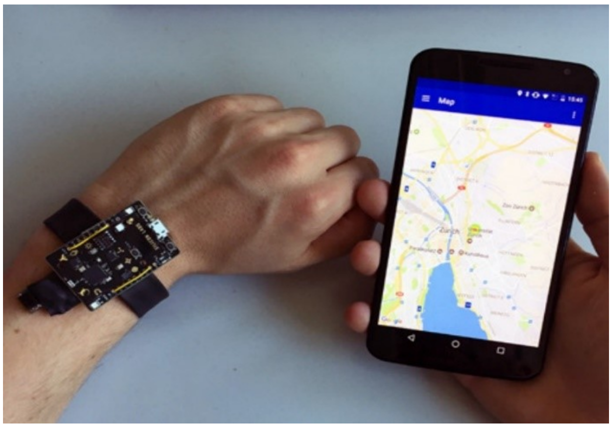

Fig. 2-18 W-air prototype and data transmission [127].

2.4.1.2.8 Common Sense: Urban Air Monitoring Prototype

The common sense is one of the most efficient prototype in its launch time. This wrist-worn is capable of several ambient air indicators (carbon monoxide, nitrogen oxides, and ozone gas sensors) and also air physical parameters (humidity and light). This waist-worn has been developed in several data transmission modes (Bluetooth, 802.15.4, or GPRS radios) and also is equipped with GPS. Orientation sensors are another aspect of the common sense. The sampling rate might be variable. The periodically data sampling, less often sampling and sampling based on the individual movement are of the features (see Fig. 2-19) [128].

Fig. 2-19 Common sense prototype for ambient air monitoring [128].

2.4.1.2.9 CitiSense: a Wireless Personal Exposure Monitoring System

If CitiSense as a solution is considered a system, thus this system consists of three main components: a wearable air pollution sensor which is the hardware sensor node and should be carried/worn by the user, the smartphone that the application is running on it and the web interface. Both wearable sensor and the smartphone must be carried by the users (or keep close in the connectivity range) throughout their day, in particular during times when exposure to pollutants would be highest, such as during a rush-hour commute. The smartphone is simply used for the real-time monitoring or so called: "in the moment observation". The web interface is used to reflect the daily data observation and tracking if the user. This prototype uses low-cost electrochemical gas sensors (carbon monoxide (CO, NO_2 and O_3). In addition to the gas sensors, air pressure, humidity and temperature also are evaluated by this board (see Fig. 2-20) [129].

Fig. 2-20 CitiSense: a wireless personal ambient air monitoring [129].

2.4.1.2.10 Safety and Health Monitoring Nodes

In [130] a hybrid wearable sensor network including safety node (CO_2 and UV index) and health node (heart rate and skin temperature), is presented. This wireless sensor network is based on IoT and utilizes a Raspbbery Pi as the gateway and cloud for data analysis and permanent storage.

This solution is demonstrated within the WBAN approach for short-range communication between two sensor nodes (BLE). The data from health node are transmitted through Low Power Wide-Area Network (LPWAN) to the gateway and WiFi for long-range communication to cloud is used. The target monitoring subjects are workers in outdoor workplaces.

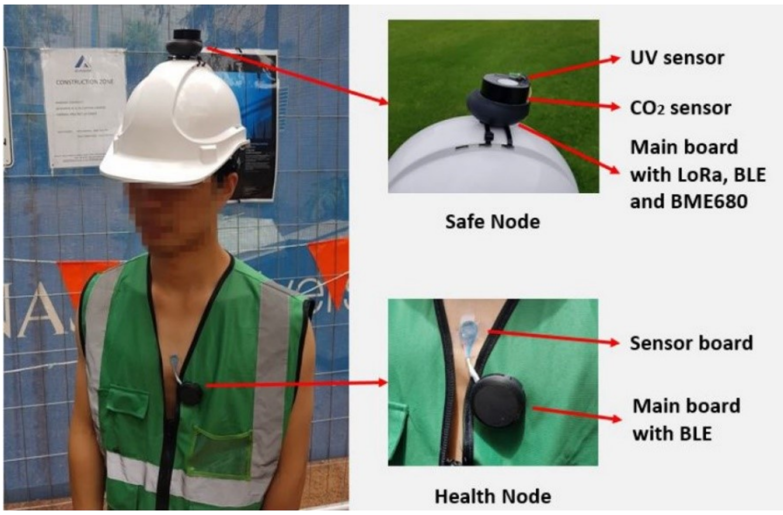

Fig. 2-21 The Safe Node and Health Node are attached to the subject' helmet and body [130].

2.4.1.2.11 Summary Of The Ambient Air Prototypes

In the previous subchapter the most recent and advanced technology mostly in the low-cost gas sensors were described. This was an essential for understanding of the gas detector devices and prototypes. The overall overview on the latest achievement in the market and also presented by the researchers (prototypes) were described in detail here. To conclude on this subchapter, a brief summary is provided as the follows:

- The heavy concentration at the moment is the ambient air monitoring in term of toxic/hazardous gases. This avoid to attract the attention for the danger of high sound level. This is a motivation and good justification to work on a prototype for noise detecting as well.
- There are many gas sensor prototypes for toxic gas detection. These devices more often are found as a single-gas and waist-worn/portable detector. In fact, the flexibility of gas sensor detectors in terms of device configuration, mode of wearability and multi-gas detecting, is a factor that requires to gain attention for improvement.
- With the great advances in technology and data transmission efficiency, still the gas sensor detectors are considered as the dependent sensor nodes which need to send the data to a gateway. In the absence of the smartphone, more often the designers do not provide the solution for the lost data.
    - Prolonged monitoring is maintained as a challenge. Power harvesting from different source of energy (e.g. body heat and movement, natural sources: sunlight and heat) can significantly assist whether in designing self-power prototypes or increasing the monitoring time through charging the battery partially. However, applying power harvesting in ambient parameters devices, requires the suitable form factor and mode of wearability. This must be considered as a step for the future developments of prototypes.
    - Although smartphone in many cases are utilized for data collection, this is more often a single way communication. Data and command transmission from the smartphone to the sensor node are not considered yet.
    - The presented prototypes and devices are designed in a pre-defined fix structure and architecture that does not open a door to the future for more comprehensive solution.
    - The future hardware and solution extension has not been considered in the aforementioned described devices and prototypes.

2.4.2 Sound Level Detectors

As the part of this research concentration, commercially available sound device detectors are presented in this section. The introduction to sound level module detectors which is necessary for sound module selection in this design will presented in next chapters.

2.4.2.1 Casella CEL 63X Sound Level Meters

This is a portable sound level meter in the range of 20-140 dBA. It is provided in the dimension of 230x72x31mm (Fig.2-21.a). It is suitable for stationary measurement or be carried by the user in some operational occupations. The Casella is equipped with a 2 GB external memory which provides the capability of data logging in low quality up to 60 hrs. This handy can distinguish the frequencies and spectrums. The total weight of the device including battery is 332 gr. Casella operates in the two following modes:

- Low Quality: 8,000 samples/s @ 8bit (64kb/s), up to 4kHz
- High Quality: 24,000 samples/s @ 8 bit (192kb/s), up to 12kHz

Furthermore, it is able to function under the 0 to 90%RH (non-condensing); -10 to +50°C (Class 1) and 0 to 40°C (Class 2); Atmospheric pressure of 65 to 108kPa [131].

2.4.2.2 3M™ Edge™ 5 Personal Noise Dosimeter with docking station, EG5-D

This is a small compact, relatively light-weighted for personal sound level monitoring. This device comes with a rechargeable lithium polymer battery that is able of 40 hours environmental sound level monitoring. It offers a shoulder mount and is in dimension of 88mm (L) x 53mm (W) x 19mm (D). A typical application is safety monitoring in healthcare (Fig.2-21.b). Although the device is comparison with the previous sound level detector is much smaller but it is not presented in a wearable mode. It is more often used as a portable one. Three weighting sound level of A, C and Z are measured by this sound level detector [132].

2.4.2.3 Sound Badge Personal Wearable Noise Dosimeter and Sound-Level Meter

This wearable dosimeter is one of the first sound level detector that can be worn. It is compact and is presented in the size of Diameter: 50mm, Height: 13mm, Weight: 35g. This sound badge is measuring the sound level in the range of 55-130 dB in three A, C and Z weights. The recording interval is 0.25 s and operates in two fast (1s) and slow (1.8s) response time. The data are monitored on the screen and are logged in an external memory (Fig.2-21.c). The device is powered by a single rechargeable lithium-ion battery that can last 16 hours and is recharged in 3 hours via USB [133].

2.4.2.4 Etymotic Wearable and Programmable Personal Noise Dosimeter Model ER-200DW8

This sound level detector has been manufactured in the form of a marker with a microphone attached at the top. The data are logged on the device and no real-time observation is possible. Instead, the dosimeter is programmable to determine the threshold and user is notified when the threshold is exceeded (Fig.2-21.d). To observe the data, this Etymotic wearable is connected to PC through USB. It is powered by three AAAA batteries. Continues monitoring of 200 hours is possible by this device. The range of 70-130 dB are detectable in the A weight [134].

(a) (b) (c) (d)

Fig. 2-22 Comparison of four available sound level detectors in the market. From left to right: (a), (b), (c) and (d).

2.4.2.5 DAP Digital Sound Level Meter

This device is a portable sound level detector and works in the range of 30 dB to 130 db. It sounds that the manual recalibration is possible by the user. The spectrum frequency in the range of 2 kHz to 8 kHz are detected by the DAP digital sound level meter. It is powered on by 1.5V (6x AAA). Although the resolution is in the scale of 0.1 dB but the precise tolerance would be 2 dB (see Fig. 2-22 .a) [135].

(a) (b) (c) (d)

Fig. 2-23 Comparison of four available sound level detectors in the market. From left to right: (e), (f), (g) and (h).

2.4.2.6 Digital Sound Level Meter, A Weighted

Another digital sound level meter in the market is “A” weighted digital sound level meter. It is functioning in 9 V. The provider indicates the 0.1 dB data resolution and +/- 3.5 dB for the device accuracy. It does not measure the sound under the 40 dB and above 130 db. The range of frequency is spread between 31.5 Hz and 4 kHz which is quite limited. The monitored data are screening though the display on the device (see Fig. 2-22.b) [136].

2.4.2.7 Testo 816-1 Sound Level Meter

This digital sound level detector with the dimension of 272 x 83 x 42 mm is working in two frequency weighting A and C. An integrated external storage and display on the device make it quite useful for data logging and observation. Testo 816-1 operates in 2 Hz sampling rate and the external memory store up to 31,000 samples. It can track the data from a slow response (1s) to a fast response (125 ms). The sound level detection from 30 dB to 130 dB is another specification of this device. The sound level spectrum frequencies are supported from 20 Hz to 8 kHz. The weight of this detector is approximately 390 grams [137].

2.4.2.8 Cesva Sc310 Sound Level Meter and Spectrum Analyzer

The SC310 is a classical user-friendly, flexible type 1 integrating sound level meter. It can be used as either a sound level meter or as a real time spectrum analyzer for both 1/3-octave bands and whole octave bands - with Type 1 filters. The sc310 is able to function in all weighting frequency. Frequency analyzer and FFT calculation also are of the features for this device. Auto and manually recalibration process are supported in Sc130. Data storage and real-time monitoring, fast and slow data response are implemented as well [138].

2.4.2.9 Summary

The available sound level meter are not limited to these devices that presented in this subsection. However, generally the dimension, features and specifications are less and more the same. This subsection was presented for an overview of the available devices which nowadays are using in industry and perhaps by individuals. A summary is presented as follows:

- The available devices mostly are portable devices.
- These devices cover a variable spectrum of frequencies based on the quality of the device.
- The measurement is mostly precise but a tolerance from 1db to 4db could be considered depending on the device.
- The calibration and recalibration is performed manually and in some devices automatically.
- These devices are mostly expensive. Basically the price range of depends on the resolution, calibration, accuracy, features and specification. Prices vary from several hundred euros up to several thousand euros.

What was presented here is only the sound level meter devices. However for sound modules which are utilized along with microcontroller a different section is considered. In that section, different microphones and modules which might be qualified for a personalized sound detection prototype are described in detail.

2.4.3 Combined Monitoring Devices For Sound Level and Hazardous Gas Detection

A device that has been developed in academic community and is able of measuring both sound level and hazardous gas with its own features and specifications is presented.

2.4.3.1 Eco-Mini

An environmental monitoring device called "Eco-Mini," is presented in [138]. This device is operating without a smartphone, sampling and recording a variety of environmental parameters (ozone, sulfur dioxide, volatile organic compounds, humidity, temperature, ambient light color balance, and sound level) as well as individual activity (3-axis accelerometer) and location (GPS) [139]. A wide range of physical and chemical parameters are evaluated by Eco-Mini. It is waist-worn and an expected location is belt connected (See Fig. 2-23).

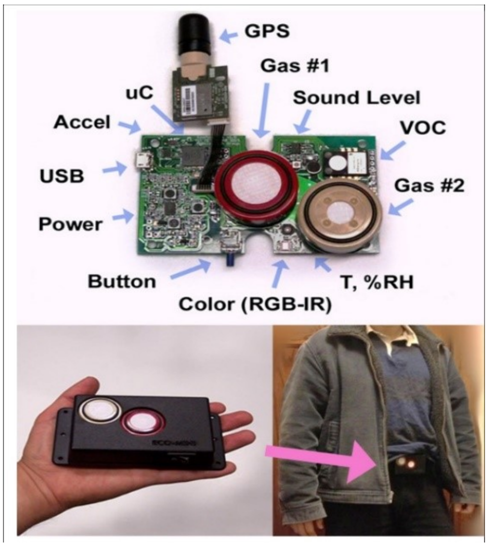

Fig. 2-24 Eco-Mini in environmental parameters monitoring [138].

As was observed this prototype is a serious contribution in the area of air quality monitoring and physical ambient assessment. However, Eco-Mini is suffering from lack of connectivity to a second part and real-time monitoring. There is no way of data transmission. All sampled data are only storage in an external memory for later observation and analysis. On the other hand, a display is not considered for instant monitoring. A possible usage of the Eco-Mini may be in clinical application for long term monitoring of non-critical situations.

2.4.4 Devices, Bracelets And Smartwatches In General Healthcare Monitoring Systems

As the ultimate target of environmental parameters monitoring is human health protection, thus to complete the state of the art, introduce the most advanced approaches and devices, briefly the general health monitoring system measuring motion tracking and vital signs are placed in this section.

2.4.4.1 E-Health Sensor Platform

In the following work the methodology and approach is described [140]. An integrated wearable health-monitoring system based on wire multi-sensor connected to microcontroller is presented [141]. It consists of a chest-worn device that embeds a controller board, an Electrocardiogram (ECG) sensor, a temperature sensor, an accelerometer, a vibration motor, a color changing Light-Emitting Diode (LED) and a push-button. In fact, in this device some of bio metric and medical parameters along with position tracking are monitored. Distinctive haptic feedback patterns can be actuated by means of the embedded vibration motor according to the user's health state. The embedded color-changing LED is deployed to provide the wearer with an additional intuitive visual feedback of the current health state. Finally, a push-button is provided for emergency cases, this button can be pushed by the user to report a potential emergency condition (see Fig. 2-24).

This system is based on the e-Health Sensor Platform V2.0 which is the first bio-metric shield for Arduino and Raspberry Pi. This device may measure the pulse, oxygen in blood, breathing airflow, body temperature, ECG, glucometer, galvanic skin response, blood pressure, patient position and muscle/Electromyography (EMG). Collected data are used in two scenarios: real time monitoring of the state of a patient and transmitting of the sensitive patient's data to a medical station for diagnosis. The data transmission possibility is through sensor e-health in one of the followings: Wi-Fi, 3G, GPRS, Bluetooth, 802.15.4 and ZigBee, depends on the application. The structural framework is based on a multi-sensor fusion approach. In particular, a client-server pattern is adopted.

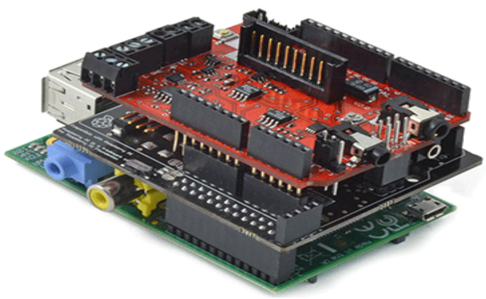

Fig. 2-25 Arduino Uno board, an Arduino Wi-Fi Shield, e-Health Sensor Shield [139].

Although a very comprehensive vital signs monitoring is demonstrated but this device does not have a license from the medical organization. Possible usage must be with care.

Every sensor is wired to the main platform. In case of willing to apply all these sensors, a large wiring is required and almost the wires cover whole body. This is critical, especially with elderly and patients. This device is not wearable and more applicable as a portable device only in emergency status where there is no accessibility to medical facilities. With number of sensors connected to the main platform and operating in high sample rate, power consumption is expected to be extremely high and need frequent battery charging. The size and weight of the device is obviously does not make it suitable for wearability.

2.4.4.2 Smartwatches And Bracelets In Market

First, at this subsection 9 devices with different features and specifications are provided in Table 2-3 and are compared [142]. The brief essential criteria on wearable devices are listed. Data storage on a memory, data transmission through a BLE, ZigBee, (short range) or WiFi (long range), prolonged operation depends on battery life, sampling rate and design efficiency, form factor, wearability and on-board sensor possibility are the most required criteria of the wearables. Another feature of a wearable might be firmware. Many of these devices come only with customized software application. To take full advantage of a development kit, in some cases, customization is a must, but not all device manufacturers provide such compatibility.

Hereinafter, 9 devices which have been used and investigated in researches are introduced and important features are listed. In the following table, all mentioned elements are compared and additional parameters including connectivity, software and firmware compatibility are taken into consideration.

These 9 devices are from different companies and manufacturers (Motion Node Bus, Opal [143], MTw development kit [144], Memsense W2 IM2 [145], STT-IBS [146], Colibry wireless [147], I2M motion SXT [148], Shimmer 3 [149], Physilog [150]). These platforms are available on the market and have been utilized in research purposes as well. It has been widely attempted to present the most recent research works and devices in the market. Comparison of different specifications of each device exhibits that only six out of the nine listed devices have the capability to be used either as data loggers or as wireless sensors networks (WSNs) [150]. Majority of the devices (eight out of nine) come with a software development kit that allow the user for customizations. The only remaining device (SHIMMER3 by Shimmer, Ireland) offers the user the capability of reprogramming its firmware (e.g. adding an onboard custom processing) [150].

Table 2-3 Comparison of 9 applied motion tracking devices available in the market in research works.

Device	Dimensions/Weight	Sensors	Battery Life	Wireless Connectivity	Sensor Network	Data log.	Software Library
Motion Node Bus [151]	Sensor:35*35*15 mm^3/10g Battery 180g	3-axes accel.; 3axes gyr. 3-magne.	5sensors: 7hrs 15sensors: 4.75 hrs	802.11g	Yes, upto 20 sensors	Yes, 4GB	Yes, open source, SDK in C++,C#, Java and Python
Opal [152]	48.4*36.1*13.4mm^3/22g (with battery)	3-axes accel.; 3axes gyr. 3-magne.	Wireless streaming: 8h Synch.: 12hrs Async.:16hrs	Low-power wireless communication protocol	Yes, up to 24 devices is possible	Yes, 8GB	Yes, SDK including support for MATLAB, JAVA, Python and C
MTw development kit [153-[154]	^34.5*57.8*14.5 mm^3/27g	3-axes accel.; 3axes gyr. 3-magne, static pressure	Continuous use:3.5 hrs Stand by :90hrs	Awinda radio protocol	Up to 32 MTw's in a configurable wireless area network	No	Yes, C,C++ and Matlab
Memsense W2 IMU [155]	40.1*33.5*15.2mm^3/not specified	3-axes accel.; 3axes gyr. 3-magne, static pressure, temperature	5hrs	Bluetooth	No	No	No
STT-IBS	36*15*46.5mm^3/ 30g	3-axes accel.; 3axes gyr. 3-magne,	Not specified	Wi-Fi, Bluetooth	No	Yes	Yes, SDK can be integrated in .Net and C++ environment
ColibriWireless	56*42*17mm^3/41 g	3-axes accel.; 3axes gyr. 3-magne. Temperature	16hrs	Wireless 2.4 GHz band operation	Yes, up to 10 trackers	No	Yes, API for implementing extended Kalman filter for tracking orientation
I2M Motion SXT	48.5*36*12mm^3/ 22g	3-axes accel.; 3axes gyr. 3-magne.	Wireless streaming: greater than 8hrs, Logging: greater than 16hrs	Proprietary low power wireless communications protocol	Yes, up to 24 STXs	Yes, 8GB	Yes, support for MATLAB, Java, Python and C
SHIMMER3	51*34*14mm^3/not specified	3-axes accel.; 3axes gyr. 3-magne., altimeter	Not specified	Bluetooth	Yes,	Yes	Yes, Labview, Matlab,

							Java/Android , C# drivers
Physilog	50*37*9.2mm^3/19g	3-axes accel.; 3axes gyr. 3-magne.,pressure sensor	< 21 hrs	Bluetooth	Yes	Yes, 4GB	Yes, ready to use code in MATLAB, C/C++, Python

In the second part of this subsection, the five most popular and applicable devices available from the market are described in detail below. The commercially name of device, country of manufacturing, tasks ability and price are provided for each one (see Fig. 2-25).

2.4.4.2.1 Fitbit Flex

The first device is Fitbit Flex (Fitbit Inc., San Francisco, California, USA), a motion tracker in wristband style, wireless enabled, and wearable. It should noticeable that Fitbit has wide range of products from Fitbit Charge1, 2, and 3 to Fitbit Ionic health, Fitbit Versa, Fitbit Alta, Fitbit Surge and Fitbit Aria. Fitbit Flex as one of the most functional and popular version of this family product is considered in this study. Fitbit flex measures both step counting and quality of steps. Fitbit flex is restricted in data transmission mode, with providing only compatibility with connection to mobile application. The device is suitable for motivation in exercise and movement. On the other side, small size of this wearable allows to be worn in various styles and locations such clipping onto a belt or clothing, carried in the pocket, or worn on the wrist as a watch. It is also able to track the quality of sleeping. The Fitbit flex also measure heart rate. A comparison different versions of Fitbit is presented in Table 2-4. This must be considered that Fitbit Flex battery life time like most of this products is 5 days. This can be compared with the features Fitbit Flex that was described. The manufacturer provides it in bangle and pendent as well. The market price of the Fitbit Flex is € 99.95 [156], [157].

Table 2-4 Comparison of Fitbit products.

Product	Price(€)*	Battery life	Type	Features
Versa	199.95	4 Days	Watch	Tracks sleep, steps, heart rate, calories and is water resistant to 50 meters.
Alta HR	149.95	7 Days	Wristband	A Smart Track feature automatically recognizes selected activities you do and records data about them.
Charge 2	159.95	5 Days	Wristband	Uses Pure Pulse to track heart rate 24/7 and offers guided breathing sessions based on heart rate
Ionic	299.95	5 Days	Watch	Tailored to serious athletes, uses Pure Pulse, built in running training programs, personal coaching.
Alta	119 and up	5 Days	Wristband	Smart Track™ technology and sleep health tracker
Ace	99.95	5 Days	Wristband	Showerproof Fitbit for kids featuring goal celebrations, badges, and sleep tracking. Recommended by the CDC.
Charge 3	149.95	7 Days	Wristband	24/7 Heart Rate Tracking, contactless payments, water Resistant to 50 M, fitness & sleep tracking, smartphone notifications
Flex 2	99	5 Days	Wristband	Measures both step counting and quality of steps. Only compatibility with connection to mobile application. Measuring exercise and movement. It is also able to track the quality of sleeping and heartrate.

* Price list 08.03.2019

2.4.4.2.2 Withings Pulse

The Withings Pulse (Withings SA, Issy les Moulineaux, France) is a WiFi enabled healthcare monitoring device that is one step further in features and specifications in contrast to the previous device that provides only motion tracking information. The Withings Pulse can count the number of individual's steps, distance traveling. It records the sleep time as well. Withings Pulse combines the heart rate and pulse measurement with the previous features. The sleep time is displayed as a percentage of the optimal sleep hours [158], [159]. Withings also provides a variety of more products in this categories with relatively same features but different dimensions.

A comprehensive comparison of features of each product is shown in detail in Table 2-5.

Table 2-5 Comparison of Withings products.

Product	Steel	Steel HR	Steel HR sport	Pulse HR
Size (mm)	36	36/40	40	44
Battery life time	Up to 25 days	Up to 8 months	Up to 25 days	Up to 20 days
Price* ($)	129.99	179.95	199.95	129.95
Features	Automatic run, steps, swimming and sleep tracking, +30 activities recognition	Automatic run, steps, swimming and sleep tracking, +30 activities recognition, heart rate measurement, connected GPS	Automatic run, steps, swimming and sleep tracking, +30 activities recognition, heart rate measurement, connected GPS	Automatic run, steps, swimming and sleep tracking, +30 activities recognition, heart rate measurement, connected GPS

*Price list 08.03.2019

2.4.4.2.3 Misfit Shine

The Misfit Shine (Misfit Inc., Apple Inc., Burlingame, California, USA) is the next motion tracker which in reality, goes much more beyond the similar devices. This device in addition to step counting, distance measurement and daily calories burnt, supports the user with following information: sleep tracker monitoring and hours of light as well as deep sleep. The Misfit Shine is compatible with Android as well as the iPhone [160]. Misfit path, Misfit Phase, Misfit Ray, Misfit Shine2 and Misfit Flare are compared in Table 2-6.

Table 2-6 Misfit products comparison.

Products	Path	Phase	Ray	Shine2	Flare
Smartphone Compatibility	iOS: 9.0 + Android: 4.4 +	iOS: 9.0 + Android: 4.4 +	iOS: 9.0 + Android: 4.4 +	iOS: 9.0 + Android: 4.4 +	iOS: 9.0 + Android: 4.4 +
Battery Life	Up to 6 months	Up to 6 months	Up to 4 months	Up to 6 months	Up to 4 months
Price(€)*	149.99	175.99	99.99	79.99	59.99
Features	Smartwatch, non-charging, steps taken, calories burned, sleep quality and duration, watch display, movement reminder, alarm	Smartwatch, non-charging, steps taken, calories burned, sleep quality and duration, watch display, movement reminder, alarm	Non-charging, steps taken, calories burned, sleep quality and duration, movement reminder, alarm	Non-charging, steps taken, calories burned, sleep quality and duration, watch display, movement reminder, alarm	Non-charging, steps taken, calories burned, sleep quality and duration, movement reminder, alarm

*Price list 08.03.2019

2.4.4.2.4 Jawbone

The Jawbone Up24 (Jawbone, San Francisco, California, USA) is the same with the previous motion tracker devices. The data transmission is performed through BLE. Jawbone allows tracking user's sleep data, eating habits, calories burned, and daily activity, including step counting and distance travelled. Wireless heart rate measurement also must be added to the features of this wrist-worn. The Jawbone Up24 is designed with only one operating button and costs US 100 [161].

Fig. 2-26 Four popular motion tracker wearable devices (wrist-worn) [156].

2.4.4.2.5 Apple Watch

One of the most advanced wearable devices in the recent years is apple watch. It has been released in series 1, 2, 3 and recently 4. The smart Apple watch is a fitness and healthcare oriented. Operating in different mode of motion recording. This device is connected to iPhone smartphone with OS version 5 and later. It can record indoor and outdoor activities as well as heart rate with configurable sample rate. Apple watch transfers the data through BLE. Apple watch measures the heart rate in a programmable time interval and transfers the data to the smartphone during a routine. This device (ex. series 3) is synchronizing through WiFi as well. The low battery life (depending on functions and usage from couple of hours to 2 day) and high price of this product (apple watch series 4 costs 429 €) are the weakness [162] (see Fig. 2-26).

Fig. 2-27 Apple watch series 3 [158].

2.4.4.2.6 Nokia Steel HR

It is a classical digital/analogue smartwatch for heart rate measurement. Nokia steel HR is compatible with both Android and iOS for data transmission. It is a good device also for sleep tracking, sleep duration and counting the number of steps. Generally, it is designed more as an activity tracker. This device is able to operates in independent mode in way that data are monitored on the display and with a large external memory size, these data are logged for several days [108A] (See Fig. 2-27) [163].

Fig. 2-28 Nokia Steel HR for heart rate measurement and activity tracking [163].

2.4.4.2.7 Summary

To conclude on the motion trackers which actually are more than only trackers, an extensive table is presented to summarize the features and specifications of the most popular wearable trackers (Table 2-7).

Table 2-7 The comprehensive and extensive comparison of the most recent wearable trackers.

Products	Apple watch 3	Fitbit Ionic	Misfit Vapor	Nokia steel HR	Garmin Fenix 3 HR [164]
Display Technology	OLED		AMOLED		
Screen Protection	Yes Scratch-resistant glass	Yes Corning Gorilla Glass, v3	Yes Scratch-resistant glass		Yes Scratch-resistant glass
Screen Size	1.5 Inch	1.4 inch	1.37 Inch		1.2 inch
Screen Resolution	272 x 340 pixels	348 x 250 pixels	326 x 326 pixels		218 x 218 pixels
Touch Screen	Yes		Yes Capacitive Touchscreen, Multi-touch		
Pixel Density Sharpness	290 ppi	306 ppi	337 ppi		257 ppi
Charging Mode	via USB, Wireless		Inductive charging via cradle	wireless	via USB
Battery Life	Up to 1 Day	Up to 4 Days	Up to 2 Days	Up to 25 Days	Up to 14 days
Alarm Clock	Yes	Yes	Yes	Yes	Yes
Goal Setting	Yes	Yes	Yes		Yes
Reminders	Yes	Yes	Yes	Yes	
Social Integration	Yes		Yes		Yes
Stopwatch	Yes	Yes	Yes	Yes	
Speaker	Yes				
Accelerometer	Yes	Yes	Yes	Yes	Yes
Pedometer	Yes				
GPS	Yes with Glonass	Yes with Glonass			Yes with Glonass
Gyro	Yes	Yes	Yes		Yes
Calories Intake Burned	Yes	Yes	Yes	Yes	Yes
Activity/inactivity	Yes	Yes	Yes		Yes
Distance	Yes	Yes	Yes	Yes	Yes
Sleep Quality	Yes	Yes	Yes	Yes	Yes
Active Minutes	Yes	Yes	Yes		Yes
Heart Rate	Yes	Yes	Yes	Yes	Yes
Steps	Yes	Yes	Yes	Yes	Yes
Hours slept	Yes	Yes	Yes	Yes	Yes
Navigation	Yes Points of interest (POI), Turn-by-turn navigation, Voice navigation	Yes Points of interest (POI), Turn-by-turn navigation, Voice navigation	Yes		Yes
Bluetooth	Yes 4.2	Yes 4.0	Yes	Yes BLE	Yes 4.0
Wireless Protocol	Yes Wi-Fi 802.11, b/g/n	Yes Wi-Fi 802.11, b/g/n	Yes Wi-Fi 802.11, b/g/n		
Compatible OS	iOS	Android v4.4, iOS	Android v4.3, iOS	Android, iOS	Android v4.3, iOS, Windows OS
Body Material	Aluminum	Aluminum		Stainless Steel	

2.5 SUMMARY AND DUSCUSSION

In this chapter, the state of the art was clearly stated. A general concept of ambient parameters monitoring in healthcare monitoring system and the effective parameters were studied. The most frequent approaches and techniques were briefly discussed. Environmental air (physical and chemical) parameters as the main focus of the research were taken into consideration and discussed.

A summary and conclusion as the base framework for the next chapter and also concept of the proposed prototype is provided as the following:

- The first mentionable point is the lack of multi-parameter wearable devices for ambient parameters monitoring. The majority of devices in the market are single-task measurement, whether it is in gas monitoring or sound level (noise) detection. As was discussed, both hazardous gas and sound level are stressor and may adversely affect the heart diseases, this combined monitoring sound quite novel, effective, reasonable and necessary to be the topic of a research.

- A survey on the bracelets and smartwatches emphasis on the popularity of wrist-worn devices. Nevertheless, the majority of bracelets and smartwatches are in the area of motion tracking, heart rate measurement, sleep tracking and body energy evaluation. However, lack of a wrist-worn device for ambient parameters monitoring is well sensed.

- With a brief look at the ambient gas monitoring, the devices are in three general categories:

    - Devices with smartphone connectivity: this devices are connected to a smartphone for data observation. Therefore a wireless communication channel (Bluetooth, BLE, Zigbee,…) is established to transmit the data to smartphone. The data are monitored as far as the connection is stable. Otherwise, the monitoring is not possible.

    - Devices with display: devices with this possibility can operate in a standalone mode. Data observation is not a function of connectivity. But the data transfer and data analysis are not possible any longer.

    - Devices with external memory: some of the devices do not support real-time monitoring. In this design, the data are monitored only and transferred to a PC at a later time.

The necessity of designing a wearable to combine all these three possibilities and more innovative features, device flexibility, user convenience and an efficient mode of wearbility is pushing the designer in this direction.

- A serious weakness of the devices in this area of research is unavailability of a configurable device. It sounds that, with a connectivity between smartphone and device, a two-way communication is feasible. The configuration may lead to sensor selection/activation from the device. This feature can result in a user-friendly and flexible wearable device that noticeably saves power consumption.

- Some devices are only launched for specific operations, applications and group(s) of working people. This research orientation is to studies and investigates the feasibility of a versatile wearable device in the area of ambient parameters monitoring which is not limited to some specific applications, places and situations.

- A multi-tasking, flexible, wrist-worn, comfortable, user friendly, easy to use, prolonged monitoring device that is supported with low-cost, could encourage the individuals to use such wearable in daily routine for health protection.

3 CONCEPT

3.1 GENERAL CONCEPT

During last decade much efforts have been performed to implement an efficient wearable device in terms of form factor, multi-parameter monitoring, prolonged observation and usability (flexibility) for pervasive environmental monitoring of the most important parameters which influence the individual health in healthcare systems. For several reasons no appropriate device has been introduced in academic level nor industry yet. As discussed in the previous chapter, WBAN and sensor data fusion as the most popular approach and technique respectively, in this area have been applied. Various algorithms and structures were proposed, although some of these devices came on operation but still users are not satisfied with the current progress, and demands are growing fast. Majority of the devices in chemical parameters measurement is introduced from the industry to the market.

In chapter 2, some of the most applicable and popular commercially available devices or research devices were presented. The state of art, challenges, criteria, bottlenecks and requirements were outlined.

Available devices and approaches show that designing a pervasive monitoring prototype requires an innovative and unique approach. Proposing a unique and applicable approach requires specific criteria, perspective and overview. An adequate design is compromising of software implementation and careful hardware design. Multi-parameter monitoring requires different sensors, therefore the use and combination of different sensors is inevitable. Thus, a physical innovative approach is necessary and hardware design is the major focus. However, this goal is not achieved without software implementation. Software implementation is an important player in the entire solution, in particular, when it can reduce the hardware complexity and consequently improves the form factor and provide easier technical solution. In fact, the software part of the work is a complementary to the hardware approach that one is not completed without the other.

3.2 CRITERIA AND REQUIREMENTS

As discussed in the related works section, a multi-parameter monitoring device with an efficient form factor is highly appreciated. This device must be capable of wearing by individuals without interference in typical daily activities. In addition, this device has to be user-friendly and operates for long-time in real-time monitoring. The device should enable safe data acquisition under any situation to avoid data lost. In the designing of such wearable, the intention is toward seeking of a solution to include the typical wearables' advantages and eliminate the weaknesses. The most important and vital criteria which accomplish both technical considerations (designer prospective) and user demands are summarized as (see Fig. 3-1):

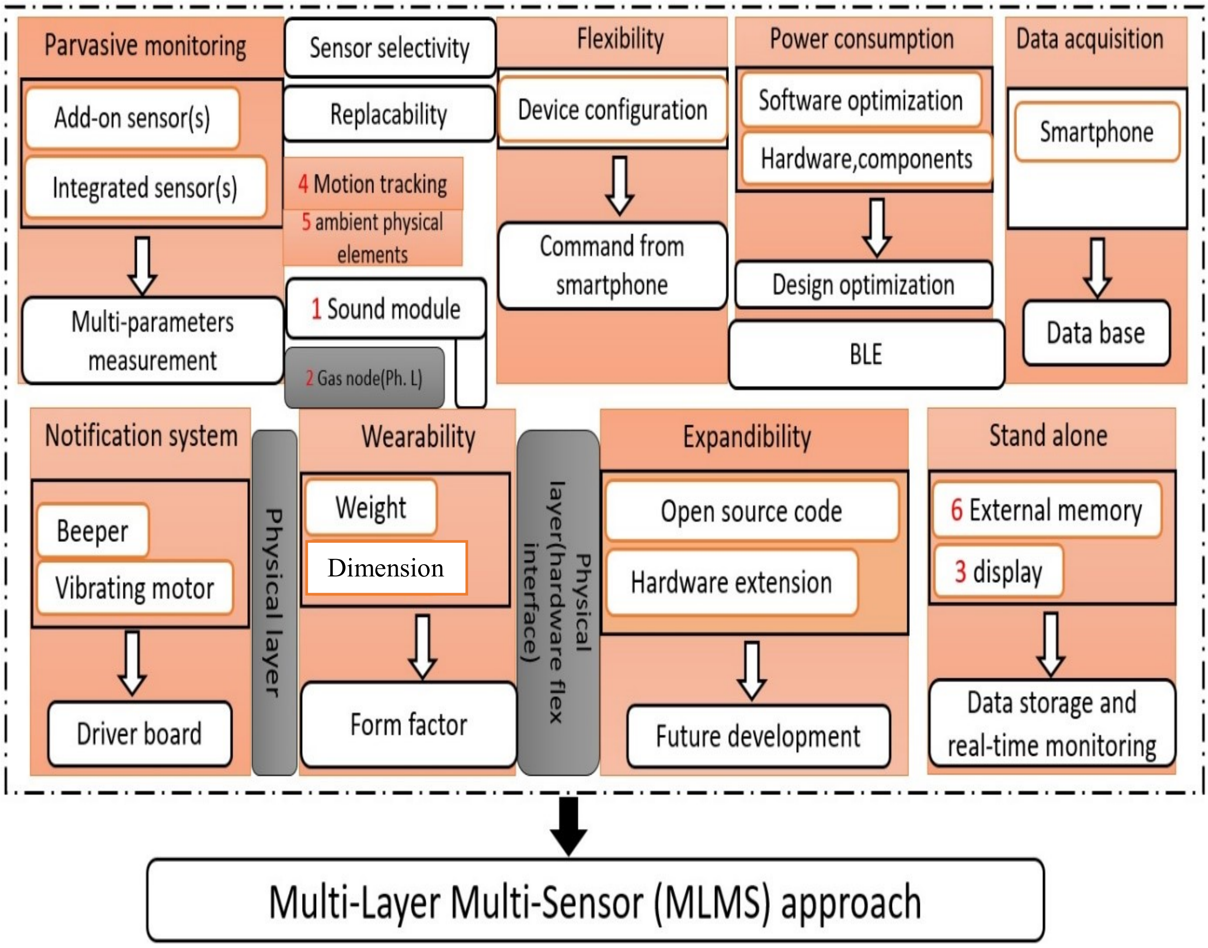

Fig. 3-1 General concept, Criteria and requirements. Some of the requirements and solutions are mutual between two parameters or more. (4), (5) and (6) are integrated on the host platform. (1), (2) and (3) are linked to the host platform via hardware flex interface.

❖ **Multi-parameter monitoring**: Available devices prove that many single task tools in the area of ambient monitoring and in particular, IOAQ are available. Each device measures a toxic or hazardous gas. As an application in occupational health, the challenge is to observe and investigate a proper influence of the parameters on the health, so that a simultaneously observation of the indicators is required. Sound level and toxic gases both are stressors and might lead to disorder heartbeat and cardiovascular disease [165], [64]. As far as both of these players are not monitored and analysed for the patients or individuals who are suffering from heart diseases, an adequate decision might not be possible by the medical supervisors.

If the user is supposed to use single tasking tools for each indicator measurement, several devices are required. Sometimes economic reasons also do not allow the user to use several devices for indicators observation.

On the other hand, by monitoring of several important environmental indicators (pervasive monitoring), more efficient self-preventive is possible. Therefore, a serious demand for multi-tasking device already is requested.

Generally, the proposed sensor node measures and collects three types of data:

- **Chemical ambient parameters**: with the major focus on CO, SO_2 and NO_2 but not restricted only to these three toxic/hazardous gases. for the solution is extended toward a solution to adopt any gas sensor within it. Although the gas sensors are distributed in wide ranges of fundamental (metal oxide, electrochemical, IR and …) and families, it is expected to cover a wider range at least in the most important indicators.

- **Ambient physical parameters**: include air pressure, air humidity, air temperature and sound level (UV index in an extended version). The sound level detection is the second wing in this proposed prototype to be observed in real-time. For two reasons, air pressure, humidity and temperature are measured:

    - More parameters are covered by the device umbrella, and it is walking toward a real comprehensive observation,
    - The chemical parameters sensors are influenced by the physical ambient air factors. Thus, these factors evaluation are important in calibration process of gas sensors.

- **Motion tracking for daily user's activities**: there is the potential of individual motion tracking by this prototype. 9 degree of freedom (DoF) is supported by the integrated sensors (magnetometer, gyroscope and accelerometer) on the main board (this is the board that is used to build the prototype based on it. This is described in realization chapter in detail). The first advantage of the motion tracking might be imagined as the activity evaluation during a routine day. When the motion tracking is integrated with ambient parameters monitoring over longer periods, a comprehensive ambient database according to urban/working area can be created. According to this database, the air condition of each region is recorded. The short target of this prototype and the major concentration is designing a prototype in the area of ambient monitoring, but the further work can be daily activities measurement that is extremely important in health of individuals. As already the raw data are collected, the algorithms for different purposes can be implemented. Fall detection of elderly, motion tracking, fast movement and many other applications can be deeply considered. Performing the second piece of this puzzle (motion tracking), may motivate to move from comprehensive ambient monitoring to comprehensive health observation by adding physiological sensors to the solution as well.

- **Form factor**: This requirement is one of the basic criteria that directly affect the device convenience. A compact, light-weighted and small wrist-worn device is highly desired. The form factor is dependent on approach, design strategy and components selection. To achieve the ideal form factor, the general strategy of the proposed wearable is based on a careful hardware design, components selection and efficient software implementation. The trade off and balance between hardware and software complexity cannot be ignored.

Individuals from different categories are less motivated to wear an inconvenient device. Users are interested to wear a device, which is useful, helpful, cost effective, performing number of tasks and does not restrict the daily manoeuvrability. According to the studies, the more appropriate mode of wearability and ease of use is wrist-worn [166], [167], [168]. Individuals are more comfortable with a wrist-worn device rather than waist-worn/arm-worn where it is inconvenient in dressing and wearer style. This requirement (wrist-worn mode), demands a small and light-weighted tool. Size and weight are the key elements of form factor in wearable devices. Therefore, the research is oriented toward implementing a wearable with a suitable form factor. In Table 3-1, the most popular wrist-worn smart watches in the market are categorized according to the market share and dimensions. This shows that a x-y dimension of these wrist-worn is between 35 to 51 mm and the height does not exceeds 18 mm. Care must be taken that these devices are commercial devices which none of them are included in ambient air monitoring, but have been considered due to popularity in the market. If these sizes are considered as the acceptable and standard, thus we expect that the proposed prototype won't be larger than 39 mm in x-y plane, where the host platform as the fundamental layer is only 33 mm. This sounds to be quite in a standard range. However, to avoid x-y extension, it is preferred to build more physical layers on top and bottom of the host platform, this still maintain the solution compact and wrist-worn and the future development also is quite possible. Altogether the size of the prototype will never touch 20 mm (out of the box). The general form factor and mode of wearability of the prototype is the function of each single components, sensor and modules that are used. Thus, each of these components are discussed regarding the criteria and requirements. Gas sensor and sound level module are the most essential to be considered here.

Table 3-1 The most popular smart wrist-worn share and dimension in the market.

Vendor	Market share (2017)	Dimension-average (mm)
Apple	15.3%	42
Xiaomi	13.6%	46
Fitbit	13.3%	35
Garmin	5.4%	47
Fossil	4.3%	51
Others	48.1%	-

- Sound module, criteria, features and specifications

Sound module detector is one of the main add on-sensors. These sensor selection can seriously influence the total mode of wearability (size and weight) of the prototype and consequently form factor is impressed. So that, briefly the criteria and merits for the sound module detector and gas sensor are discussed:

There are two ways to implement it:

- Design and Implementation of a module from the scratch,
- Use an off the shelf module and change according to the requirements of the final design.

According to the fact that nowadays with advances in semiconductor and technology, wide range of sound modules are available commercially. It sounds that spending much time on designing a module while the similar is in market is not the best way. Instead, a module is selected according to the final prototype and the changes are applied according to the criteria. Form factor, gain and sensitivity are the most important factors in sound level detection. This sound module also must be compatible with the main platform in power supply. The effective factors on sound module selection are listed as below:

- Form factor: here, the form factor is extremely important. In addition to length and width of the module, the thickness also is playing very important role. The microphone positioning and orientation also has to be considered. In the final design, the sound module should stand vertically and microphone is outside oriented to avoid and reduce self-user conversation detection.

- Voltage supply: although to have a qualified output signal detected by the host platform, the input voltage should be higher, but this might be compensated by gain adjustment. However, the sound module has to meet the requirements of sensitivity, gain and resolution.

- Output signal: the output signal from the sound module must meet the least requirements. The output signal must be detectable by the host platform for processing, but the resolution could be enhanced by the Analogue to Digital Converter (ADC) resolution for better sound level detection. It is also possible to amplify the gain and adjust the sensitivity.

- Low-cost: as a policy in this design, all components should be as low-cost as possible to do not affect the final prototype cost and still affordable by individuals.

These are the parameters that influence the noise module selection process. Based on this criteria and discussion, in the next chapter the sound module is selected and features are discussed in detail.

- Gas sensor, criteria, features and specifications

In the second step, the merits of a suitable gas sensor for the proposed prototype are outlined. Gas detection in this prototype is performed by gas sensor node. The gas sensor node consist of gas sensor and gas sensor driver. When the gas sensor driver board is designed and implemented, the gas sensor is attached on top of it and forms the gas sensor node.
To create a gas sensor node, the first step is to select an appropriate gas sensor family which is fit within the design. Features and specifications of the sensor are critical in final device performance and efficiency. Moreover the gas sensor shape and dimension, seriously can influence the form factor, size and weight of the final prototype design. The most critical factors in gas sensor selection are listed in the followings [169], [170], [171], [172], [173], [174]:

Size, weight, power consumption, operation mode (V/A), output external components, products of the same family, technology, package, response time, wear ability, reusability and life time.

These criteria are the merits that lead to gas sensor selection in the proposed prototype. In the realization chapter, the selected gas sensor with the features and specification in more detail is introduced.

- ❖ Notification system: Healthcare systems are working toward preventive and predictability (P^2health). Thus, the ambient parameters monitoring has to protect the individual by preventing (warning) the user from dangerous situations. A notification system is absolutely required to notify the user in abnormal statuses. In particular, in gas detection such CO, that does not have a smell or flavour and high exposure concentration can lead to death, notification system sounds necessary. Once the necessity of a notification system is clarified, an efficient methodology to attract the individual attention, must be implemented.

  The primary choice is a beeper operating in adjustable frequency according to the degree of risk. But as a concern, the beeper may not be able to attract the user attention in noisy operational area/urban. Thus, a haptic notification to touch the wearer is proposed. A vibrating motor touching wrist can probably tackle this problem. To conclude, a notification system with combination of beeper and vibrating motor is an adequate system to cover different situation under various conditions.

- Vibrating motor, criteria, features and specifications

A vibrating motor is used to attract the attention of the wearer in operational working places that are noisy. In addition, vibrating motor is engaged with haptic sense which is one of most sensitive human sense. To choose an appropriate vibrating motor, first the requirements and criteria are listed out:

- Size and localization: the target wearable as a wrist-worn is restricted by several parameters. One of these elements is size. As the space for each component must be carefully designed and located, thus the applied vibrating motor must be small in diameter and length. Weight also is important which should not be forgotten. Vibrating motor localization is the second priority. In the future proposed design, the general shape of the device is rounded while the case is designed in a combined structure. A part is rounded, a part is straight and a small corners are tilted. Therefore, some spare space is found between the device and case for vibrating placement. On the other hand, the best position of the vibrating motor is vertical to touch the individual's hand in working status.

- Power supply and energy specifications: a repetitive consideration in wearable should be considered. Power supply of the operational vibrating motor should be in the range of the whole design. The vibrating motor must generate enough rotation to attract the attention while the power consumption must be too high.

- Cost and ease of use: as this device is going to be a low-cost end product, each component is limited in price. Furthermore, the shape of the vibrating motor is an effective factor in final selection.

A careful consideration of these merits, drive the designer toward narrow selection of vibrating motor available in the market. In realization chapter (chapter 4), the final decision on vibrating motor is discussed in detail.

- Beeper, criteria, features and specifications

Beeper is a feet of notification system that is activated in different modes in abnormal status. However in an alarm generating component, it is expected that the volume is high enough to attract the individual's attention.

In the policy with the vibrating motor, the following criteria and concerns must be relied on in beeper selection:

- Size and localization: a wearable wrist-worn prototype with several add on-sensor(s), components, features and specifications definitely encountering size issue. Every component has to be added to the solution very carefully. Therefore the size, weight and shape of beeper is the matter for designer. Altogether with concerning the final design and shape of the prototype, the localization of the beeper is demonstrated on the body of box that cover the sensor node.

- Power consumption: although the notification system only is activated in abnormal statuses and thus it is not more often. However, still the power consumption is one of the major drawbacks in wearable design. We do the best to select a beeper which satisfy the requirements and also is low in power dissipation. On the other hand, the beeper should be adopted in voltage supply of the system.

- Ease of use and integration with the system: in working on the very small scale design, the caution in dealing with every step in the design and implementation is necessary. The beeper hardware integration mode with the notification driver and whole solution is a matter. So that, wire/pin compatibility is also considered in beeper selection.

These criteria are considered to conclude for the beeper selection in next chapter.

- Power consumption and prolonged monitoring: in an efficient prolonged monitoring, battery life time is the most critical player. Energy dissipation, might directly and indirectly affects the performance of the observation through sample rate, data transmission time interval and even form factor. To reach an efficient form factor, the battery size must be reduced, thus an appropriate circuit design and architecture definition are compulsory in terms of components and sensors [175], [176], [177], [178].

  Prolonged monitoring provides a reliable evaluation and larger database with no interrupt. In addition to a battery capacity, efficient hardware design and component selection, a careful device configuration and sensors' sampling rates can significantly extend the battery life and the monitoring period.

  One of the features that is applied in software side is adjustable sampling rate. The battery level is divided into five portions and each segment covers twenty percent of the battery level. Due to some concerns then last two area are combined and cover forty percent of the battery level. Each battery level has its own specific sampling rate. With this algorithm, as the battery level is reduced the sampling rate is reduced too.

  With sensor selection feature also, the proposed device always operates in an optimal mode. This prototype potentially can be used by different individuals' categories from workers for noise detection, to office working people for gas detection in laboratories. Each may demand different time observation. One can only be interested to power on the prototype when is working (ex. Workers and chemist) for eight hours, some other may be interested even measure when he/she is at home for sixteen hours and some can demand for twenty-four hours protection (ex. elderly). If the request of third group of users is satisfied, consequently two others are in the range as well. In this design, with a careful hardware design, appropriate modular approach, configurable prototype and variable sampling rate, the operational time of battery is expected to be greater than twenty-four hours. In addition, in low battery level, individual is able to remove unwanted sensor(s) or reduce the sampling rate by sending command from the smartphone.

  - Independent operation: although creation of a database from data transmission to a smartphone and then server is privilege in personalized parameters monitoring but it is on condition of the smartphone accessibility and BLE connectivity. Here is the place that standalone operation could significantly improve the proposed device application. It is a part of technical solution to still observe and collect the data on real-time while the BLE is disconnected and smartphone is not available. In this case, an external memory and display can bring the independent capability to the prototype.

As was notified in some previous papers, the wearable devices are suffering from the real-time data observation in emergency status. In case of battery running in low level, or smartphone unavailability and data transmission to a smartphone is disconnected, the possibility of data observation must be provided. This is a serious and crucial demand in wearable devices for independent operation. For an independent monitoring, two conditions should be satisfied:

- Real-time monitoring: more often data from a wearable are sent to a smartphone for data protection (avoiding data lost) and real-time monitoring. As a solution, a display for the parameters monitoring can eliminate the necessity of the smartphone in this case. In some prototypes/devices, the data are directly sent to a smartphone or stored in an external memory, and then at some other time, are transferred to a PC for observation and analysis. Although this can be solution to maintain the data for investigation but cannot help the individual instantly. To overcome of this drawback, in this proposed prototype the sampled and collected data are instantly transmitted to smartphone (when BLE is connected) or is perceived on the display. So, the user in any case is able to monitor the data instantly and be notified on the environmental conditions. Depending on the nature of monitored parameters, the sampling rate for each is different. It is 0.2, 1 and 2 Hz for gas, physical parameters and noise respectively.

- Data loss: data are re-transmitted to the smartphone for creating a database and data loss avoidance. If data can be logged somewhere interim as long as the communication channel is resumed again or smartphone is available, then this data can also be transmitted in an appropriate time. An external memory for data logging is proposed for data protection in emergency status.

To address the issue, when the data transmission to a second party is disconnected, the data are observed on a display in real-time and at the same time are storage in an external memory and as soon as the connection is resumed these logged data are transferred as the history to the smartphone for further analysis (based on the individual decision) [179], [180].

The second concept in independent operation, refers to modular design. In modular design each part, sensor and actuators are functioning without an intersection functionality with other parts. As the proposed wearable consist of several sensors, components and actuators, it is a fact that an independent and modular design is essential.

The display and sound level are designed in the modular methodology. This provides a flexibility and selectivity to the user to remove or switch off the sound level and display modules, if required. This facility results in power saving as well. Display is located at the top of final prototype horizontally.
In addition, the display is utilized to notify the environment status in term of sound level and gas and BLE connection state, on the screen.
Although display integration on the sensor node creates several advantages, but requires a careful selection and localization. The display that is supposed to be used in this prototype must have the following characteristics:

- Low power consumption: the range of power supply does not have to exceed than 3.3 v due to the host platform power supply limitation.

- Size and weight: these factors are important in each module and sensor that is applied to the design, as the final prototype is limited in size and is wrist-worn.

- Mode of communication: as in this work, several sensors and modules are operating. The number of pins available from the microcontroller are limited to 24 (compatible with board to board connector), and each pin must be carefully used, the mode of operating is critical. Therefore, a display with possibility of I2C communication is preferred. In addition, the display must have the least complexity in hardware (number of active pins) and instead a display with the least number of pins and more sophisticated in software implementation is appropriate for the purpose of this proposed device.

- Resolution: where the display must be small and light, therefore a high resolution with clarity data observation is necessary.

❖ Data acquisition and analysis: The ultimate target of any environmental indicators is health monitoring and analysis. As far as the sampled data are not transferred to a cloud server for permanent storage, the solution is not completed. Therefore, an efficient low power data transmission channel must be established to send the data to a smartphone as a hub and from there to a cloud server. These data might be taken into consideration by a medical station for diagnosis [181], [182], [183], [17].

Where this wearable operates as a personalized ambient parameter monitoring, therefore, data collection and further analysis is necessary.

❖ Expandability: technologies and demands are continuously changing toward enriching the quality of life. Thus, in designing this proposed prototype, it is considered to keep the window of development open. The wearable has the potential of being developed in hardware/software in future development. With the tight collaboration of hardware and software implementation in the sensor node, the complexity and size of the hardware significantly reduced and consequently more space are reserved for adding sensor(s) and module(s). With the great advances in wearable sensor, microelectronics and integration technology, the next generation of components might be available shortly in close future. Therefore, it is important to implement a modular and expandable prototype so that the intended sensors, modules, features and components can be added to the structure or replaced without changing the whole solution in software/hardware.

❖ Device configuration and sensor(s)/display activation: from the application point, the proposed prototype can be widely applied in healthcare and ambient parameters monitoring. But these two areas are not the only applications, it may cover the range of smart home, smart city, agriculture, chemical and life science automations and so on. As a result, the target users of the proposed prototype are not limited. This sensor node may be worn by anyone from any working type. Each working area needs its own parameters monitoring (gas sensor). With this regard, it is designed for using by anyone in anywhere for any parameter evaluation (covered by the sensor node). To do so, the proposed prototype must be capable of configuration by the user. While there are different sensors on the prototype, but the decision is taken by the user for sensor activation. The configuration feature is implemented due to hardware limitation, power consumption, flexibility and user friendly. The two-way communication between sensor node and the smartphone, specially sending command from the smartphone, can significantly bring the prototype on the stage of monitoring of a wide range of environmental monitoring. The sensor is installed, calibrated and only is activated by the user. With a universal gas sensor driver, the software implementation makes this solution feasible. The second advantages of sensor node configuration are adjusting the sensor sampling rate according to his/her requirements. It is quite straightforward and user needs only to press the intended sampling rate of the target on the application from the smartphone.

The commands for the sensor activation from the smartphone to the sensor node are sent periodically with the fixed time interval for each. The time interval for gas and noise sensors are different. In fact, the time interval of command transmission indicates on the sensor sampling rate.

Furthermore, the logged data transmission from the external memory to the smartphone also is implemented according to the received command from the smartphone. The difference is once the command is sent from the smartphone, the procedure is continued until all logged data are sent to the smartphone.

3.3 METHODOLOGY AND APPROACH

The criteria discussed at the top are the main highlights. To achieve each goal, there are several requirements that must be considered at the same time. Depending on the criteria, a requirement(s) can be common between two/three criteria. At some point, there are more than one mutual point between more than one requirements.

Multi-parameters monitoring, device flexibility, mode of wearbility and configurability, prolonged monitoring, real-time data acquisition are all important factors in designing the wearable that one without another cannot be granted. So, these should be considered at the same time with an appropriate approach

Designing and implementation of a wrist-worn prototype with the described features and specifications requires a specific concept and approach.

For wearability, avoiding timing conflict and synchronization, secure data acquisition, efficient pin utilization and ease of use, a centralized data processing with distributed sensors is used. There sensors are utilizing different modes of interfacing (inter-integrated circuit (IIC), SPI and ADC) to the microcontroller.

For an efficient mode of wearability (wrist-worn) and user convenience, in spite of conventional wearable design the "$x - y$" plane is not extended for sensor placement. Instead "z" axis is extended from both directions for sensor utilization, feature implementation and specifications accomplishment.

In this approach, each layer is designed and devoted to a special task. Gas sensor node and notification system, each has its own layer which are linked directly (notification system) and indirectly (gas node) to the host platform layer.

Host platform includes all integrated sensors and chip antenna as well. The display and sound module are connected to the host platform through a physical layer called hardware interface. In fact, this layer does not host any sensor but only facilitate the module, sensors and layer connection and avoid the device height extension. The layers are stuck on top of each other and Multi-Layer (ML) approach is constructed.

Hardware interface plays a critical role in the proposed approach and is the heart of the hardware approach. It is a layer with capability of layer connection from two sides (top and bottom) and module and actuator connection from the pinned tail side. The hardware interface assists to utilize every space and distribute the components around the physical solution. The common pins are shared through a board to board connector. This connector also causes to build a layer on top of another in a firm way.

The bottom layer of the solution is battery holder consist of button cell battery. To make the approach firm, compact easy to handle and locate into the case in further progressing, the wire connection between battery and host platform is removed and it is pined and soldered instead.

To use this methodology some serious concerns are addressed.

The operational sensors are placed in two general groups. In addition, the monitored parameters, due to limited number of pins and space are categorized in two general protocol communications for an efficient communication:

- Integrated sensors (I2C)
- Add-on sensors (ADC)

According to this sectioning, Physical air sensors including air pressure, air humidity and air temperature, from one side and motion tracking with three gyroscope, magnetometer and accelerometer sensors on the other side, are integrated sensors and sharing I2C bus with each specified sampling rate.

In addition to these integrated sensors, display also is used in I2C communication protocol mode. Sound module measurement as an add-on sensor is using ADC. In some sensors, there are cross section for using ADC and I2C. Gas sensors are add-on sensors using both I2C (sensor initialization and configuration) and ADC (output).

3.3.1 Features and Specifications

In order to reach multi-parameters monitoring goal in an efficient form factor some features must be granted:

- Replaceability: from the design and implementation prospective, the only possibility to have the possibility of several gas parameters monitoring and yet maintain the solution compact, is to design the gas sensor node in replaceable way. The layer is readily replaced by another gas sensor node. The gas sensor node including an electrochemical gas sensor and a gas sensor driver attached together which construct a single light and small united node. Two advantages are addressed by this feature:

  - Where this proposed prototype is intended for using in wide range of applications, therefore, the user from different categories are able to use the target gas sensor according to the condition, requirements and environment.

- ➢ In spite of traditional gas sensor devices features that number(s) of predefined and fixed toxic/hazardous gases are evaluated, this capability, avoids operation of several gas sensors (in most cases is not essential) simultaneously that in consequence lead to lower power consumption and smaller, compact and lighter weighted prototype.

- Configurability: to reduce the hardware complexity for sensor activation in replaceable mode and avoid gas sensor timing conflict, the sensor(s) and display are activated/deactivated via command from the smartphone. The sensor activation is not only limited to gas sensor selection, but sound module, display and logged data feature are also control by the user. In sensor selectivity and device configuration, even no sensor may be selected if not necessary. This is discussed more in detail in next subsections and chapters.

3.4 GENERAL SYSTEM OVERVIEW

The criteria and requirements which are mentioned earlier are standing for general concepts, but what can create these factors, is a well-defined platform compatible with these features and criteria. This makes the platform flexible and adopts various number of sensors. The primary platform selection process is the most important step for a correct decision. A platform that is compatible with the already mentioned points such as: Multi-parameters, multi-tasking, light-weight, high processing, high performance, small in size, expandable (hardware/software) and standalone.

In addition to the physical hardware approach for the wearable implementation, the general structure of the system also is important. In large scale this project is structured into three tiers: sensor node (prototype), gateway and server/cloud. Sensor integration, data sampling, data acquisition, data storage (temporary), and data observation (on the display) are performed in the first island that is the concentration of this work (sensor node). The data transmission to gateway (the second island) sounds necessary due to permanent data storage, data/command communication and data observation (software implementation). As the most convenient and popular one, smartphone with Bluetooth low energy (BLE) transmission mode might be considered as the gateway in this project. In particular, in preventive medicine, the data analysis and sensor/data fusion are playing an important role in user health protection. Thus, these data are transmitted from the smartphone to a cloud/server for permanent storage (the third island). Different analysis, algorithms and predictions may be implemented in this stage. The bridge between sensor node and gateway from one side and between gateway and server from the other side, can complete the proper path for the data communication between sensor node and server as well (in other word a direction connection is established between end user and medician). The data communication between sensor node and gateway is considered as the short-range communication and utilizes BLE. BLE is the most appropriate means for the communication, as almost all smartphones are using it nowadays. The long-term data transmission between server and gateway might be accomplished by WiFi, once the smartphone is connected to internet. Therefore, a complete solution from user to server is supported to protect the data collection. In addition, a complementary information from data analysis can be provided to the individual. However, design and implementation of each island has its own concerns that only the first island design is discussed in detail in this thesis.

3.5 CONTRIBUTIONS

The main contribution of this research is to provide a scientific solution in comprehensive ambient monitoring through parameters (physical and chemical) measurement applicable in healthcare, occupational and preventive medicine. But the end effect prototype is not only limited to this application. The solution is compatible to be applied in ecosystem, agriculture evaluation, smart home and cities as well. Furthermore, this solution might be extended to the chemical laboratory environment assessment.

The device is highly intended to be considered as an individual companion. This device is implementing to fill the gap of a comprehensive environmental monitoring via a compact, multi-tasking and battery efficient wearable. The designer is willing to provide an independent and modular tool for long time individual's ambient and motion tracking monitoring. In this approach, the device in independent mode, operates as a standalone and data are monitored in real time through a display and data might be storage in an external memory and in a regular mode, data collection are transmitted through smartphone for permanent storage, the smartphone is an intermediate hub to direct the obtained data from the different sensors to a web server for additional medical analysis. To support the prototype with user convenience, mode of wear-ability, form factor (weight and size), multi-tasking, device configurability and flexibility and future extendibility are deeply investigated.

To make the device more user friendly and flexible, it is configurable through smartphone. The user may choose the sensor according to the needful.

However, to design a standalone wearable and prolonged monitoring, features of data logging, real-time data monitoring, configurability and adjustable sampling rate are considered as well.

Motion tracking data are collected to specify a complete database during daily activity of the wearer as well as fitness analysis in necessary. This can be done through data fusion in smartphone. In preventive medicine the target is to protect before corruption, thus the prototype is equipped with a user notification system in abnormal status. This notification is operating in both mode of haptic through a vibrating motor and beeper.

At the end of this dissertation, the efficiency and possibility of MULTIPLE sensors on ONE sensor node, is verified.

In large scale monitoring, the intension is to support and demonstrate the following prospective:

- MULTIPLE nodes on ONE individual,
- MULTIPLE individuals on ONE cloud system.

4 REALIZATION (Implementation of a Wrist-Worn Environmental Sensor Node)

In our proposed architecture in this research, each group of sensors is located on a separated physical layer; wiring is eliminated. Instead of the wiring, layers are located on top of each other through board to board connector.

The first step to begin with the experimental implementation, is an appropriate host platform selection. An adequate host platform is the foundation to construct the layers on top of it. The challenge is how efficiently distribute the sensors on the wearable and start the realization by building the prototype. For this reason, a platform with the capability of layers (hosting the sensors and modules) construction on top of each other is required. More efficient is to extend the solution in both side of z axis in top and bottom. Furthermore, this host platform has to also be equipped with chip antenna for data transmission.

As described in concept chapter, the sensors in the proposed approach are categorised into integrated sensors and add-on sensors. As a requirement of eligible host platform, it must include all integrated sensors to facilitate the data processing, sensor communication, weight, and size and space utilization. In this methodology the size of the final device is maintained constant in x-y plane and the prototype is extended in z axis.

4.1 LAYER AND COMPONENTS DESCRIPTION

In this section, the concept that was described in the previous chapter is verified and the Multi-Layer Multi-Sensor (MLMS) concept is verified. So that each layer, sensor selection and approach is described. Prior to this, the criteria of the main host platform as the fundamental layer of this approach is explained and discussed.

4.1.1 Eligible Host Platform Selection And Alternatives (First Step)

Host platform selection consists of two major concerns:

- Microcontroller: is the heart of platform and brain of the whole solution. Therefore, it must be capable of fast data processing by a qualified core, support the data transmission over BLE, independent firmware development, rich connectivity, compatible with different software stacks in development, data encryption for security protection (future work), numbers of pins for add on-sensor utilization. Full set of digital interfaces including SPI, I2C and UART for such prototype which includes several sensors from different categories and in various working conditions, is mandatory. Moreover, ADC with high resolution can facilitate the data conversion and calibration process for gas and noise sensors. However, nevertheless the selected microcontroller is not limited only to these specifications, but these are the least that must be accomplished. To find a microcontroller with such merits, three latest families of (at the time microcontroller and platform selection) Nordic semiconductors and Texas Instrument (TI) are the first candidates. In Table 4-1 the most important features and criteria of the microcontrollers (Nrf51, STM32 and MSP430) are listed and compared:

Table 4-1 The most qualified microcontrollers from TI and Nordic semiconductor comparison.

Microcontroller	Nrf51 [184]	STM32 [185]	MSP430 [186]
core	ARM® Cortex™-M0 32 bit processor •275 µA/MHz running from flash memory •150 µA/MHz running from RAM • Serial Wire Debug (SWD)	ARM® 32-bit Cortex®-M3 CPU Core • 72 MHz maximum frequency, 1.25 DMIPS/MHz (Dhrystone 2.1) performance at 0 wait state memory access •Single-cycle multiplication and hardware division	• 16-Bit RISC Architecture, 62.5-ns Instruction (A/D) Conversion Cycle Time • Brownout Detector – Internal Very-Low-Power Low-Frequency • Serial Onboard Programming, (LF) Oscillator No External Programming Voltage Needed, – 32-kHz Crystal Programmable Code Protection by Security
Memory	• 256 kB or 128 kB embedded flash program memory • 16 kB or 32 kB RAM	•64 or 128 Kbytes of Flash memory • 20 Kbytes of SRAM	• 256 KB of Flash memory • 256 KB of RAM
DFU OTA compatibility	On-air compatibility		
Power management	• Supply voltage range 1.8 V to 3.6 V • 4.2 µs wake-up using 16 MHz RCOSC • 0.6 µA at 3 V OFF mode • 1.2 µA at 3 V in OFF mode + 1 region RAM retention •2.6 µA at 3 V ON mode, all blocks IDLE • On-chip DC/DC buck converter	•Sleep, Stop and Standby modes •VBAT supply for RTC and backup registers	• Ultra-Low Power Consumption – Active Mode: 230 µA at 1 MHz, • Low Supply-Voltage Range: 1.8 V to 3.6 V • Five Power-Saving Modes – I 2 • Ultra-Fast Wake-Up from Standby Mode in C™ Less Than 1 µs
Analogue to digital conv.	8/9/10 bit ADC - 8 configurable channels	• 2 x 12-bit, 1 µs A/D converters (up to 16 channels) • Conversion range: 0 to 3.6 V •Dual-sample and hold capability	• 10-Bit 200-ksps Analog-to-Digital (A/D) • On-Chip Comparator for Analog Signal Compare Function or Slope Analog-to-Digital
General purpose pins	31 General Purpose I/O Pins	Up to 80 fast I/O ports	• Up to 24 Capacitive-Touch Enabled I/O Pins • Package Options – TSSOP: 20 Pin, 28 Pin – PDIP: 20 Pin – QFN: 32 Pin
Counter	•One 32 bit and two 16 bit timers with counter mode •Real Timer Counter (RTC)	7 timers • Three 16-bit timers, each with up to 4 IC/OC/PWM or pulse counter and quadrature (incremental) encoder input •16-bit, motor control PWM timer with dead time generation and emergency stop •2 watchdog timers (Independent and Window) •SysTick timer 24-bit down counter	• Two 16-Bit Timer A With Three • On-Chip Emulation Logic With Spy-Bi-Wire Capture/Compare Registers Interface • External Digital Clock Source Fuse • Basic Clock Module Configurations Converter With Internal Reference, Sample- – Internal Frequencies up to 16 MHz With and-Hold, and Auto scan Four Calibrated Frequency
Digital interface	SPI Master/Slave • Two-wire Master (I2C compatible) • UART (CTS/RTS)	•7 channel DMA controller •Peripherals supported: timers, •ADC, SPIs, I 2Cs and USARTs	• Universal Serial Communication Interface (USCI) 2.2 V •Enhanced UART Supporting
Security	AES HW encryption		

The microcontroller comparison is a part of platform selection. As it is seen, these three microcontrollers' families are similar in features and specifications, but without careful study and investigation of the main platform, the selection is not possible. Therefore, to complete the process, the most applicable platforms which have the criteria of a main platform in this solution are compared and studied.

- Host platform: host platform selection even can be more important than microcontroller. The solution, architecture, hardware development, add on-sensors, and general structure must be compatible with the host platform. In addition, where the prototype is consisting of several physical layers stuck on top of each other, the accessibility to the hardware for programming especially during development might be quite difficult, thus Over-The-Air (OTA) Device Firmware Upgrade (DFU) sounds necessary. Physical air parameters (air temperature, humidity and pressure) and motion tracking sensors, have been developed greatly with advances in technology of semiconductor, and size of these sensors are shrinking dramatically. As a result, the best performance is achieved when a platform with already integrated sensors is utilized.

The infrastructure of the solution must be defined as a well-suited platform to handle the architecture. In addition, as the fundamental requirement, this host platform must be capable of physical extension. The next point in the target wearable is to eliminate all wires between any components and sensors to host platform. Instead each two layers are linked through board to board connector (distributed sensors). This led to a firm solution and sharing a pin easily between all layers. Therefore, the host platform must be equipped with board to board connector. A platform that has been designed for a low power wireless solution. Hereafter the most qualified platforms based on the discussed microcontroller are compared. Dimension, form factor, expansion, compatibility with the whole solution, flexibility, power consumption and efficient data communication are the factors which are considered for platform selection.

Table 4-2 Potential platforms comparison.

Platform	WEMS [122]	Nrf51822 Beacon [187]	Adafruit WICED WiFi Feather [188]	STM32F103VET6 Development board [189]	iProtoxi BTL3H3 [189]
Dimension (mm)	75 x55	20	51 x 23 x 8	61	32
Integrated sensors	Accelerometer, Temperature, Humidity, UV, gas sensors	No	No	No	Accelerometer, magnetometer, gyroscope, Humidity, temperature, air pressure,
External memory	Yes	No	No	No	Yes
Data transmission mode	BLE	BLE	WiFi	BLE	BLE
Solution compatibility	Yes	Yes	Yes	Yes	Yes
Display	Yes	No	No	Yes	No
Power consumption	High	Ultra-low	High	High	Ultra-low
Voltage supply (v)	5	3	3.3	3.3-5	2.7-3.3

4.1.1.1 Discussion On The Platform Selection And The Alternatives

From the beginning it was expected that no platform can fully satisfied the requirements. But it would be the best to gain the most from the selected platform and not start from the scratch. So that a platform with an adequate dimension and integrated sensors which is capable of hardware expansion is a suitable candidate. An overview from the concept chapter, requirements and expected proposed prototype, drive the designer smoothly toward a multi-layer physical approach. The reason is to fulfil the form factor that is supposed to be wrist-worn. Therefore, all candidate platforms above are potentially expandable in height and flexible is structure and hardware design.

Two platforms (Nrf51822 beacon and iProtoxi BTL3H3) are based on Nrf51822 and two are developed depending on STM32 (Adafruit WICED WiFi Feather, STM32F103VET6 development board) and the last platform is utilizing MSP430 microcontroller (WEMS).

Fig. 4-1 Modular, compact and light weight Nrf51822 beacon [186].

All these platforms satisfy the instructions processing and can be developed in both hardware and software. According to this point Nrf51822 beacon is excluded where no integrated sensor/display/external memory is demonstrated on the board. Nevertheless, still as a hardware extension solution may be considered.

Adafruit WICED WiFi Feather is a qualified platform in terms of dimension and hardware extension. However, it is suffering from the lack of integrated sensors and also high power consumption. This platform is using WiFi in data transmission mode that dissipate a lot of energy. Where a personalized ambient monitoring device must work in prolonged mode and sampled data must be protected, unavailability of Internet can cause a problem in data transmission. In addition, where the prototype is going to be considered as a companion and in short range of communication usage to the smartphone, BLE is sufficient.

Fig. 4-2 Adafruit WICED WIFI Feather [187].

An investigation on STM32F103VET6 development board shows that it is a high power consumption board due to touch screen display. This board is using BLE for data transmission that is quite common and popular nowadays. This development board does not support DFU-OTA programming mode. The common point of the recent two platforms is pin to pin connection for hardware expansion. If these platforms are supposed to be extended in hardware, the new developed physical layer should be attached to the platform through pin to pin connector. Regarding the available pin connector and the considered pins of platform, this might extend the height of solution dramatically.

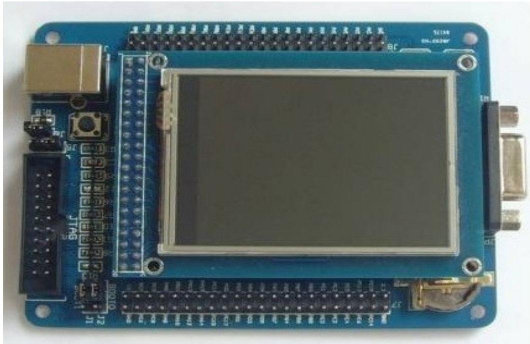

Fig. 4-3 STM32F103VET6 Development board [188].

The last two remaining platforms are good candidates for selection in the proposed prototype. A careful comparison is required to conclude the advantages and disadvantages of each. WEMS is features with different categories of sensors which might be potentially a perfect selection. The physical air ambient sensors (humidity, temperature and UV index) are supporting the platform. In addition motion tracking is less and more provided with integrated accelerometer sensor. External memory and display support the independent operation mode fully. The feature and specifications of this platform are not only restricted to what was mentioned.

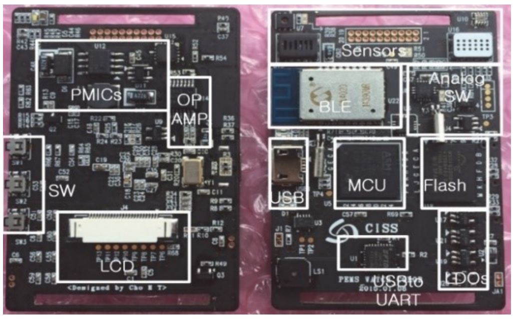

Fig. 4-4 WEMS (top and bottom side) [122].

A double channel metal-oxide gas sensor is utilized on the board as well. The data transmission is performed in BLE mode too. All these advantages are quite tempting for this hardware selection. Before final decision, a careful study of features and characteristics are demonstrated.

As one of the major concentration of the proposed prototype in concept chapter, form factor is extremely influencing the final decision. The square shape of this platform although bring it on the stage for a tight competition but relatively large scale make it more suitable for waist-worn mode rather than wrist-worn.

The second point is power consumption which due to a very high consuming display make it inadequate. In fact, if this platform is chosen as the main platform, the power consumption, adjusting sampling rate of each sensor and prolonged monitoring would be a bottleneck.

The next remarkable issue is the hardware expansion. A limited number of pins on the board can restrict the functionalities of the system. Number of add on-sensors in this design can dramatically increase in the future work. Furthermore, adding physical layer on top of the platform can cause the same problem as previous ones.

Predefined, fixed and metal-oxide gas sensors are the next issue. The used double channel gas sensor is from the metal-oxide technology which needs a long time warming up and high power consumption. A calibration and re-calibration process requires more effort and frequent verification.

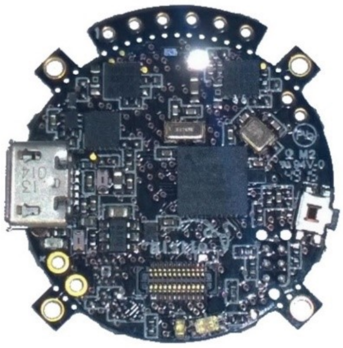

Fig. 4-5 The final candidate of the prototype, iProtoxi- BTL3H3 [189].

In the following the last candidate platform is closely investigated in features, specification and possible scenarios.

Aistin blue platform is based on Nordic nrf51822 microcontroller and is designed by iProtoxi company (iProtoXi Oy, Teknologiantie 18, 90590 Oulu, Finland). The platform is equipped with chip antenna and capable of hardware extension and add on-sensors. There are two integrated board to board connectors on the platform which make it capable of expansion from both sides in height.

The platform is including the sensors for detecting 3D-acceleration, 3D-magnetism, 3D-rotation which provide a 9 DoF for a precise motion tracking on one side, and humidity, air pressure and temperature on the other side (integrated sensors).

In this host platform, the sensors are distributed in both sides. The host platform is equipped with the chip antenna and support the BLE data transmission (Fig. 4.6) [190].

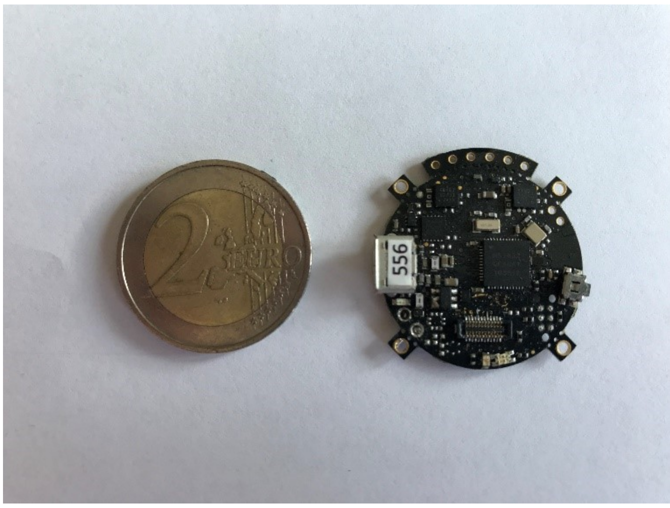

Fig. 4-6 Host platform selection in first step.

Furthermore, the host platform is enriched with an integrated external memory. This external memory can be well suited within the entire architecture to operate in standalone mode. Low power consumption, BLE data transmission mode, an ideal dimension and weight along with easy hardware expansion for the future work, provide the most essential requirements and can gain the most from the host platform.

Therefore:

BTL3H3 from the iProtoxi as a small and rounded platform with the diameter of only 32 mm and thickness of 4.2 mm is considered as the host platform.

BTL3H3 top and bottom sides with the component's placement is depicted and described in detail in Fig.4-7 and Fig.4-8. The integrated sensors and external memory also are referenced in Table 4-3 and Table 4-4.

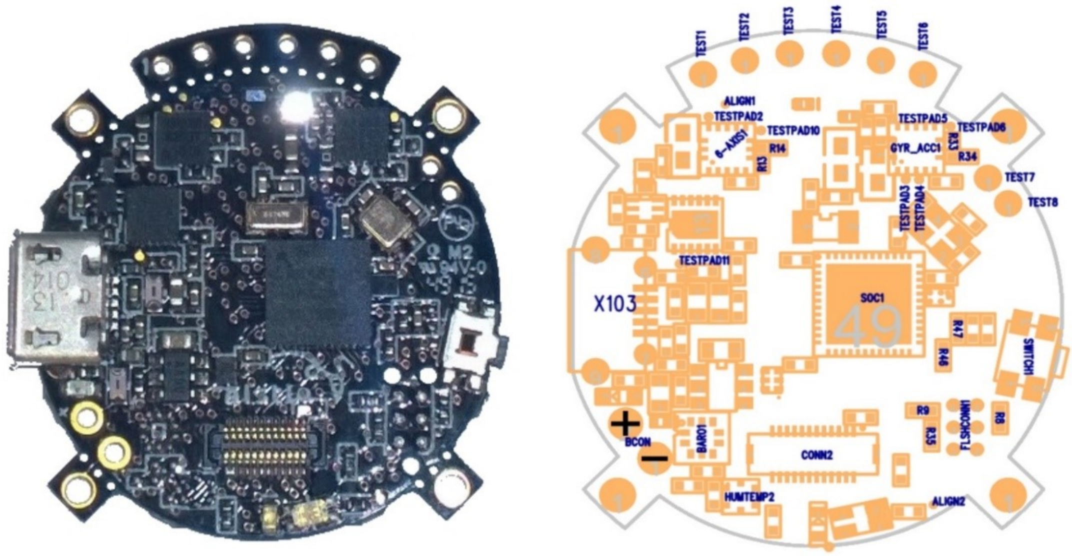

Fig. 4-7 The host platform top side, Left: BTL3H3 image, Right: the top side components placement [191].

Table 4-3 Top side component references.

Reference	Component
6-AXIS1	KMX62-1031
GYR_ACC1	KXG03
BARO1	not assembled
HUMTEMP2	not assembled
CONN2	Aistin 2 connector
X103	USB connector
BCON	Battery connector(B2B-PH-K-S(LF)(SN))(Optional)

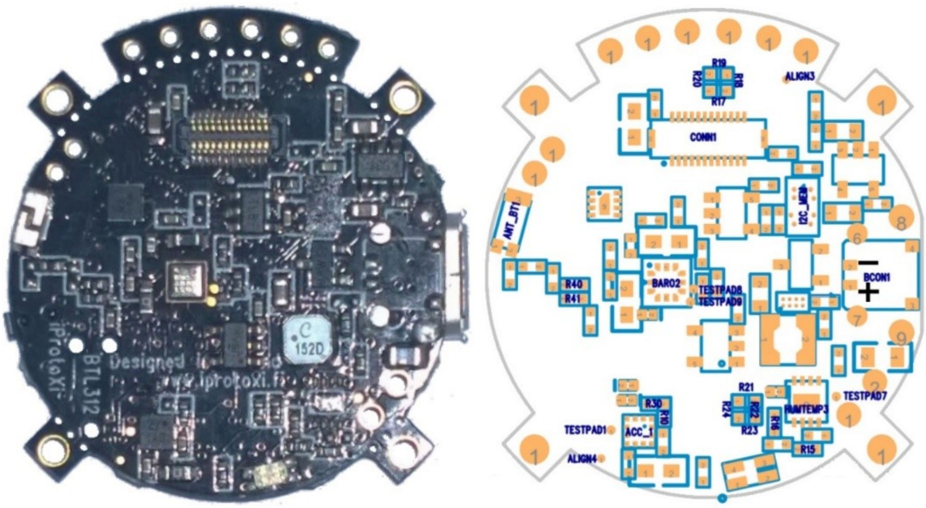

Fig. 4-8 The host platform bottom side, Left: BTL3H3 image, Right: the bottom side components placement [191].

Table 4-4 Bottom side component references.

Reference	Component
CONN1	Aistin 1 connector
I2C_MEM	M24M02-DRCS6TP/K
BARO2	BM1383(A)GLV
ACC1	KX122-1037
HUMTEMP3	SHT31-DIS-B
BCON1	Battery connector (BM02B-ACHSS-GAN-ETF)(Optional)

4.1.1.2 BTL3H3 Technical Consideration Regarding Antenna And Motion Trackers Sensors

As this host platform is used to be used with other electronics layers, care must be taken to keep BT2.4GHz antenna and the KMX62-1031 accelerometer/magnetometer uncovered by metal sheets or wiring. Metal covering will affect the performance of these parts significantly. Using plastic enclosure is recommended. For best performance, assembly screws should be non-magnetic material (nylon / beryllium-copper alloy / bronze-aluminum alloy) (see Fig. 4-9).

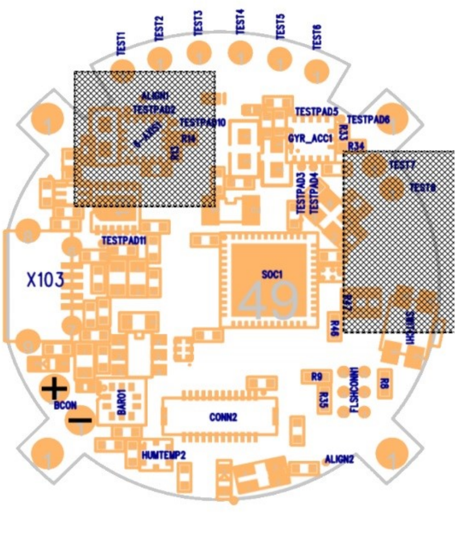

Fig. 4-9 Accelerometer and antenna area should not be covered by metal material [190].

To avoid physical interference with the USB and also fit the designed layer with the BTL3H3 (hardware aspect) in size, the host platform is applied in the status of USB down and antenna top. Thus, the gas sensor node is located at the top layer (connected to bottom side of BTL3H3) and the notification system driver that is much smaller in size, is located at the bottom of the solution (connected to the top of BTL3H3).

4.1.2 Gas Sensor Node

Toxic and hazardous gas measurement is one of the main parts in this research. It is not desired to restrict the indicators evaluation rather, it is intended to provide a solution for a wide range of gas measurement. Gas sensor must be exposed to the target gas freely. In this architecture, a layer including target gas sensor and gas sensor driver is constructed and is called gas sensor node. This layer consists of the gas sensor and gas sensor driver board and is located at the top of the proposed wearable device to be exposed in the target gas.

To address the multi-tasking and sensor selectivity of the device, gas sensor layer is designed in replaceable mode. Each gas sensor node is replaced with another target gas readily by the user. By using this feature, the user may decide where and when, which gas sensor is located and comes on operation. Care must be taken to design a versatile sensor driver to be compatible with different gas sensors. This requires the driver flexibility and configurability.

A gas sensor driver board is designed to include all external components such as external resistor gain adjustment, external filter and enable pin for output signal conversion and run the gas sensor as well. A configurable, low power consumption and flexible analogue front-end amplifier (EFA) is required to be compatible with reducing and oxidizing gases with different bias, zero internal and gain adjustment configurations. This feature addresses a versatile device in wide range of applications.

4.1.2.1 Gas Sensor Selection

To design a gas sensor layer, compatible with the final prototype, the gas sensor node in terms of size and sensor performance must be optimized.
The gas sensor layer (gas sensor node) includes two individual layers:

- Gas sensor,
- Gas sensor driver board.

When gas sensor driver board is designed and implemented, the gas sensor is attached on top of it and form the gas sensor node.
To create a gas sensor node, the first step is to select an appropriate gas sensor family which is fit within the design. Features and specifications of the sensor are playing very important role in final device performance and efficiency. The most critical factors in gas sensor selection were already listed in the concept chapter extracted from [169], [170], [171], [172], [173], [174].

In the introduction chapter different gas sensors, implemented with various technologies and the most recent wearable devices were mentioned. To design a gas sensor node, the most effective criteria, features and specifications of the most well-known gas detectors are summarized and compared in details in Table 4-5.
A wide and comprehensive feature comparison of the most popular gas sensors, in terms of critical factors such as power consumption, size, mode of operation, response time, calibration

and recalibration process bring the conclusion that, the most adequate sensor which is adopted within the final design is Spec [192].

It provides a good response time (<15 s), and high resolution (this feature is a function of the type of gas sensor). This manufacturer also has NO_2, CO, SO_2, H_2S and O_3 which are similar in size and operation but need their own configurations and calibrations. This sensor requires the least external components with very low power consumption (approximately 10^{-6}W) and is an electrochemical sensor which the operation is based on real gas measurement. Each sensor requires different configuration and calibration process, this issue is addressed in the gas sensor layer design. It is mentionable that, sensors from Cambridge Company were good candidate for this architecture but, were not available at the time of design for the next 1 year. Although this company has very limited products for different hazardous gases that might restrict its usability due to different hardware requirements as well.

Table 4-5 Features and specifications of the most qualified sensors from different families.

Features	Spec	Figaro (Rounded)	SGX	Cambridge CMOS	PyreOS (Rounded)
Size(mm)	15×15×3	14.7×49.8	5×7×1.55	2.7×4.0×0.6	20×20
Weight (g)	1-2	12	NA	NA	NA
Power consumption (mW)	0.01	38	30-81	<1.2	NA
Operation mode (V/A)	A	V	V	V	V
Output signal	A	A	A	D	A
Output ext. comp.	yes	yes	yes	no	yes
Products	CO, NO_2 SO_2, H2s, O_3	CO, NH_3,CH_4,CH_6,O_2	CO, NO_2,	IAQ	CO_2,CO, SO_2,NO
Channel	1	2	1,2,3	1	1,2,4
Technology	Elec. Ch.	Elec. Ch.	(MEMS)	(CMOS)	Wave length IR
Package	SMD	Pins	SMD	SMD	TO
Response time (sec)	< 15	15	Dependent on gas concentration	on condition	Dependent on gas concentration
Wear ability	yes	On cond.	yes	yes	on cond.
Reusability	yes	no	perhaps	perhaps	no

4.1.3 Notification System

To avoid user exposure of long time in risky status, a notification system is implemented to operate if necessary. This system is designed for various situations and workplaces. A vibrating motor located at the bottom of the final prototype which touches the user's wrist and a beeper are the means of notification system in addition to notification system's driver. The vibrating motor as the haptic mean may help to notify the individuals who are on operational and noisy environments where the beeper does not attract the attention. These beeper and vibration motor are connected to the notification board driver which is located at the bottom of the host platform (Fig. 4-10- right). The notification driver as the main part of notification system is linked to the host platform directly through board to board connector.

So far, a wearable with three physical layers has been described. As shown in Fig. 4-10, a visualized system with two layers at the top and bottom of host platform is depicted.

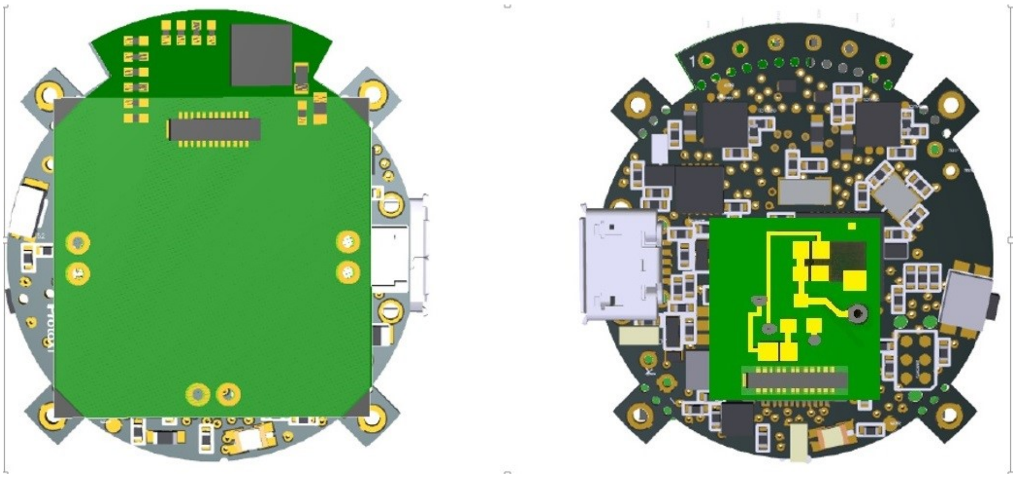

Fig. 4-10 Left- gas sensor layer with external components at the top, right-notification driver board at the bottom.

4.1.3.1 Vibrating Motor Selection

Previously was discussed what are the criteria and merits for the selection of a vibrating motor. Here three vibrating motors that can be adopted within the solution are compared in different features and the final decision is taken according to Table 4-6.

The number of miniature size vibrating motor are summarized and compared as:

Table 4-6 Comparison of features and criteria for three small-size vibrating motor.

Name and brand (model)	QX MOTOR	Pololu	Pololu shaftless
Form factor	Encapsulated/Enclosed	Encapsulated/Enclosed	Button shape
Current consumption(mA)	65	Less than 60	60 mA (80 mA max)
Dimension	6×10mm	11.6×4.6mm	10x3.4mm
Voltage supply	3v	2.4-3.5v	2.5-3.5v

This tiny DC motor (Pololu) is used in the final design. It produces vibrations by spinning an eccentric shaft at over 10,000 RPM when powered at 3 V. Motors like this are commonly found in cell phones and other devices that use vibration for tactile feedback. Its small size (11.6 × 4.6 × 4.8 mm) and light weight (0.8 g) make it easy to integrate into the system with tight space constraints. The motor is encased in a removable rubber sleeve that gives it flat surfaces for mounting and prevents it from chattering against whatever it is mounted to. This vibrating motor is used in 3.3 V (2.4 V to 3.5 V recommended) in the proposed wrist-worn prototype. The polarity is not important (the motor can run Clockwise (CW) or Counter Clockwise (CCW)).

4.1.3.2 Beeper Selection

A sound generator (buzzer/beeper) is the initial mean of the notification system. It is quite suitable for office working users and also non-operational environments. However the only beeper does not work out in all environments and situations and needs a complementary mean (vibrating motor). In addition, to cover all groups of people including disables (people with hearing disability) the vibrating motor sounds essential.

The beeper selection as same with the vibration motor step, requires some criteria that should be considered.

In spite of vibrating motor, the beeper does not consume much power. The majority of efforts on finding an appropriate beeper is concentrated on size, generated torque and positioning. Low voltage supply (2.8-3.3 V) is the parameter that severely strict the number of potential beeper. A 3 V mini passive electric buzzer is used in the target prototype. By selection of vibrating motor and beeper the notification system is completed.

4.1.4 Hardware Interface And Linked Components

To avoid expansion of the size of prototype, and design a modular and flexible wrist-worn, a layer called hardware interface is considered. This physical layer does not include any integrated sensor but plays the role of an intermediate linker. This flex is physically designed similar to the gas sensor driver and consist of two male and female board to board connectors at the top and bottom and is located between gas sensor layer and host platform to connect these two layers. Furthermore, the hardware flex interface includes a thin and long tail connector which reserves number of pins for sensors or module usage (see Fig. 4-11). During the development process the hardware interface has been improved in dimension, form and numbers of implemented and reserved pins as: “ready to use”. The first version as also is seen in Fig. 4-5 in yellow color was designed in larger size. The sound module and display were soldered through the wire to the hardware interface.
In the latest version, the hardware interface is more compact, all wires are removed and display is located and connected through pin. The expandability of the solution in term of add on-sensor/module has been significantly improved. In addition to final size of prototype, the usability of the solution also is improved (Fig. 4-12, Fig. 4-13).

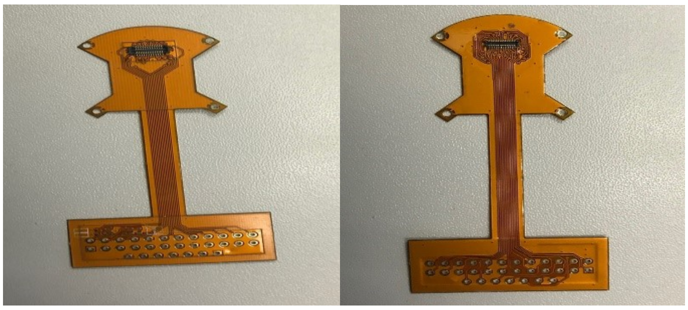

Fig. 4-11 First version of hardware interface, bottom and top layer.

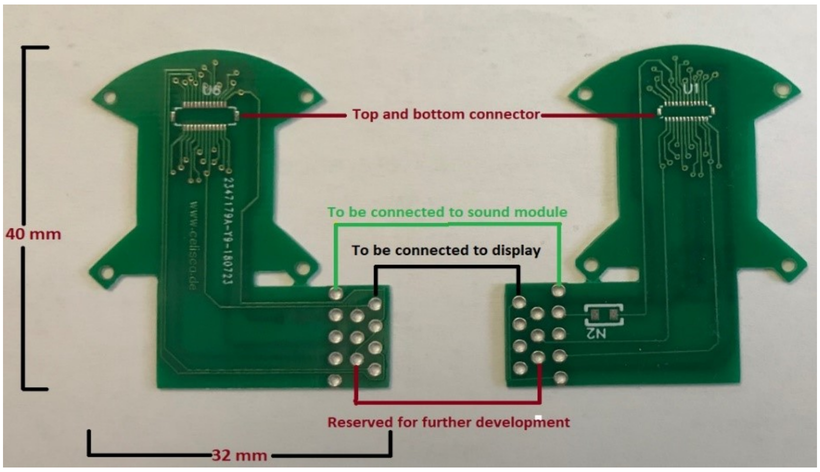

Fig. 4-12 Developed prototype version of hardware interface.

In the second version of hardware interface, in addition to smaller size, the reserved pins for further development also has been assigned (e.g. UV index). The solution does not need wiring and even in some versions due to firm and compact shape, as the example used for fixed station, the housing (covering box) is not required.

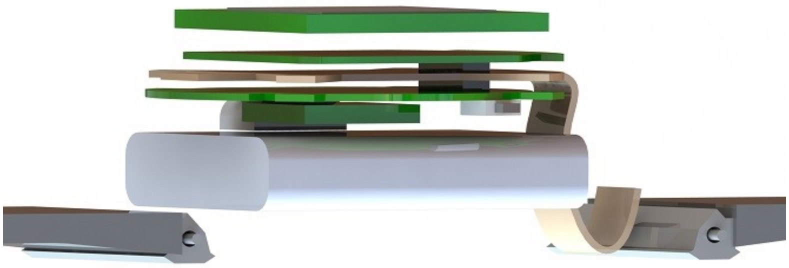
Fig. 4-13 Hardware visualized design of multi-layer approach.

4.1.4.1 Sound Level Module

A three pin sound level module is connected to the tail of flex interface to communicate to the host platform. The module must be modified in hardware to be adopted within the design and is located at the body of the final prototype vertically.
Criteria of sound module’s selection features, and specifications are discussed, summarized and compared in the following Table 4-7 shortly but hardware, software implementation, data conversion, calibration and evaluation are discussed in a separate chapter in detail.

Table 4-7 Features and specifications of sound module candidates for the final application.

Sound module	[[193] 	[194] 	[195] 	[196] 	[197] 
Voltage supply(v)	5	3.3-5	5	4-6	2.5-5.5
Length	Not fitted	Not fitted	Not fitted	Not fitted	Fitted
Width	Fitted	Fitted	Fitted	Fitted	fitted
Thickness	Not fitted	Not fitted	Not fitted	Fitted	Not fitted
Output signal	Fair	Good	Good	Good	Good
Adjustable gain	Yes	Yes	Yes	Yes	Yes

"Analog sound sensor V2 (SKU: DFR0034)" is the candidate for the sound level measurement in the final prototype [198]. Small size, low price, accuracy, good output signal quality, appropriate gain, straightforward tuning, analogous and working in wide range of voltage supply (3 to 5 V) are the features and specifications that satisfy the necessities to apply this module in final design (see Fig. 4-14).
The microphone type of module is Electret condenser which is producing very low level voltage in a few mili-volts, therefore amplification is mandatory [199], [200].

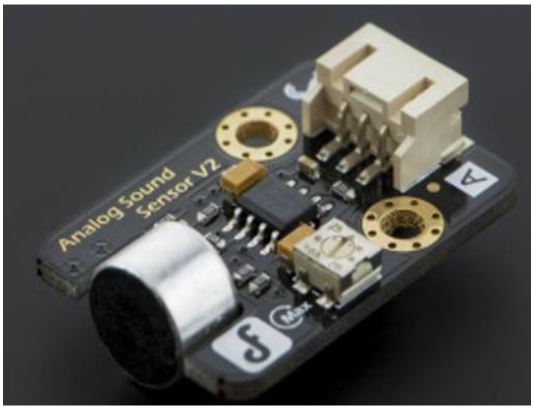

Fig. 4-14 Sound module in prototype design (Analog sound sensor V2)[189].

4.1.4.2 Display

Display is an important feature in standalone operation of the solution. Communication mode with the microcontroller (due to numbers of sensors on operation and avoid operational conflict), power consumption, cost, quality of graphic and scale of the display are the most important concerns in display selection.

Apart from the display selection, its localization and adoption in the solution also is important. From one side the display should be quite visible to the user (top side) and from the other side, gas sensor should be located at the top due to readily exposure of target gas. So that the display link to the hardware interface and also stands side by side of the gas sensor.

An Organic Light-Emitting Diode (OLED) display with the size of 0.91 inches and resolution of 32×128 pixels is used in the final prototype [201]. The display is operating in I2C mode with the dedicated address which bring the possibility of using along with other I2C working sensors with different addresses. The integrated chip on the OLED display for utilization is SS1306 [202] (see Fig. 4-10). The rest of potential display candidates are compared with the respected features and specification in Table 4-8.

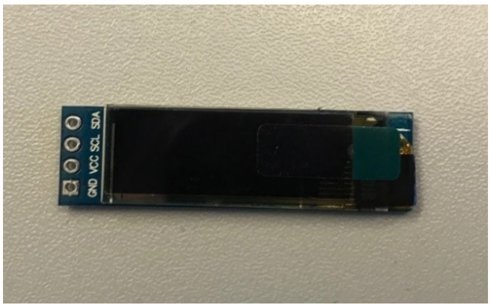

Fig. 4-15 Selected display for the prototype.

The number of displays are studied and compared in the Table 4-8.

Table 4-8 The specifications and features of most five appropriate displays are compared.

Brand (model)	Description	Active Area(mm)	Display Colors	Signal Interface	Input Volt.(v)	Used pins
Sharp(LS012B7 DH02)	CG-Silicon,1.2 inch, 240×240	30.48×30.48	Monochrome (1-bit)	SPI	3	10
Wisechip (UG-6448HLBEG03)	PM-OLED,0.66 inch, 64×48	13.42×10.06	Mono(Blue) (1-bit)	SPI, I^2C	2.8/7.25	28
Wisechip (UG-9616TSWCG02)	PM-OLED,0.69 inch, 96×16	17.26×3.18	Mono(White) (1-bit)	I^2C ,	2.8/7.25V	14
Truly (OEL9M0068-W-E)	PM-OLED,0.91 inch, 128×32	22.38×5.58	Mono(White) (1-bit)	SPI, I^2C	-	15
LG (LH154Q01-TD01)	a-Si TFT-LCD,1.54 inch, 240×240	27.72×27.72	262K (6-bit) , CIE1931 50%	MIPI(1data lane)	3.3/1.8	12
Univision (UG-2832HSWEG04)	PM-OLED,0.91 inch, 128×32	22.384×5.584	Mono(White) (1-bit)	4-wire SPI	2.8/7.25	15
OLiGHTEK (SVGA060SC)	AM-OLED,0.60 inch, 800×600	12.06×9.06	16.7M (8-bit)	Dependent	1.8/5.0/-1.5	Depend.

4.2 PROTOTYPE DESIGN IN TWO VERSIONS

The final prototype is designed in two versions. Although both of these versions in functionalities, gas sensor node design, display, notification system and configuration are the same, they differ in the bottom layer.

In the first version in Fig. 4-16 number of layers on top of each other is shown. The hardware interface tail is at the right side of the picture. In this version the utilized battery is Li-ion that is connected to the main host platform through wire. This battery is smaller in size and capacity (250 mAh).

In Fig. 4-16 a proper prototype of the final device is depicted. In this figure all sensors, modules, layers and components are shown.

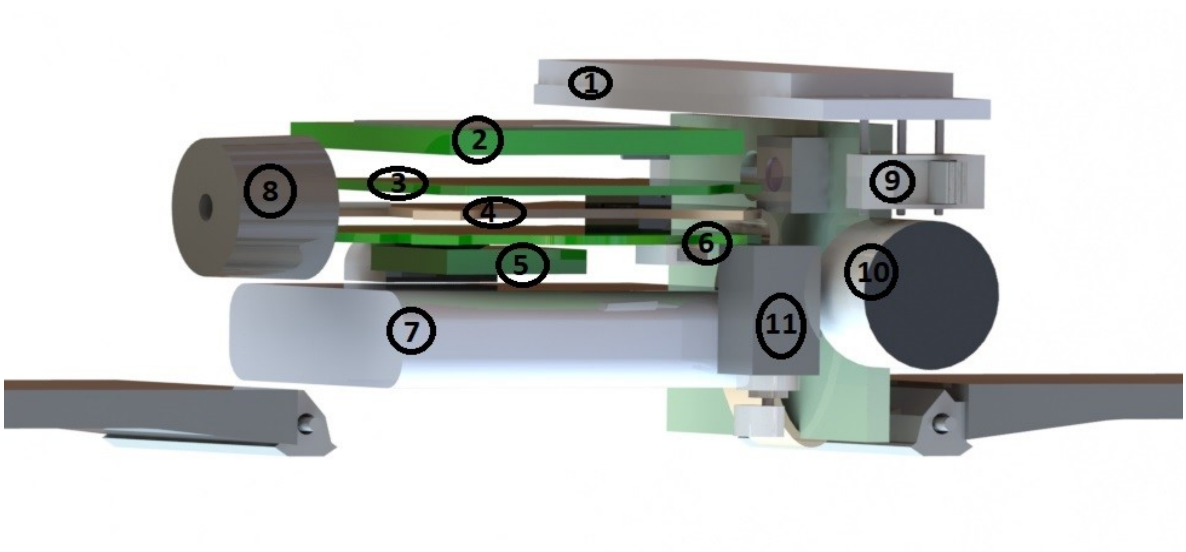

Fig. 4-16 Multi-Layer Multi-Sensor visualized (MLMS) approach (V1). 1: display, 2: gas sensor, 3: gas sensor driver, 4: hardware interface, 5: notification driver, 6: host platform, 7: battery, 8: beeper, 9: sliding switch, 10: microphone, 11: vibrating motor.

In the second version (see Fig. 4-17) the Li-ion battery is replaced with a coin cell battery which is larger in size and capacity (300 mAh). Where the coin cell battery does not have wire for connection, therefore an additional layer is designed to hold the battery and also connect it through the pin to the host platform.

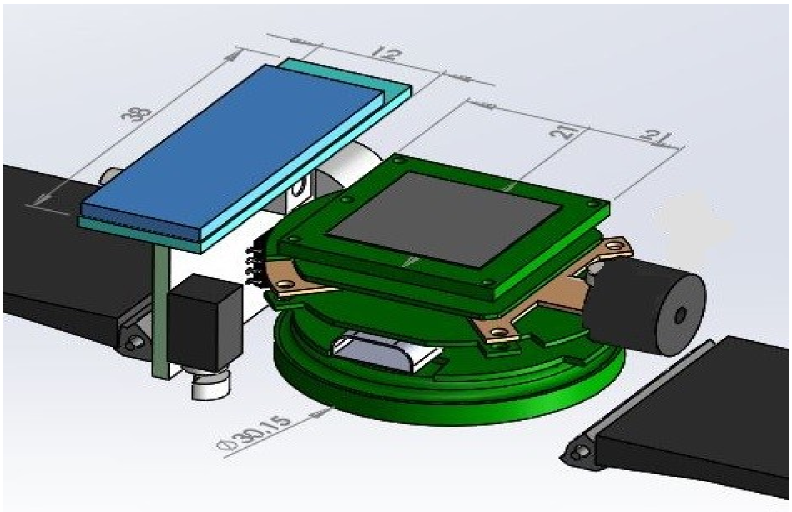

Fig. 4-17 Multi-Layer Multi-Sensor visualized (MLMS) approach with coin cell battery (V2).

4.2.1 Battery Holder And Button Cell Battery

For a prolonged data monitoring, a battery with higher capacity is required. The target battery is button cell. To remove the wire connection due to compact, firm and easy handling of the wearable, the battery holder is considered and is soldered via pins to the host platform. The battery holder is located at the bottom of the solution. A 300 mAh Li-ion capacity battery supplies the device.

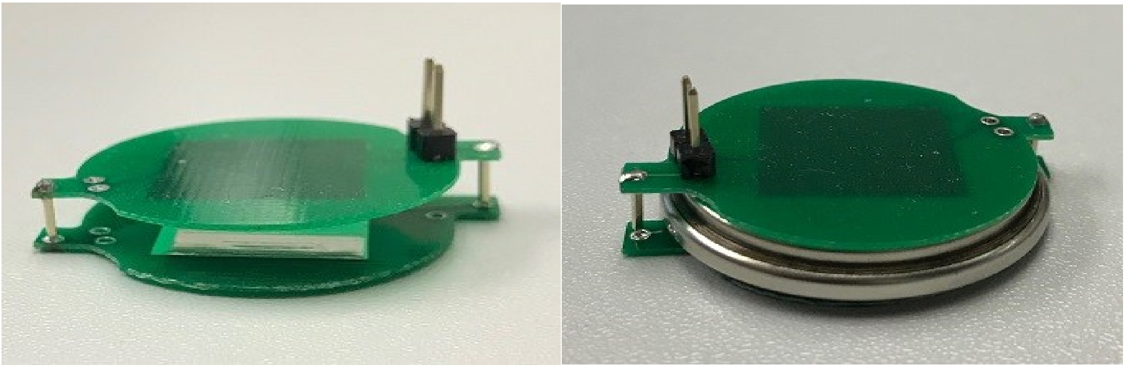

Fig. 4-18The design of battery holder in two layer(left) and layers including the battery (right).

4.3 CIRCUIT DESIGN AND LAYERS

The proposed solution consists of 5 physical layers. Two of these physical layers (gas sensor node includes gas sensor and gas sensor driver and battery holder layer is constructed of battery holder and coin cell) are including two parts. In addition, display and sound module are linked to the host platform through hardware flex interface.

In Fig. 4-19, host platform is considered as the layer 3. The gas sensor (1) and gas sensor driver (2) are soldered to form the gas sensor node. This layer is connected to host platform via hardware flex interface. The electronics circuit design of the gas sensor driver is depicted. Notification system driver (5) is directly linked to host platform (circuit design also with beeper and vibrating motor are included). Display (4A) and sound module (4B) and antenna also are mentioned. The customized pin number and name according to bus 24 protocol are specified in the figure.

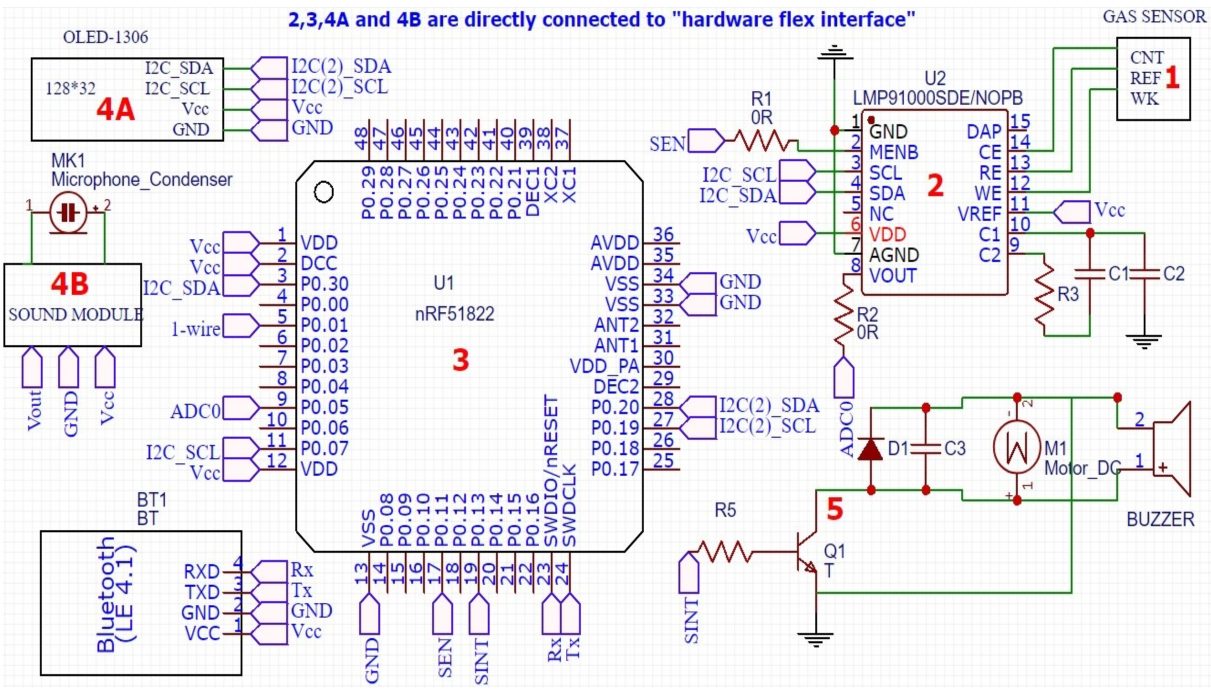

Fig. 4-19 Electronics circuit design and components of the proposed wearable for the gas sensor node, notification system and sound module. No. (4A), (4B), (3) and (1,2) are directly linked to hardware flex. No. (5) is connected to host platform (3).

By now, physical approach, layers, components and features have been introduced and a visualized version of the final prototype were presented. In Fig. 4-20 and Fig. 4-21 a completed visualization of the final prototype including the coin cell battery are presented. In these pictures all detail which will be considered in implementation including the box and 3D housing are shown. It is expected that a good understating of the solution, features specifications, components and sensors description approach and methodology have been presented so far. The implemented prototype in next chapters is the same with what is provided in these pictures. It must be mentioned that in the next chapters, circuit design of gas sensor driver, gas sensor calibration, sound sensor calibration, data validation and experimental prototype tests are discussed in much more detail.

Fig. 4-20 Graphic design of device in solid work, layers, components and case. (1):top part of 3D housing, (2):gas sensor, (3):display, (4):gas sensor driver, (5):sound module, (6):screw of 3D housing, (7):hardware flex interface, (8):host platform and charging USB, (9):on/off button of 3D housing to the host platform, (10):vibrating motor, (11):screw of 3D housing, (12):battery holder, (13): coin cell battery, (14):bottom part of 3D housing to cover the battery, (15):the main part of 3D housing to hold the prototype, (16): bracelet.

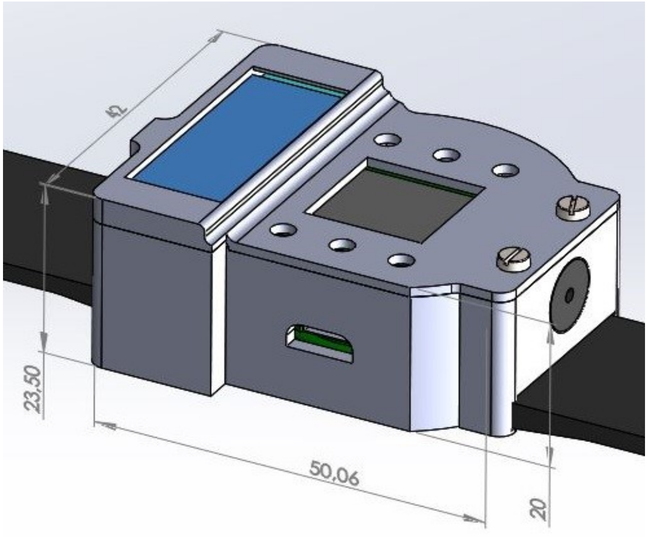

Fig. 4-21 The final design of prototype with covering box.

4.4 PROPOSED STRUCTURE

The framework is based on two main facts: multi-sensor system and multi-layer add on-board sensors which is the innovative part. In particular, a client-server pattern is adopted, and smartphone is acting as an intermediate hub (gateway) to communicate between client and server. The wrist-worn device is considered as a client and remotely communicates with a smartphone through BLE. In this two-way communication data are sent from the client (wrist-worn) to smartphone as the intermediate hub in short-range communication and from smartphone to cloud server in a long-term communication. But the return way data communication from the smartphone to the wearable device is operated when required only. As an example, when the data are sent from the smartphone to a server, stored and thus are analyzed by a medical doctor. An appropriate decision is made according to obtained data from the device, now it’s time to command necessary recommendations to the applicant by his/her wearable device or some other defined algorithms before. Server is where the logic of this architecture is implemented. The communication way from the smartphone to the sensor node is established when user intends to activate/deactivate a sensor, display or even when it is required to adjust (increase/decrease) the sampling rate of sensors. The data packets for gas sensor, and noise are separated and are sent to the smartphone in 2 and 0.2 Hz respectively. The time interval for motion tracking sensors is 20 ms and this is 1 s for physical parameters including air pressure, humidity and temperature. The temperature, humidity and air pressure are integrated into one packet due to data transmission efficiency. The data are stored in the smartphone and can be utilized in csv format. The general architecture and overview of sensor node that include sensors and data sequence in different modes (BLE connected/disconnected) are discussed as a part of careful data protection in this system.

The general strategy of this architecture is shown in Fig. 4-22. It indicates the prototype operation in standalone (BLE disconnected) and configurable mode (BLE connected). Each of these operational modes has its own configuration.

In standalone mode, the prototype works in fixed predefined sampling rate and is not adjustable from the smartphone. Display and NO_2 gas sensor be default are activated. In addition sound module detector also operates at when the prototype is switched on.

The major differences in configurable mode is sensor activation and sensor sampling adjustment from the smartphone. In fact in this mode, the user has the chance to select which gas sensor is operating. Furthermore, he/she can decide display and sound detector are required to operate or not. This feature can significantly improve the prolonged monitoring. Power consumption of each sensor, module, display and all other parts are discussed and calculated in power consumption chapter (see Fig. 4-22).

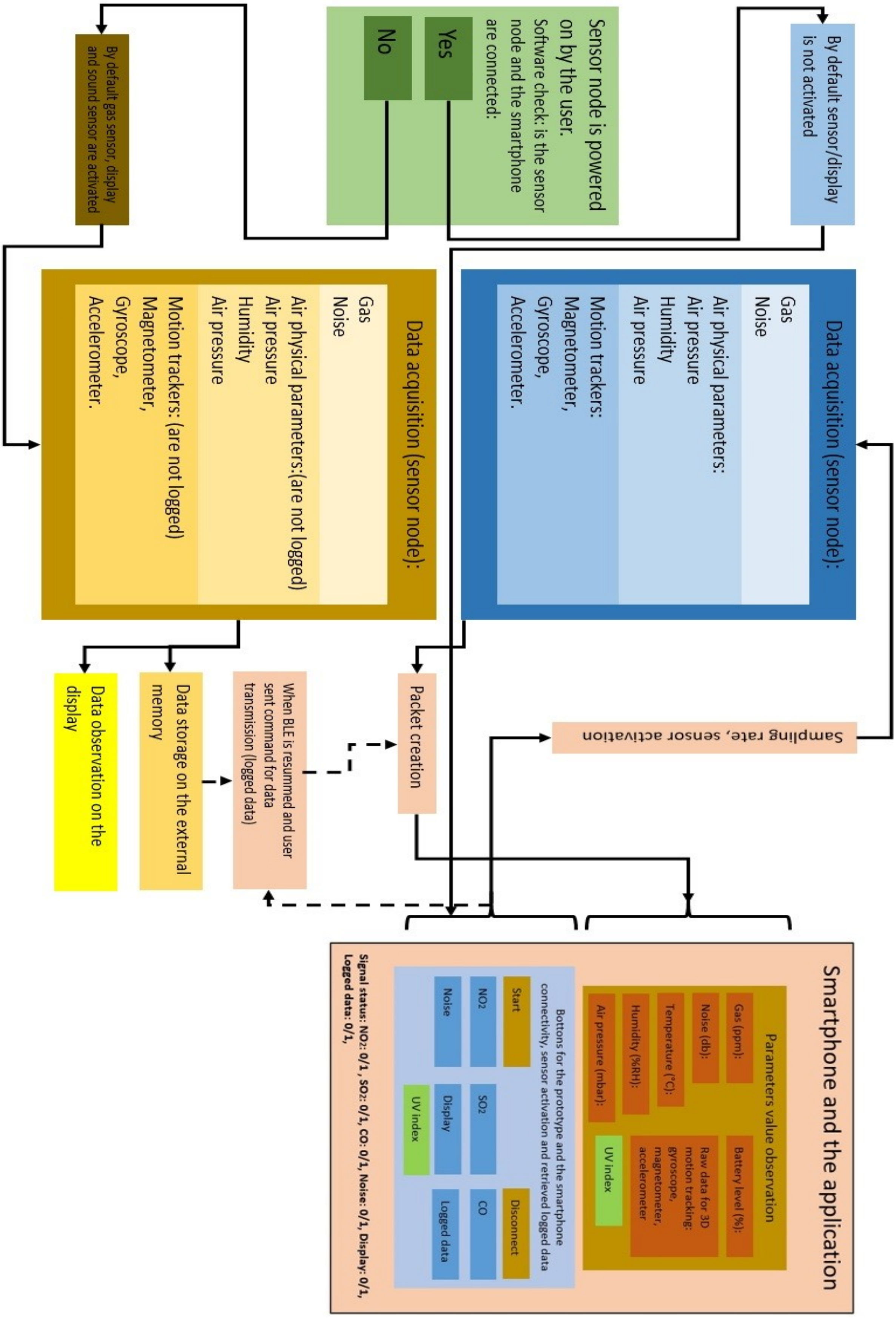

Fig. 4-22 General strategy of the proposed prototype in standalone and configurable mode.

I2C and ADC digital interface are more often used for data acquisition in sensor node. Gas and sound values are always in protected mode of operation. These data are transmitted to the smartphone when BLE is connected and are stored in the external memory when the BLE is disconnected. As is seen, external memory also is a part of configuration block. It means that user can decide when is intended to transmit the data from the external memory. In the mode of BLE disconnected display is activated by default and all sensors are operating in predefined sampling rates. In addition when the BLE is connected the gas sensors, sound module, display and external memory are accessible for configuration by the used from the smartphone.

4.4.1 Client (Wrist-Worn Device)

The proposed wearable device gathers different ambient and movement data from various integrated and add on-board sensors. In particular, it is a light, small and wrist-worn device (Fig. 4-23) that consists of a microcontroller, add on-board sensors, display and notification components which are powered by means of a micro USB or Li-Ion battery.

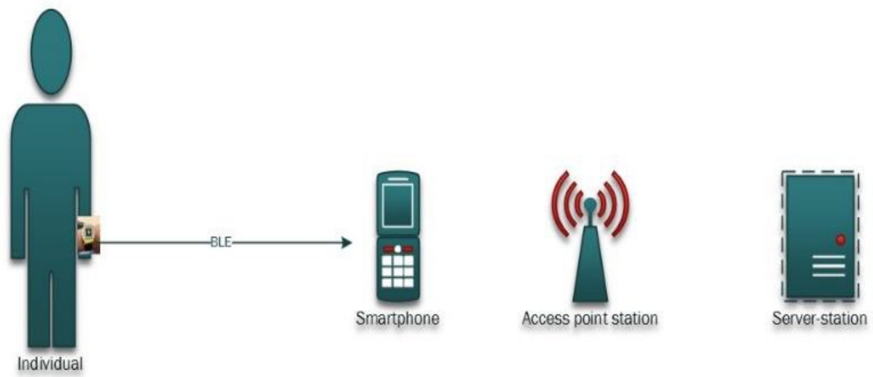

Fig. 4-23 Structure of the whole system.

The host platform (described in chapter 4) must be capable of short-range data transmission and providing radio connectivity with integrated crystal antenna. A smart power control management block gives this capability of being used for long term monitoring with small battery, for several hours. To establish a channel for data transmission between the smartphone and sensor node, the application that has been developed for this purpose must be used. If the application called "P^{2}health" is opened, once the user press the "start" button, if sensor node is accessible, then the channel is established and immediately data transmission is started. The BLE and NUS (Nordic UART Service) service is used for data communication.

4.4.2 Multi-Threading And Multi-Level Hierarchical Server

When data are collected by wrist-worn, these data must be sent to a server to be stored. Therefore, the server has to implement a multi-threading and multi-level control program, depends on the status and operations, different decisions are made in various levels. This allows to simultaneously and efficiently collect data from different users. To be able of performing a sequence of operations with lowest errors, strict real-time criteria are adopted. Moreover, the Multi-threading and multi-level hierarchical, improve performance and scalability.

The communication between the smartphone and the prototype is two-way. In the majority of the work in this area, the smartphone only is used for data collection to protect data from the lost and at the second order to send them to a server for permanent storage and analysis.

In this work, the smartphone is given a higher weight. It is used to configure the sensor node to work with different sampling rates and also provides the possibility of sensor activation for the user. A closer look is taken at the application that is running on the smartphone (Fig. 4-24).

Two major sections are seen in the application. The first part is parameters value on the screen to observe. Gas, sound, ambient physical parameters and the motion trackers and one sensor (UV index) that is considered as the future development are seen on the Fig. 4-24.

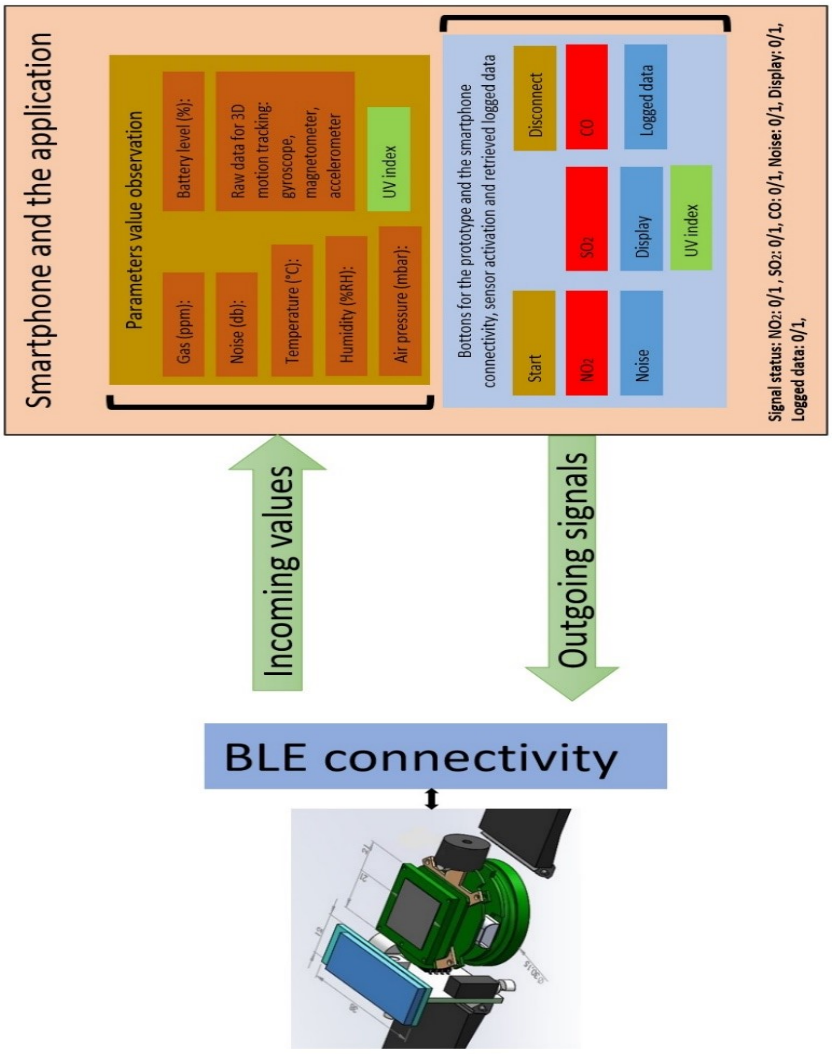

Fig. 4-24 Two-way data communication between sensor node and the smartphone.

In this part the communication arrow is from the sensor node to the smartphone. In fact the acquired data on the sensor node are transmitted to the smartphone for storage and observation.

The second part indicates on the sensor node configuration. There are several buttons for interaction. These buttons have to be pressed for activation. The first row of these buttons take the sensor node to BLE connected and disconnected mode (data transmission is established).

The second row indicates on the gas sensor selection and activation. Where at each time only one gas sensor is activated therefore user is able to select the target gas sensor.

The next row is dedicated to display, logged data and noise detector. Each of these options may be activated by pressing the button.

The UV index button at the last row is to show the future development that at the moment is not activated.

A line at the bottom of the application indicates on the signal status send from the smartphone to the sensor node. In fact, if the value in the front of each parameter is set to 1, it means that that sensor/feature is activated. At the following the command transmission from the smartphone to the sensor node is discussed. The command length duration determines the sampling rate and the activation status of the sensor and features in the prototype.

The type command for all sensors and features send from the smartphone is the same. But what make the difference is the command duration. This duration for the gas sensors/sound is adjustable and depending on the requirements can be changed and adjusted. But this command for display and logged data activation is continuous. The transmission of logged data is defined as an independent operation that once starts will transmit all logged data and cannot be interrupted. On the other hand, for continuous observation of data on the display (especially in standalone mode), it is preferred to send continuous command, nevertheless this can be modified as well (see Fig. 4-25).

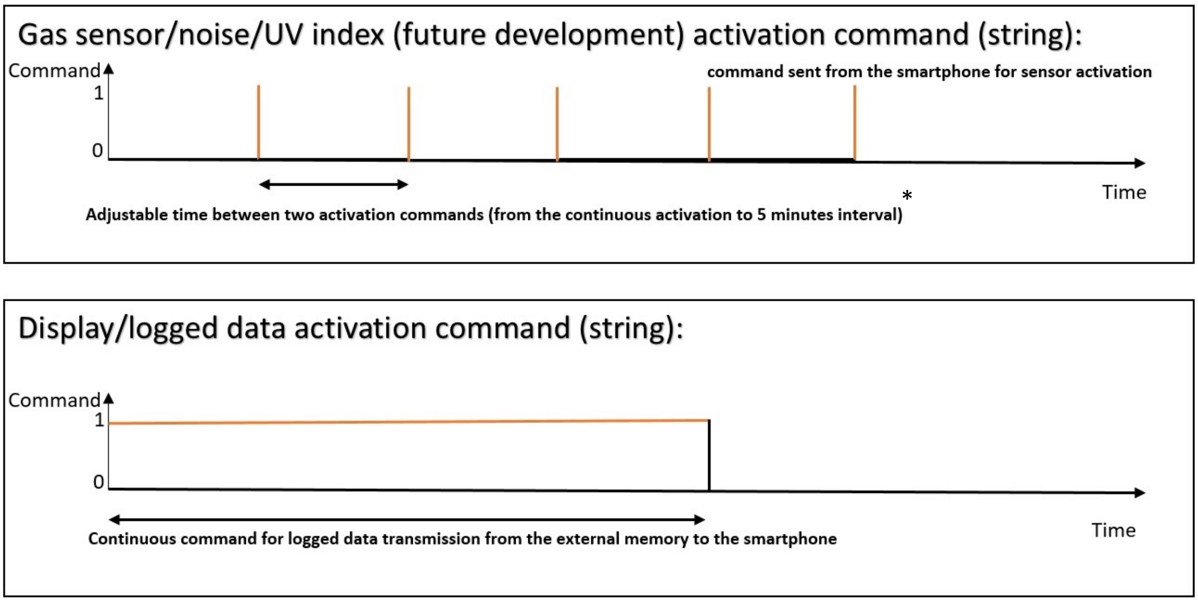

Fig. 4-25 Command description from the smartphone to the sensor node.

*This figure indicates on the transmitted pulse from the smartphone to the prototype to activate the target sensor which can be a toxic/hazardous gas sensor and sound or include UV index sensor in future development. The time interval of the command is adjusted on the smartphone.

5 GAS SENSOR LAYER DESIGN AND RESULTS

In this chapter, the full consideration is given to gas sensor's layer design. The evolution progress of the gas sensor layer from the first design is presented. Result of the first design, physical appearance, performance and reasons for moving forward to the more efficient design to the latest version are described in detail.

The sensor selection criteria already was described in the previous chapter and Spec sensors was chosen as the qualified gas sensor in the designing a personalized ambient air monitoring prototype. At the beginning of this chapter, sensor driver design that is compatible with the NO_2 and CO gas sensors and also supports the wide range of oxidizing and reducing gas sensors are described. The section is followed with sensor output accuracy, calibration process and data validation. Eventually, the methodology is supported with experimental results.

The final design must be able to measure several toxic and hazardous gases in IOAQ. This target must be achieved while, the final prototype still should present a small, light and compact solution. The fact is people from different group ages and working classes, require their own demands. Each can be in a different application with others. To cover the most of these applications and demands, the solution must be flexible to cover wide range of parameter monitoring with ease of switching from one gas to another while still the solution, structure and architecture is the same (fixed hardware). This feature does not have to change the hardware solution from one to another parameter evaluation. As the second matter of fact, and with a brief investigation on the application and individual's expectation, it is realized that more often only one gas pollutant is under measurement at each time and place (this is correct in particular, in personalized ambient parameters monitoring).

Therefore, the gas sensor node is designed and implemented in replaceable mode. In this feature, the target gas sensor node is readily replaced with some other target gas sensor by the user in hardware. Prior than switching from a gas sensor node to another, it should be cleared that the software implementation including sensor initialization and calibration has been demonstrated and is embedded in the microcontroller's code for each gas sensor separately. So that at the activation step, user activates the predefined embedded piece of code only by sending command from the smartphone to the sensor node. This feature improves the flexibility and user friendly factors of the sensor node and reduce the power consumption significantly by avoidance of operation of several gas sensors at the same time.

5.1 GAS SENSOR DRIVER DESIGN – Scenario 1

Designing and implementation of the gas sensor driver was not in the current version at the beginning. It was started with gas sensors from SGX Company's gas sensors. The sensor's shape are quite in an ideal scale, and some of sensors are supported with multiple channel (several gases detection simultaneously). Of course the gas sensor driver for this type of gas sensor is distinguished with the gas sensor driver for the Spec gas sensor (final and applicable gas sensors). However, the structure and approach (Multi-Layer) is still the same for both gas sensors.

To give a clear idea of the gas sensor design progressing, both gas sensor driver tests and results are presented.

5.1.1 Structure

Double channel SGX gas sensor (MICS 5414) was the first candidate for the sensor node design [203]. Two gases measurement at the same time, light-weighted, small and fair response time are the reasons for the gas sensor selection. SGX is able to measure NO_2 and CO with separate channels on the same sensor.

Beside these advantages, there are number of disadvantages that the sensor is suffering from them. The first mismatch with the main host platform is 5v voltage supply operation. While the host platform is powered on by 2.8 V (later with redesigning will be shifted to 3.3 V), and sensor is compatible with 5.5 V, a DC-DC converter is required. An electronics circuit parts for sensor operation and measurement is divided to 3 sections:

- A DC-DC convertor to shift the power supply from 2.8 to 5 V and applicable to the gas sensor,
- Sensor implementation,
- Output signal conversion to I2C mode for host platform usability.

The electronics circuit of a sensor node for IOAQ measurement is depicted in Fig. 5-1.

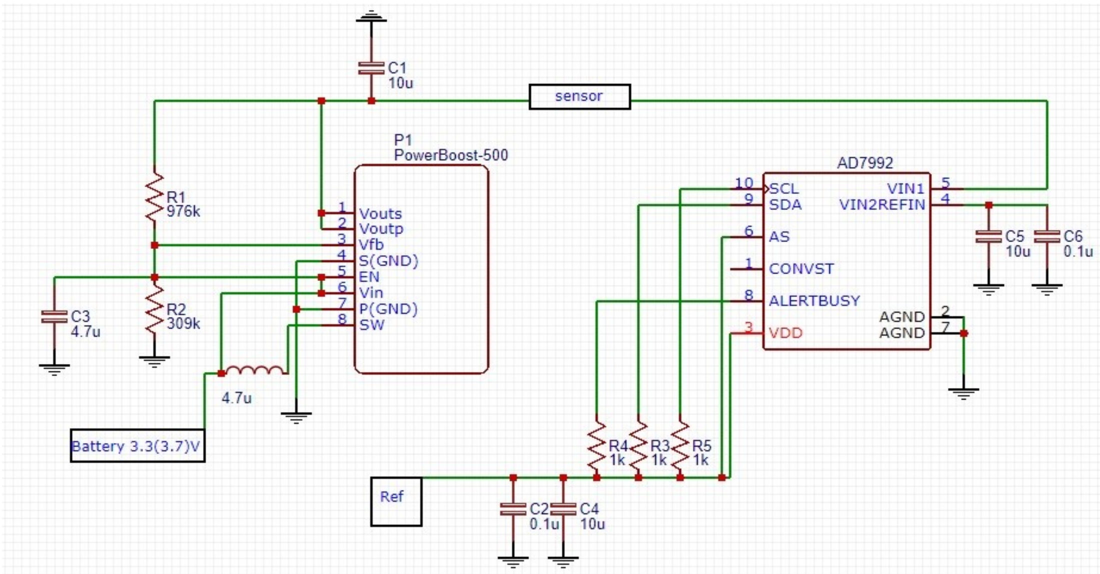

Fig. 5-1 Electronics circuit design for MICS 5414.

A DC-DC converter with the least leak out current is carefully designed to shift the level of power supply to 5V compatible with the sensor. The output of the sensor is going through the second section of the circuit. This circuit changes the mode of communication from analogous to I2C. Where the number of target gases at the prototype are multiple, I2C communication mode is well suited to address several sensors.
The first version of the case (chassis) for the wearable prototype with measuring NO_2 and CO target gases in 3-D was designed to host the multi-layer device. The assembled prototype to be worn is depicted in Fig. 5-2 and Fig. 5-3.

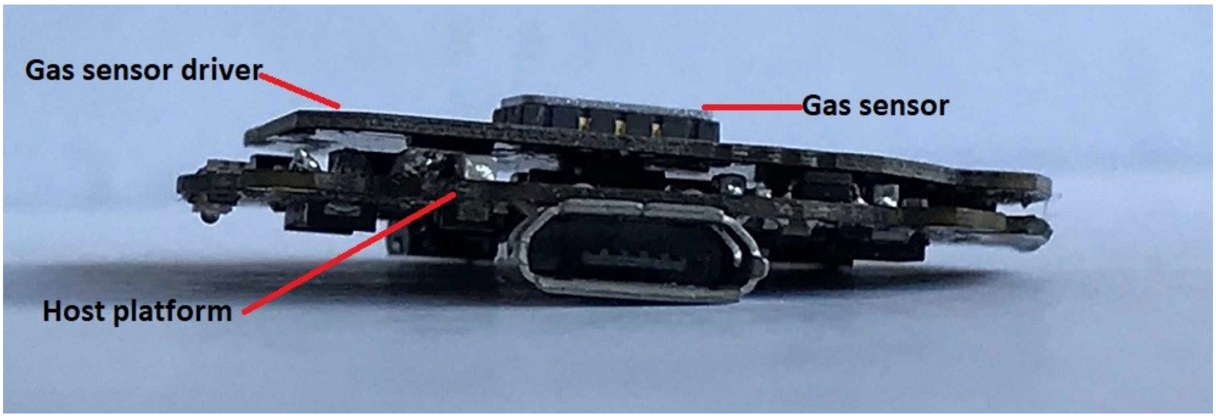

Fig. 5-2 Two layers proposed wearable with SGX gas sensor.

Fig. 5-3 First version of multi-layer gas sensor measurement.

5.1.2 Experimental Results, Observation and Evaluation

The described setup is applied to CO and NO_2 in preliminary measurements. Output of experimental results are evaluated in terms of accuracy, response time, recovery time and power consumption. CO and NO_2 stand in two different gas categories, one is oxidizing and another is reducing. From the other prospective, CO is an active gas and NO_2 is a reactive gas. The output of the sensors is monitored on the oscilloscope. In Fig. 5-4, the blue line is representing the CO gas output's signal and the yellow line is indicating on NO_2.

Base on the set up, the nature of the gases and sensors' internal fundamental operation, the reference level of both gases (in non-exposure target gas) is 1.945 V (NO_2) and 2.6 V (CO). These values are valid for the room temperature conditions. When sensors are exposed to the various levels of gas concentration respectively, output voltage of the sensor is ascended for CO (reducing internal resistance) and is reduced for NO_2 (increasing internal resistance) due to changes in load resistance, configured for each one.

Basically, long exposure to NO_2 can lead to serious health problem when it exceeds 2ppm. The NO_2 concentration which normally is observed in urban area does not exceed 0.7 - 0.8 ppm. In Fig. 5-5-LEFT, the output voltage of sensor while is exposed to the target NO_2 gas between 0.03 to 2.3 ppm are exhibited. The obtained results in the range of 0 – 1 ppm with a good approximation may be considered linear. The response time measurement from the gas sensor exposure to the first gas detection by the sensor is less than 30 seconds and the stability time is a function of exposed gas concentration but mostly does not exceed than 60 seconds. The stability time is reduced when the gas concentration is greater than 1.2 ppm.

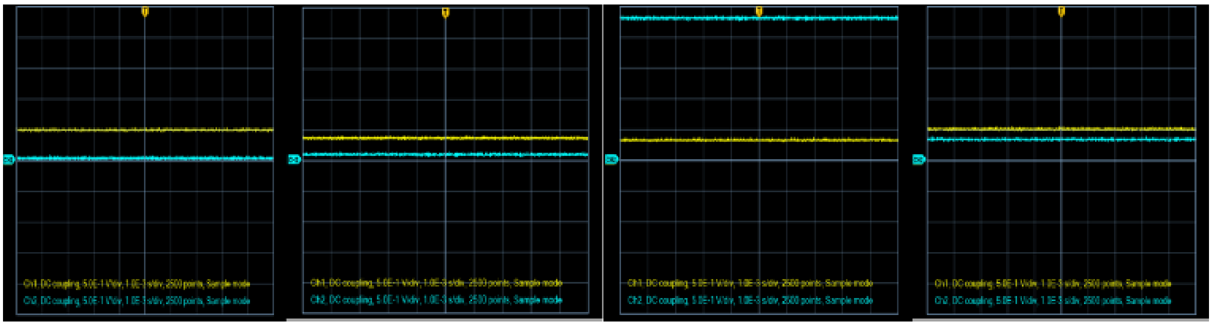

Fig. 5-4 Output results of MICS-5414 monitored on oscilloscope.

Recovery time is the next vital indicator in sensor performance evaluation. Sensor recovery time is the "necessary time for the sensor to reach from non-zero gas concentration to zero gas concentration (reference level) and is ready to perform the next measurement".
In the performed experiments, was observed that a long recovery time (50 minutes) is required. In the first 5 minutes, the sensor reaches to 51% of the maximum gas concentration, the sensor behavior during this time is quite linear (see Fig. 5-5-Right). In the next 13 minutes (18 minutes) the sensor is recovered by 78%. The slope rate of recovery time is reduced within the remaining 22%. The recovery process time is completed in 50 minutes.

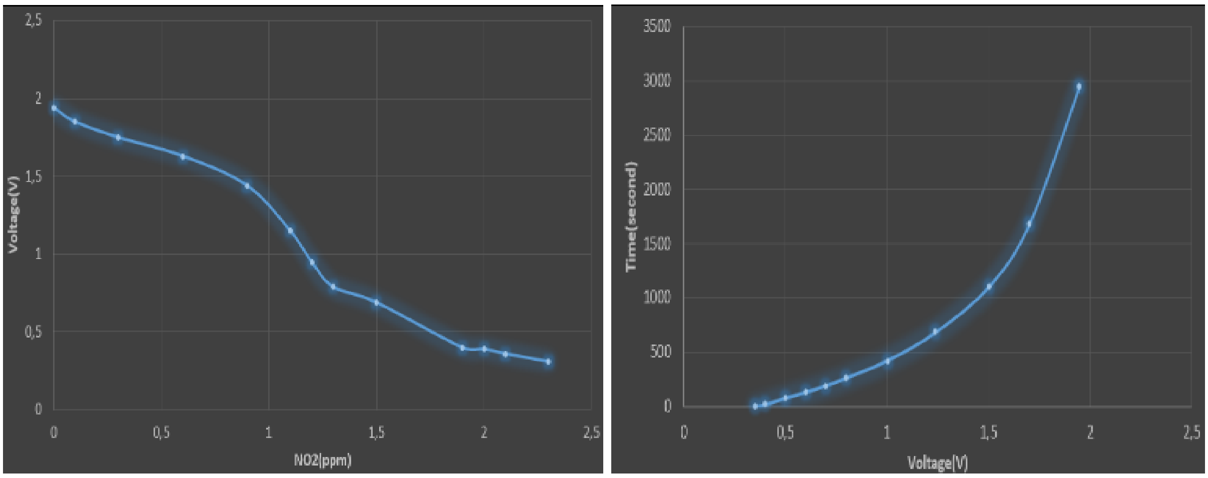

Fig. 5-5 Left, voltage to ppm conversion for MICS-5414. Rigth, Recovery time.

A Li-ion battery with capacity of 250 mAh is used on the prototype. The used gas sensors in this prototype consumes up to 30 mA. The power consumption of other components plus data transmission in BLE connected status, will increase the power dissipation to greater than 140 mW (> 45 mAh). The life of monitoring is the function of gas sensor sampling rate. With a lower sample rate during monitoring, device may run longer.

However, although this design might fit within the prototype (hardware), but the power consumption and recovery time, and the number of external components are the weaknesses.
From the other side, the sensor is metal based structure, which requires a long time warming up before operation [204]. With what was achieved by the SGX sensor in experimental tests, it is found out that, this scenario is not fit with the proposed wearable criteria and requirements, in particular in term of power consumption and recovery time.

5.2 GAS SENSOR DRIVER DESIGN - Scenario 2

In spite of well-defined mechanical design and adoption, the first scenario didn't satisfy the general requirements of the expected solution. In particular, power consumption, and recovery time raise the serious issues.

So that the gas sensor is shifted from the sensors based on metal oxide technology to sensors manufactured using electrochemical technology. It is expected that a gas sensor node with much lower warming up and power consumption and more straightforward circuit design is implemented. As a consequence, the gas sensor driver also is changed accordingly.

5.2.1 Structure

In the second gas sensor layer design, the observed issues from the first scenario are considered to avoid. In this design, enable pin is taken into consideration for sensor activation (at the beginning by sliding switch and at the latest version by sending command from the smartphone: hardware to software shifting for reducing the design complexity and improving the prototype flexibility).

The gas sensor driver must be designed in a way of compatibility with any type of gas sensors from Spec family. Output signal from the sensor is typically in current, to feed this signal to the ADC of microcontroller, this signal is processed in two steps:

- Current to voltage conversion,
- Amplification through an appropriate amplifier,
- Filtering.

Gas sensor layer compatibility with each gas sensor requires different gain magnitude for each, specific bias for each different type sensor, load resistance and zero internal voltage. With such demands, an amplifier is required to combine amplification and conversion proportionally. Furthermore, amplifier must be programmable in different mode with the least required external components and power consumption. LMP91000 as an Analogue Front End (AFE) amplifier provides a proper solution [205].

LMP91000 is described as the followings:

- Seven programmable internal resistors level to adjust the gain for each sensor separately,
- Three internal zero states for reducing and oxidizing gases,
- Twelve levels of biases.

This AFE has a straightforward circuit design with low power consumption with wide operational range (2.7 to 5 V) make it appropriate in the architecture. The output signal of the amplifier must be filtered to eliminate the noise amplified through the AFE. The filtering process is the function of sensor type which might be in one or two steps. Based on the type of sensors, the gain of LMP91000 is adjusted. In some reactive sensors (NO_2 and SO_2) mostly the provided gain through the internal programming and configuration is not satisfied, thus an external resistor is required with large value to produces larger gain.
This sensor driver must be connected to the hardware interface to communicate to host platform through a male board to board connector.

Therefore, the sensor driver board includes an AFE amplifier which converts sensed current by the sensor to voltage proportionally, a 24-pin male Hiros board to board connector [206], two filters on output signal and as a feedback, one external resistor to adjust the gain if required for oxidizing gases, and enable pins for each desired gas sensor. The output signal of AFE is fed to the host platform microcontrollers ADC pin for processing (see Fig. 5-7, 5-6).

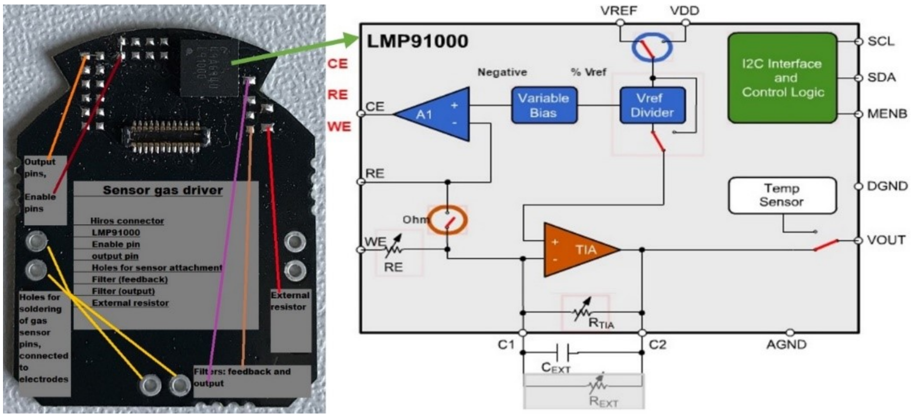

Fig. 5-6 Gas sensor driver design in detailed with external components location.

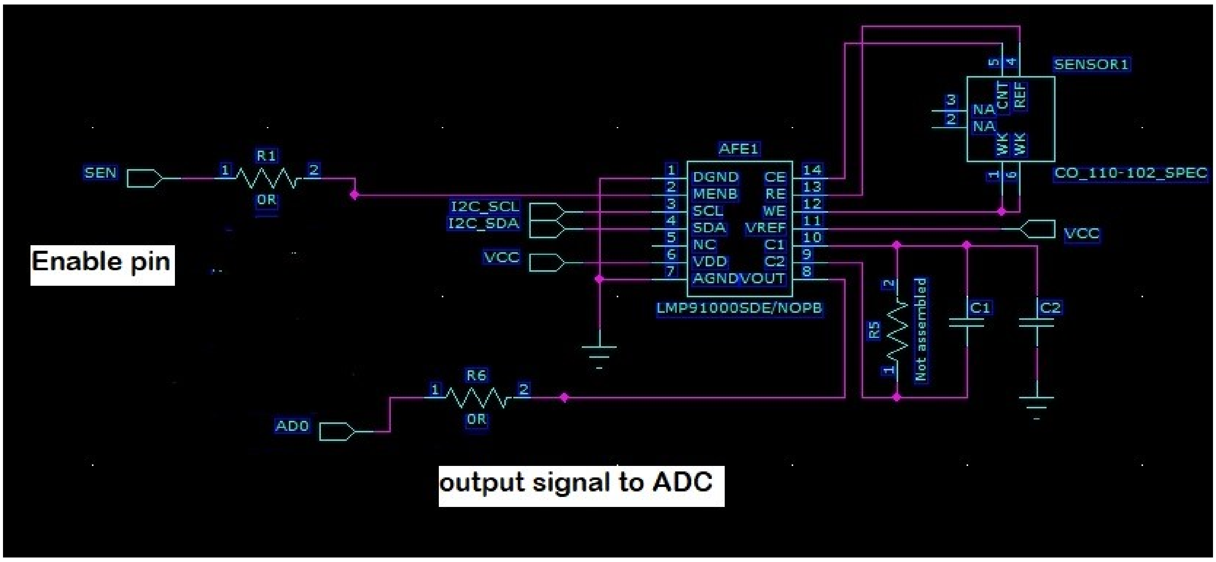

Fig. 5-7 The initial gas sensor driver board design in schematic.

5.2.2 Developed Version of Gas Sensor Driver (V2, V3)

The first version of the gas sensor driver already discussed and evaluated. This universal gas sensor driver activates and drives the gas sensors from two different categories: oxidizing and reducing.

Basically the reducing gases stand on the lower baseline voltage and with increasing the target gas concentration, the output current and in turn voltage is increased (ex. CO). For this type of gas sensors which are mostly active, the output signal more often satisfies the requirements demanded by the ADC. But for the oxidizing gases such as NO_2 which also is extremely reactive, the output signal is heavily function of the biasing voltage. Even some millivolts changes in the input voltage of the gas sensor can interfere with the correct operation of the gas. In the second version, this issue was tackled by integrating a reference chip on the board in the new design. Under this design, the voltage for the second time was fixed through the Precision Low Power FGA Voltage Reference chip in the gas sensor driver (U5: Intersil

ISL60002DIH320Z-TK [207]). Furthermore, the possible ripple also was eliminated by the filter implemented on the gas sensor driver.

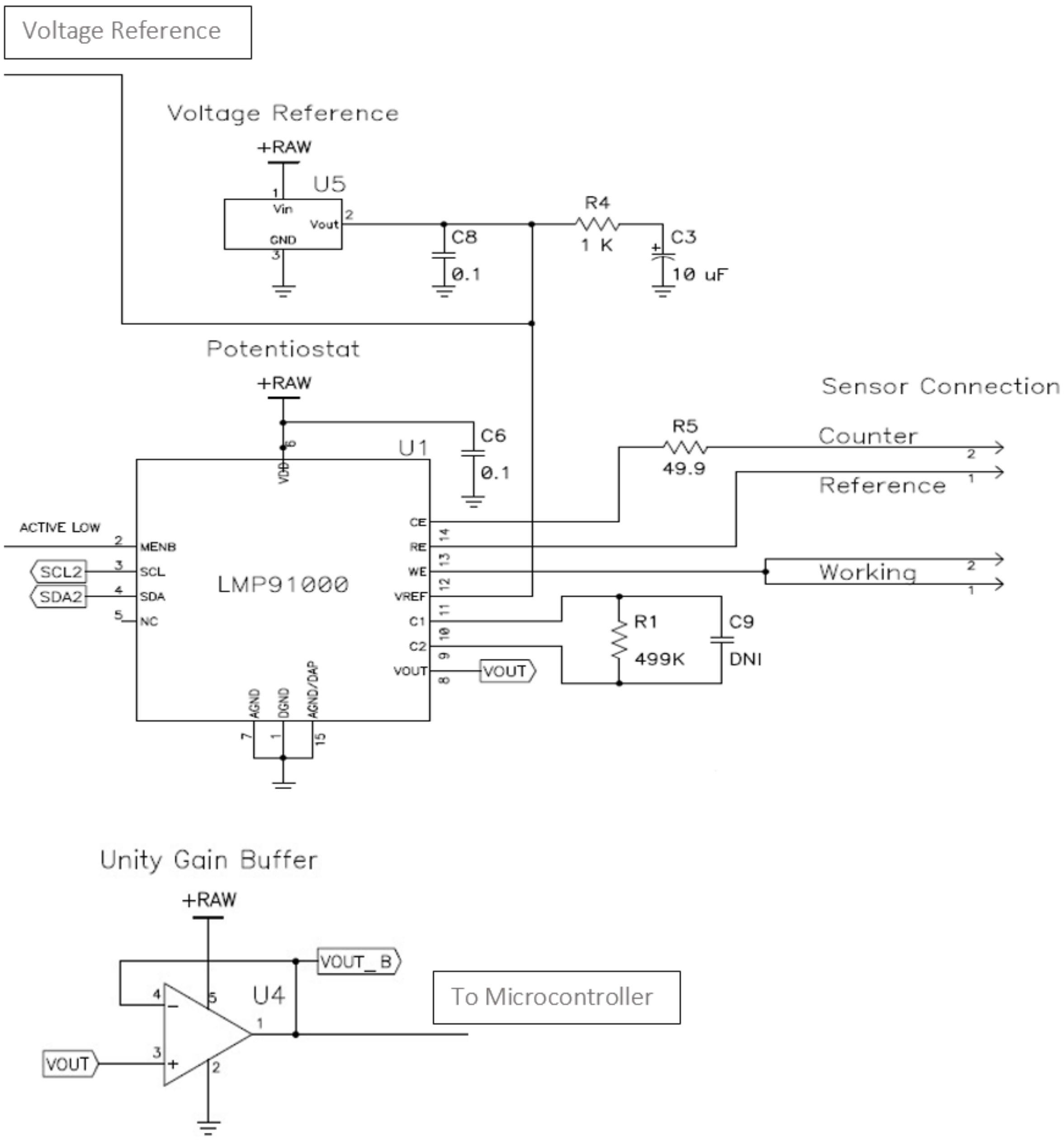

Fig. 5-8-a. The circuit gas sensor driver for the second and third version (reference voltage and gain unity buffer)[2].

[2] In this circuit, documents from TI and Spec have been partially used.

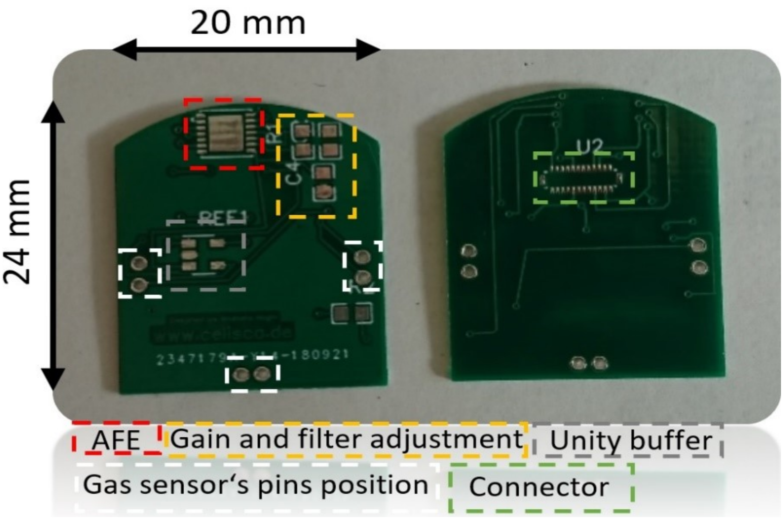

Fig. 5-8-b. The second version of gas sensor driver.

In the third version (V3), the possible mismatch impedance between the output signal of the gas sensor and the ADC microcontroller is tackled. A gain unity buffer (U4: MicroChip MCP6041T-I/OT [208]) is considered to solve the problem. This improves the quality of the feed signal to the microcontroller. The V2 and V3 of the gas sensor driver and also PCB design are shown in Fig. 5-8 and Fig. 5-9.

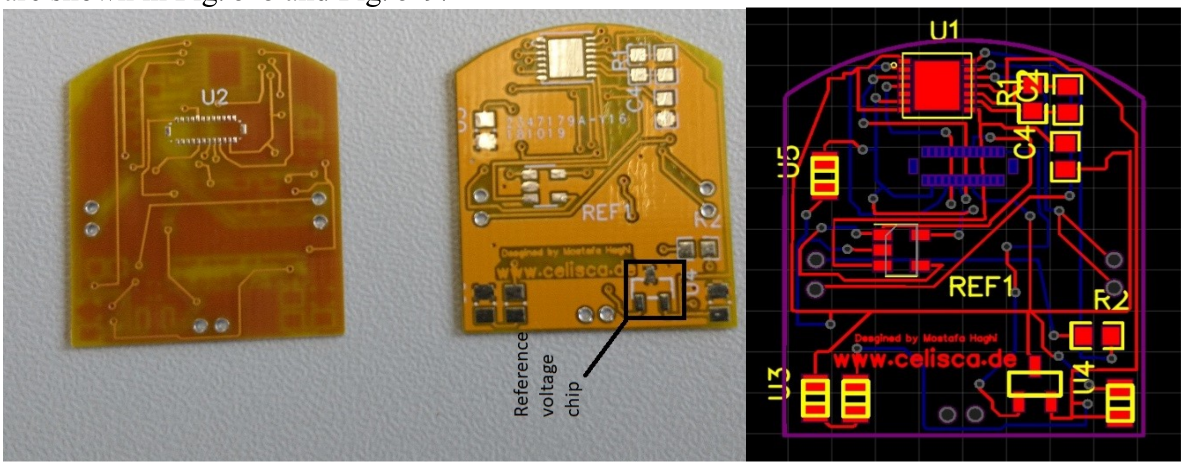

Fig. 5-9 The third version of gas sensor driver (left) and PCB design (right).

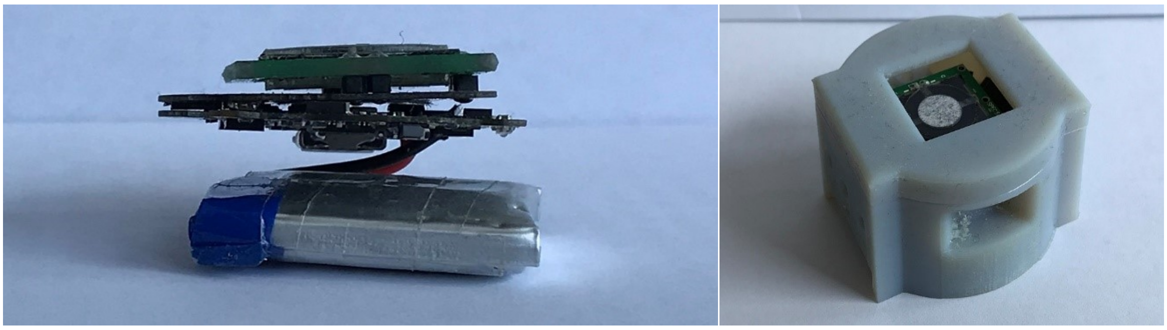

Fig. 5-10 Two layers proposed wearable with Spec sensor (left). The proposed wearable in the case.

5.2.3 Calibration Process

The gas sensor output signal is influenced by the ambient physical parameters. Depending on the type of gas, this effect might be less and more. When the output signal of the gas sensoris fed to the microcontroller, the calibration process is prior to data conversion to gas concentration according to part per million (ppm). The calibration process and investigation are performed for two different gas sensors CO (active) and NO_2 (reactive). The process for the rest of the sensors follows the same policy.

The ambient physical parameters (air pressure, air humidity, and temperature) are measured for two reasons in the final prototype:

- A comprehensive monitoring is demonstrated,
- These parameters affect the gas sensors performance.

Calibration process is performed in two steps. As a matter of fact, the physical parameters might change the:

- Zero baseline,
- Span of the sensor measurement.

Zero baseline is: “the value that is shown in non-exposure status”. This factor at the room condition, for a calibrated gas sensor, is zero. But as the physical ambient parameters affect the sensor performance, the baseline value might be drifted as well. This value after the calibration must be always equal to zero. *Zero baseline* or so called *zero drift* correction is the first step in calibration.

Span of gas sensor, “shows the range of gas variability in exposure of the target gas”. Due to physical parameters presence this might be different with the real gas concentration in the environment. This is the second step forward in gas sensor calibration.

At the following the physical parameters footprint on the gas sensor performance is studied.

5.2.4 Humidity Dependence

Basically, only an instant large humidity change in the environment may cause a rapid spike in baseline value for tens of ppb (part per billion). This change direction is compatible with the direction of increasing (positive baseline change) humidity and descending (negative baseline change), but it comes to a stability quickly in seconds (see Fig. 5-11).

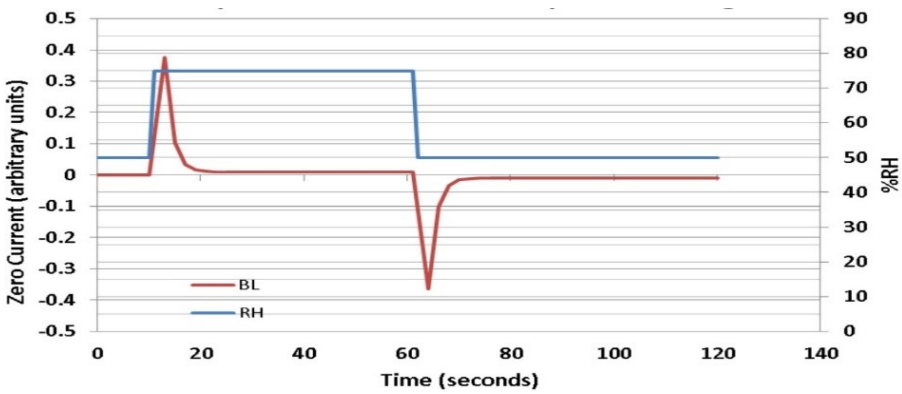

Fig. 5-11 Instance effect of humidity on gas sensors.

The rapid change of humidity (+/- 30 %) bring approximately five seconds of instability. At the final design prototype, according to the nature of gas sensors (15 seconds response time) and the requirements, the gas sensor sample rate is every 2 minutes data transmission. As is shown in Fig. 5.11, the response of the baseline value of the sensor to rapid humidity changes is

ignorable in long period of measurement. This figure is an average and might be slightly changed for each type of sensor. The exact values are obtained in experimental results.
From the other side, span effect of short-term and mediocre humidity change on the sensor sensitivity is very low and negligible. The measured experimental and investigated data from the data base, indicate an air humidity of between 33% and 55% in winter, affects NO_2 and CO by 1 ppm and maximum rate of 3 ppm within 45 days. In summer this drift in baseline response would be slightly more. The drift occurs within 45 days of first operation and afterwards, the baseline generated current is not changing significantly (see Fig. 5-12).

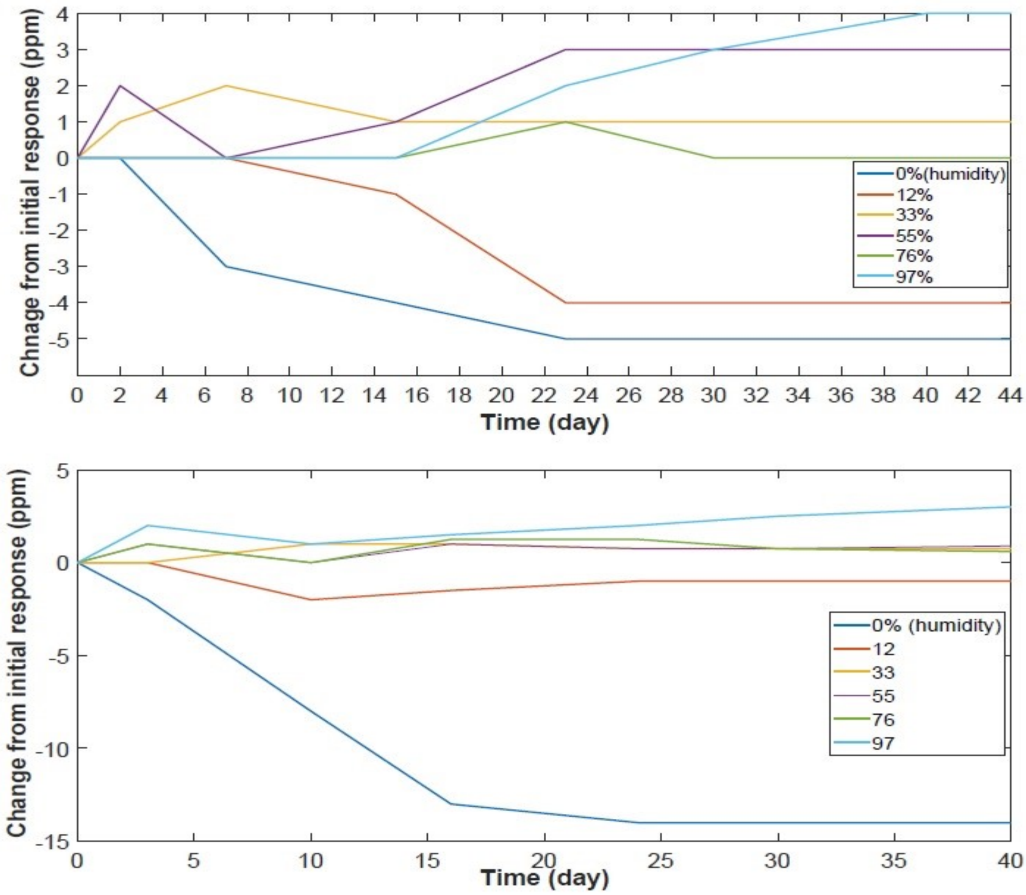

Fig. 5-12 Humidity effect on baseline vale of NO_2 (top) and CO (bottom).

5.2.5 Pressure Dependence

Generally, target gas sensors (NO_2 and CO) from Spec family are designed to operate under standard conditions (23+/- 3 C, 40–60 %RH, and sea level atmospheric pressure) for the best performance.
Although, these sensors in higher humidity range, are operating still very well with software compensation. The measured pressure in ***celisca,*** where the calibration has been performed, shows that, in different floors and laboratories the pressure is in the range of 1009 to 1019 atm, that is acceptable and protect the sensor from any pressure calibration. On the other hand, the measured pressure in Rostock (Germany) [209], where tests have been performed, exhibits the relatively same range during the year 2017 (minimum and maximum values in each month are mentioned, see Table. 5-2).

Table 5-1 Pressure investigation during 2017 in Rostock.

Month	Jan.	Feb.	March	April	May	June	July	Aug.	Sept.	Oct.
Max. air pressure(m bar)	1035	1033	1025	1036	1025	1020	1014	1019	1022	1020
Min. air pressure(m bar)	1011	987	991	1010	1007	993	1000	1005	1000	1009

5.2.6 Flow Rate Dependence

The sensitivity, response time and accuracy of the sensor is affected by the air flow rate [210]. This factor in an indoor measurement and investigation is well controlled as the flow rate of the air in a closed environment does not interfere with the sensor performance. Although the architecture design is targeted to be applied more often in workplace environments which the air flow rate is typically 0.1 – 0.2 m/s and this flow rate is compatible with the released gas in the used calibrator container, but for the sensor protection and avoid flowing air directly to the sensor face, a porous PTFE membrane [43] is used at the top of the sensor. Furthermore, the sensor is protected by the physical case, which surrounds the sensor by 1–2 mm higher height avoiding direct air flow to the sensor node.

Using a porous PTFE membrane will also protect the sensor from condensation and accumulating dust and oil vapors.

5.2.7 Temperature Dependence

A physical factor that significantly influences the performance of the gas sensor is temperature [211], [212]. Temperature compensation is the most important factor that play an important role in sensor calibration. The sensor response to temperature variation is investigated within a wide range of -10 °C to + 40 °C. For a precise calibration, care must be taken that, calibration is performed in two steps:

- Zero baseline
- Span of sensor

Both of these factors are affected by temperature. Therefore, to utilize the gas sensors in the performance and accurate operation, it is necessary to correct both factors. Although, this may be demonstrated in hardware aspect, but the preference is software compensation. Due to the nature of each gas sensor, oxidizing gases such as CO are more affected by the physical parameters, with the same investigation, reducing gases (NO_2) are less or not affected significantly by these parameters. In Fig. 5-13 (top) the temperature changes, almost is negligible in zero drift. Regarding NO_2 gas sensor in the entire range of measurement (-10 to +40 C). During experimental tests, it is observed that, the maximum effect of temperature on the zero current is less than 0.5 ppm.

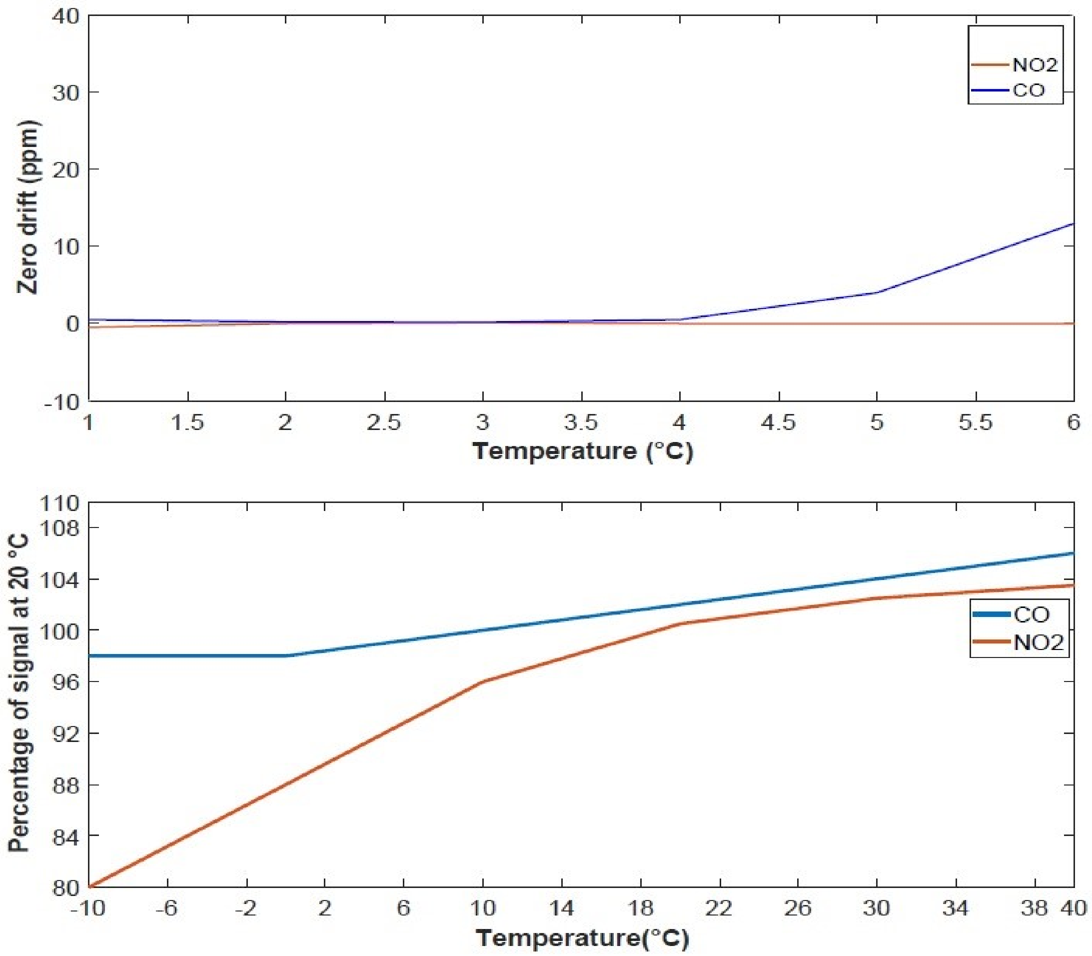

Fig. 5-13 Effect of temperature variant on NO_2 and CO baseline (top) and span (bottom).

Regarding CO gas sensor, the temperature compensation on baseline (zero drift) is more important where the intensity of effect is increased in higher temperature. The temperature behavior is divided into 3 major linear portions:

- Between -10 °C and +20 °C, the zero drift with a good approximation is negligible,
- From 20 °C to 30 °C, by increasing the temperature, the baseline is varied between 1 – 4 ppm,
- While shifting to the higher temperature, the zero drift is influenced more where the change is between 4 – 12 ppm.

The behavior of temperature on the zero drift in all three portions is quite linear which make the compensation straightforward through software.
The maximum observed change of zero drift for NO_2 was +/-0.5 ppm per each temperature degree during experimental tests.
The equations, calculations and policy without calibration is presented and the calibration policy is followed in the next subsection.
The applied temperature is obtained from the LMP91000. This AFE is able to work in two modes:

- Output signal from the gas sensor,
- Measuring temperature.

This mode switching is implemented in software (see Fig. 5-14 and Fig. 5-15).
LMP91000 is switched to temperature mode in each measurement process before entering to the calibration routine.

```
void lmp91000_temperature_cfg(void)
{
  uint8_t result;


  nrf_gpio_pin_clear(LMP91000_CO_MENB_PIN);
  nrf_delay_ms(1);

  do
  {
    result = lmp91000_get_status();
  } while (result != 1);
  lmp91000_clear_lock();
  //nrf_delay_ms(1);
  Twiface_writeReg(This, LMP91000_TIACN_REG, LMP91000_TIA_GAIN_14KOHM | LMP91000_TIA_RLOAD_10);
  //nrf_delay_ms(1);
  Twiface_writeReg(This, LMP91000_REFCN_REG, LMP91000_REF_SOURCE_EXTERNAL | LMP91000_INT_ZERO_20 | LMP91000_BIAS_POSITIVE | LMP91000_BIAS_0);
  //nrf_delay_ms(1);
  Twiface_writeReg(This, LMP91000_MODECN_REG, LMP91000_SHORTING_FET_DISABLED | LMP91000_OP_MODE_TEMP_MEASURE_TIA_OFF);
  lmp91000_set_lock();
  nrf_delay_ms(1);
  nrf_gpio_pin_set(LMP91000_CO_MENB_PIN);
}
```

Fig. 5-14 LMP91000 configuration to temperature mode.

```
void lmp91000_adc_start(void)
{
  uint32_t temp, i, sensor_value, temp_value, base_value, templ;
  unsigned char lcd_str[50];

//  if(!strcmp(cmdData, "NO2"))
  {
    lmp91000_cfg();
    lmp91000_temperature_cfg();
  }

  NRF_ADC->INTENSET   = ADC_INTENSET_END_Disabled;
  NRF_ADC->CONFIG     = (ADC_CONFIG_RES_10bit << ADC_CONFIG_RES_Pos)  |
    (ADC_CONFIG_INPSEL_AnalogInputOneThirdPrescaling << ADC_CONFIG_INPSEL_Pos) |
    (ADC_CONFIG_REFSEL_VBG << ADC_CONFIG_REFSEL_Pos)  |
    (LMP91000_VOUT_ADC << ADC_CONFIG_PSEL_Pos)     |
    (ADC_CONFIG_EXTREFSEL_None  << ADC_CONFIG_EXTREFSEL_Pos);
  NRF_ADC->EVENTS_END = 0;
  NRF_ADC->ENABLE     = ADC_ENABLE_ENABLE_Enabled;
  nrf_delay_us(200);

```

Fig. 5-15 Embedded LMP91000 configuration in calibration process.

The detected gas concentration based on ppm without temperature compensation is calculated in (1):

$$C_x = \frac{1}{M}\left(V_{gas} + V_{gas0}\right) \quad (1)$$

Where:
C_x is the gas concentration (ppm),
V_{gas} is the output signal voltage (mV) for the measured concentration,
V_{gas0} is the output signal voltage (mV) in a clean-air environment,
M is the sensor calibration factor (V/ppm). M, is calculated by (2):

$$M\left(\frac{V}{ppm}\right) = \text{ Sensitivity code } \left(\frac{nA}{ppm}\right) \times TIA\left(\frac{kV}{A}\right) \times 10^{-9}\left(\frac{A}{nA}\right) \times 10^{3}\left(\frac{V}{kV}\right) \quad (2)$$

Where:
The sensitivity factor (Code) is provided on the sensor label, and TIA Gain is the gain of the trans-impedance amplifier (TIA) circuit in the calculation process. The V_{gas0} value is represented in (3):

$$V_{gas0} = V_{ref} + V_{offset} \quad (3)$$

V_{offset} must be adjusted according to the experimental results, but to start with calibration $V_{offset} = 0$ is a primary estimation.

As the equations of the preliminary calculation were presented, the calibration process is applied at the next step and will conclude with the corrected output signal.

In software compensation, basically the calibration (error correction) is implemented in two steps:

Baseline correction:

The calibration is started with baseline correction in eq. (4). In fact, the whole calculation is based on zero drift signal, therefore in the first step, the zero-corrected voltage (mV) is subtracted from the raw signal. The reference temperature according to the experiments is 20 °C.

$$I_z(T_m) = I_z(T_0) + [\frac{1}{°C} \times (V_{gas} - V_{gas})] \quad (4)$$

Where:
T_0: the reference temperature point at 20 °C,
T_m: the temperature that is gas measurement is made,
$I_z(T_m)$: raw signal for zero concentration at Tm,
$I_z(T_0)$: raw signal for zero concentration at T0,
I/°C : baseline response to temperature.
All currents values units are in nA.

I_z at the T_m is the baseline output at non-exposure gas (zero concentration) that is corrected at the equation 7. Since we are able to directly measure the output signal in mV, the current under each temperature is calculated through TIA gain and external resistor. Equations eq. (5) and eq. (6) indicate the calculation.

$$\text{Sensitivity code } \left(\frac{nA}{ppm}\right) Gas\ concentration\ span(ppm) = sensor\ output\ current \quad (5)$$

$$V_{out}(\text{mV at 0 ppm}) = sensor\ output\ current\ \times R_{TIA} + V_{ref} \quad (6)$$

Where:

V_{ref} for NO_2 is:

$$V_{ref} = 0.67 \times V_{cc}$$

V_{ref} for CO is:

$$V_{ref} = 0.2 \times V_{cc}$$

Where:
V_{cc} = 3.3 V.
The minimum span for the CO is 1000 ppm and this is 20 ppm NO_2. Gas sensitivity is constant for each gas sensor and is obtained from the data sheet. In NO_2, R_{TIA} is replaced with R_{ext}. When the baseline is corrected, the output signal must be self-calibrated and shows the current 0ppm at any environmental conditions.

Correct the net span:

When the output signal exhibits the correct signal value for non-exposure status, the calibration is extended to cover the net span. Therefore, in eq. (7) and eq. (8) span is compensated under gas concentration:

$$I_c(T_m) = I_u(T_m) - I_z(T_m) \quad (7)$$

Where:
$I_c(T_m)$: is zero corrected signal at measurement temperature,
$I_u(T_m)$: is uncorrected signal for concentration at Tm.

$$ppm = (\frac{1}{CF}) \times I_c(T_m) \times [1- (\frac{\%}{°C}) \times (T_m - T_0)] \quad (8)$$

Where:
CF: calibration factor nA/ppm at the experiment temperature,
%/°C: span temperature correction factor is extracted from Fig.4.9 (bottom),
CF: is dedicated to each sensor even for the same gas sensors. This value is written at the back side of each sensor by the manufacturer and is necessary in calibration process.

After these two steps, the obtained output signal is corrected and indicates on real compensated output signal.

The implemented version of the device in two layers is shown in Fig. 5-16.

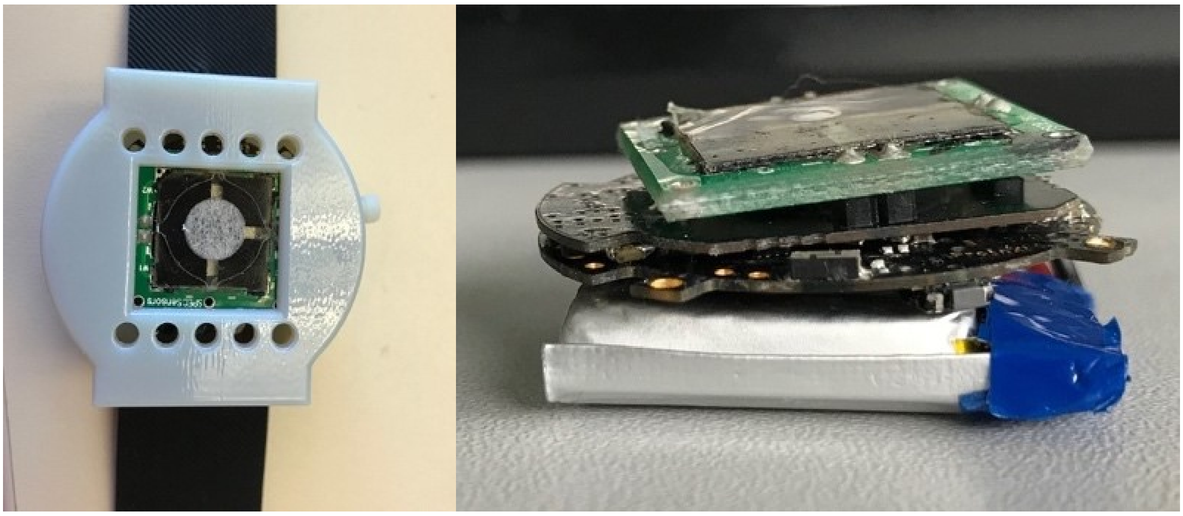

Fig. 5-16 Implemented version of device with replaceable gas sensor in two layers.

5.2.8 Experimental Results: CO

The efficiency and performance of CO sensor and driver are evaluated in several parameters. Depending on the application of the device and where it is used, effective elements might be bolded. When sensor is exposed to the toxic gas, the quick detection is coming to the first priority as the long exposure may lead to death. The time that is required by the sensor to react to the hazardous gas and generates the output signal, is called response time.

The second parameter that is worth to pay attention to, is the required time by the sensor to reach from a non-zero value ppm to 0 ppm (when the gas is removed) and sensor is ready for the next measurement, this is called recovery time.

This is important in environments such chemical laboratories, which measuring the gas is performed in close intervals (seconds). Response time and recovery time are evaluated in the Fig. 5-17 for CO gas sensor. In this investigation, wide range for the CO gas is covered (0 – 1620 ppm). While the degree of danger and the adverse effect on health at each level of concentration is different, thus the majority of experiments are performed in the range of 0 300 ppm.

Resolution stands as the next valuable factor in the experiments. The resolution is divided into two areas, 0 - 30 ppm with resolution of 7.5 ppm and 30 1620 ppm with resolution of 5 ppm. This resolution might be improved to 1 ppm as well, but at the moment it is not a priority.

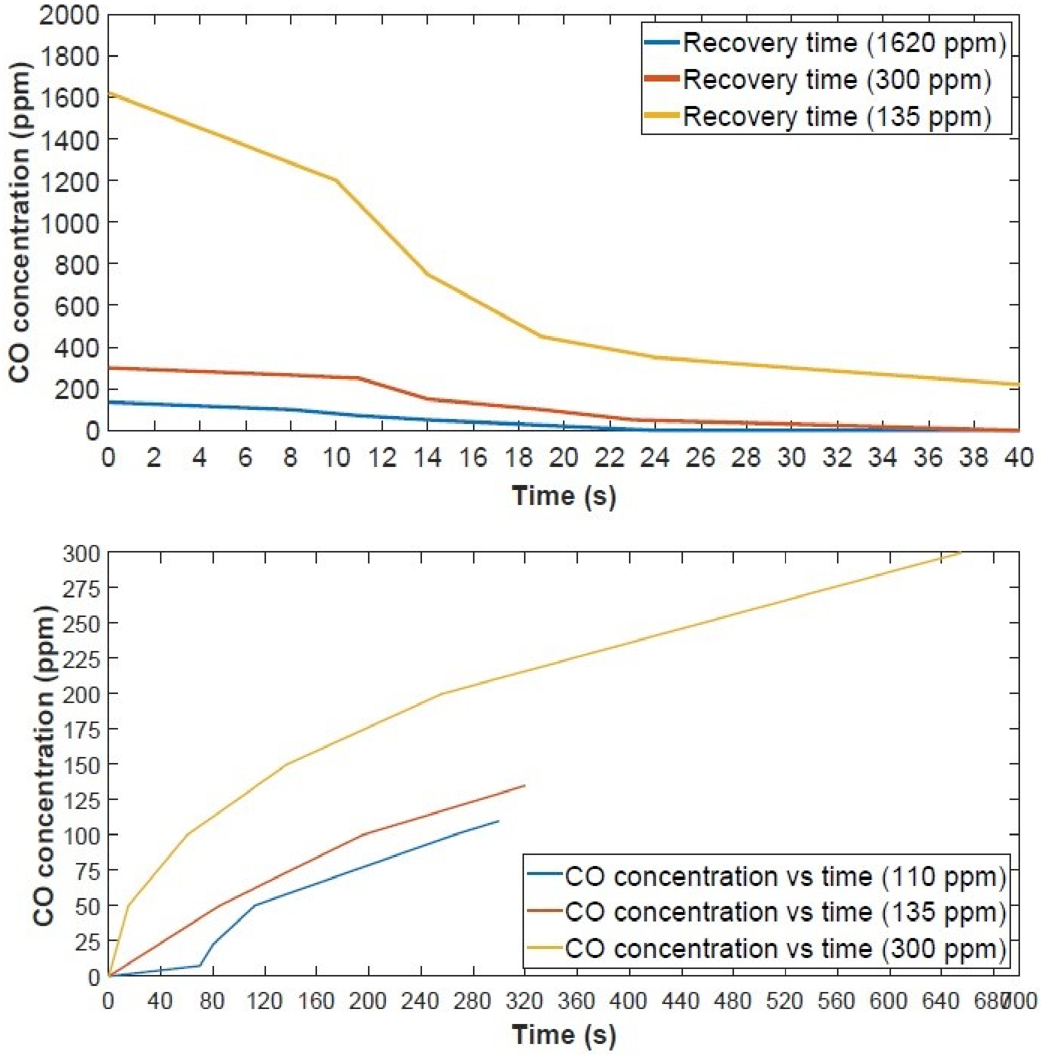

Fig. 5-17 Evaluated recovery time (top) and response time (bottom) under three CO concentration.

In Fig. 5-19 mean values and standard deviation are depicted where the experiment has been repeated for 10 times after calibration process. The test environment was celisca laboratories 1, 2 in Rostock University (Germany) [213]. The temperature was between 19 °C and 28 °C at 38% RH and 1atm.
(It is mentionable that, possibility of test error between 1–2% due to human performance is considerable).

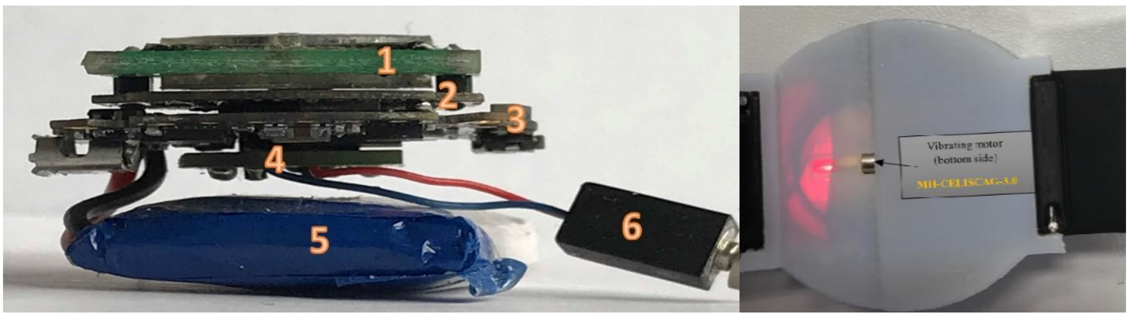

Fig. 5-18 Three-layer sensor node with notification system driver and vibrating motor (left). Back side of case (right).

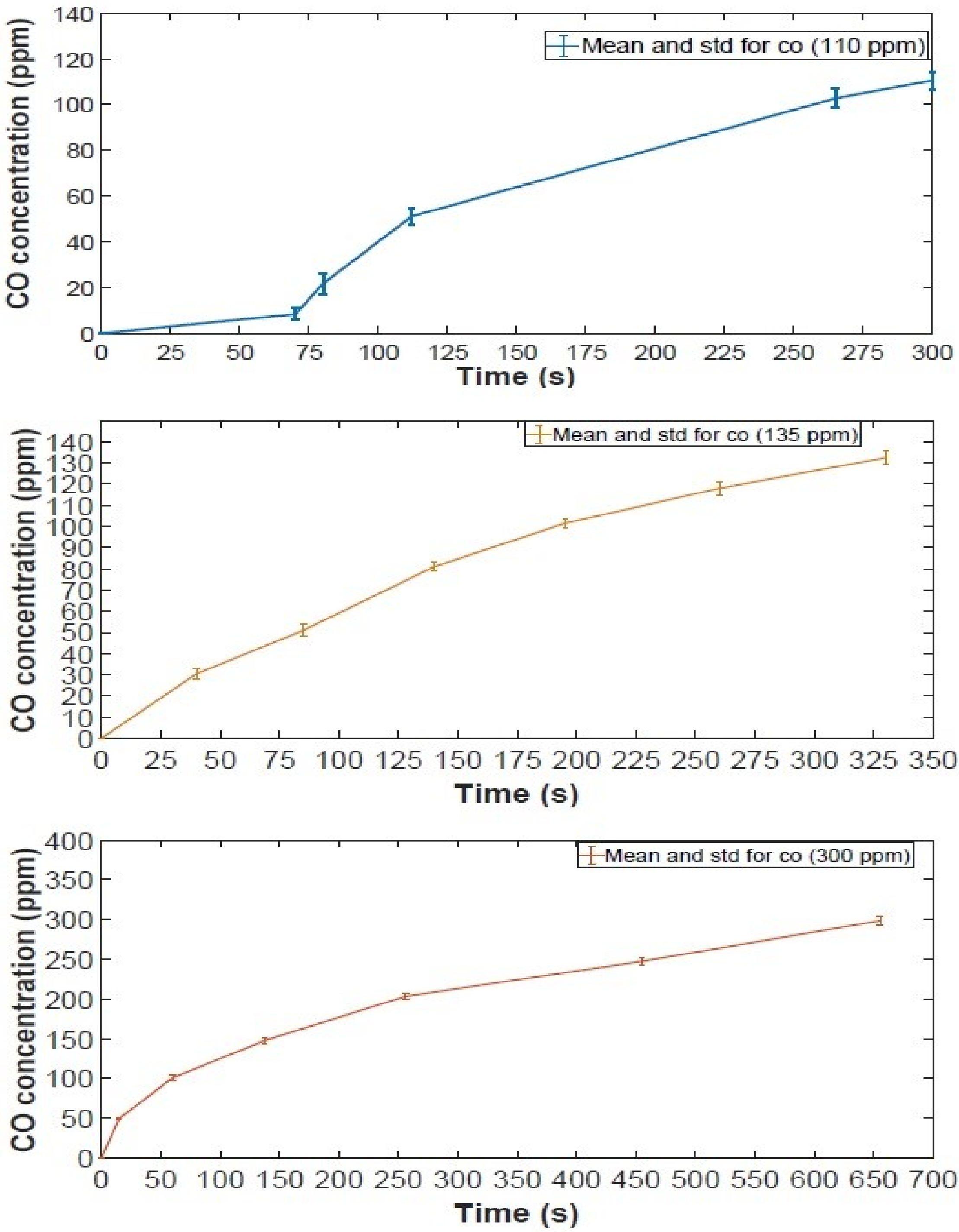

Fig. 5-19 Evaluation of mean value and standard deviation under 110, 135 and 300 ppm CO concentration.

Steady estate

Some technical points and observations are listed briefly by taking a closer look at the CO gas behavior under the experimental tests.

To bring the experimental results into the linearity scope, the resolution is provided in two scales:

The resolution is 7.5 ppm for concentrations < 50 ppm and 5 ppm for concentrations > 50 ppm up to 1,620 ppm.

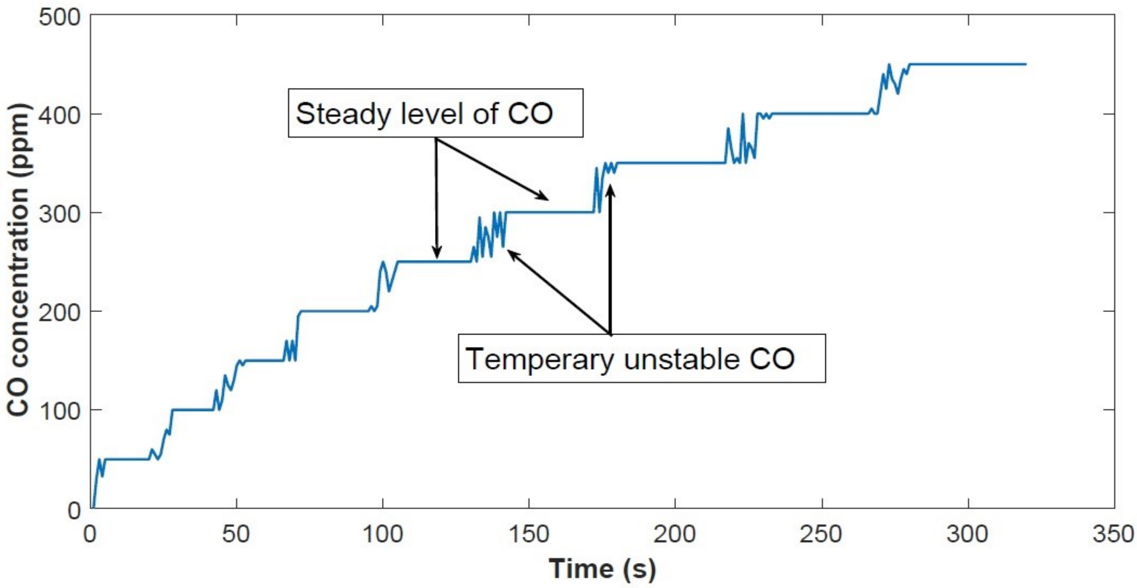

Fig. 5-20 Stable level and halt time for 1,620 ppm concentration (for the detail description refer to *).

*During the experiment, several significant observations were perceived:

- The key point in resolution and the correct recorded values is the time. All measurements under different gas concentrations must be recorded for the same time. For example, the time for 110 ppm and 300 ppm to reach from non-exposure gas to 50 ppm is quite different. Therefore, always for each measurement, time and concentration must be mentioned to validate the values.
- In Fig. 5-20, two states of values are differentiated called: steady state and temporary unstable level. Depending on gas concentration, this situation might occur or not. Steady state is defined as the time that gas sensor value is quite fixed and stable. Sometime before and after, the gas values are swinging to reach the steady state.
- The unstable states of the gas measurement are an area before reaching to the steady state level. In fact, it follows the pattern to reach the stable level quickly. In a very high concentration, the unsteady points are not involved in the measurement at the beginning of the test and the concentration values monitoring are observed clear and straight.
- Calibration process of the prototype has been demonstrated in conjunction with well-known BW CLIP [214]. This calibrator is limited to 300 ppm (used for data validation).
- In Table 5-3, a general measurement comparison is provided for prototype accuracy assessment and data validation. The majority of the measurements are covering the calibrator instrument results. With the obtained results, accuracy of the monitoring results is higher than 93.3 %. This accuracy is strongly being the function of "when the data are read by the individual"- The majority of tests are concluded and recorded within 5 minutes. In addition, the experiment conditions may influence the results.
- The average time to read the concentration value is 5 minutes. This time may be varied to 10 minutes as well. Due to structure of electrochemical sensors, the more device is kept exposed to the target gas, more the recorded value is close to the final saturation concentration, but in majority of the cases, evaluation reaches to the 75-80 % of the final result at the first 5 minutes.
- Due to the power consumption, data are sent to the smartphone every two minutes, therefore, power is saved and with each data transient, the observed data on the smartphone are getting closer to the final results.

Table 5-2 Comparison of prototype results with the calibrator.

MLMS-EMGN-3.1 (ppm)	45	67.5	105	115	150	302
Calibrator (ppm)	42	65	111	126	152	300

5.2.9 Experimental Results: NO_2

NO_2 is an extremely reactive gas belongs to oxidizing gas families. Working and calibration of this gas sensor demand precise setting and configuration. The initial bias voltage is set to maximum (67%) of the supply (reference) voltage. The gain adjustment require an external resistor placement (499 k ohm). The purpose of voltage reference design and gain unity buffer mostly is to cover the reactive and oxidizing gases. The NO_2 was tested in chemical laboratories by technicians and different groups of biology students to measure the generated NO_2 from the opening vessels.

Each vessel depending on the material which has been filled with, contains different gas concentration. So that before experimental results, it is expected that the prototype should record different concentrations. This test was in the laboratories under the room temperature and in a realistic demonstration. The user does not access to the logged data and cannot change any of the gas setting configuration. The wearer is only carrying the prototype and at the end the recorded data are investigated from the smartphone.

The first results of test is shown in Fig. 5-21:

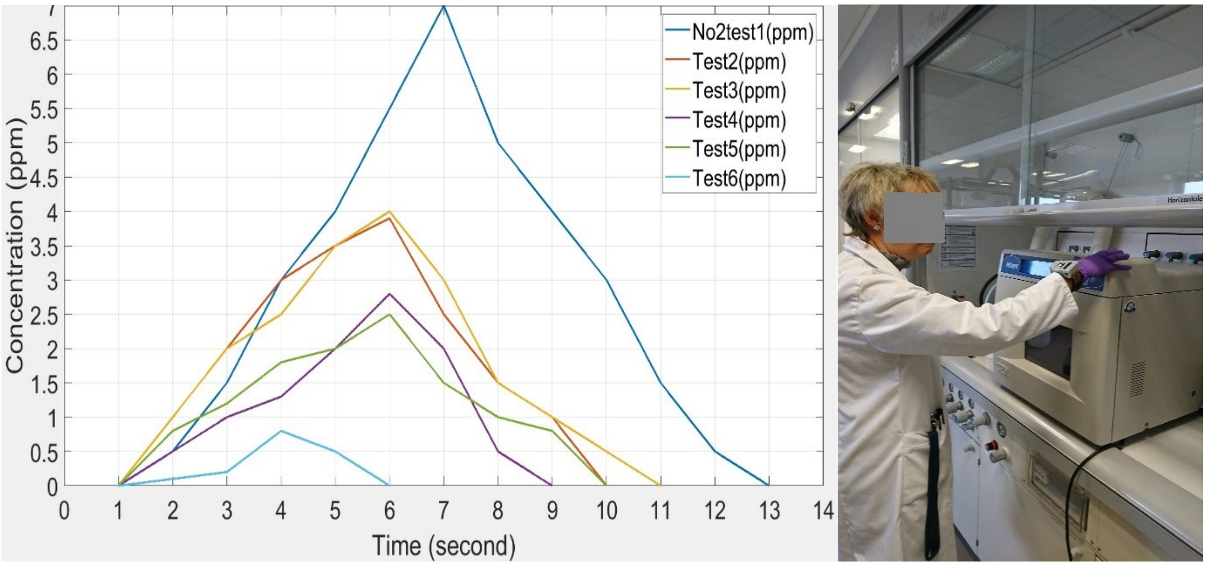

Fig. 5-21 The experimental results for NO_2 tests.

The recorded values in Fig. 5-21 are for six opening vessels. Each color indicates on a vessel and the recorded concentrations are according to random measurement of the vessels. Response time, recovery time, maximum and minimum concentration of the tests are clearly depicted on the figure.

In the second test of sensor node for NO_2 detection, ten vessels each contains different rate of gas concentration were considered. In this test, the time interval between opening each two vessels almost can be ignored. Vessels were opened one after another continuously. However, the next vessel become open to release the gas if and only if the previous vessel gas was completely leaked out. Duration of test was approximately fifteen minutes. Due to high number of vessels and fast test, and for data validation in this test, the sampling rate was increased to 0.25 Hz. It means every four seconds one sampled was collected that lead to 201 samples.

In Fig. 5-22 some gaps are seen that indicates on zero ppm, this mostly is the time between the end of test for the vessel 1 and reaction time to open and detects the vessel 2.

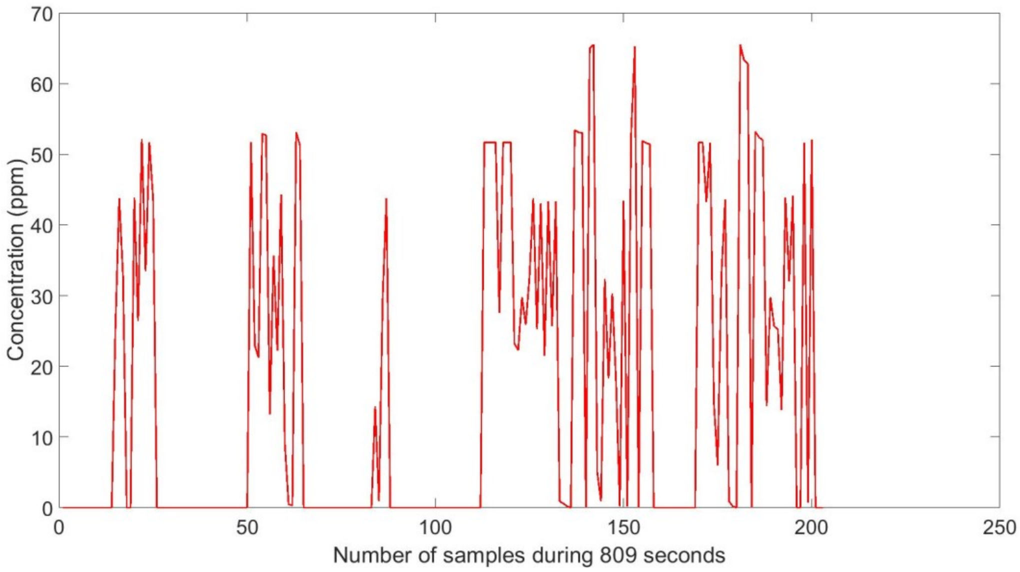

Fig. 5-22 Results of second test of NO_2.

In the test that was performed in the laboratory for the measurement of NO_2 digestion, seven vessels were available. The duration of this test was approximately fifteen minutes and seven vessels were opened in sequence with a time interval of 10 -15 seconds between each two. The released volume of gas from each vessel was different and varied between 0 to 52.70 ppm.

In this test the sampling rate was set to 1 Hz to collect the majority of data without lost. The lowest concentration is recorded for the vessel number 3 and the most risky situation was observed while opening the vessel number 4.

The notification system was activated in type two mode (highest degree of risk).

Recovery time and response time are depicted as well in Fig. 5-23. It is observed that the longer recovery time is a consequence of exposure to higher gas concentration for longer. Thus, in vessel number 4, the response time is the least, the period of remaining in the peak of concentration in the longest and consequently the recovery time is the longest in contrast with other vessels. This correlation is perceived in the rest of vessels observation. The rate of recovery time and also the stability are briefly discussed. In fact, the rate of recovery time is the function of concentration, duration of exposure, and the removing source of gas. This means if the source of gas is instantly removed, thus the recovery starts immediately.

Furthermore, whatever the aforementioned parameters above are longer (duration of exposure) and higher (gas concentration), reaching stability (0 ppm) is taking longer. This is the reason the swinging waves are observed in vessels 2, 4, and 6.

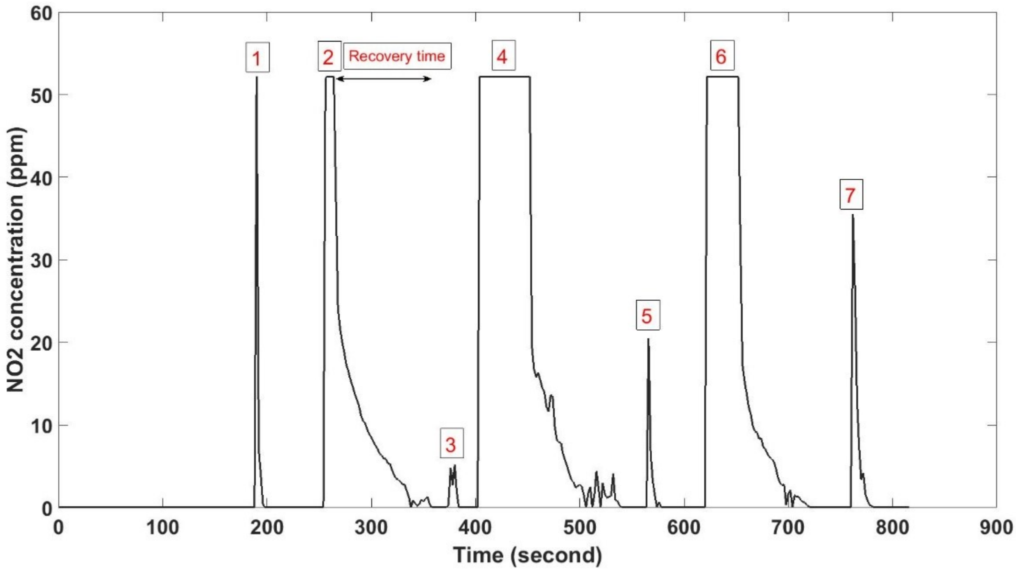

Fig. 5-23 Results of test for 7 vessels containing of NO_2. Duration of this experiment is fifteen minutes with the sampling rate of 1 Hz.

The nature and instruction for No_2 detection in following test is different than the previous test. In this test, the Nitric acid is manually pipetting to cupper which leads to NO_2 production. The technician who was demonstrating this instruction worn the prototype and the smartphone for the data logging was located in the range of BLE coverage. The sampled and transmitted data to the smartphone are seen in Fig. 5-24 (a) for NO_2 and Fig. 5-24 (b) for noise detection (will be discussed in detail in the next chapter) simultaneously. Technician would added Nitric acid in different dozes to the cupper (locating in a container for safety) gradually and resulted in NO_2 production after the chemical reaction. This was performed in 3 major general tests (3 piece of copper) with random acid volume and random time interval between each two pipetting during approximately 22 minutes. The NO_2 boundary is limited between 0 and 52 ppm. Adding higher doze of acid to cupper accelerating the chemical reaction (until the metal is disappeared due to reaction). This is the reason for continuous multi-level measurement of NO_2 with various concentrations in Fig. 5-24 (a). As it is observed, at some points (twice in part 1, three times in part 2 and once in part 3), the acid has been added before the measurement from the previous reaction reaches to 0 ppm which indicates the performance and proper detection of the prototype.

In addition, the generated noise (sound level) by different machines and facilities in the laboratories and technicians were measured as well. The recorded values indicate a noisy environment with sound level is between 40 to 77 dB in this test.

Noise detection and experimental results are discussed in detail in Chapter 6.

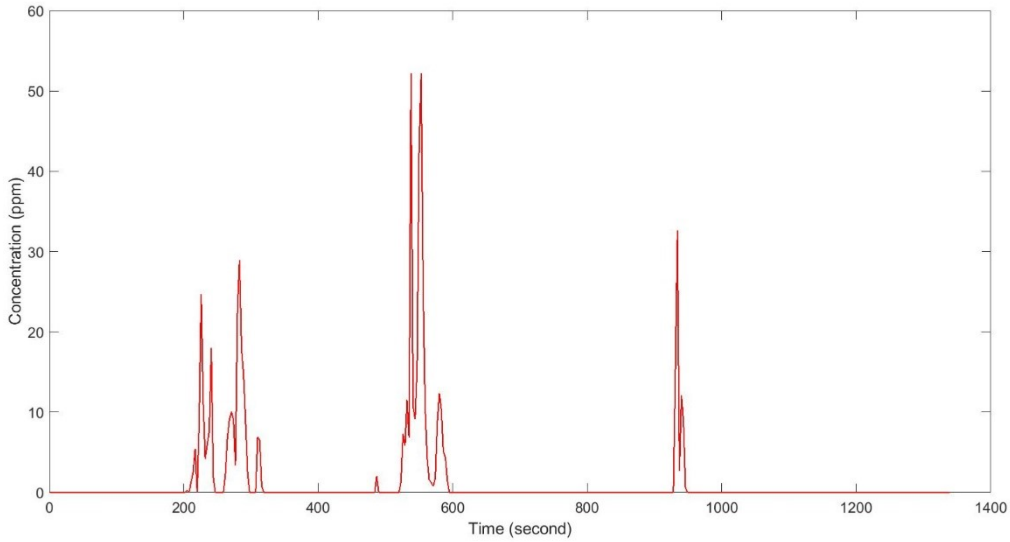

(a)

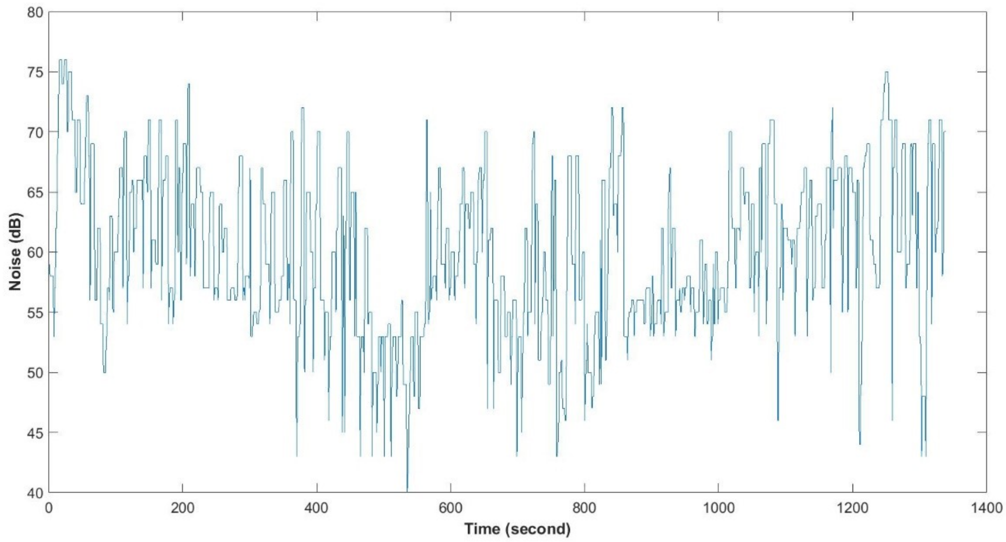

(b)

Fig. 5-24 Manual chemical procedure for NO_2 detecting (a) and noise test (b). This experiment was conducted in 22 minutes with the sampling rate of one Hz and two Hz for NO_2 and sound detection respectively.

6 SOUND Monitoring MODULE

During the development process, to demonstrate the MLMS approach, the gas sensor node as the top layer that is connected to the main host platform is designed and implemented to construct the second layer. Sound level module is implemented after the gas sensor. The module is connected to the host platform through hardware interface attached to the tail. This module is implementing vertically at the side of the prototype with outside oriented microphone.
The sound module and display both are communicating to the host platform directly but are attached to the solution via hardware interface. To integrate the sound module in the system in this section, the gas sensor node is removed, and hardware interface is located directly to the host platform. So that gas sensor node is again located on top of hardware interface. Sound module is connected to the tail of hardware interface and hereafter is adopted mechanically and also as the data acquisition sensor (see chapter realization for hardware interface detail).

Several analog and digital sound level modules are already commercially available in the market. The most challenging parts of sound level module selection, in addition to performance are sufficient gain, compatible power consumption, quality of signal and the size of module. The limited height and length of the final prototype's chassis restricts the designer for module selection. A trade is made between sensitivity, performance, price, supported power supply and the scale of module to finalize the module. This step already verified in chapter 3 and 4. Hereafter, the sound module implementation, hardware redesign, data validation, calibration and experimental results are discussed in detail.

6.1 SOUND MODULE IMPLEMENTATION AND STEPS

The sound level detection is the second part of major concentration of this proposed device (the first part is hazardous gases). Generally, in sound level detection, three steps (decisions) are involved:

- Hardware adoption,
- Data conversion,
- Data validation and calibration.

The criteria, features and specifications that lead to a sound module selection, were discussed in previous chapters. Sound Module Analogue V.2 was selected for the hardware adoption. With a light hardware refining, it's located and adopted readily into the system.

6.1.1 Sound Module Positioning

It is very critical to decide for sound module positioning to still keep the solution compact and light-weighted with high quality signal acquisition. As was discussed in realization and concept chapters, to avoid height extension, the sound module is linked to the host platform through hardware flex interface. Thus, the sound module is carefully located in side of the prototype and positioned on the wall of the case. It is firm and also avoid size extension. The microphone is outside oriented to measure the environmental noises. The sound module is located vertically in the front of the whole solution, edge by edge of display and hardware flex. Both versions of hardware interface were considered to implement the prototype.

6.1.2 Sound Module Conversion And Calibration

The output signal of the sound module is in analogous. To obtain an adequate signal for feeding to microcontroller's 1-wire pin (selected for receiving the signal from the sound module), there are two steps in hardware and software sides to be performed. Before calibration, due to the size of module, it must be modified in both height and length and be adjusted with the final prototype device. Furthermore, as the module is used with the 3.3 v power supply, the gain has to be redesigned to compensate the amplification process.

6.1.2.1 Hardware Redesign And Gain Adjustment

Although the sound module is operating in the range of 3-5 V, but it is utilized in 3.3 V due to host platform power supply. As a matter of fact, operation in lower level of power consumption reduces the amplification gain and the output signal detection is difficult. As a consequence, a circuit redesign in gain adjustment is performed. Furthermore, to implement the module in the chassis, the scale is shortened by 4 mm from each side which shrink the altitude of the module. To produce an amplified signal by the microphone from one side and maintain the sensitivity from the other side, LM358 amplifier gain must be redesigned and regulated. The output gain (Av) is calculated for wide range of frequencies.

When signal amplification, sensitivity tuning and gain adjustment are completed, the signal is prepared to be passed to the microcontroller for further processing. For higher resolution and accuracy and to differentiate between each level of sound, a loop for signal accumulation and average generation was implemented to collect the raw signal sensed by the microphone. Basically, sound level conversion is a logarithmic mathematic function. This logarithmic function was implemented to map the very large scale of decimal values to a smaller area.
The application of logarithmic mathematical function maps the raw signals to the range of 406-492.

6.1.2.2 Sound Level Pattern And Equations

When the software implementation maps the data in smaller and readable values, a calibrator device is used for data conversion to sound level unit (dB) [215]. Both prototype and calibrator are located at the same place to measure the sound level. This procedure was demonstrated in celisca laboratories 1 and 2 for approximately 100 times to find a pattern for data conversion to dB.

6.1.2.3 Pattern Description

In general, this device is able to measure the sound levels between 32 to 93 dB. The calibration and data validation was performed at the distances of five, ten, and fifteen cm. Five patterns were extracted while experimental tests for this range. Both linear and non-linear equations are observed in the equations. Each equation covers partially a range of final conversion. The range between 406 - 407 and 408 - 413 are covered by two linear equations. The next two patterns are non-linear and cover the range of 414 - 417 and 418 - 433 respectively. The last and widest pattern is created by a linear equation which cover the range of 434 - 492.
Each unit represents one dB.
The equations and range of coverage are provided in Table 6-1 and Fig. 6-1 In the following:

Table 6-1 Equations and extracted patterns from data conversion.

Equation	Range of raw signal
$F(x) = 0.45x - 148.7 + k_1$	406-407
$= 01.82x - 706.66 + k_2$	408-413
$= 0.0002981x^{2} - 0.5800x - 223.59 + k_3$	414-417
$= -0.000176x^{2} + 0.6488x - 187.12 + k_4$	418-433
$= 0.63x - 211.8 + k_5$	434-492

The final step in the calibration process is to add constant value to the equation patterns for calibration and re-calibration. These constant values are experimentally obtained and are unique for each portion.

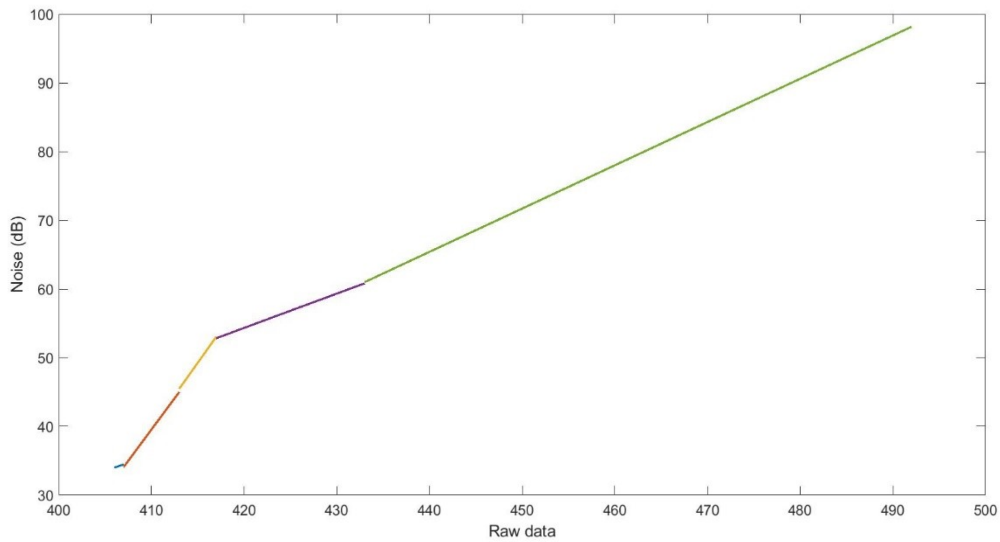

Fig. 6-1 Equations patterns for data conversion to sound level (dB).

The complete procedure of data conversion is depicted in Fig. 6-2. As it is observed, the raw data obtained from the microphone are going through the mathematical logarithmic function to map to a smaller scale. The second step is to add constant values to each range and eventually feed to scope of the equations is the final step. But care must be taken that, the signal gain adjustment and amplification is prior than these steps.

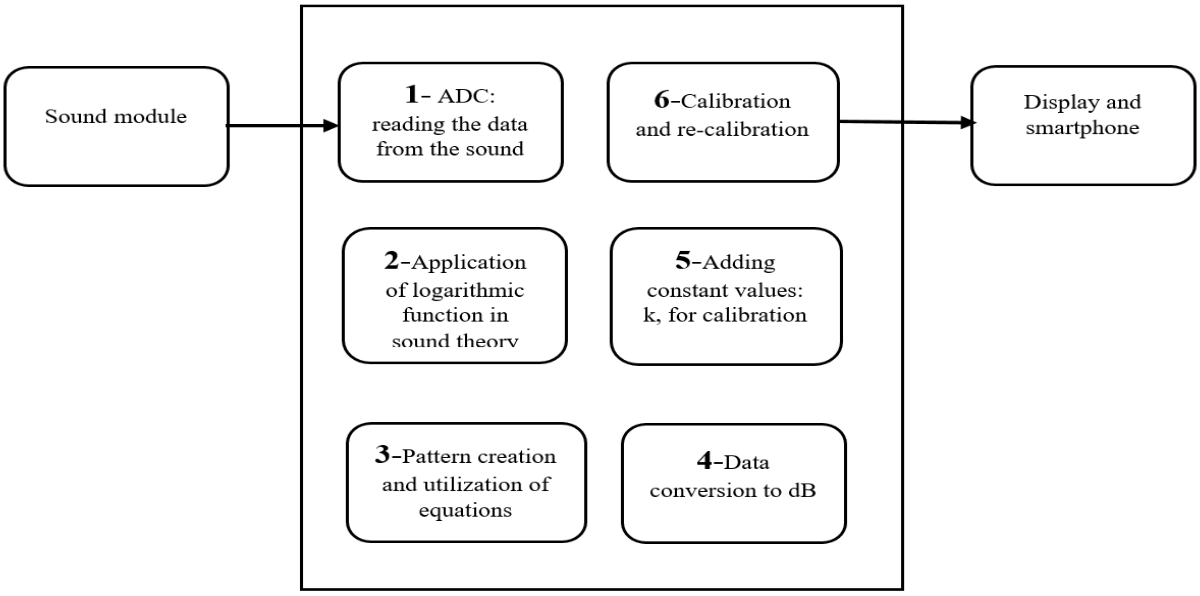

Fig. 6-2 Implemented procedure of data conversion to sound level (dB).

Fig. 6-3 depicts the prototype with 4 layers including replaceable gas sensor node, host platform hardware flex interface and the sound level module. The hardware interface is intermediated between the host platform and sound module to facilitate hardware connection. The hardware flex interface consists of 24 pins (exactly as the same with board to board connector) and reserves number of pins for further development in the future improvement. A completed version of the prototype is seen in Fig. 6-4 (with the latest version of hardware interface).

6.1.2.4 Recalibration

The recalibration is necessary for the prototype as it is a part of instruction for every commercial device as well. The period of re-calibration depends on various factors. The physical touch of microphone, environmental parameters (humidity) and changing the bias of sound module may changes the performance. Therefore as is seen in Table 6-1, different constant values for each linear and non-linear parts are considered (K_1, K_2, K_3, and k_4). If the device is calibrated these values are 0, each part can be separately recalibrated by adding/reducing values to each equation. K is a member of "Z" and therefore can be: $K > 0$, $K < 0$ or $K = 0$ (if calibrated).

Defining 4 calibration factors facilitate the re-calibration. Each part is independent of the other part and this improves the re-calibration efficiency and reduce the effort.

6.2 EXPERIMENTAL RESULTS

In this subsection, the experimental results of measuring the sound level in different realistic environments in compared with the calibrator and an android application are presented (all devices were calibrated before tests). It is mentionable that measuring sound level while calibration and data validation without distance is not significant. The experiments were demonstrated in several realistic environments by tens of people from different ages and working categories from children and primary students to master students, biologists and ordinary people who do not have an idea of the technical background for better feedback. The prototype has been tested for long time (>24 hrs) in several scenarios but due to the restricted space, only some of results are presented,

First a basic introduction to Sound Pressure Level (SPL) calculation and mathematical functions are briefly presented [216], [217], [218].

Basically, SPL is calculated by eq. (1):

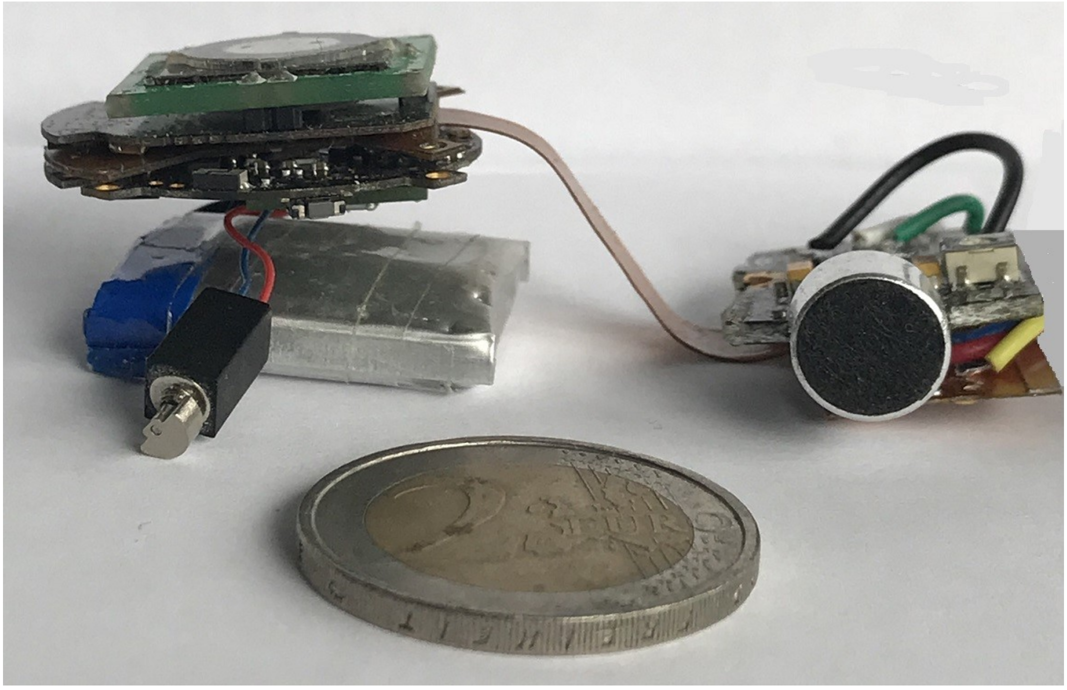

Fig. 6-3 The completed sound level and gas sensor solution in Multi-Sensor Multi-Layer approach.

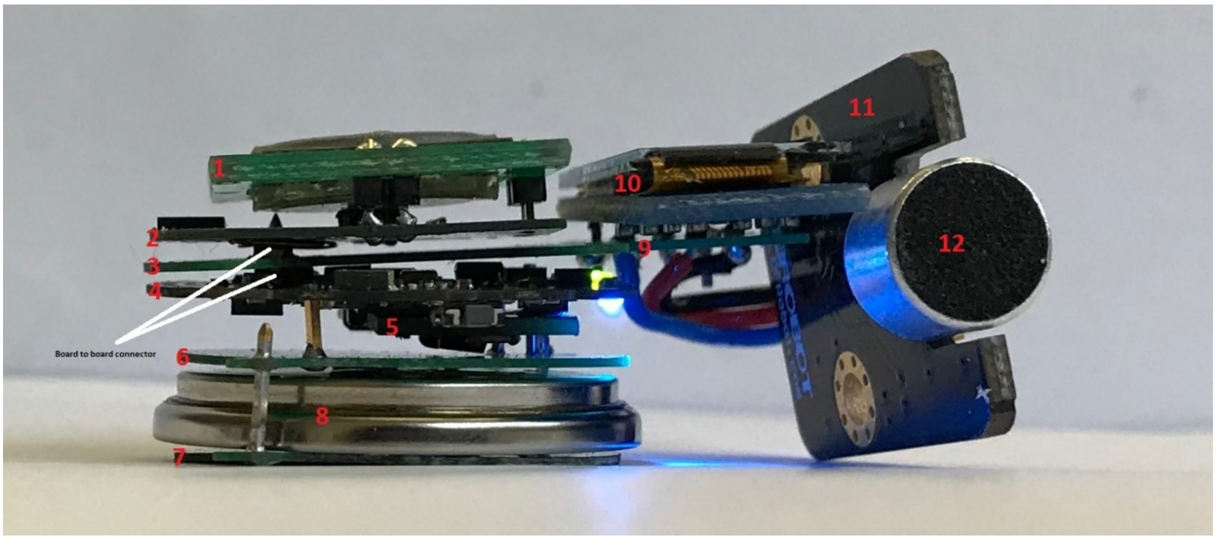

Fig. 6-4. The completed version of assembled prototype. First layer (1,2): gas sensor, gas sensor driver. Second layer (3,9): hardware flex interface, tail of hardware flex interface. Third layer (4): host platform. Fourth layer (5): notification system driver. Fifth layer (6,7,8): positive and negative pole of battery holder, coin cell battery. (10): display, (11): sound module, (12): microphone.

$$SPL = 20.\log_{10}(p_s/p_0) \qquad (1)$$

Where:
$P_0 = 2 * 10^{-5}$ Pa,
And ***Ps*** is pressure level directly sensed by the microphone. There is difference between sound pressure and sound intensity which is sound energy quantity. In this investigation, the concentration is on SPL calculation and observation. There are following equations on:

$$P_1 = 1/r_2,\ P_2 = 1/r_1 \tag{2}$$

Where ***P*** is pressure sensed on the microphone that is converted to signal proportionally and ***r*** is the distance between microphone and sound source. While this equation for sound intensity is changed as:

$$I = P^2 \tag{3}$$

Thus: Where I is sound level pressure, and from eq. (2) and eq. (3):

$$\left(\frac{r_1}{r_2}\right)^2 = \frac{I_2}{I_1} \tag{4}$$

Should have differentiated between sound intensity and sound level, sound level equation with distance is as:

$$L2 = L1 - 20.\log_{10}(r1/r2) \tag{5}$$

L1 and L2 are the sound level for the microphone 1 and 2 from the sound source in Fig. 6-5.

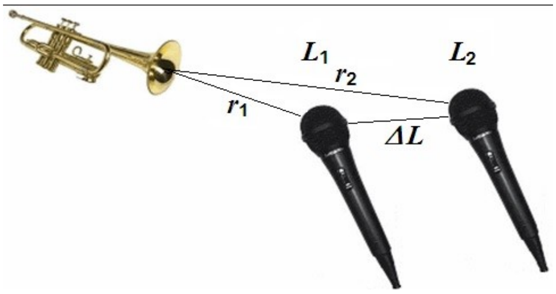

Fig. 6-5 Sound source, microphone and correlation. At the experimental tests, calibrator and device were placed at three different distances from the sound source. Distance between the two tools was 5 cm. The desired range of measurement is between 35 and 80 dB.

Hereafter the prototype device is called Multi-Layer Multi-sensor Environmental Monitoring (Gas, Noise) MLMS-EMGN-4.0 . 4 indicates on number of physical layer and 0 is the version of device. MLMS-EMGN-4.0 and calibrator tool (Brel & Kjr Sound Level Meter Investigator 2260, Denmark) are located in office 206 in celisca at the determined distance from the source. The results are presented in Table. 6-2. This test is demonstrated in 3 distances under the same conditions.

Table 6-2 Sound Level Measurement in three distances.

R_1 = 10 cm		R_2=20 cm		R_3=30 cm	
MLMS-EMGN	Calibrator	MLMS-EMGN	Calibrator	MLMS-EMGN	Calibrator
R_1	R_1	R_2	R_2	R_3	R_3
48	46.6	45	43.5	37	40
54	53.9	50	50.1	45	45.2
60	59.6	57	57.2	51	51.8
66	63	63	63	53	54.7
78	75	76	74	73	71.5

The second and third experiments were performed in analytical laboratory of Celisca with three various tools for better comparison. MLMS-EMGN-4.0, sound meter as an Android application (before using was calibrated) and 2260 calibrator are the three devices in these two experiments. The resolution for the MLMS-EMGN-4.0 is 1 dB, and the maximum error in the whole test is 4 dB (which occurs only twice during the tests). The rest of results are very close to the calibrator and in some cases, it is indicating the precise measurement (see Fig. 6-6).
The Fig. 6-7 is presented to notify the importance of constant values in calibration process. This test was performed under the same condition with the same tools in lab 1. As is observed this test has been recorded before final calibration process of MLMS-EMGN-4.0. A constant accuracy distance from the calibrator values are observed. This error is tackled with the added constant value in calibration process.

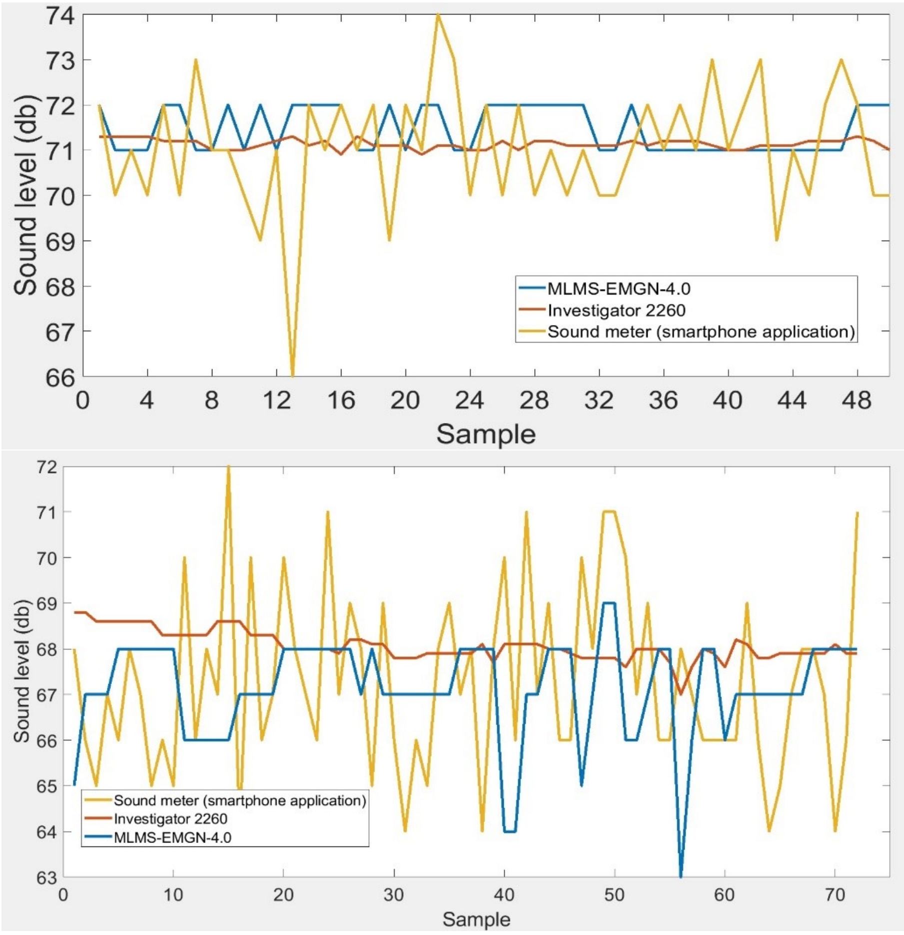

Fig. 6-6 Accuracy comparison of the prototype, calibrator and the android application in Lab.1, 2. This test was performed for 24 and 72 seconds repectively.

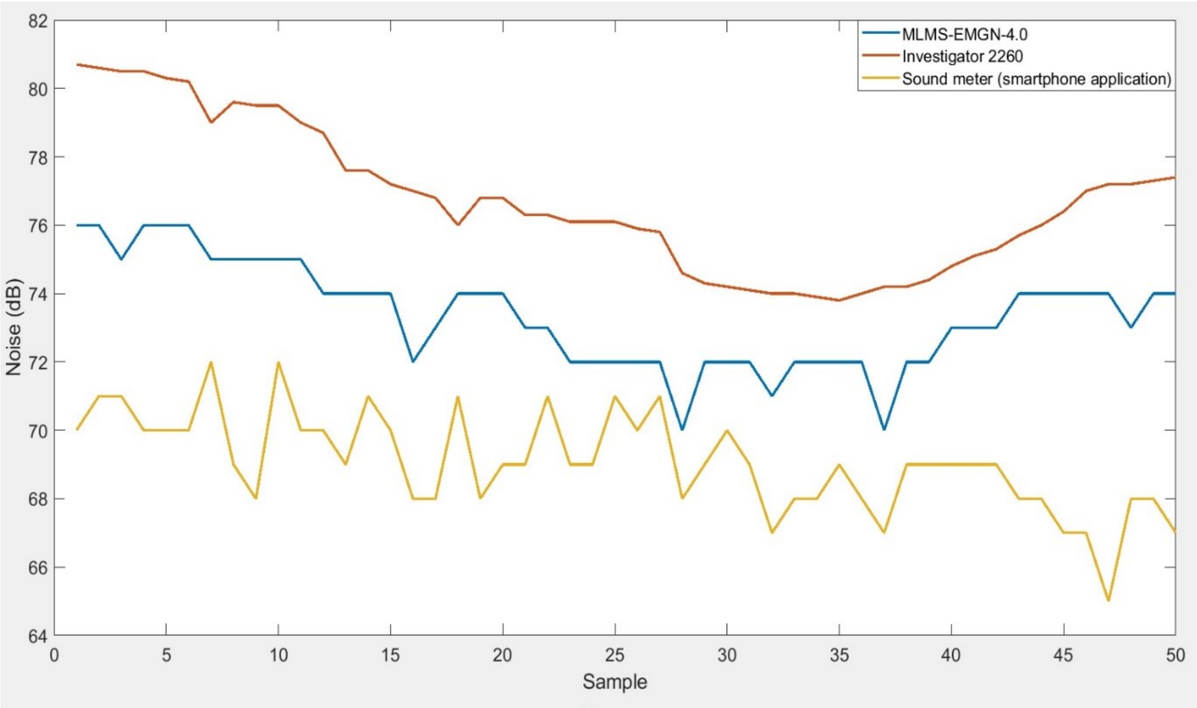

Fig. 6-7 Data conversion without constant values of calibration (the samples have been collected in 25 seconds).

After a careful prototype calibration in several hardware and software steps and data validation in comparison with the calibrator, the prototype is tested under realistic conditions during daily routine activities of individuals (indoor/outdoor). The latest version of the prototype was carried by several users for several days. However, due to large generated number of data, only a limited data are shown in Fig. 6-8, Fig. 6-10 and Fig. 6-11 to support the performance of the prototype. To differentiate the variation of noise levels in indoor and outdoor environment and to identify the efficiency of the prototype, one minute sampling in 4 status of indoor/outdoor and walking/cycling/sitting and in general a daily routing of an individual are presented. The presented data show the results of two test days with two users under various conditions (see Fig. 6-8 and Fig. 6-11). The first day included user tests in an indoor environment for 8 hours. The test was started at 8:30 am and ended at 4:30 pm. The individual performed a typical daily activities in two floors, several offices and laboratories. The prototype was carried during the lunch time as well. The notification system's threshold was 70 dB for > 1 hour exposure. User notification was activated at 11:30 am. A disconnection was experienced due to long distance between the smartphone and the sensor device.

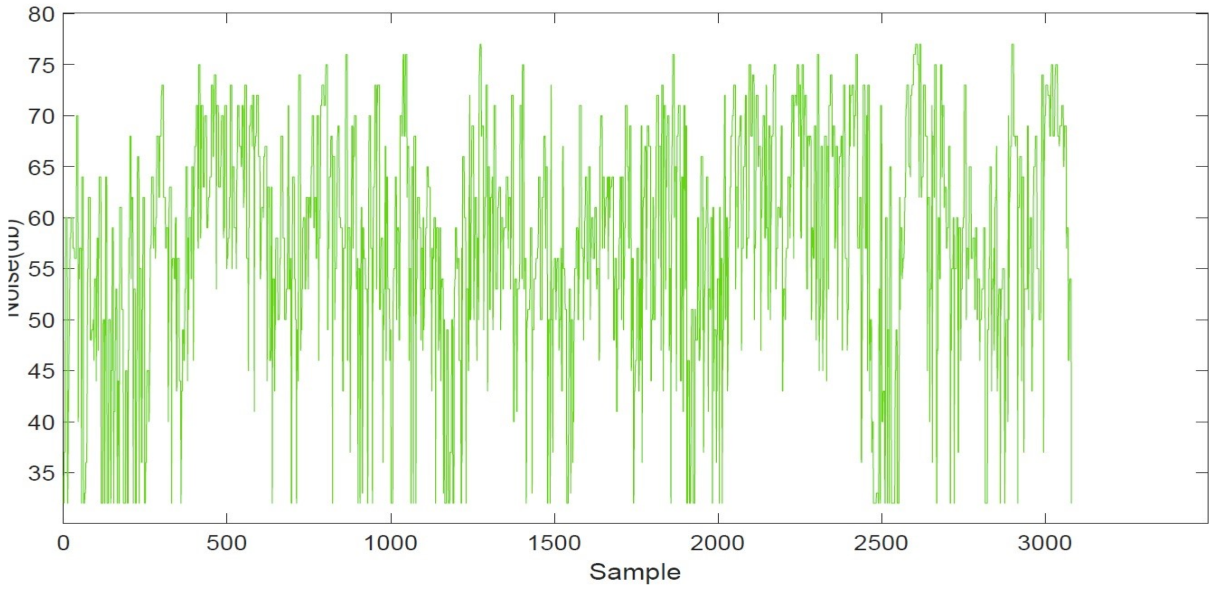

Fig. 6-8. The result of first day test (indoor), Sampling rate is set to two Hz.

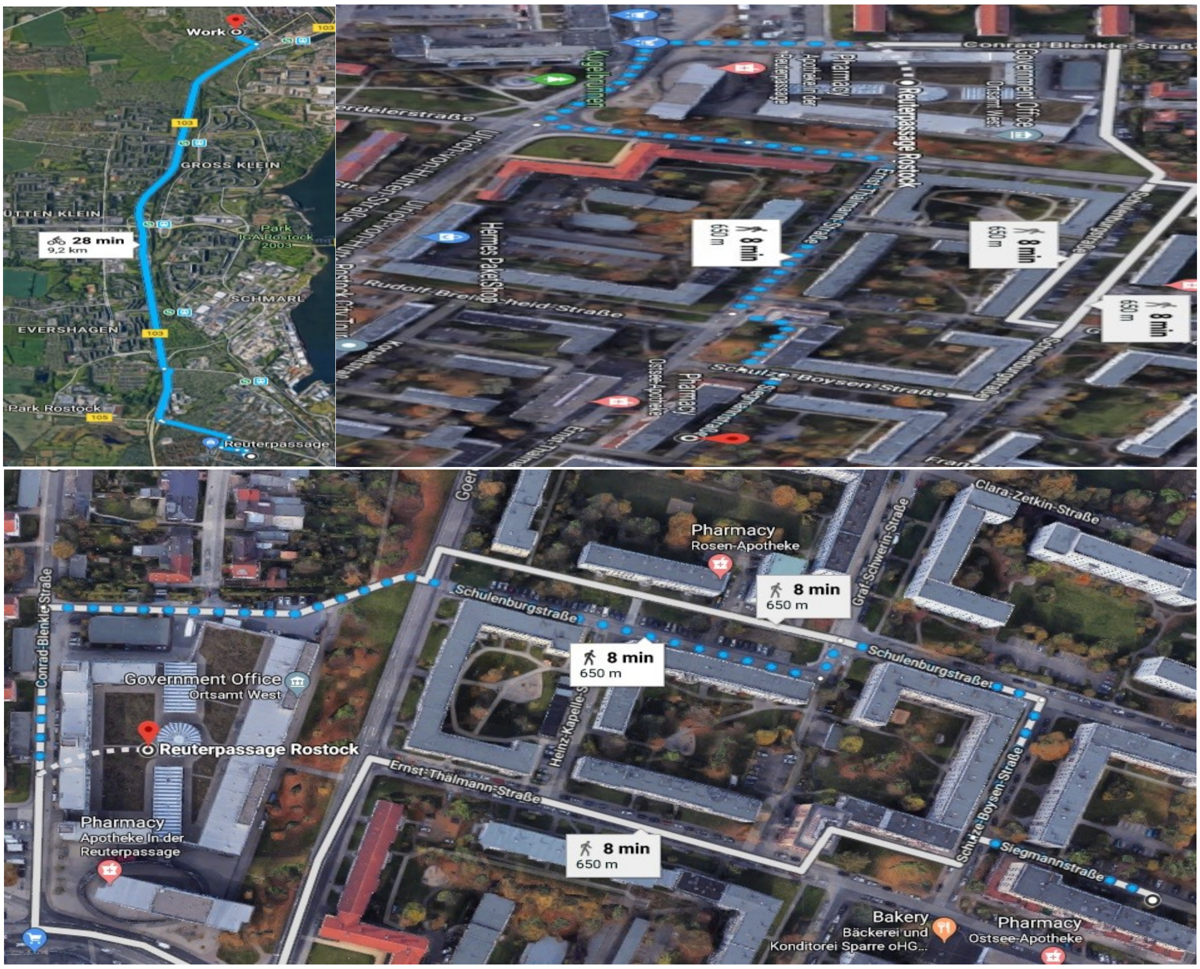

Fig. 6-9. The routes and transportation modes of the second test.

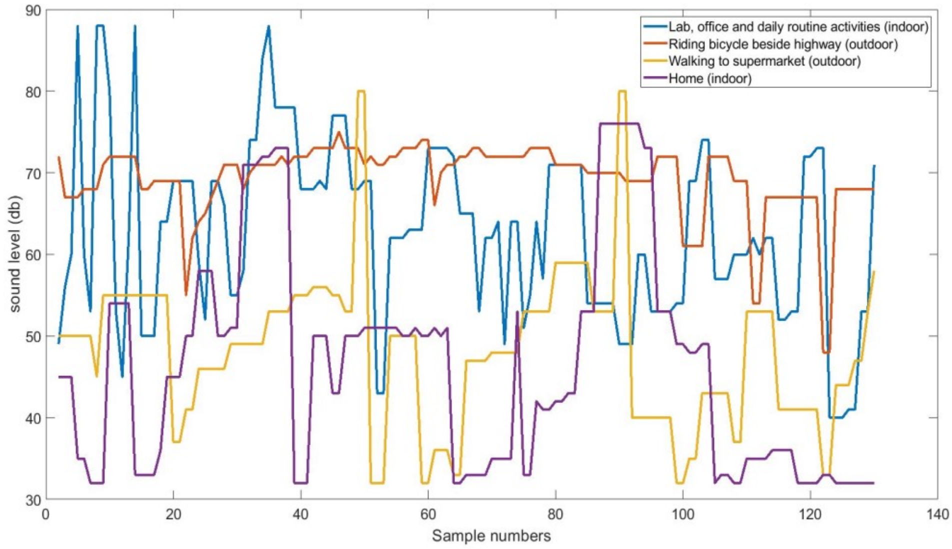

Fig. 6-10. The sound level test under a daily routine activities (indoor/outdoor) with two Hz sampling rate in 65 seconds collecting 130 samples.

The results are from indoor and outdoor under different modes of transportation and various conditions and area of the city (Fig. 6-9). For a clear perspective of the noise measurements, the average noise measurement also is added to Fig. 6-11 (bottom).

The second day included tests in outdoor and indoor environment under three modes of riding bicycle, walking and being at home. The wearer carried the prototype for almost 30 minutes cycling, 20 minutes walking in streets to supermarket for shopping and 2.5 hours at home (see Fig. 6-9). 1 minute sampling from the first day and 3 minutes noise evaluation in second day (1 minute in each mode) are shown in Fig. 6-10. The data presented are the complete day test without specific parameters consideration. The noise is swinging between 32 (the lower boundary detection of the prototype) to 80 dB.

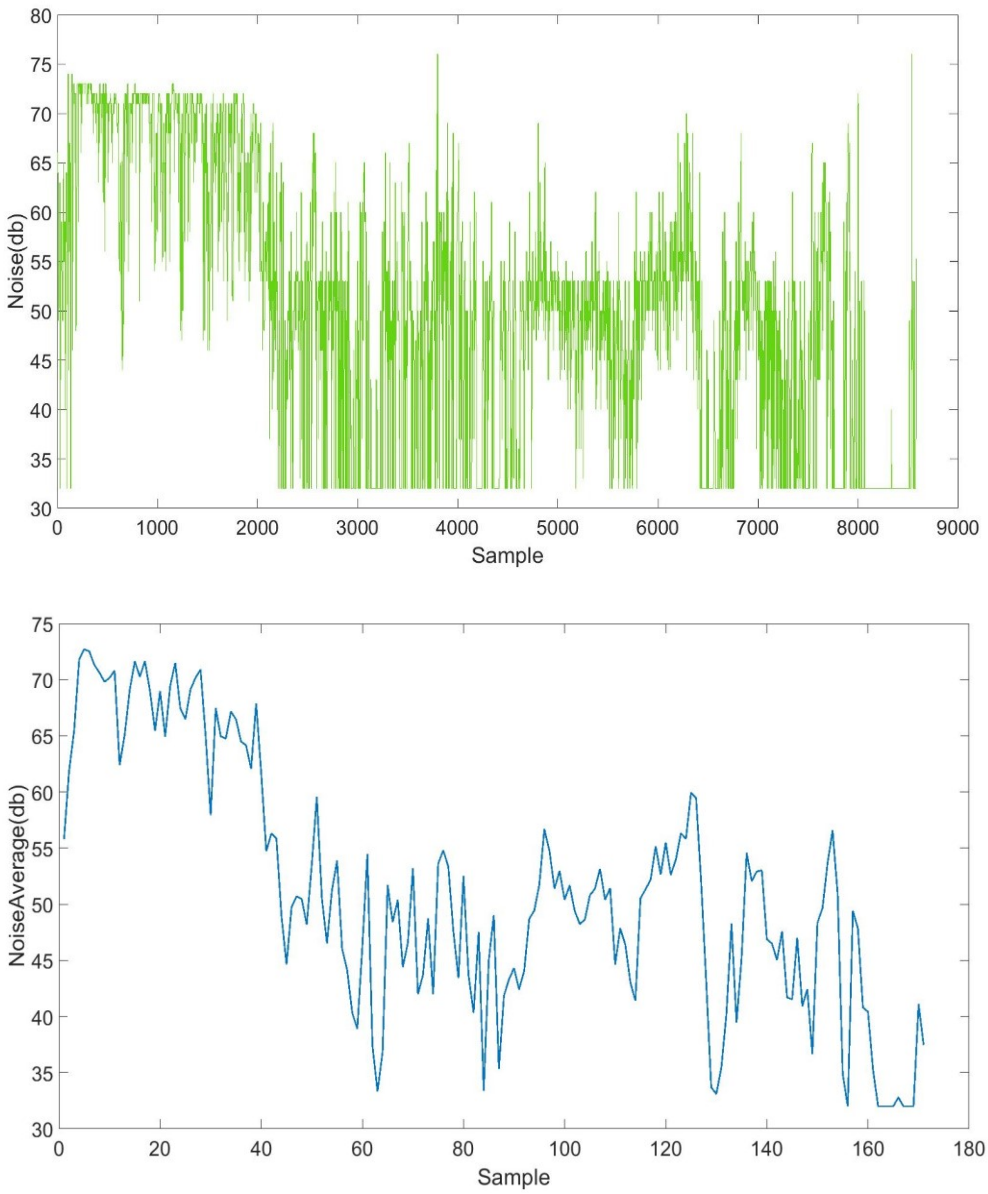

Fig. 6-11. The result of part of first day test during 75 minutes with sampling rate of two Hz (indoor), instant values (top), average (bottom).

A realistic day test is demonstrated in different mode of activities and transportations and in various places as well. In this test the subject worn the prototype at 4:30 P.M. in the afternoon and start his daily routing from Warnemunde Werft from the office. The subject walks to the bus station through the street and passes the highway and reaches to the bus station. He waits for the bus for 10-12 minutes and then gets on bus for the approximately 18 minutes. The subject leaves the bus and walk to the train station to follow his way. After 5 minutes of riding train, he gets off and walks to the tram station for 1 minute. Riding tram takes approximately 8 minutes and the subject continue to his plan by walking to a restaurant. Spending nearly two hours at restaurant and having his dinner is the next plan. At the end of this experiment (part 1) subject walks back home and spend the rest of his time from 8:20 P.M. at home for personal stuff. During home time, the prototype was placed at the kitchen. Watching TV, listening to music and etc. was part of the subject's routine (see Fig. 6-12).

This experiment lasted for 27 hours and 40 minutes up to the next day 20:10 P.M. Due to the lack of space and huge number of data and figures, it is avoided to bring it here. The data was logged in external memory after the smartphone went low level of battery.

The average of sound level for each part of this experiment is recorded under each figure (see figure 6-13 (a) to (i)).

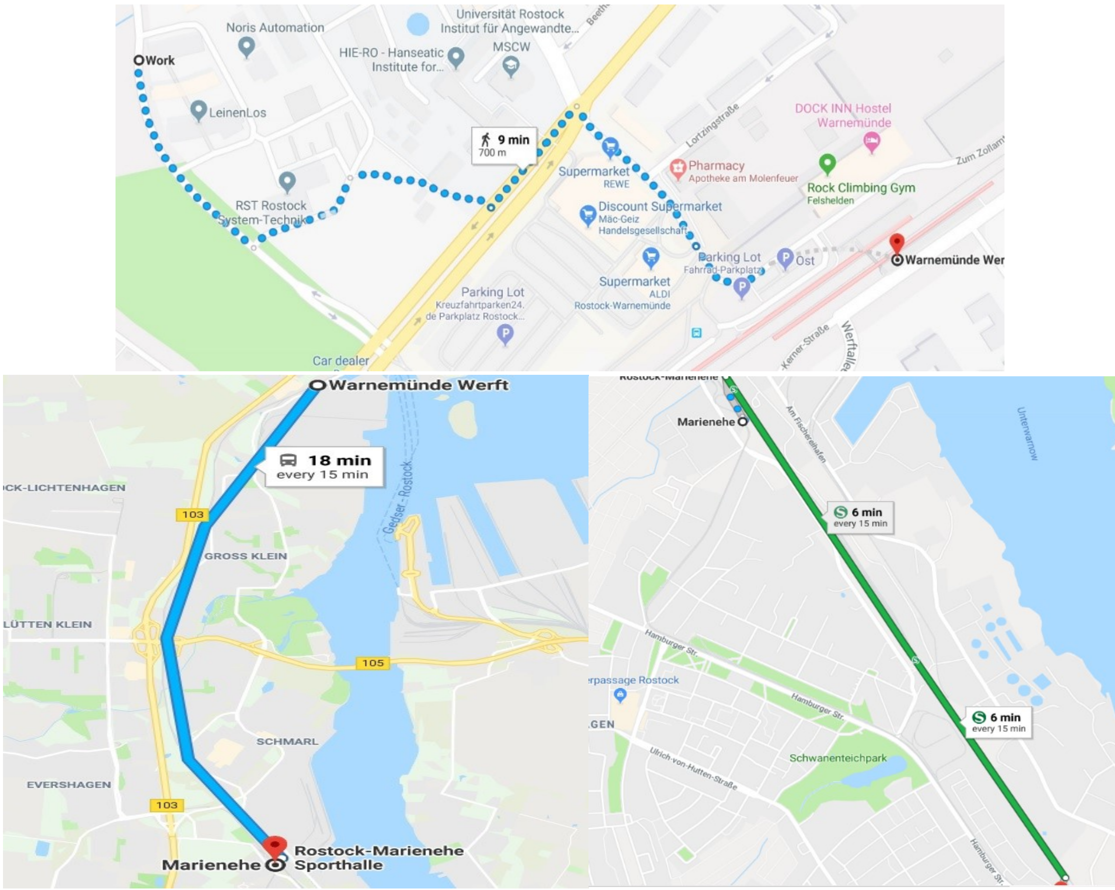

Fig. 6-12-(a) The route of subject during the prototype usage.

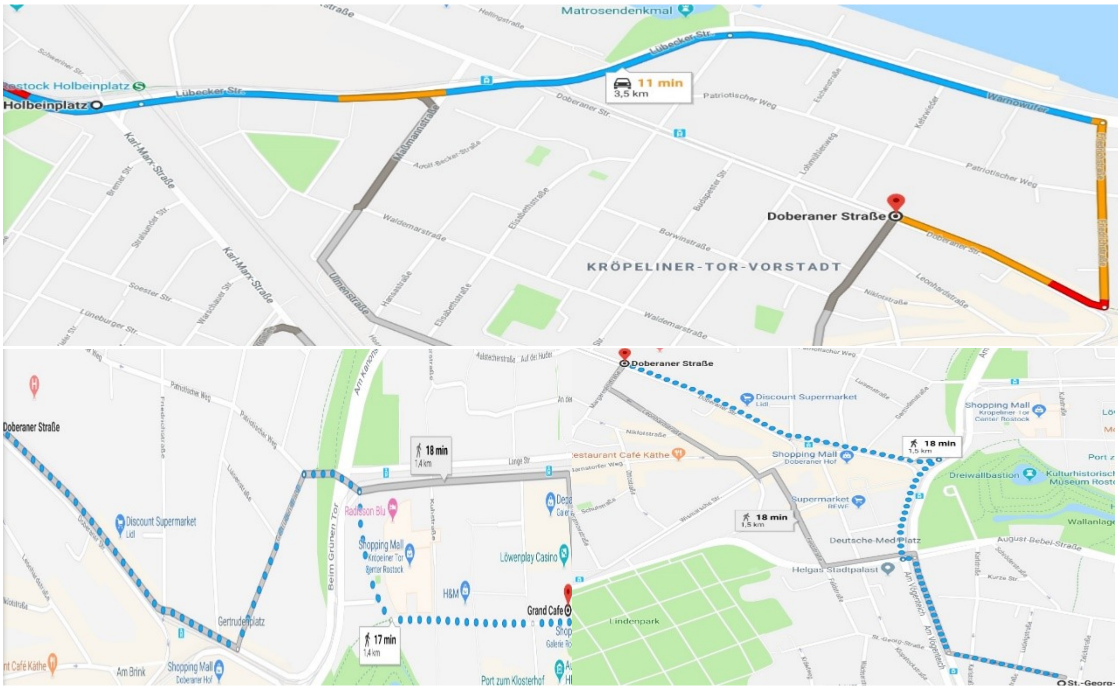

Fig. 6-12-(b) The route of subject during the prototype usage.

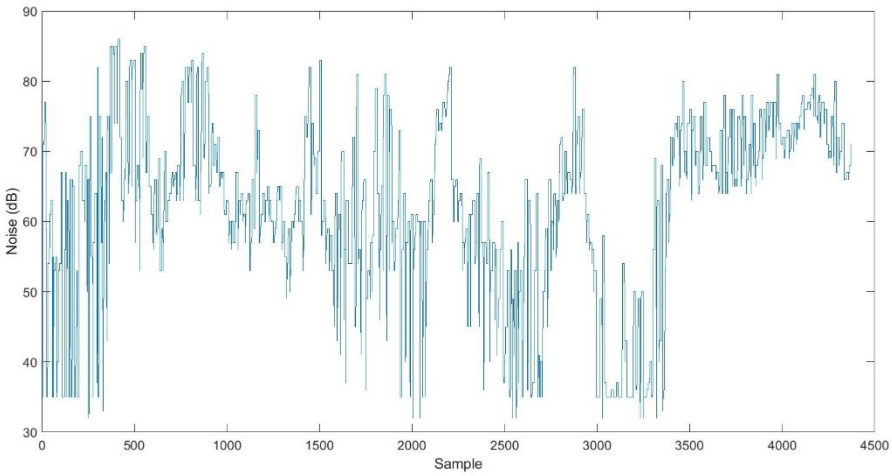

Fig. 6-13 Experimental tests' results collected from a daily routing in different activities (40 minutes).

(a) Walking from office (start point) to bus station, noise average: 63, 2 dB

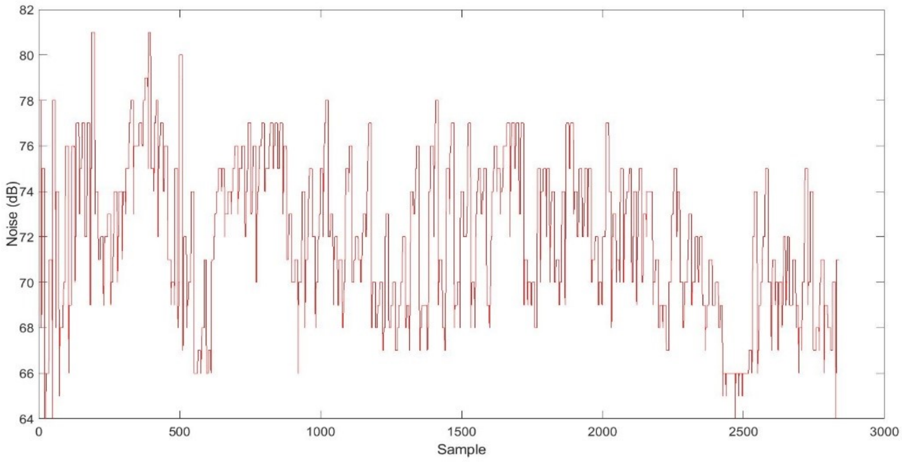

(b) Riding a bus to the train station, noise average (24 minutes): 72, 31 dB

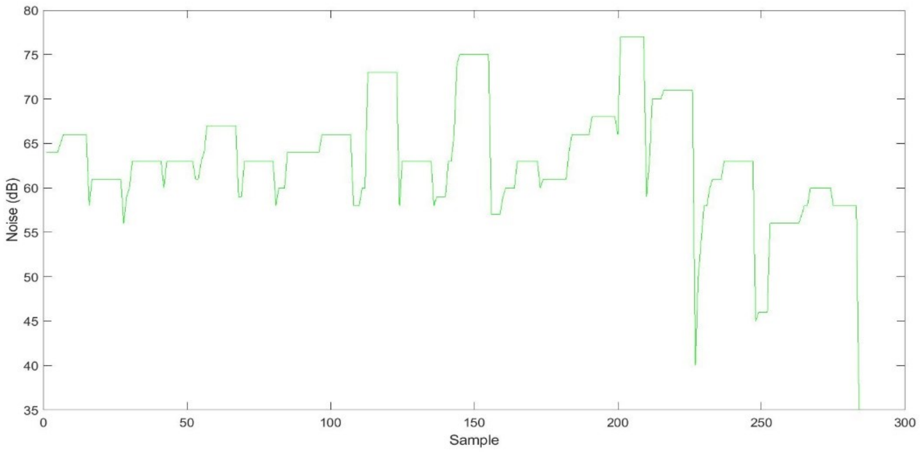

(c) Walking from bus station to train station, noise average (140 seconds): 63, 59 dB

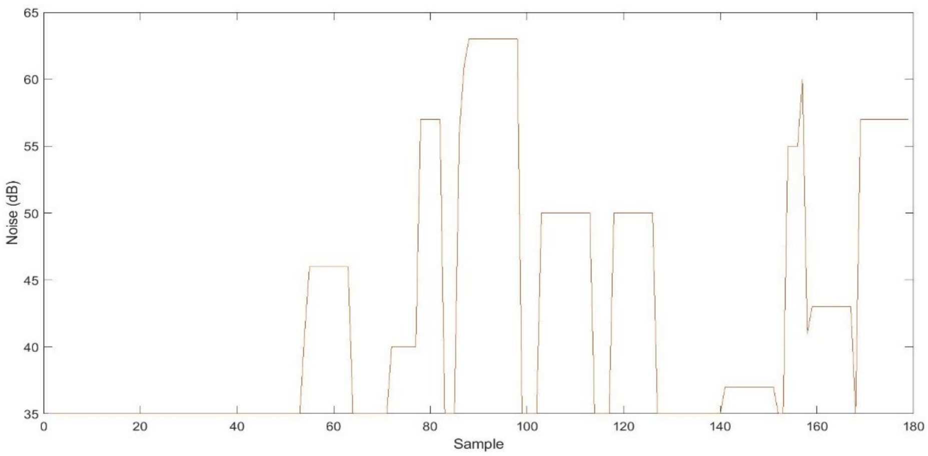

(d) Walking from train station to tram station, noise average (90 seconds): 42, 37 dB

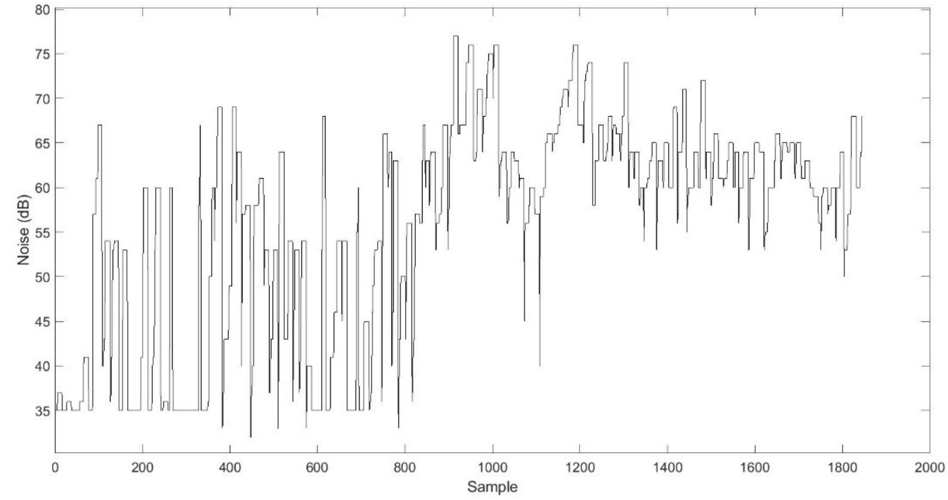

(e) Riding a tram to Doberane Platz, average noise (fifteen minutes): 56, 29 dB

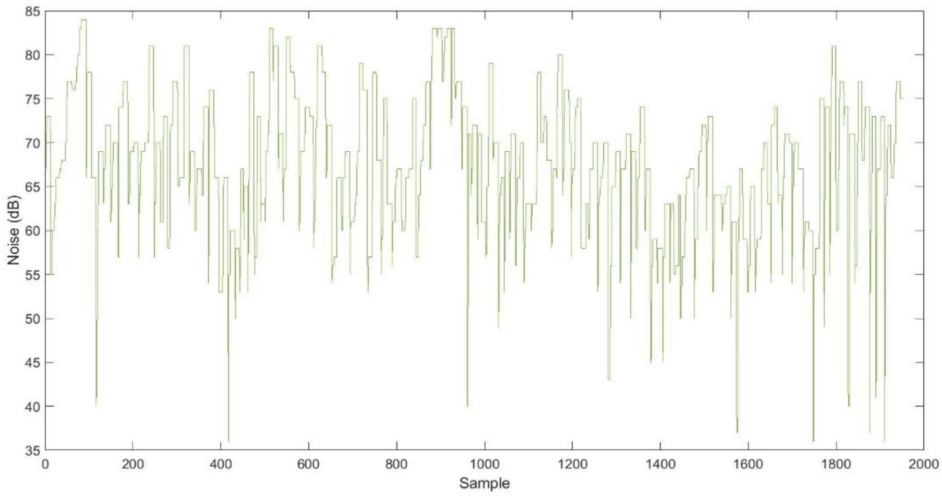

(f) Walking from Doberane Platz to restaurant, noise average (17 minutes): 68,13 dB

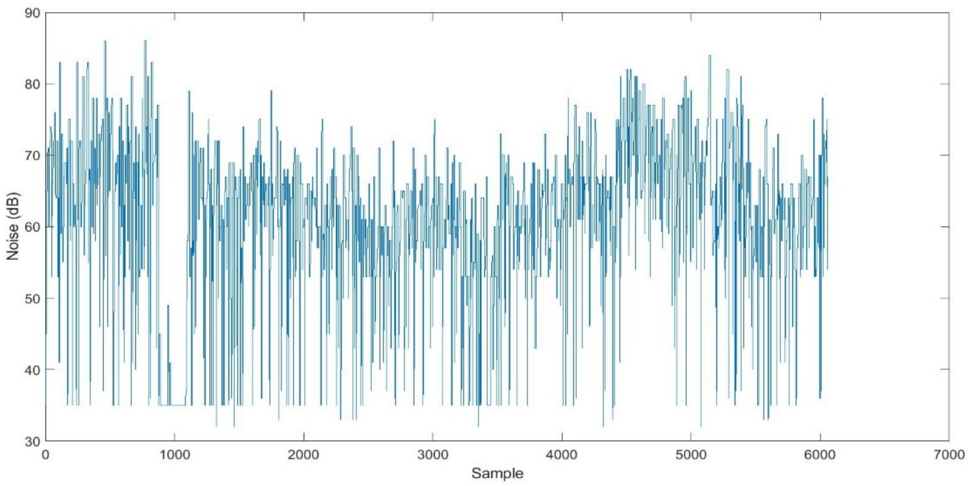

(g) Sitting in the restaurant1, average noise (50 minutes): 62,86 dB

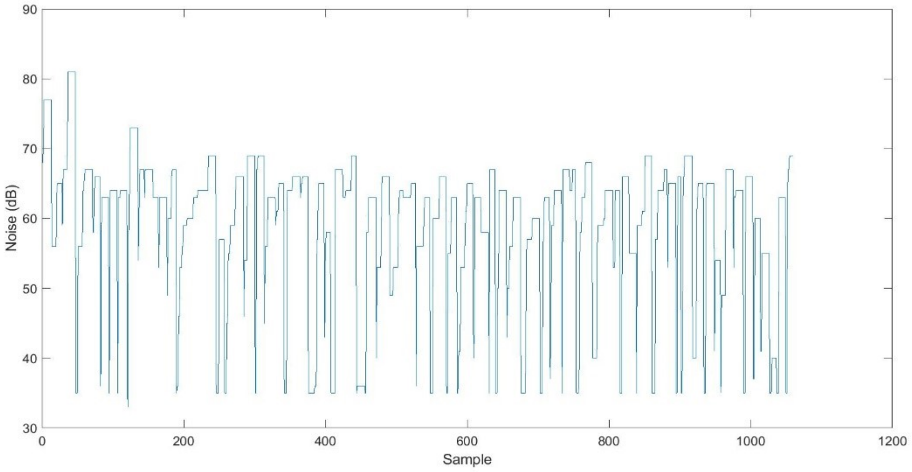

(h) Sitting in the restaurant2, average noise (10 minutes): 59,29 dB

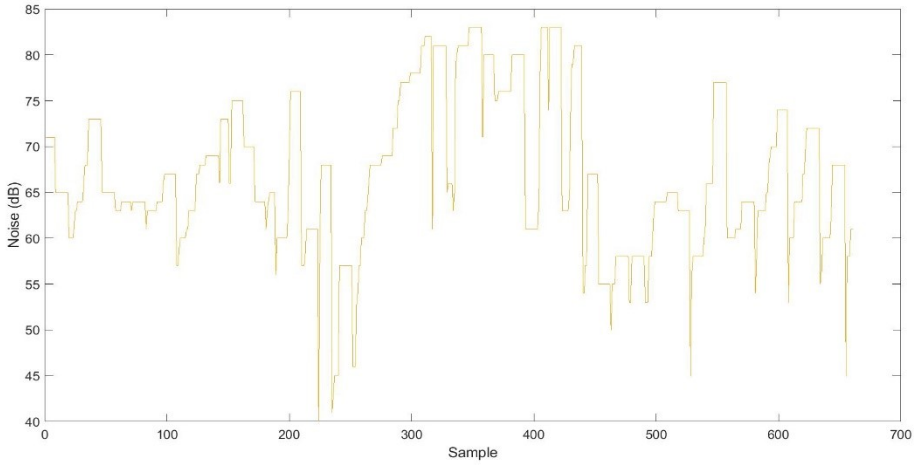

(i) Walking from the restaurant toward home, average noise (six minutes): 67,07 dB

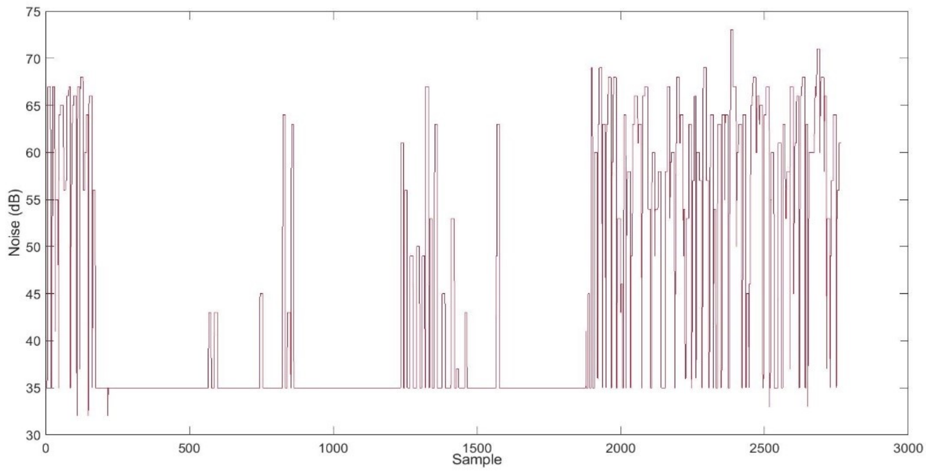

(j) At home, average noise (24 minutes): 44,88 dB

7 NOTIFICATION SYSTEM AND REAL-TIME MONITORING

This chapter is dedicated to notification system and display description. The display also is considered as the part of notification system that monitors the values of the parameters and notify the status of BLE (connected/disconnected) and data transmission (logging/sending). At the first subsection the notification system design, usage and advantages are described and the chapter is followed with details on display, real-time monitoring, implementation and benefits of display demonstration.

7.1 NOTIFICATION SYSTEM

The system features, applications and specifications were described in details in the previous chapters. MLMS-EMGN-4.0 is applied in environmental parameters (physical and chemical) observation to protect individual health. But the only measurement may not be sufficient in some cases such as toxic and hazardous evaluations. A system must be implemented to warn the user on ambient status to avoid long time exposure which may lead to irrecoverable damages or losses. A well-designed and adequate notification system can carry out this duty in risky situations which the wearer requires protection.

As well designed, versatile and applicable notification system in different environments and situations might combine more than one features to attract the user attention in various status.

As a consequence, the MLMS-EMGN-3.0 notification system, combines both haptic warning through a vibrating motor as well as a beeper. This is a good combination which can be applied for either noisy situations (operational occupations) that only the beeper (sound generator) can't be loud enough to gain the user attention (so the vibrating motor can do the job) and also in quiet environments (offices) which beeper is sufficient.

7.1.1 Notification System Design

As the final prototype is restricted in size and weight and has been designed as a wrist-worn sensor node, So that the notification system must be carefully designed to avoid additional imposed weight and size.

Generally the notification system consist of:

- Driver board,
- Vibrating motor,
- Beeper.

The vibrating motor and the beeper need to be activated. This is performed through a driver board which is called notification system driver. This driver is designed as a physical layer and is located at the bottom of host platform. Therefore, an electronics circuit to operate in risky situations is designed and implemented (see Fig. 7-1). The main component of the circuit is a transistor that operates whether in saturation/off mode.

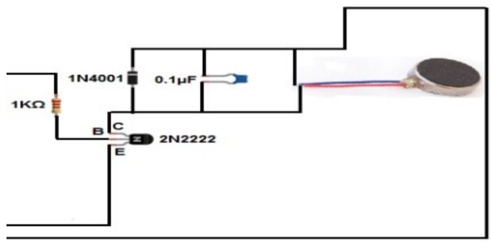

Fig. 7-1 Notification system electronics circuit.

Both vibrating motor and beeper are connected to the notification system driver layer. The activation is set according to each parameter's threshold. More often this feature is used to monitor the chemical elements in risky status.

7.1.2 Notification System Activation

The notification system is one of the most important concept in designing of the wearable in preventive medicine. The vibrating motor and beeper are the means of this system to operate. The criteria, merits and essential requirements already were discussed in concept chapter and the selected tools were introduced in realization chapter.

Vibrating motor and beeper are activated when receive the activated signal from the notification driver. Hence for each gas and also sound level detection according to the needful a threshold has been determined. Threshold of each gas is determined based on the degree of risk and notification system driver is activated in 3 states:

Normal: when the monitored parameter does not exceed the threshold, therefore the notification driver is switched off and it does not take any operation.

Low degree of risk: in this state, the notification system driver is activated through the micro controller signal and consequently, the vibrating motor and beeper are operating in low frequency. So that the duty cycle is 0.5. The notification driver is activated for one second and is switched off for one second. This continued until the target parameter is less than the threshold.

High degree of risk: this is the most dangerous situation which make a serious issue for the user. Thus the notification system driver is operating in the highest degree of frequency to attract the individual attention.

In this status, the duty cycle is 0.75. It means that the driver is operated for three seconds and is switched off for 1 second.

If CO is taken as an example, the proposed wearable's notification system begins to activate the vibrating motor and beeper at 70 ppm. The notification system operates at the highest frequency when the CO exceeds 200 ppm, where it can hurt the heart patients.

At the Fig.7.2 the code configuration for three mentioned status are presented. The data are raw signal and equivalent with ppm concentration after the conversion.

```
readMotion(connected);
lmp91000_adc_start();
sound_sensor_adc_start();
if(old_gas_value != sensorRAW)
{
  temp1 = sensorRAW / 10;
  temp2 = sensorRAW % 10;
  sprintf(lcd_str, "GAS(PPM) = %d.%d  \t", temp1, temp2);
  ssd1306_put_char(0, 0, lcd_str);
  old_gas_value = sensorRAW;

  if(sensorRAW > 2000 && sensorRAW < 5000)
  {
    vibration_type = 1;
  }else if(sensorRAW > 5000)
  {
    vibration_type = 2;
  }else
  {
    vibration_type = 0;
    vibration_counter = 0;

  }
}
```

Fig. 7-2 Code implementation for notification system activation.

When the notification system layer is designed and code implementation is created for the activation, the layer is attached to the bottom of MLMS-EMGN-3.0. By adding one more physical layer to the prototype, by now, it is called MLMS-EMGN-4.0.

The implemented notification system layer with both gas sensor node and sound module, are presented in Fig. 7-3 and Fig. 7.4.

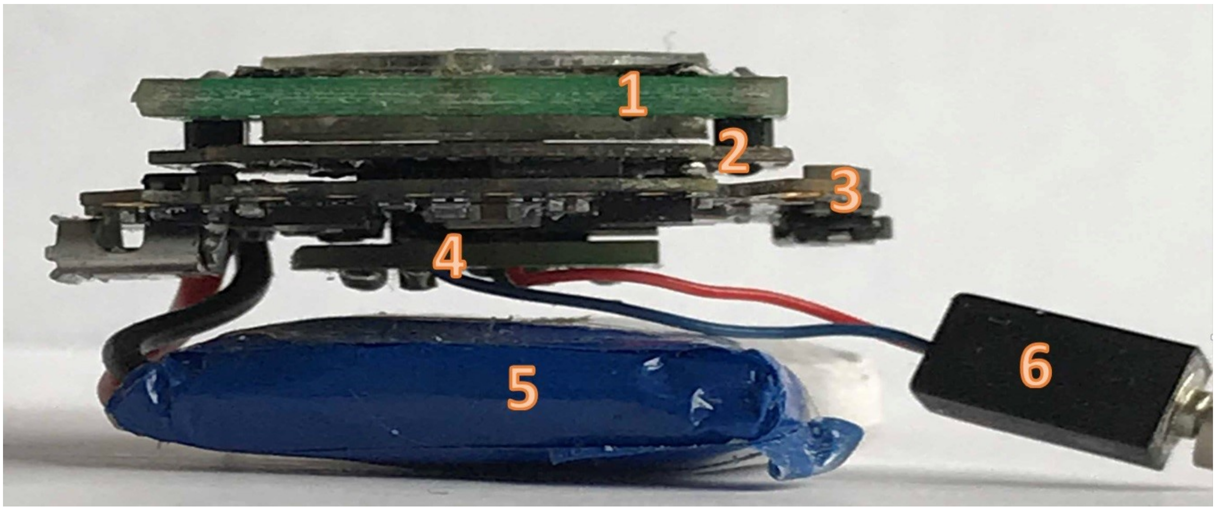

Fig. 7-3 Implemented notification system layer in prototype with gas sensor node. (1): gas sensor, (2): gas sensor driver, (3): Host platform, (4): Notification system driver, (5): Battery Li-ion 250 mAh, (6): vibrating motor.

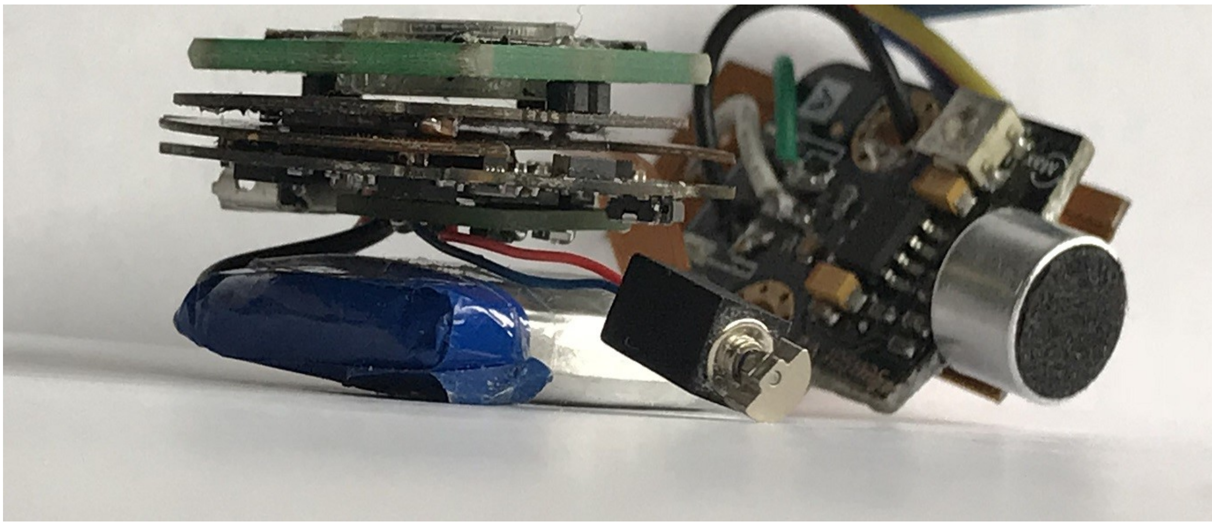

Fig. 7-4 Implemented notification system layer with gas sensor node and sound module.

7.2 DISPLAY AND REAL-TIME MONITORING

Standalone operating means the device is capable of working independent of the smartphone availability and BLE connectivity and still data are accessible (data are not lost) and observed in real-time by the user.

Therefore, to create the ability of working as an independent wearable which does not need a smartphone for operating, a display implementation is essential. The display is considered for this wearable for several reasons:

- Real-time monitoring: with a display, data are sampled and sent to the display in real-time with the desired sample rate, rather than sending to smartphone in real-time which make it inefficient in power consumption.
  In this scenario, the data are sent in two different sample rates to display and smartphone (In real-time are sent to display, two Hz for sound level and 0.2 Hz for gas sensor. In average value are sent to the smartphone, 0.2 Hz for sound level and 0.02 Hz for gas sensor).

- Secure data monitoring: in data transmission from a wearable to smartphone, there is the possibility of communication channel interruption and BLE disconnection. In this scenario in the case of lack of a display the individual is not able to observe the ambient parameters any longer.

- Power consumption: another reason that make a display efficient to be implemented is power consumption saving. In case that, the battery is running in low, whether it is in smartphone or wearable, there is the possibility to disconnect BLE and observe the data in real-time yet.

- Two types of data collection: while data are sending to both display and smartphone, the individual is observing two types of data:

- ❖ Instant real-time monitoring from the sampled sensors,
- ❖ Average values of ambient parameters on the smartphone.

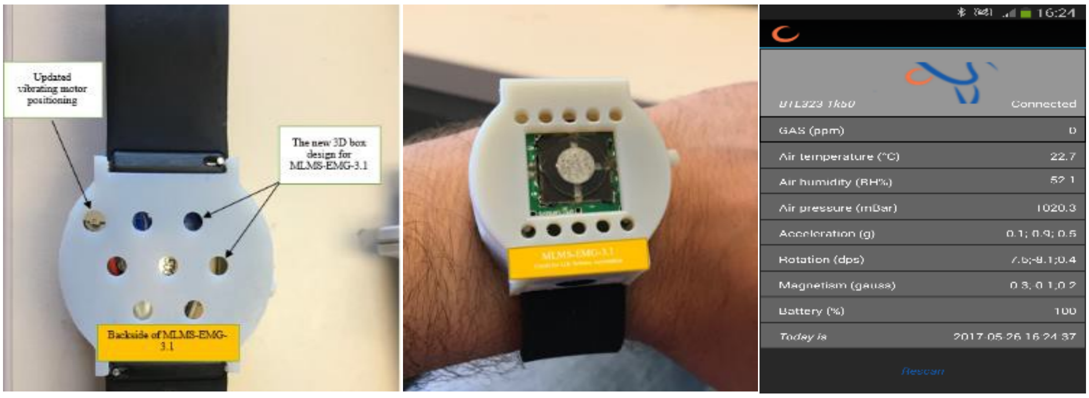

Fig. 7-5 The case with ventilation holes (left and middle) and application (right).

7.2.1 Display Implementation

The OLED display is connected to the tail of hardware interface for microcontroller communication. In the final prototype, the display is implemented on the top of the chassis for user convenience and data observation.

Both chemical parameters (toxic and hazardous gases) and sound level are monitored on the display.

A general structure view of the solution and the embedded display is exhibited in Fig. 7-6.

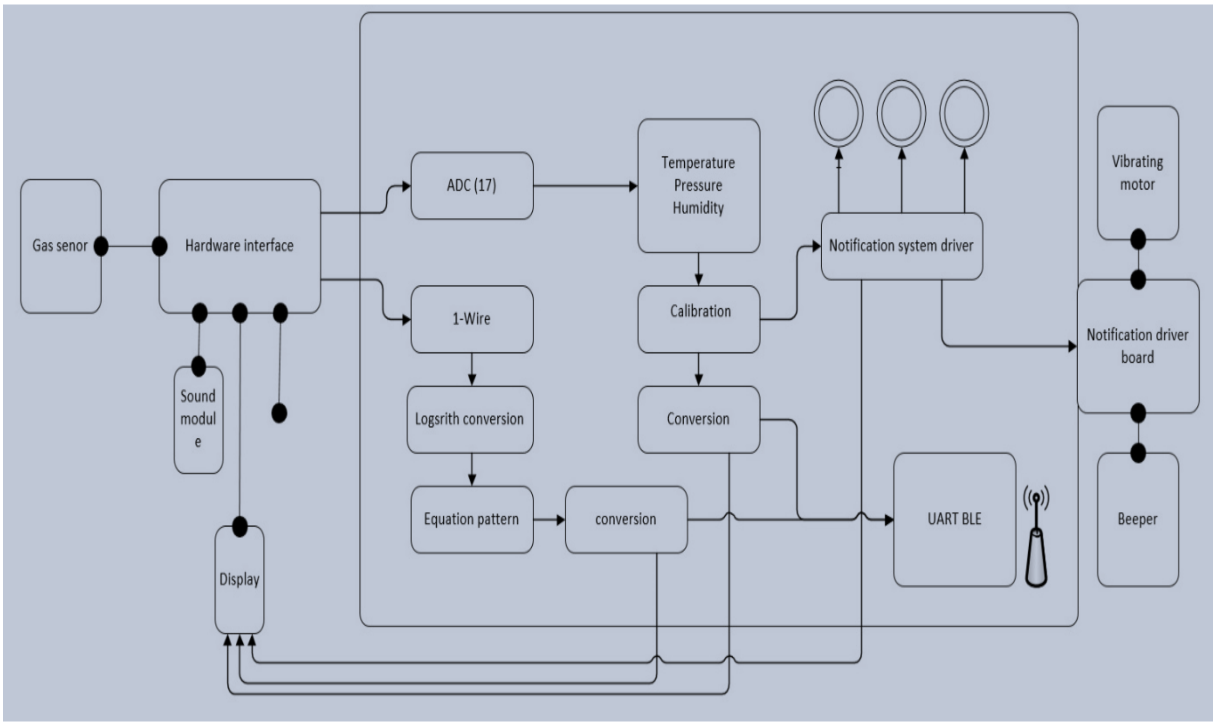

Fig. 7-6 A complete structure view of the whole solution.

The display and sound level are integrated in the system as modular components. Therefore, there is the possibility for the user to switch off/remove these modules if the operation is not required. This may lead to less power consumption in the whole system.

An implemented version of the device called: MLMS-EMGN-4.1 from different prospective is depicted in the Fig. 7-7, Fig. 7-8.

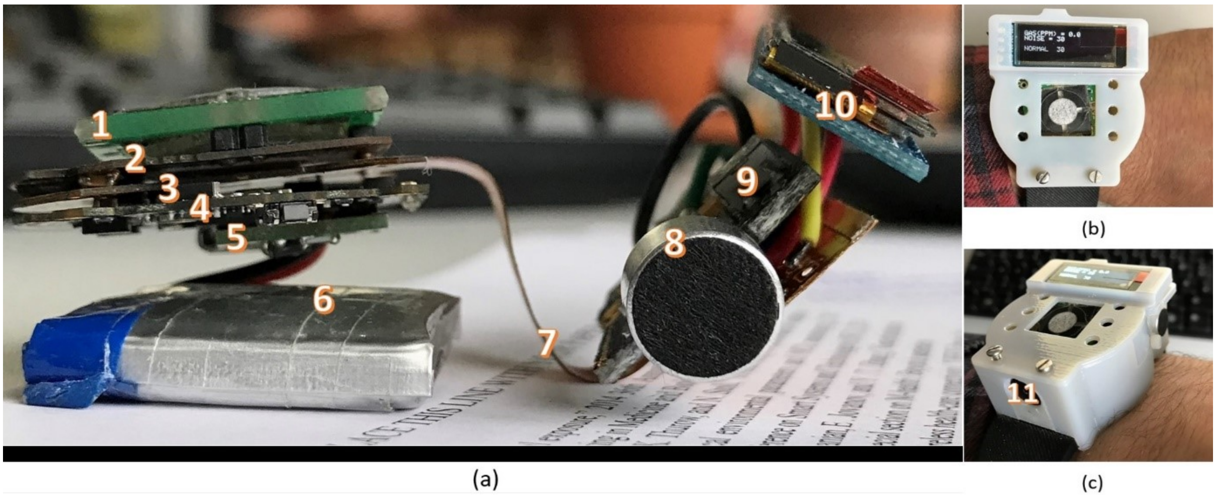

Fig. 7-7 Assembled proposed device. (a) Layers and components stuck on top of each other: (1) gas sensor, (2)gas sensor driver, (3)hardware flex interface, (4) Host platform, (5) notification system driver, (6) battery, (7) tail of flex interface, (8) microphone, (9) sound module, (10) display. (b) Top view of MLMS-EMGN-4.0. (c) Side view of MLMS-EMGN-4.0: (11) beeper.

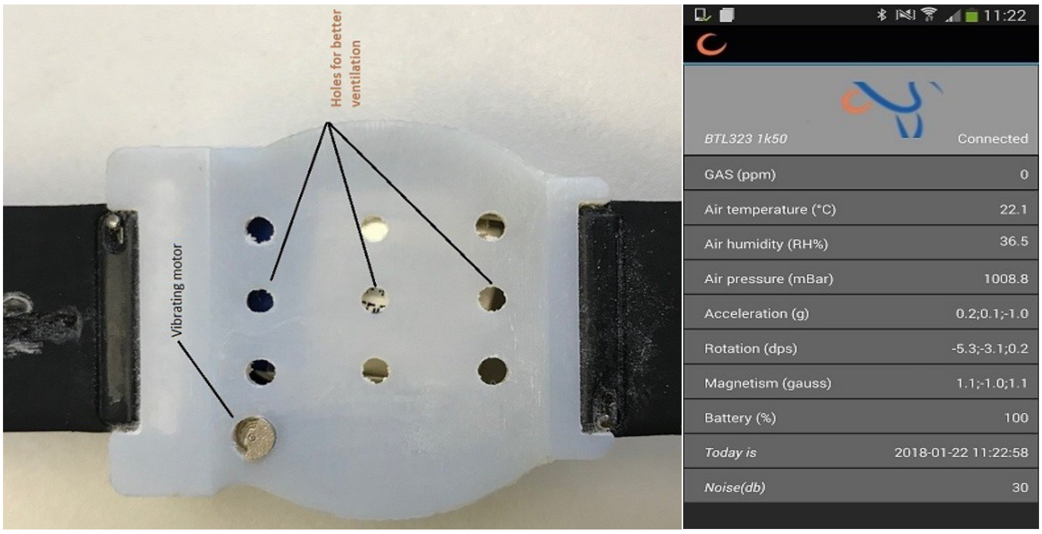

Fig. 7-8 The back side of four-layer wearable prototype for physical and chemical ambient monitoring and data monitoring in real-time on the smartphone.

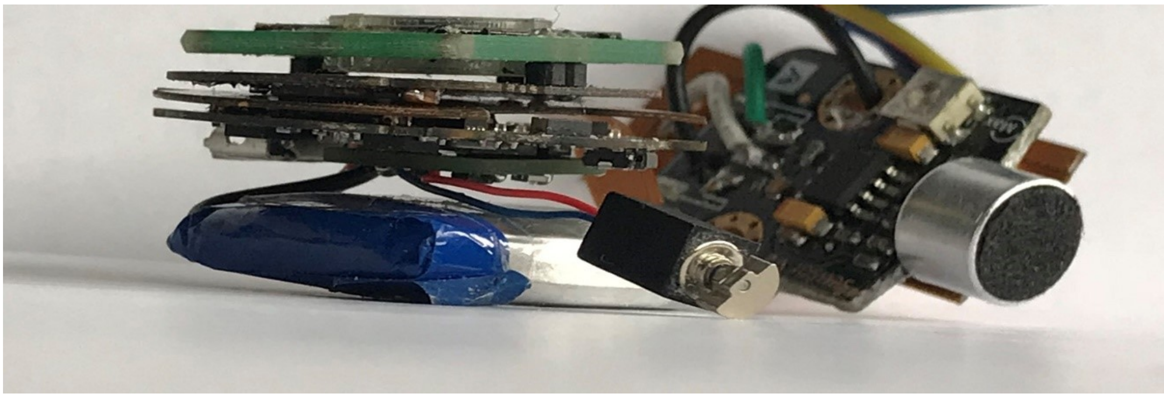

Fig. 7-9 A complete prototype solution with gas sensor, sound module and notification vibrating motor.

8 GENERAL STRATEGY OF THE PROTOTYPE OPERATION

In this chapter the sensor data sampling, transmission and data logging while BLE is connected/disconnected is described. In general, the strategy of operation in two modes of BLE connected/disconnected is discussed. The chapter is followed up with sensor selection and activation, data communication protocol between the smartphone and the proposed device, and device configuration.

8.1 GENERAL STRATEGY OF DATA SAMPLING AND ACQUISITION

The operation of the prototype for the general strategy of data sampling, storage and acquisition is according to the BLE status (connected/disconnected) (see Fig. 8-1). Depending on the BLE status, two general scenarios are predicted and implemented:

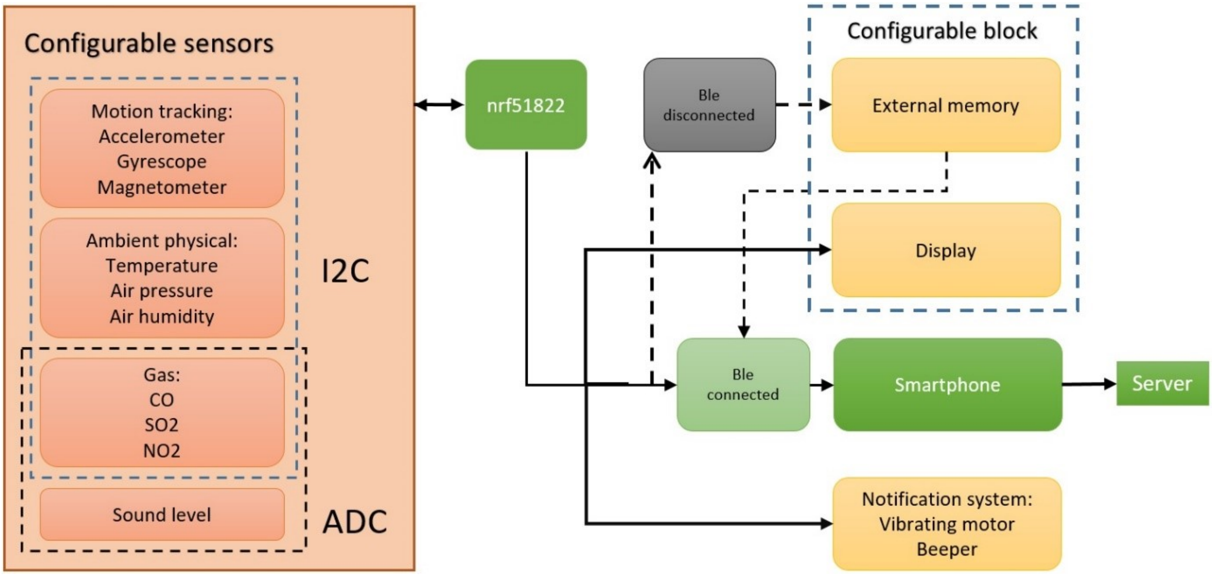

Fig. 8-1 General strategy in two BLE connected/disconnected mode.

8.1.1 BLE Is Connected

Device configuration and sensor selection is one of the main features and specifications of the proposed device that bring multi-tasking capability and efficient form factor directly and indirectly. In addition, this feature contributes in power consumption efficiency, wider range of gas evaluation, flexibility. User may select the desired sensor by sending a command to MLMS-EMGN-5.1. Hereafter, this version of the proposed wearable is called MLMS-EMGN-5.1. When MLMS-EMGN-5.1 is turned on and the communication channel with the smartphone is established, the display is switched off by default, and motion trackers' sensors and ambient air physical sensors are on operation. As the air physical parameters are important in gas sensor calibration, as far as a gas sensor is on operation, the physical parameters also are required to be measured. At the same behavior, motion tracker sensors also are utilized during the daily activities for the individual's daily routine analysis. The reason for off-display is less power consumption while the data may be observed on the smartphone. However, the display can be switched on by user command from the smartphone. Due to full configuration of MLMS-EMGN-5.1 by the smartphone, when the communication channel is established both gas sensor node and sound module detector are switched off. Unless, the wearer is going to switch on gas sensor node, sound module and display according to his/her needs. In addition, user also is able to switch off/on any combination of these sensors, actuator and module (see algorithm 8-1).

Algorithm 1: MLMS-EMGN-5.1 configuration

```
The device is configured by the smartphone. The user by pressing
  predefined buttons on the smartphone decides for the sensor(s) and
  actuator selection. NO2, CO, SO2, noise, noisegas and datalog
  are the buttons on the smartphone.
Result: Write here the result
S_n1 ← sampling rate(noise);
S_g1 ← sampling rate(gas);
if BLE is disconnected then
    display is initialized();
    display starts();
    external memory is initialized;
    disply ← "BLE is disconnected"
    noise module is initialized();
    LMP91000 is initialized();
    LMP91000 is configured by default to CO();
    S_n1 is set;
    S_g1 is set;
    noise module starts();
    gas sensor starts();
    return noise;
    disply ← noise value
    external memory ← noise
    return gas;
    display ← gasvalue;
    external memory ← gas
end
else
    display ← BLE is connected
    if CMD ← display then
        display is initialized;
        disply starts();
        disply ← "BLEisconncted"
    end
    if CMD ← gas then
        LMP91000 is initialized;
        LMP91000 is configured to gas
        gas is calibrating;
        returngas; display ← gas;
        BLE ← gas
    end
    if CMD ← Noise then
        Noise module is initialize
        noise module start sampling
        return noise
        display ← noise;
        BLE ← noise;
    end
    if CMD ← NoiseGas then
        both procedure of noise and gas are done
    end
    if CMD ← DataLog then
        BLE ← dataarereadfromexternalmemory
    end
end
```

Algorithm 8-1. MLMS-EMGN-5.1 functionality in BLE disconnected status.

The user by pressing predefined buttons on the smartphone decides for the sensor(s) and actuator selection. NO2, CO, SO2, noise, noise gas and data log are the buttons on the smartphone (in the extended version UV index also is implemented).

If all available sensors in the proposed device are:

$$Sensor|actuator \text{ collection } = \{\mathrm{G, S, M, HPT, D}\}$$

Where:

$$G = \{G_1, G_2, \dots, G_n\}$$

And in this work;

$$G = \{NO_2, SO_2, CO\}$$

$M = \{\text{Gyroscope, Magnetometer, Accelerometer}\};$

$D = \{\text{Display}\};$

$S = \{\text{Sound module}\};$

From these collection, motion trackers and air physical sensors are excluded for sensor configuration, thus:

$$Configurable\ sensor, actuator = \{\mathrm{G, S, D}\}$$

At each time, from G_1, G_2 and G_3 only one gas sensor can be selected in combination with sound level detector and display. There are following combination configuration modes:

$$Possible\ combination\ configurations = \{\mathrm{G1|G2|G3}\}\{\mathrm{D}\}\{\mathrm{S}\}\{\mathrm{G1|G2|G3, S}\}\{\mathrm{G1|G2|G3, D}\}\{\mathrm{D, S}\}\{\mathrm{G1|G2|G3, S, D}\}$$

8.1.2 BLE is Disconnected (standalone operation)

When BLE is disconnected, MLMS-EMGN-5.1 is set to standalone mode automatically. In this mode of operation, the display is switched on for real-time data monitoring and external memory is initialized for data logging. By default, all sensors (ambient air physical and chemical and motion trackers) are initialized and sensors sampling is started based on the fixed sampling rate of 0.2 Hz for gas sensor, 1 Hz for ambient air physical and 2 Hz for sound module. To extend the time of standalone operation from one side and avoid important data lost due to limited external memory space from the other side, only gas sensors values and sound levels are stored in external memory. The capacity of the external memory is 256 kB (see algorithm 8-2).

To evaluate the number of samples that can be stored in the external memory, the following phrases are stated for noise sensor:

$$\text{Data length in each sample} = 3\text{B}$$

For: $\text{sampling rate} = 2\text{Hz}$

$$\text{number of samples in one minute} = 120$$

Therefore:

$$\text{number of bytes in one minute sampling} = 360$$

The same calculation for gas sensor shows that:

$$\text{data length in each sample} = 3\text{B}$$

For: $\text{sampling rate} = 0.2\text{Hz}$

$$\text{number of samples in one minute} = 12$$

Therefore:

$$\text{number of bytes in one minute sampling} = 36$$

$$\text{The summation of stored bytes for gas and sound module is } 396\text{B}$$

$$\text{Total time of data storage} = 256\text{K}/396 = 10.77\text{ hrs}$$

This calculation says that, if BLE is disconnected, the external memory is logging data for nearly 11 hours under the constant sampling rates of sensors. In the next chapters will see that, due to efficient ambient evaluation and saving power consumption (prolonged monitoring), the sampling rates of gas sensor and sound module are variable and adjustable according to the level of battery. According to the adjustable sampling rate, as the level of battery is reduced, the sampling rate is reduced too. This results in a smaller number of samples in some specific period (ex. 1 minute) and therefore, a smaller number of bytes must be logged into the external memory. Less number of samples extend the external memory for longer time of data logging.

Algorithm 2: MLMS-EMGN-5.1 sampling rates

The $noise$ and NO_2, CO, SO_2 sampling rates are variable according to the battery level. Four battery levels are considered and as the level is reduced the sampling rate decreases.

Input : $L_j \leftarrow battery\ level$
$j = 1, 2, 3, 4;$

Output: $S_{ni} \leftarrow sampling\ rate(noise);$
$S_{gi} \leftarrow sampling\ rate(gas);$

$where:$

$samplingrate(noise) = \frac{4}{2^i};$

$samplingrate(gas) = \frac{1}{5 \times i^2};$

$i = 1, 2, 3, 4;$

Reading the battery level is prior than sensor sampling;

$read\ battery\ level();$

if $(80 \preceq battery\ level \preceq 100)$ **then**
- $L_1 \leftarrow battery\ level;$
- $S_{n1} \leftarrow sampling\ rate;$
- $S_{g1} \leftarrow sampling\ rate;$
- $read\ noise;$
- $read\ gas;$

end

else if $60 \preceq battery\ level \prec 80$ **then**
- $L_2 \leftarrow battery\ level;$
- $S_{n2} \leftarrow sampling\ rate;$
- $S_{g2} \leftarrow sampling\ rate;$
- $read\ noise;$
- $read\ gas;$

end

else if $40 \preceq battery\ level \prec 60$ **then**
- $L_3 \leftarrow battery\ level;$
- $S_{n3} \leftarrow sampling\ rate;$
- $S_{g3} \leftarrow sampling\ rate;$
- $read\ noise;$
- $read\ gas;$

end

else
- $L_3 \leftarrow battery\ level;$
- $S_{n3} \leftarrow sampling\ rate;$
- $S_{g3} \leftarrow sampling\ rate;$
- $read\ noise;$
- $read\ gas;$

end

Algorithm 8-2 MLMS-EMGN-5.1 functionality in BLE connected status.

Another configuration that has been implemented is logged data transmission. When BLE is disconnected, the data are logged in external memory. While the communication channel is resumed, these data have to be retrieved for permanent storage. To prevent interference with normal data transmission, a button is implemented on the smartphone's application for logged data transmission. User is fully authorized to transmit the logged data at any time that is appropriate according to the device application and tasks.

8.2 DATA AND STRUCTURE OF PACKET TRANSMISSION

The two-way communication protocol and packet architecture are depicted in Fig.8-2. In this figure, each packet is described in detail. In MLMS-EMGN-5.1 data are transmitted in 4 packets: The data from the same group of sensors are combined and sent in one packet for data efficiency transmission and power consumption. For each packet a unique ID is assigned for identification in application side.

8.2.1 $\mathbf{F_1}$: Motion tracking, 19 bytes (including 2bytes don't care)

To follow the motion, this packet is sent every 20ms. A $3DoF\ accelerometer$, $3DoF$ gyroscope and $3DoF$ magnetometer are combined for a precise user tracking. Each sensor reserves 12 bits. The $Seq.$ in the packet is used as the data sequence number. F_1 is a data ID identification, byte separation and recognition process in android APK. The last two bytes are reserved for further development.

8.2.2 $\mathbf{F_2}$: Physical Environmental Parameters (temperature, air pressure, humidity), 12 bytes

This packet is sent to the smartphone every second. It is started with seq. and followed by F_2 and then air pressure, temperature and humidity. All environmental elements are using 2 bytes split to higher and lower byte.

8.2.3 $\mathbf{F_4}$: Gas ($\mathbf{NO_2/CO/SO_2}$), 4 bytes

4 bytes for gas data transmission is sufficient. These data are sent every 2 minutes due to sensor nature, application requirement, lower power consumption and sensor response time.

8.2.4 $\mathbf{F_5}$: Sound Level, 4 bytes

The construction of sound level packet is similar to gas. Data are sent to Android in 2 Hz.

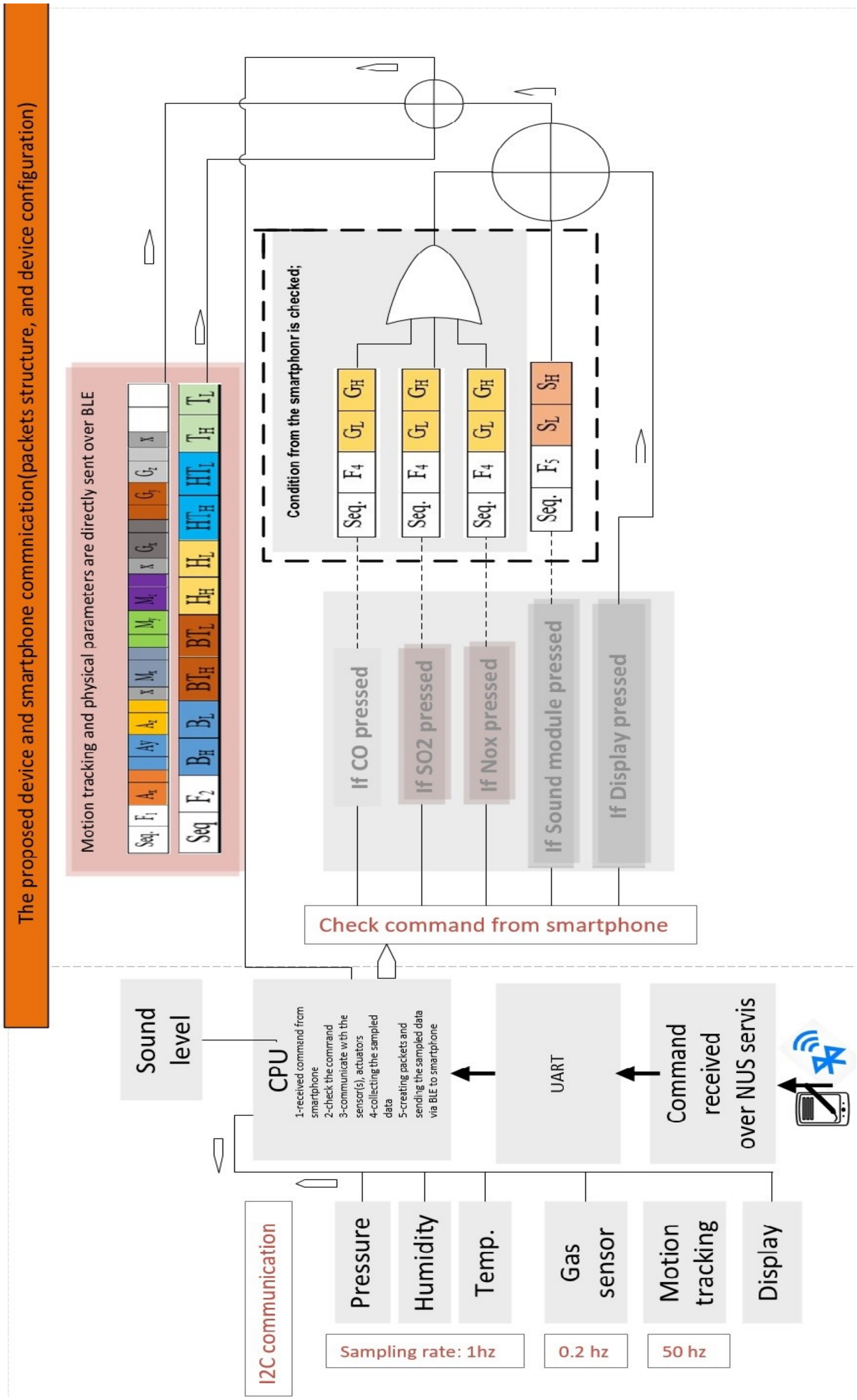

Fig. 8-2 Two-way data communication between the proposed device and smartphone. The MLMS-EMGN-5.1 is configured by the commands from the smartphone and the sampled data are logged in the smartphone.

9 EVALUATION OF POWER CONSUMPTION

9.1 EVALUATION OF CURRENT CONSUMPTION FOR EACH SENSOR AND MODULE

The prolonged monitoring always is a critical aspect of wearable design. In particular, in MLMS-EMGN-5.1 that is evaluating number of parameters, a careful design and implementation in both hardware and software is playing an important role. In this section the power consumption of each one of sensors and actuator are measured separately. Motion trackers, ambient air physical parameters, gas sensor, sound module and display are evaluated. Furthermore, the power dissipation of the external memory in disconnected BLE status and BLE while it is used to transmit the data are evaluated. The effect of external memory while is initialized in disconnected BLE and wireless communication channel on battery life are embedded in the calculations.

Motion trackers are the first evaluated sensors. These sensors due to required accuracy have the highest sampling rate (50 Hz). The current consumption of these sensors is less than 5 mA. The next group of sensors is ambient air physical sensors (air temperature, humidity, and pressure) with the sampling rate of 1 Hz. When the first and second group of sensors are operating at the same time, an over lapping in data transmission is observed due to synchronization sample rate every one second. The high peak of current consumption in every second is due to the summation of motion trackers and environmental physical parameters every.

The third section in the Fig. 9-1 belongs to the display. The display is initialized with each sound level module monitoring. This caused a swinging current consumption between 6 and 8 mA.

The Fig. 9-1 in the fourth segment, is regarding the evaluation of gas sensor. During this period, display is switched off to only measure the current consumption of the gas sensor but two first groups of sensors are on operation (the gas sensor's current consumption is calculated from reduction of total measured current from the summation of ambient physical and motion tracker sensors which were calculated in first two parts). The peaks with large amplitudes which are seen every 5 seconds are due to synchronization with motion trackers and ambient air physical. The maximum of the peak occurs when all sensors from the segment 1, 2, and gas sensor measurement are synchronized.

In green part, sound level module is evaluated along with first two groups, while gas sensor goes off. Due to 2 Hz sampling rate of sound level detector, the summation with first and second group may occur every 0.5 and 1 second respectively.

Before the communication channel is established, all sensors and the actuator are switched on for current consumption evaluation. Care must be taken that external memory's power dissipation is embedded during sound level detector and gas sensor observation.

The last part of power estimation is dedicated to BLE connection while all sensors and actuator are working. As it is observed the maximum current consumption is 15.8 mA. This is reached every 5 seconds at most, when all sensors are synchronized with gas sensor (with lowest sampling rate). However, to calculate the battery life time in worst case, we have:

$$Battery\ life = \frac{300\ (mAh)}{15.8\ (mA)} = 19\ hrs$$

When BLE is disconnected, external memory is initialized for samples storage of gas and sound level detector. Thus, the power consumption of external memory is embedded in the gas and sound module section (see Fig. 9-1).

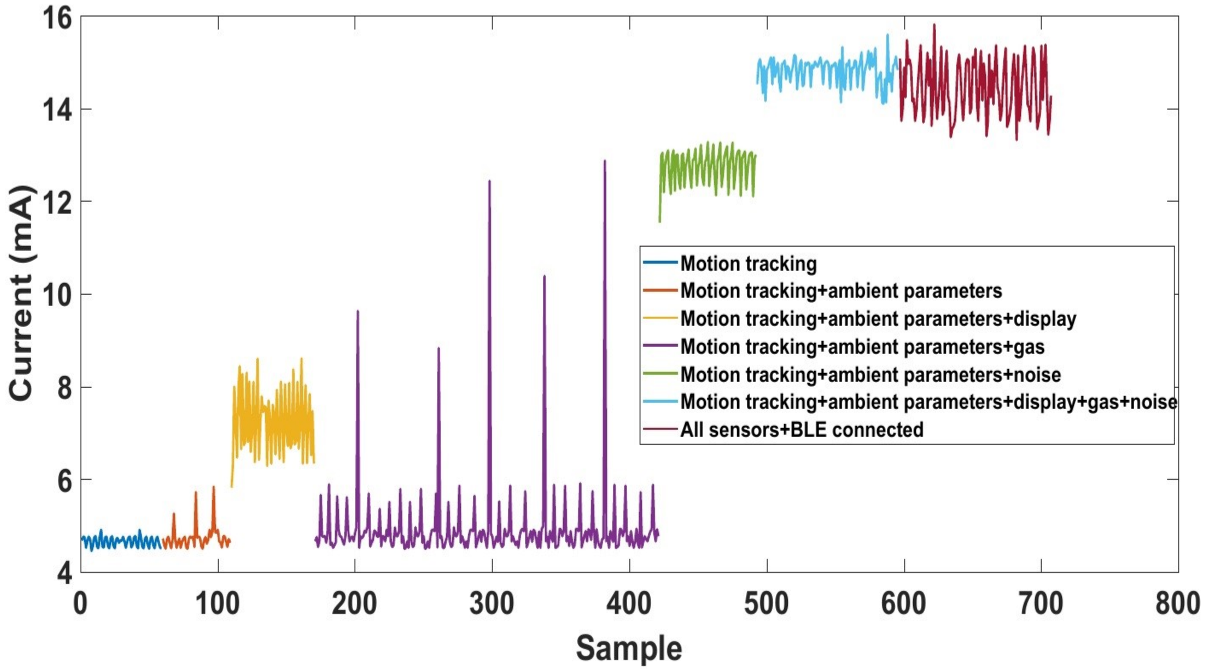

Fig. 9-1 Power consumption estimation of Ubiqsense in BLE connected/disconnected status (the experiment has been performed in several completed cycles of sensors data collection).

9.2 ADJUSTABLE SAMPLING RATE AND POWER CONSUMPTION

The current consumption was evaluated in the previous subsection for the highest sampling rates (the largest current consumption). Generally, due to direct correlation of sampling rates and power consumption, if the sampling rates of sensors is reduced, it is expected that the current consumption is less than what was calculated. In this subsection, a technique is applied to improve the battery life. As an obvious point, the battery life is the function of sampling rate directly. Due to accuracy of motion tracking, It is not intended to change the motion tracking sampling rate. Sound module and gas sensors are two candidates for sampling rate adjustment. Nevertheless, the sampling rate adjustment does not apply in the way that the regular environmental parameters evaluation is sacrificed for long-time monitoring.

As it is depicted in Algorithm 2, the battery level is divided into 5 areas. As the battery charge is reduced by 20%, the sampling rate of both gas sensor and sound module is reduced but in different rates. As the sound level generation is at a moment and also might be disappeared instantly, therefore the sound level detector's sampling rate is reduced in smaller rate, therefore:

$$Battery\ Level = \{L_i\}\ and\ \mathrm{i} = \{1,2,3,4\},$$

Where L_1 is the level of battery between 80 % and 100 % and L_4 is the level of battery for less than 40 % each level is reduced by 20 %. Then:

$$Sampling\ rate\ (noise) = \left(\frac{2}{2^i}\right) \qquad (1)$$

The same calculation from eq. (1) is implemented for gas sensor sampling rate but in sharper sampling reduction.

$$Sampling\ rate\ (gas) = \left(\frac{1}{5\times i^2}\right) \qquad (2)$$

Gas measurement in higher time interval does not affect the device's accuracy significantly, because still 1sample of gas is acquired in 40 seconds.

To calculate the battery life extension when the sampling rate formula is applied, the following formula is applied:

$$\text{Total current consumption} = \sum_{i=1}^{6} I_{ti} \qquad (3)$$

Where:

$$I_{ti} = \begin{cases} I_M + I_{HPT} + I_D + (I_G + I_N) + I_{E.M.} & , \quad If\ BLE\ is\ Disc. \\ I_M + I_{HPT} + I_D + (I_G + I_N) + I_{BLE.} & , \quad Otherwise \end{cases}$$

During the calculation, always the largest current consumption is considered. While between the BLE connected (data transmission through BLE) and disconnected (external memory for data logging is initialized) status, BLE connected status dissipates more power. Thus the second case is taken for calculation. To evaluate the effect of sampling rate, the basic power consumption in the lack of gas sensor and sound level module is defined as:

$$I_{base} = I_{ti} - (I_G + I_N) \qquad (4)$$

The average current consumption in basic status (excluding gas and sound module) is approximately 9.1 mA. This average for gas sensor is 2.2 mA (14% of total current consumption) and 4.5 mA (28% of total current consumption) for sound level detector. Then it is expected that the current consumption in correlation with battery level and sampling rate is calculated as the followings:

$$current\ consumption\ (noise) = \left(4.5\ \times \frac{4}{2\times 2^i}\right) \qquad (5)$$

$$current\ consumption\ (gas) = \left(2.2\ \times \frac{5}{5\times i^2}\right) \qquad (6)$$

$$Where: i = 1,2,3,4\ \forall\ L_i = Battery\ Level$$

The total battery extension according to hour is calculated based on:

$$Extended\ battery\ life = \frac{300\ (\text{mAh})}{I_{base} + I_{GiAve} + I_{SiAve}\ (mA)} = 26.75\ hrs$$

$$I_{Gi} = \sum_{i=1}^{3}\left(\frac{5}{5\times i^2}\right) + 2\times 2.2\times \frac{5}{5\times i^2} \qquad (7)$$

$$I_{GiAve} = \frac{I_{Gi}}{5} \qquad (8)$$

And for the average current consumption of sound module the same calculation with its own sampling rate is repeated:

$$I_{Si} = \sum_{i=1}^{3}\left(4.5\frac{4}{2\times 2^i}\right) + 2\times 4.5\times \frac{4}{2\times 2^i} \qquad (9)$$

$$I_{SiAve} = \frac{I_{Si}}{5} \qquad (10)$$

Therefore, in the worst case, the battery life is extended for 29 %. It should be noticed that, the higher sampling rates of environmental air parameters and motion trackers which consumes much less power consumption (higher weights) for reliable calculation were ignored.

MLMS-EMGN-5.1 is depicted in detail in Fig. 9-2

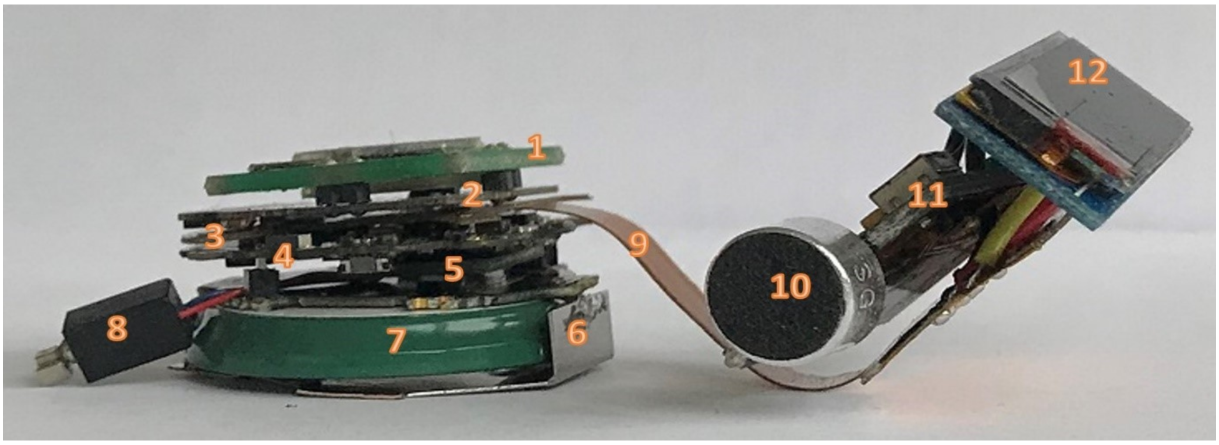

Fig. 9-2 The assembled proposed wearable (MLMS-EMGN-5.1). (1): Gas sensor, (2): Gas sensor driver, (3): Hardware flex interface, (4): Host platform, (5): Notification system driver, (6): Battery holder, (7): Coin cell battery, (8): Vibrating motor, (9): Tail of hardware flex interface, (10): Microphone, (11): Sound module detector, (12): Display.

The general application of the healthcare system (developed in celisca) including ambient parameters monitoring and data observation are shown in Fig. 9-3.

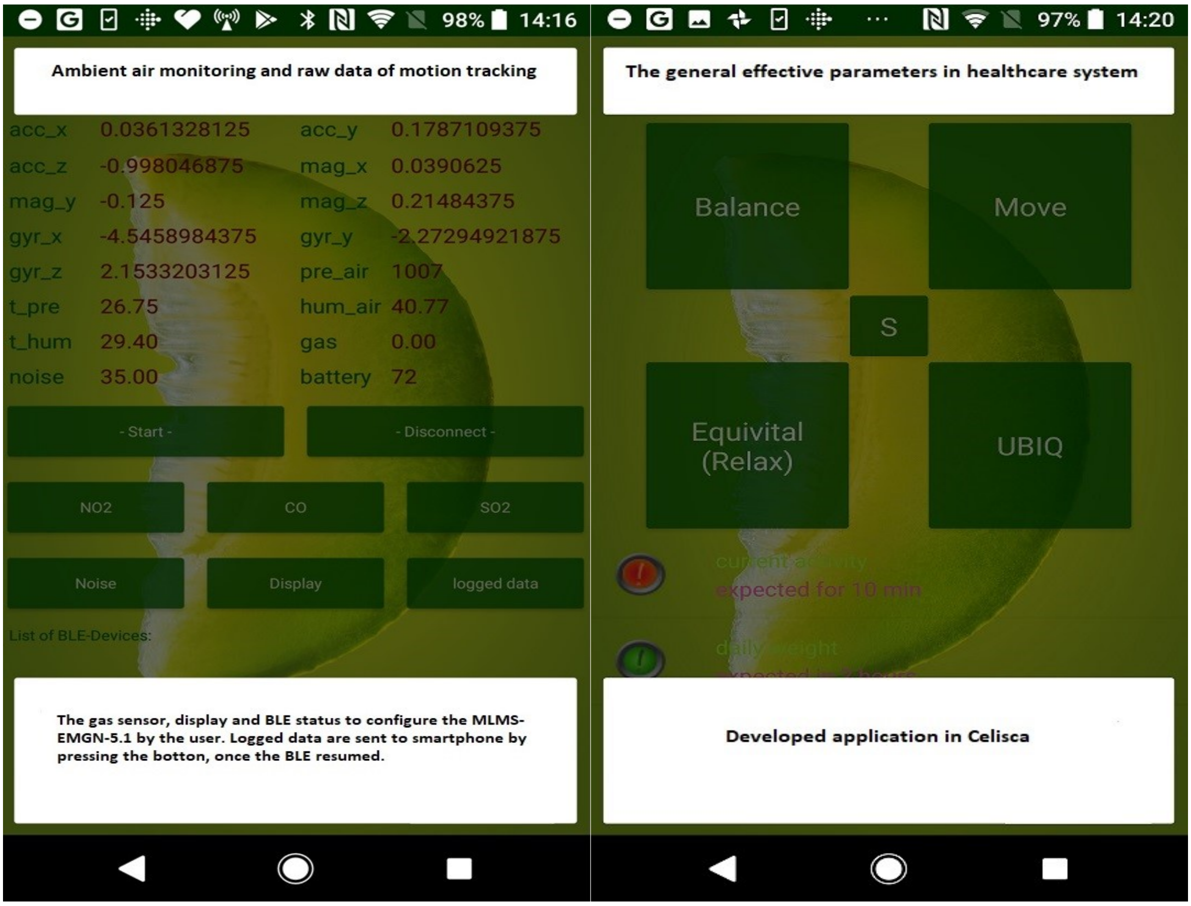

Fig. 9-3 The real-time ambient data monitoring and configuration (left), the general system of healthcare system (right).

9.3 COMPREHENSIVE INVESTIGATION

At the end of this work a comprehensive Table 9-1 is provided. In this table the most applicable wearables in this same area of research are compared in wide range of features and specifications with the proposed prototype. Configurability and sensor activation features are not presented in the table because it is only applied in the proposed prototype and are unique. The devices and prototypes provided in this table are mostly presented in chapter 2 as well.

Table 9-1 Comprehensive investigation on the features of the most applicable devices and prototypes.

Device	Size(mm)	Weight(gr)	Wearability	Connectivity	Structure	Sensor Replaceability	Display	Sound level
Gas sensor EVM [60]	26 × 26 × 50	NA	portable	BLE	flexible	no	no	no
TIDM-1CHP [61]	107.31 × 75.69	NA	waist-worn	no	fixed	two	yes	no
Gas alert extreme [32]	50 × 95 × 40	110	waist-worn	no	fixed	no	yes	no
MLMS-EMG-4.0 [50]	50 × 42 × 24	51.18	wrist-worn	BLE	flexible	yes	yes	yes
Eco Mini [49]	NA	NA	waist-worn	no	fixed	yes	no	yes
W-Air [43]	30 × 45	NA	wrist-worn	BLE	fixed	no	no	no
WEMS [51]	42 × 56 × 15	NA	waist-worn	BLE	fixed	no	yes	No
MLMS-EMGN-5.1	50 × 42 × 23	51.18	wrist-worn	BLE	flexible	yes	yes	yes

Temp. pressure humidity	Motion tracker	Resolution (ppm)	Vibrating motor	beeper	Software	hardware	Data storage	Battery life time(hrs)	Price(€)
No	No	0.1	No	No	Yes	No	No	CR2032-NA	599
No	No	0.1	No	No	yes	yes	No	USB-Battery	NA
No	No	0.1	Yes	Yes	no	no	No	1.5 years	338
Yes	Yes	0.1-7.5	Yes	Yes	yes	yes	No	15	160
Yes	Yes	NA	No	No	no	no	Yes	950 mAhr LiPol-NA	NA
Yes	Yes	4.3-64ppb	No	No	yes	yes	No	NA	38
Yes	Yes	NA	No	Yes	yes	no	Yes	2.5	NA
Yes	yes	0.1-7.5	yes	yes	yes	yes	yes	26	130

10 SUMMARY AND FUTURE WORK

10.1 SUMMARY

WHO has announced that individual's exposure to air pollutants is recognized as one of the main reasons in every seven death. In a larger scale of view, ambient parameters including toxic/hazardous gases and noise influence people's health, in particular who are suffering from cardiovascular, asthma, and heart patients. Elderly and children also have to be added to this critical group. The main focus of healthcare is gradually shifting from traditional treatment (treatment after diagnosis) to preventive medicine. Prediction and prevention according to history tracking record of an individual is fundamental theory of the new era of healthcare. In comprehensive monitoring of healthcare, four general parameters are involved (stress level, vital signs, ambient parameters and motion daily activities), and monitoring of environmental parameters in terms of physical and chemical (hazardous/toxic gases, noise, UV index, air temperature, humidity, and pressure) is one of the major considerations. Environment is of serious concern due to rapid industrialization and urbanization in the modern world. Environmental monitoring can be widely applied in different applications from industrial condition monitoring, occupational health and ecosystem changes to safety observation in chemical laboratories. After promising experiences with electronic health (e-Health) and mobile health (m-Health), the medical treatment is on the way to the new generation of systems, called the Internet of Things (IoT). Some researchers are oriented toward IoT based systems which are widely spread over all fields of applications. IoT, in concept, is a palm that links all fingers of different sizes and characteristics. The penetration rate of technologies from various scales and types (smart city, home, healthcare, and many more) characterized by comfort, flexibility, smart decision and control in conjunction with ease of use, motivates many people to use wearable smart devices in different areas. In particular, in healthcare and ambient parameters monitoring (focus of this paper) sensor integration, multi-parameters monitoring, centralized data collection and accessibility, secure transmission, and ease of use are the most important demands from many of users. IoT is the concept that may bring all these demands together under the same umbrella by means of wearable devices and advanced communication protocol technologies. In this work, we pay more attention to wireless sensor network (WSN) as the first tier of IoT. WSN is a spatially distributed network of autonomous sensors for the monitoring of environmental conditions, such as toxic gases, UV index, temperature, sound level (noise), pressure, and humidity. The WSN is built of "nodes" – here wearable. However, the WSN might be extended by adding nodes in healthcare, motion tracking and other fields. To conclude, the design of an efficient wearable device in environmental monitoring and in general, all fields related to real-time healthcare monitoring is playing an important role in WSN and consequently comprehensive parameters monitoring and IoT.

An environmental monitoring device can contribute to the routinization of workplace safety and to the collection of important health indicators. A wearable device capable of data transmission and communication with a gateway (eg. smartphone)-cloud, facilitates a suitable fusion with other sensor nodes within IoT. Therefore, the first step is to design an efficient wearable device for environmental monitoring with a special focus on wearability, prolonged operation, multi-parameter monitoring and data transmission.

The available ambient monitoring devices are mostly limited to portable (hand-held/waist-worn) and single-task devices. In particular, these devices are associated more often with hazardous gas detection and noise monitoring. Many of these devices are unaffordable to the average consumers especially when intention is multi-parameter monitoring (several single-task devices are required). In addition, the multi-parameter monitoring by several single-task wearables, reduces user convenience (e.g. interfering with daily routing activities) and increases the final cost. Wearable market's statistics indicate, many individuals from different professions and ages are highly interested in using wearables for ambient and healthcare parameters monitoring. Demands of users are mainly toward the wearability (form factor and convenience), prolonged, multi-parameter monitoring, and cost effective tools which do not interfere with daily routine activities. Sensor and device configurability, Big data, ease of data monitoring (on a smartphone an display), secure and straightforward data transmission (star configuration), data lost protection (storage in an external memory), and early user notification in abnormal status (beeper and vibrating motor) are expected as the major features of an efficient wearable device (in environmental monitoring) based on a new approach for an easy adoption in IoT. Healthcare parameters monitoring is not restricted to a special group of people and is important to everyone. Thus, to reach more users, the device must be affordable. In addition, a long monitoring time is essential. To conclude, a device with multi-parameters monitoring, a suitable form factor (light-weighted and compact), convenient mode of wearability (wrist-worn), beside the prolonged monitoring and cost-effective is more attractive for the users. These are the missing points in many manufactured products from industry.

To achieve the aforementioned requirements, a careful hardware design based on efficient electronic circuits and appropriate components selection is considered. Although software development and task distribution between software and hardware may reduce the hardware complexity and grant the criteria. In recent decades, semiconductor technology has been significantly improved, but reaching to promising points of size reduction in wearable technologies, requires some longer "time". For instance, to get a better gas sensor with lower response time, higher resolution and smaller in size, the technology must be more advanced in membrane. The alternative of "waiting for future" is to design a wearable device according to a tight strategy: Multi-Physical-Layer

.

The concentration is on "3D space utilization" as the concept and infrastructure of designing of a wearable in ambient parameters monitoring. This strategy is implemented according to "multi-layer" approach. In this approach, each group of parameters from the same category is monitored by a modular physical layer enriched with the respected sensors. Depending on the number of parameters and layers, each physical layer is located on top of another. The intention is to implement a device for "everyone in everywhere for everything". If the wearability and multi-parameters monitoring are given the highest priority at the foreground, consequently several drawbacks (form factor, weight, size, comfortness, and user friendly) are tackled behind the scene. In spite of many traditional structures, in this approach the hardware expansion is not done in x-y plane. The physical layers for different tasks are stuck one on top of the other through board to board connector in z direction. As the consequence, final scale of x-y is maintained constant (based on initial basic platform) and is adequate to be considered as a wrist-worn device. However, the altitude of device is slightly expanded while still keeping the solution compact. Designers believe that every tiny space must be utilized for components placement. The qualified initial basic platform compatible with the requirements (dimension, data transmission, capable of hardware expansion and integrated sensors) is chosen to host the physical layers. This host platform is enriched with the integrated ambient physical sensors, distributed on both sides. Gas sensor node is placed at the top layer of the device for easy exposure and a notification driver for early user warning in abnormal status is located as the bottom layer. Heart of this design is a hardware interface located between the host platform and the gas sensor node. Noise, UV index module and display are linked to the host platform through the hardware flex. The hardware interface is capable of linking more numbers of sensors to expand the wearable. The gas sensor layer consists of a universal gas sensor driver (compatible with two/three-lead gas sensors) and gas sensor itself. To provide multi-gas monitoring (one at each time), gas sensor layer is replaceable with other two/three-lead gas sensor (this is easily done by the user). To complete the multi-gas observation, sensor selection/activation is performed by sending a command from the smartphone to the device by the user. This feature can add several advantages to the wearable such as lower power consumption, compact form factor and prolonged ambient monitoring. In this design, data are always protected from lost whether by sending to the smartphone or storage in an external memory (when Bluetooth low energy (BLE) is disconnected). Real-time data monitoring via display/smartphone is supported. This wrist-worn is modular and can also operate independent of the smartphone.

10.2 FUTURE WORK

The intention to Link the Current Version to Future Development: Leading to Comprehensive Healthcare Monitoring (Motion Tracking and Vital Signs):

- The prototype is capable of covering the majority of ambient parameters to monitor. UV index can be considered as an add-on sensor.
- The available 9 DoF integrated inertial sensors provides motion tracking and user activities recording. By acquiring raw data in the smartphone, different algorithms may be implemented regarding various possibilities of user activities. This may include fall detection (especially for elderly), distance and in general motion tracking.
- Due to the adequate approach and a modular design, vital signs (e.g. heart rate and skin temperature) can be added to the prototype as a new physical layer to the current version.
- To extend the battery life, power harvesting by natural resources/body heat is a potential field of research in future development of this prototype.
- This device as a multi-parameter monitoring wrist-worn is capable of bidirectional data transmission. Therefore, it has the merit to be adopted in IoT.
- If this device is widely used for environmental monitoring by individuals during daily routine, the collected data by server (wearable-gateway-server) from each individual can be utilized for evaluation of very small scale area in urban environmental parameters

evaluations (e.g. a street). This may overcome to the issue of stationary climate sites which are rare in cities due to size, cost and maintenance.

11 REFERENCES

References

[1] P. Wang, R. Valerdi, S. Zhou, and L. Li, “Introduction: Advances in IoT research and applications,” *Inf Syst Front*, vol. 17, no. 2, pp. 239–241, 2015.

[2] http://dx.doi.org/10.1109/TETC.2015.2390034, “The Emerging Internet of Things Marketplace From an Industrial Perspective: A Survey,” *IEEE Trans. Emerg. Topics Comput.*, vol. 3, no. 4, pp. 585–598, 2015.

[3] L. D. Xu, W. He, and S. Li, “Internet of Things in Industries: A Survey,” *IEEE Trans. Ind. Inf.*, vol. 10, no. 4, pp. 2233–2243, 2014.

[4] S. M. Riazul Islam, D. Kwak, M. Humaun Kabir, M. Hossain, and K.-S. Kwak, “The Internet of Things for Health Care: A Comprehensive Survey,” *IEEE Access*, vol. 3, pp. 678–708, 2015.

[5] Holler, J., Tsiatsis, V., Mulligan, C., Avesand, S., Karnouskos, S., & Boyle, D., *From machine-to-machine to the Internet of Things: Introduction to a new age of intelligence,* Amsterdam: Academic Press, 2014.

[6] G. Kortuem, F. Kawsar, V. Sundramoorthy, and D. Fitton, “Smart objects as building blocks for the Internet of things,” *IEEE Internet Comput.*, vol. 14, no. 1, pp. 44–51, 2010.

[7] K. Romer, B. Ostermaier, F. Mattern, M. Fahrmair, and W. Kellerer, “Real-Time Search for Real-World Entities: A Survey,” *Proc. IEEE*, vol. 98, no. 11, pp. 1887–1902, 2010.

[8] D. Guinard, V. Trifa, and E. Wilde, “A resource oriented architecture for the Web of Things,” in *2010 Internet of things: (IOT 2010) Tokyo, Japan, 29 November- 1 December 2010*, Tokyo, Japan, 2010, pp. 1–8.

[9] L. Tan and N. Wang, “Future internet: The Internet of Things,” in *2010 3rd International Conference on Advanced Computer Theory and Engineering*, Chengdu, China, Jan. 2010, V5-376-V5-380.

[10] *Internet of Things Applications USA 2018 | 14 - 15 Nov | Santa Clara Convention Center, CA, USA.* [Online] Available: https://www.idtechex.com/internet-of-things-usa/show/en/. Accessed on: Dec. 18 2018.

[11] W. Gao *et al.,* “Fully integrated wearable sensor arrays for multiplexed in situ perspiration analysis,” (eng), *Nature*, vol. 529, no. 7587, pp. 509–514, 2016.

[12] S. Xu *et al.,* “Soft microfluidic assemblies of sensors, circuits, and radios for the skin,” (eng), *Science (New York, N.Y.)*, vol. 344, no. 6179, pp. 70–74, 2014.

[13] M. Haghi, K. Thurow, and R. Stoll, “Wearable Devices in Medical Internet of Things: Scientific Research and Commercially Available Devices,” (eng), *Healthcare informatics research*, vol. 23, no. 1, pp. 4–15, 2017.

[14] Institute of Electrical and Electronics Engineers, *The fourth international symposium on wearable computers*: IEEE Comput. Soc, 2000.

[15] T. Martin, E. Jovanov, and D. Raskovic, “Issues in wearable computing for medical monitoring applications: A case study of a wearable ECG monitoring device,” in *The fourth international symposium on wearable computers*, Atlanta, GA, USA, 2000, pp. 43–49.

[16] P. A. Rauschnabel and Y. K. Ro, “Augmented reality smart glasses: An investigation of technology acceptance drivers,” *IJTMKT*, vol. 11, no. 2, p. 123, 2016.

[17] U. Anliker *et al.,* “AMON: A Wearable Multiparameter Medical Monitoring and Alert System,” *IEEE Trans. Inform. Technol. Biomed.*, vol. 8, no. 4, pp. 415–427, 2004.

[18] C.-C. Yang and Y.-L. Hsu, “A review of accelerometry-based wearable motion detectors for physical activity monitoring,” (eng), *Sensors (Basel, Switzerland)*, vol. 10, no. 8, pp. 7772–7788, 2010.

[19] S. Patel, H. Park, P. Bonato, L. Chan, and M. Rodgers, “A review of wearable sensors and systems with application in rehabilitation,” (eng), *Journal of neuroengineering and rehabilitation*, vol. 9, p. 21, 2012.

[20] P.-C. Hii and W.-Y. Chung, “A comprehensive ubiquitous healthcare solution on an Android™ mobile device,” (eng), *Sensors (Basel, Switzerland)*, vol. 11, no. 7, pp. 6799–6815, 2011.

[21] S. Imani *et al.,* “A wearable chemical-electrophysiological hybrid biosensing system for real-time health and fitness monitoring,” (eng), *Nature communications*, vol. 7, p. 11650, 2016.

[22] *2015 IEEE Jordan Conference on Applied Electrical Engineering and Computing Technologies (AEECT)*.

[23] P. J. Soh, G. A.E. Vandenbosch, M. Mercuri, and D. M.M.-P. Schreurs, “Wearable Wireless Health Monitoring: Current Developments, Challenges, and Future Trends,” *IEEE Microwave*, vol. 16, no. 4, pp. 55–70, 2015.

[24] D. Spirjakin, A. Baranov, and S. Akbari, “Wearable Wireless Sensor System with RF Remote Activation for Gas Monitoring Applications,” *IEEE Sensors J.*, p. 1, 2018.

[25] R. Miramontes *et al.,* “PlaIMoS: A Remote Mobile Healthcare Platform to Monitor Cardiovascular and Respiratory Variables,” (eng), *Sensors (Basel, Switzerland)*, vol. 17, no. 1, 2017.

[26] P. van Daele, I. Moerman, and P. Demeester, “Wireless body area networks: Status and opportunities,” in *Ultra Wideband Wireless Body Area Networks : 9th International Conference on Body Area Networks : Ultra Wideband Wireless Body Area Networks : Co-Operative and Energy Efficient Body Area and Wireless Sensor Networks for Healthcare Applications : Academic Press Library in Biomedical Applications of Mobile and Wireless Communications: W: 2014 XXXIth URSI General Assembly and Scientific Symposium (URSI GASS)*, Beijing, China, 2014, pp. 1–4.

[27] Q. Zhang, D. Zhou, and X. Zeng, “Highly wearable cuff-less blood pressure and heart rate monitoring with single-arm electrocardiogram and photoplethysmogram signals,” *BioMed Eng OnLine*, vol. 16, no. 1, p. 1879, 2017.

[28] M. A. Al-Taee, W. Al-Nuaimy, A. Al-Ataby, Z. J. Muhsin, and S. N. Abood, “Mobile health platform for diabetes management based on the Internet-of-Things,” in *2015 IEEE Jordan Conference on Applied Electrical Engineering and Computing Technologies (AEECT)*, Amman, Jordan, pp. 1–5.

[29] M. M. Rodgers, V. M. Pai, and R. S. Conroy, “Recent Advances in Wearable Sensors for Health Monitoring,” *IEEE Sensors J.*, vol. 15, no. 6, pp. 3119–3126, 2015.

[30] *vivante-iot-ecosystem.jpg (1500×933).* [Online] Available: https://bensontao.files.wordpress.com/2013/10/vivante-iot-ecosystem.jpg. Accessed on: Nov. 27 2018.

[31] R. Negra, I. Jemili, and A. Belghith, “Wireless Body Area Networks: Applications and Technologies,” *Procedia Computer Science*, vol. 83, pp. 1274–1281, 2016.

[32] A. A. Lazakidou, S. Zimeras, D. Iliopoulou, and D.-D. Koutsouris, Eds., *mHealth ecosystems and social networks in healthcare*. Cham: Springer, 2016.

[33] World Health Organization and https://www.facebook.com/WHO, *WHO Global Ambient Air Quality Database (update 2018).* [Online] Available: https://www.who.int/airpollution/data/cities/en/. Accessed on: Dec. 20 2018.

[34] G. Li, C. Fang, S. Wang, and S. Sun, “The Effect of Economic Growth, Urbanization, and Industrialization on Fine Particulate Matter (PM2.5) Concentrations in China,” (eng), *Environmental science & technology*, vol. 50, no. 21, pp. 11452–11459, 2016.

[35] M. Crippa *et al.,* “Forty years of improvements in European air quality: Regional policy-industry interactions with global impacts,” *Atmos. Chem. Phys.*, vol. 16, no. 6, pp. 3825–3841, 2016.

[36] *Air quality in Europe — 2016 report.* [Online] Available: https://www.eea.europa.eu/publications/air-quality-in-europe-2016. Accessed on: Feb. 19 2018.

[37] J. M. Samet and J. D. Spengler, “Indoor Environments and Health: Moving Into the 21st Century,” *Am J Public Health*, vol. 93, no. 9, pp. 1489–1493, 2003.

[38] N. Bruce *et al.,* “WHO indoor air quality guidelines on household fuel combustion: Strategy implications of new evidence on interventions and exposure–risk functions,” *Atmospheric Environment*, vol. 106, pp. 451–457, 2015.

[39] J. Lelieveld, J. S. Evans, M. Fnais, D. Giannadaki, and A. Pozzer, “The contribution of outdoor air pollution sources to premature mortality on a global scale,” (eng), *Nature*, vol. 525, no. 7569, pp. 367–371, 2015.

[40] S. A. Sattar *et al.,* “Decontamination of indoor air to reduce the risk of airborne infections: Studies on survival and inactivation of airborne pathogens using an aerobiology chamber,” (eng), *American journal of infection control*, vol. 44, no. 10, e177-e182, 2016.

[41] J. Lelieveld, A. Haines, and A. Pozzer, “Age-dependent health risk from ambient air pollution: a modelling and data analysis of childhood mortality in middle-income and low-income countries,” *The Lancet Planetary Health*, vol. 2, no. 7, e292-e300, 2018.

[42] L. Du *et al.,* “Particle Concentrations and Effectiveness of Free-Standing Air Filters in Bedrooms of Children with Asthma in Detroit, Michigan,” (eng), *Building and environment*, vol. 46, no. 11, pp. 2303–2313, 2011.

[43] S. Li, *Proceedings of the 2009 International Symposium on Environmental Science and Technology*. Beijing: Science Press, 2009.

[44] P. Wargocki and D. P. Wyon, “Ten questions concerning thermal and indoor air quality effects on the performance of office work and schoolwork,” *Building and environment*, vol. 112, pp. 359–366, 2017.

[45] X. Zhang, P. Wargocki, Z. Lian, and C. Thyregod, “Effects of exposure to carbon dioxide and bioeffluents on perceived air quality, self-assessed acute health symptoms, and cognitive performance,” (eng), *Indoor air*, vol. 27, no. 1, pp. 47–64, 2017.

[46] H. Maula, V. Hongisto, V. Naatula, A. Haapakangas, and H. Koskela, “The effect of low ventilation rate with elevated bioeffluent concentration on work performance, perceived indoor air quality, and health symptoms,” (eng), *Indoor air*, vol. 27, no. 6, pp. 1141–1153, 2017.

[47] C. Huang *et al.,* “Potential Cardiovascular and Total Mortality Benefits of Air Pollution Control in Urban China,” (eng), *Circulation*, vol. 136, no. 17, pp. 1575–1584, 2017.

[48] B. J. Hubbell *et al.,* “Understanding social and behavioral drivers and impacts of air quality sensor use,” (eng), *The Science of the total environment*, vol. 621, pp. 886–894, 2018.

[49] G. Li *et al.,* “Association between fine ambient particulate matter and daily total mortality: An analysis from 160 communities of China,” (eng), *The Science of the total environment*, vol. 599-600, pp. 108–113, 2017.

[50] C. B.B. Guerreiro, V. Foltescu, and F. de Leeuw, “Air quality status and trends in Europe,” *Atmospheric Environment*, vol. 98, pp. 376–384, 2014.

[51] A. Kamal *et al.,* “Principle component analysis of flue gas exhaust and health risk estimates for the population around a functional incinerator in the vicinity of Rawalpindi Pakistan,” *Arabian Journal of Chemistry*, vol. 10, S2302-S2306, 2017.

[52] C. Wiedinmyer, R. J. Yokelson, and B. K. Gullett, “Global emissions of trace gases, particulate matter, and hazardous air pollutants from open burning of domestic waste,” (eng), *Environmental science & technology*, vol. 48, no. 16, pp. 9523–9530, 2014.

[53] P. S. J. Lakey *et al.,* “Chemical kinetics of multiphase reactions between ozone and human skin lipids: Implications for indoor air quality and health effects,” (eng), *Indoor air*, vol. 27, no. 4, pp. 816–828, 2017.

[54] Elisabeth, “Carbon-Monoxide-Risks-at-Low-Levels,” https://www.spec-sensors.com/wp-content/uploads/2016/05/Carbon-Monoxide-Risks-at-Low-Levels.pdf.

[55] R. Khaiwal *et al.,* “Assessment of noise pollution in and around a sensitive zone in North India and its non-auditory impacts,” (eng), *The Science of the total environment*, vol. 566-567, pp. 981–987, 2016.

[56] T. Münzel *et al.,* “Environmental stressors and cardio-metabolic disease: Part I-epidemiologic evidence supporting a role for noise and air pollution and effects of mitigation strategies,” (eng), *European heart journal*, vol. 38, no. 8, pp. 550–556, 2017.

[57] M. Basner *et al.,* “Auditory and non-auditory effects of noise on health,” *The Lancet*, vol. 383, no. 9925, pp. 1325–1332, 2014.

[58] S. A. Stansfeld, “Noise pollution: Non-auditory effects on health,” *British Medical Bulletin*, vol. 68, no. 1, pp. 243–257, 2003.

[59] A. Recio, C. Linares, J. R. Banegas, and J. Díaz, “The short-term association of road traffic noise with cardiovascular, respiratory, and diabetes-related mortality,” (eng), *Environmental research*, vol. 150, pp. 383–390, 2016.

[60] D. Banerjee, “Association between transportation noise and cardiovascular disease: A meta-analysis of cross-sectional studies among adult populations from 1980 to 2010,” (eng), *Indian journal of public health*, vol. 58, no. 2, pp. 84–91, 2014.

[61] D. Vienneau, C. Schindler, L. Perez, N. Probst-Hensch, and M. Röösli, “The relationship between transportation noise exposure and ischemic heart disease: A meta-analysis,” (eng), *Environmental research*, vol. 138, pp. 372–380, 2015.

[62] T. Münzel *et al.,* “Environmental Noise and the Cardiovascular System,” (eng), *Journal of the American College of Cardiology*, vol. 71, no. 6, pp. 688–697, 2018.

[63] W. Passchier-Vermeer and W. F. Passchier, “Noise exposure and public health,” (eng), *Environmental health perspectives*, vol. 108 Suppl 1, pp. 123–131, 2000.

[64] T. Münzel, T. Gori, W. Babisch, and M. Basner, “Cardiovascular effects of environmental noise exposure,” (eng), *European heart journal*, vol. 35, no. 13, pp. 829–836, 2014.

[65] R. Rylander, “Physiological aspects of noise-induced stress and annoyance,” *Journal of Sound and Vibration*, vol. 277, no. 3, pp. 471–478, 2004.

[66] M. G. Smith, I. Croy, M. Ogren, and K. Persson Waye, “On the influence of freight trains on humans: a laboratory investigation of the impact of nocturnal low frequency vibration and noise on sleep and heart rate,” (eng), *PloS one*, vol. 8, no. 2, e55829, 2013.

[67] E. E. M. M. van Kempen *et al.,* “The association between noise exposure and blood pressure and ischemic heart disease: a meta-analysis,” (eng), *Environmental health perspectives*, vol. 110, no. 3, pp. 307–317, 2002.

[68] E. Murphy, E. A. King, and H. J. Rice, “Estimating human exposure to transport noise in central Dublin, Ireland,” (eng), *Environment international*, vol. 35, no. 2, pp. 298–302, 2009.

[69] V. Pathak, B. D. Tripathi, and V. k. Mishra, “Evaluation of traffic noise pollution and attitudes of exposed individuals in working place,” *Atmospheric Environment*, vol. 42, no. 16, pp. 3892–3898, 2008.

[70] A. Piccolo, D. Plutino, and G. Cannistraro, “Evaluation and analysis of the environmental noise of Messina, Italy,” *Applied Acoustics*, vol. 66, no. 4, pp. 447–465, 2005.
[71] A. Gidlöf-Gunnarsson and E. Öhrström, “Noise and well-being in urban residential environments: The potential role of perceived availability to nearby green areas,” *Landscape and Urban Planning*, vol. 83, no. 2-3, pp. 115–126, 2007.
[72] R. Gravina, P. Alinia, H. Ghasemzadeh, and G. Fortino, “Multi-sensor fusion in body sensor networks: State-of-the-art and research challenges,” *Information Fusion*, vol. 35, pp. 68–80, 2017.
[73] H. Cho, Y.-W. Seo, B.V.K. V. Kumar, and R. R. Rajkumar, “A multi-sensor fusion system for moving object detection and tracking in urban driving environments,” in *Robotics and Automation (ICRA), 2014 IEEE International Conference on: May 31 2014-June 7 2014 : [Hong Kong, China]*, Hong Kong, China, 2014, pp. 1836–1843.
[74] M. Mubashir, L. Shao, and L. Seed, “A survey on fall detection: Principles and approaches,” *Neurocomputing*, vol. 100, pp. 144–152, 2013.
[75] IEEE Conference on Computer Vision and Pattern Recognition; CVPR, *IEEE Conference on Computer Vision and Pattern Recognition (CVPR), 2013: 23 - 28 June 2013, Portland, Oregon, USA ; proceedings*. Piscataway, NJ, Piscataway, NJ: IEEE, 2013.
[76] P. J. Figueroa, N. J. Leite, and R. M.L. Barros, “Tracking soccer players aiming their kinematical motion analysis,” *Computer Vision and Image Understanding*, vol. 101, no. 2, pp. 122–135, 2006.
[77] I. Wachsmuth and T. Sowa, Eds., *Gesture and Sign Language in Human-Computer Interaction: International Gesture Workshop, GW 2001 London, UK, April 18-20, 2001 Revised Papers*. Berlin, Heidelberg: Springer, 2002.
[78] D. Hutchison *et al., Ubiquitous Intelligence and Computing: 6th International Conference, UIC 2009, Brisbane, Australia, July 7-9, 2009. Proceedings*. Berlin, Heidelberg: Springer Berlin Heidelberg, 2009.
[79] L. Vito, O. Postolache, and S. Rapuano, “Measurements and sensors for motion tracking in motor rehabilitation,” *IEEE Instrum. Meas. Mag.*, vol. 17, no. 3, pp. 30–38, 2014.
[80] C. Fuchs, N. Aschenbruck, P. Martini, and M. Wieneke, “Indoor tracking for mission critical scenarios: A survey,” *Pervasive and Mobile Computing*, vol. 7, no. 1, pp. 1–15, 2011.
[81] S. O. H. Madgwick, A. J. L. Harrison, and A. Vaidyanathan, “Estimation of IMU and MARG orientation using a gradient descent algorithm,” (eng), *IEEE ... International Conference on Rehabilitation Robotics : [proceedings]*, vol. 2011, p. 5975346, 2011.
[82] *Wireless Communications, Networking and Mobile Computing, 2009. WiCom '09. 5th International Conference on*: IEEE / Institute of Electrical and Electronics Engineers Incorporated, 2009.
[83] E. Jovanov, “System architecture of Wireless Body Sensor Networks,” in *6th International Workshop on Wearable Micro and Nano Technologies for Personalized Health (pHealth), 2009: 24 - 26 June 2009, Oslo, Norway*, Oslo, Norway, 2009, pp. 45–48.
[84] M. M. Hassan, K. Lin, X. Yue, and J. Wan, “A multimedia healthcare data sharing approach through cloud-based body area network,” *Future Generation Computer Systems*, vol. 66, pp. 48–58, 2017.
[85] J. Shen, S. Chang, J. Shen, Q. Liu, and X. Sun, “A lightweight multi-layer authentication protocol for wireless body area networks,” *Future Generation Computer Systems*, vol. 78, pp. 956–963, 2018.
[86] M. Waheed, R. Ahmad, W. Ahmed, M. Drieberg, and M. M. Alam, “Towards Efficient Wireless Body Area Network Using Two-Way Relay Cooperation,” (eng), *Sensors (Basel, Switzerland)*, vol. 18, no. 2, 2018.
[87] G. Fortino *et al.*, “Advances in multi-sensor fusion for body sensor networks: Algorithms, architectures, and applications,” *Information Fusion*, vol. 45, pp. 150–152, 2019.
[88] J. Xing and Y. Zhu, “A Survey on Body Area Network,” in *Wireless Communications, Networking and Mobile Computing, 2009. WiCom '09. 5th International Conference on*, Beijing, China, 2009, pp. 1–4.
[89] D. P. Tobon, T. H. Falk, and M. Maier, “Context awareness in WBANs: A survey on medical and non-medical applications,” *IEEE Wireless Commun.*, vol. 20, no. 4, pp. 30–37, 2013.
[90] A. Boulemtafes and N. Badache, “Design of Wearable Health Monitoring Systems: An Overview of Techniques and Technologies,” in *Annals of information systems, 1934-3221*, vol. 20, *mHealth ecosystems and social networks in healthcare*, A. A. Lazakidou, S. Zimeras, D. Iliopoulou, and D.-D. Koutsouris, Eds., Cham: Springer, 2016, pp. 79–94.
[91] H. Klauk, *Organic electronics II: More materials and applications / edited by Hagen Klauk*. Weinheim: Wiley-VCH, 2012.
[92] T. Rai, P. Dantes, B. Bahreyni, and W. S. Kim, “A Stretchable RF Antenna With Silver Nanowires,” *IEEE Electron Device Lett.*, vol. 34, no. 4, pp. 544–546, 2013.
[93] Y. Zhang *et al.*, “A Batteryless 19 $\\mu$W MICS/ISM-Band Energy Harvesting Body Sensor Node SoC for ExG Applications,” *IEEE J. Solid-State Circuits*, vol. 48, no. 1, pp. 199–213, 2013.
[94] R. Rosini and R. D'Errico, “Comparing On-Body dynamic channels for two antenna designs,” in *Loughborough Antennas and Propagation Conference (LAPC), 2012: 12 - 13 Nov. 2012, Burleigh Court Conference Centre, Loughborough University, UK*, Loughborough, Leicestershire, United Kingdom, 2012, pp. 1–4.
[95] H. Giddens, D. L. Paul, G. S. Hilton, and J. P. McGeehan, “Influence of body proximity on the efficiency of a wearable textile patch antenna,” in *2012 6th European Conference on Antennas and Propagation*, Prague, Czech Republic, 2012, pp. 1353–1357.
[96] R. Cavallari, F. Martelli, R. Rosini, C. Buratti, and R. Verdone, “A Survey on Wireless Body Area Networks: Technologies and Design Challenges,” *IEEE Commun. Surv. Tutorials*, vol. 16, no. 3, pp. 1635–1657, 2014.
[97] A. Sani, A. Alomainy, and Y. Hao, “The effect of various human body tissue models on radiowave propagation from a bladder implanted wireless source,” in *2009 IEEE International Symposium on Antennas and Propagation and USNC/URSI National Radio Science Meeting: [Charleston, S.C., June 1-5, 2009*, North Charleston, SC, USA, 2009, pp. 1–4.
[98] L. Martens, D. Kurup, W. Joseph, and G. Vermeeren, “In-body path loss model for homogeneous and heterogeneous human tissues,” in *XXXth URSI general assembly and scientific symposium, 2011: [URSI GASS 2011] ; 13 -20 Aug. 2011, Istanbul, Turkey*, Istanbul, 2011, pp. 1–4.
[99] A. S. Abiodun, M. H. Anisi, I. Ali, A. Akhunzada, and M. K. Khan, “Reducing Power Consumption in Wireless Body Area Networks: A Novel Data Segregation and Classification Technique,” *IEEE Consumer Electron. Mag.*, vol. 6, no. 4, pp. 38–47, 2017.
[100] T. Hayajneh, G. Almashaqbeh, S. Ullah, and A. V. Vasilakos, “A survey of wireless technologies coexistence in WBAN: Analysis and open research issues,” *Wireless Netw*, vol. 20, no. 8, pp. 2165–2199, 2014.
[101] International Association of Computer Science and Information Technology; Singapore Institute of Electronics; IEEE Computer Society, *2009 International Conference on Information Management and Engineering: Proceedings, Kuala Lumpur, Malaysia, 3-5 April 2009*. Los Alamitos Calif.: IEEE Computer Society, 2009.

[102] E. Jovanov, "Wireless Technology and System Integration in Body Area Networks for m-Health Applications," in *Engineering in Medicine and Biology Society, 2005: IEEE-EMBS 2005 : 27th Annual International Conference of the Engineering in Medicine and Biology Society : 1-4 September, 2005, [Shanghai, China]*, Shanghai, China, 2005, pp. 7158–7160.
[103] *Cairclip : the autonomous pollution sensor - Cairpol.* [Online] Available: http://cairpol.com/en/expertise-autonomous-systems-for-monitoring-low-concentration-pollutants/products-cairnet-cairtube-cairclip-capteur-cairsens/cairclip-autonomous-pollution-sensor/. Accessed on: Feb. 26 2018.
[104] G. Mulhern, "lbna26394enn," http://publications.jrc.ec.europa.eu/repository/bitstream/JRC86499/lbna26394enn.pdf.
[105] gerbomi, "Microsoft Word - EUR23676.doc,"
[106] L. Spinelle, M. Gerboles, M. G. Villani, M. Aleixandre, and F. Bonavitacola, *Field calibration of a cluster of low-cost available sensors for air quality monitoring. Part A: Ozone and nitrogen dioxide.* [Online] Available: https://www.infona.pl/resource/bwmeta1.element.elsevier-81a5da2b-6140-387f-ad30-f3bf61d43a88. Accessed on: Feb. 26 2018.
[107] *Document Display | NEPIS | US EPA.* [Online] Available: https://nepis.epa.gov/Exe/ZyNET.exe/P100MOXD.txt?ZyActionD=ZyDocument&Client=EPA&Index=2011%20Thru%202015&Docs=&Query=&Time=&EndTime=&SearchMethod=1&TocRestrict=n&Toc=&TocEntry=&QField=&QFieldYear=&QFieldMonth=&QFieldDay=&UseQField=&IntQFieldOp=0&ExtQFieldOp=0&XmlQuery=&File=D%3A%5CZYFILES%5CINDEX%20DATA%5C11THRU15%5CTXT%5C00000015%5CP100MOXD.txt&User=ANONYMOUS&Password=anonymous&SortMethod=h%7C-&MaximumDocuments=1&FuzzyDegree=0&ImageQuality=r75g8/r75g8/x150y150g16/i425&Display=hpfr&DefSeekPage=x&SearchBack=ZyActionL&Back=ZyActionS&BackDesc=Results%20page&MaximumPages=1&ZyEntry=2. Accessed on: Feb. 26 2018.
[108] E488676, "TechData_O3_3E1F_rev201111," https://www.citytech.com/PDF-Datasheets/o33e1f.pdf.
[109] *City Technology Gas Sensors.* [Online] Available: https://euro-gasman.com/gas-sensors/citytech.html. Accessed on: Feb. 26 2018.
[110] *City Technology Ltd, Global Leaders in Gas Sensor Technology.* [Online] Available: https://www.citytech.com/index.html. Accessed on: Feb. 26 2018.
[111] *Alphasense | The Sensor Technology Company.* [Online] Available: http://www.alphasense.com/. Accessed on: Feb. 26 2018.
[112] *Default Page Title.* [Online] Available: http://www.alphasense.com/index.php/products/nitrogen-dioxide-2/. Accessed on: Feb. 26 2018.
[113] I. T. Department, "Microsoft Word - a1a-mics-2710_2_s1.doc," https://www.cdiweb.com/datasheets/e2v/mics-2710.pdf.
[114] *MICS-4514, Gas Sensor - MetalOxide, SGX Sensortech Limited (formerly e2v).* [Online] Available: https://sgx.cdistore.com/ProductDetail/MICS4514-SGX-Sensortech-Limited-formerly-e2v/333417/. Accessed on: Feb. 26 2018.
[115] "5042pdf," http://www.figarosensor.com/products/5042pdf.pdf.
[116] *Carbon dioxide : Select by target gas - Gas Sensors & Modules | Products - Figaro Engineering Inc.* [Online] Available: http://www.figaro.co.jp/en/product/sensor/target-gas/co2/. Accessed on: Feb. 26 2018.
[117] *OEM Modules - ELT SENSOR.* [Online] Available: http://tccelt.co.kr/2016/products/oem_modules/sub_main.html. Accessed on: Feb. 26 2018.
[118] L. Spinelle, M. Gerboles, M. G. Villani, M. Aleixandre, and F. Bonavitacola, "Field calibration of a cluster of low-cost available sensors for air quality monitoring. Part A: Ozone and nitrogen dioxide," *Sensors and Actuators B: Chemical*, vol. 215, pp. 249–257, 2015.
[119] *Gas Sensors for the Internet of Things.* [Online] Available: https://www.spec-sensors.com/. Accessed on: Dec. 20 2018.
[120] *Home.* [Online] Available: https://pyreos.com/. Accessed on: Dec. 20 2018.
[121] N. N. Samotaev, A. V. Ivanova, K.Y. Oblov, and A. A. Vasiliev, "Wireless digital platform for environmental gas monitoring," in *2015 International Siberian Conference on Control and Communications (SIBCON): 21 - 23 May 2015, Russia, Omsk*, Omsk, Russia, 2015, pp. 1–4.
[122] *2015 9th International Conference on Sensing Technology (ICST): Date*. Piscataway, NJ: IEEE, 2015.
[123] *GasAlert Extreme Single Gas Detector.* Accessed on: Feb. 20 2018.
[124] *Multi Gas Detectors.* [Online] Available: https://www.bw-gasmonitors.com/multi-gas-detectors-gasalertmicroclip-xt-multi-gas-detectors.html. Accessed on: Feb. 20 2018.
[125] *TIDA-00056 Gas Sensor Platform with Bluetooth Low Energy | TI.com.* [Online] Available: http://www.ti.com/tool/TIDA-00056. Accessed on: Feb. 20 2018.
[126] *Ambient Sensor.* [Online] Available: http://www.bosch-presse.de/pressportal/de/en/ambient-sensor-35987.html. Accessed on: Feb. 20 2018.
[127] B. Maag, Z. Zhou, and L. Thiele, "W-Air," *Proc. ACM Interact. Mob. Wearable Ubiquitous Technol.*, vol. 2, no. 1, pp. 1–25, 2018.
[128] D. Culler, Ed., *Proceedings of the 7th ACM Conference on Embedded Networked Sensor Systems*. New York, NY: ACM, 2009.
[129] W. Kaiser and R. McCray, Eds., *Proceedings of the Conference on Wireless Health*. [Place of publication not identified]: ACM, 2012.
[130] F. Wu, T. Wu, and M. R. Yuce, "An Internet-of-Things (IoT) Network System for Connected Safety and Health Monitoring Applications," (eng), *Sensors (Basel, Switzerland)*, vol. 19, no. 1, 2018.
[131] *Noise Monitoring.* [Online] Available: https://www.casellasolutions.com/products/casella_us_en/by-application/noise-monitoring.html. Accessed on: Dec. 20 2018.
[132] *3M™ Edge™ 5 Dosimeter Kit EG5-D, Docking Station 1 Kit EA/Case.* [Online] Available: https://www.3m.com/3M/en_US/company-us/all-3m-products/~/3M-Edge-5-Dosimeter-Kit-EG5-D-Docking-Station-1-Kit-EA-Case/?N=5002385+3294756827&rt=rud. Accessed on: Dec. 20 2018.
[133] *soundBadge.* [Online] Available: https://www.panacoustics.com/soundbadge.html. Accessed on: Dec. 20 2018.
[134] *ER-200DW8 Personal Noise Dosimeter with Data Logging | ADCO HEARING PRODUCTS.* [Online] Available: https://adcohearing.com/product/er-200dw8-personal-noise-dosimeter-data-logging. Accessed on: Dec. 20 2018.
[135] *DAP Digital Sound Level Meter - günstig bei LTT.* [Online] Available: https://www.ltt-versand.de/Ton/Audio-Tools-und-Zubehoer/Audiomessgeraete/DAP-Digital-Sound-Level-Meter::55712.html?language=de&utm_source=google&utm_medium=shopping&gclid=CjwKCAiA0uLgBRABEiwAecFnk4lpzkD-WKaRpfoCAH34CWMe7S_Gsa4cWLOIRiSz3PNKsw-9ZWr7_RoC-wcQAvD_BwE. Accessed on: Dec. 20 2018.
[136] *Digital Sound Level Meter, A Weighted.* [Online] Available: https://www.grainger.com/product/GRAINGER-APPROVED-Digital-Sound-Level-Meter-5URG3. Accessed on: Dec. 20 2018.
[137] *Testo 816-1 Sound Level Meter.* [Online] Available: https://www.testoaus.com.au/testo-816-1-sound-level-meter. Accessed on: Dec. 20 2018.

[138] N. Acoustics, *SC310 Class 1 Sound Level Meter | NOVA Acoustics Ltd | Sound Testing Specialists | Sound L...* [Online] Available: https://www.novaacoustics.co.uk/acoustic-equipment/sound-level-meters/cesva-sc310-class-1-sound-level-meter. Accessed on: Dec. 20 2018.

[139] R. R. Fletcher, N. M. Oreskovic, and A. I. Robinson, "Design and clinical feasibility of personal wearable monitor for measurement of activity and environmental exposure," (eng), *Conference proceedings : ... Annual International Conference of the IEEE Engineering in Medicine and Biology Society. IEEE Engineering in Medicine and Biology Society. Annual Conference*, vol. 2014, pp. 874–877, 2014.

[140] F. Sanfilippo and K. Y. Pettersen, "A sensor fusion wearable health-monitoring system with haptic feedback," in *2015 11th International Conference on Innovations in Information Technology (IIT): Innovations 2015 : proceedings : 01-03 November 2015, Dubai, United Arab Emirates*, Dubai, United Arab Emirates, 2015, pp. 262–266.

[141] *e-Health Sensor Platform V2.0 for Arduino and Raspberry Pi [Biometric / Medical Applications].* [Online] Available: https://www.cooking-hacks.com/documentation/tutorials/ehealth-biometric-sensor-platform-arduino-raspberry-pi-medical. Accessed on: Feb. 20 2018.

[142] G. M. Bertolotti *et al.,* "A Wearable and Modular Inertial Unit for Measuring Limb Movements and Balance Control Abilities," *IEEE Sensors J.*, vol. 16, no. 3, pp. 790–797, 2016.

[143] O. Aziz, E. J. Park, G. Mori, and S. N. Robinovitch, "Distinguishing near-falls from daily activities with wearable accelerometers and gyroscopes using Support Vector Machines," (eng), *Conference proceedings : ... Annual International Conference of the IEEE Engineering in Medicine and Biology Society. IEEE Engineering in Medicine and Biology Society. Annual Conference*, vol. 2012, pp. 5837–5840, 2012.

[144] IEEE International Conference on Service-Oriented Computing and Applications; IEEE/ION Position, Location and Navigation Symposium; IEEE/ION PLANS, *IEEE/ION Position, Location and Navigation Symposium - PLANS 2014, 2014: 5 - 8 May 2014, Hyatt Regency, Monterey, California*. Piscataway, NJ, Piscataway, NJ: IEEE, 2014.

[145] X. Yun, E. R. Bachmann, H. Moore, and J. Calusdian, "Self-contained Position Tracking of Human Movement Using Small Inertial/Magnetic Sensor Modules," in *IEEE International Conference on Robotics and Automation, 2007: 10 - 14 April 2007, [Roma, Italy]*, Rome, Italy, 2007, pp. 2526–2533.

[146] G. Epelde *et al.,* "Universal Remote Delivery of Rehabilitation: Validation with Seniors' Joint Rehabilitation Therapy," *Cybernetics and Systems*, vol. 45, no. 2, pp. 109–122, 2014.

[147] A. Reiss and D. Stricker, "Aerobic activity monitoring: Towards a long-term approach," *Univ Access Inf Soc*, vol. 13, no. 1, pp. 101–114, 2014.

[148] K. Frank, E. M. Diaz, P. Robertson, and F. J. F. Sanchez, "Bayesian recognition of safety relevant motion activities with inertial sensors and barometer," in *IEEE/ION Position, Location and Navigation Symposium - PLANS 2014, 2014: 5 - 8 May 2014, Hyatt Regency, Monterey, California*, Monterey, CA, USA, 2014, pp. 174–184.

[149] M. Schulze *et al.,* "Development and clinical validation of an unobtrusive ambulatory knee function monitoring system with inertial 9DoF sensors," (eng), *Conference proceedings : ... Annual International Conference of the IEEE Engineering in Medicine and Biology Society. IEEE Engineering in Medicine and Biology Society. Annual Conference*, vol. 2012, pp. 1968–1971, 2012.

[150] M. C. Schall, N. B. Fethke, H. Chen, S. Oyama, and D. I. Douphrate, "Accuracy and repeatability of an inertial measurement unit system for field-based occupational studies," (eng), *Ergonomics*, vol. 59, no. 4, pp. 591–602, 2016.

[151] F. Foerster, M. Smeja, and J. Fahrenberg, "Detection of posture and motion by accelerometry: A validation study in ambulatory monitoring," *Computers in Human Behavior*, vol. 15, no. 5, pp. 571–583, 1999.

[152] F. Dadashi, G. P. Millet, and K. Aminian, "Estimation of Front-Crawl Energy Expenditure Using Wearable Inertial Measurement Units," *IEEE Sensors J.*, vol. 14, no. 4, pp. 1020–1027, 2014.

[153] *MTw Development Kit (legacy product) - Products - Xsens 3D motion tracking.* [Online] Available: https://www.xsens.com/products/mtw-development-kit/. Accessed on: Feb. 26 2018.

[154] M. J. Mathie, A. C. F. Coster, N. H. Lovell, and B. G. Celler, "Detection of daily physical activities using a triaxial accelerometer," *Med. Biol. Eng. Comput.*, vol. 41, no. 3, pp. 296–301, 2003.

[155] G. Uswatte *et al.,* "Objective Measurement of Functional Upper-Extremity Movement Using Accelerometer Recordings Transformed With a Threshold Filter," *Stroke*, vol. 31, no. 3, pp. 662–667, 2000.

[156] *fitbit flex - Google Search.* [Online] Available: https://www.google.de/search?q=fitbit+flex&rlz=1C1CHBF_enDE756DE756&oq=fitbit+&aqs=chrome.3.69i57j0l5.4872j0j7&sourceid=chrome&ie=UTF-8. Accessed on: Feb. 26 2018.

[157] *Fitbit Flex 2™ Fitnessarmband.* [Online] Available: https://www.fitbit.com/de/flex2. Accessed on: Feb. 26 2018.

[158] *Withings Pulse – Nokia.* [Online] Available: https://support.health.nokia.com/hc/en-us/categories/200118227-Withings-Pulse. Accessed on: Feb. 26 2018.

[159] *Best Fitness Trackers 2018.* [Online] Available: https://www.tomsguide.com/us/best-fitness-trackers,review-2066.html. Accessed on: Feb. 26 2018.

[160] *Smartwatches, Fitness Trackers & Wearable Technology - Misfit.* [Online] Available: https://misfit.com/de_de/. Accessed on: Feb. 26 2018.

[161] *UP App by Jawbone | Live happier and healthier with our free app.* [Online] Available: https://jawbone.com/up. Accessed on: Feb. 26 2018.

[162] *Watch.* [Online] Available: https://www.apple.com/lae/watch/. Accessed on: Feb. 26 2018.

[163] *Hybrid Smartwatch | Steel HR - Withings.* [Online] Available: https://www.withings.com/de/de/steel-hr. Accessed on: Dec. 20 2018.

[164] Garmin, *fēnix® 3 Tutorial Videos | Garmin | United States.* [Online] Available: https://www.garmin.com/en-US/learning-center/fenix-3. Accessed on: Dec. 20 2018.

[165] A. Muzet, "Environmental noise, sleep and health," (eng), *Sleep medicine reviews*, vol. 11, no. 2, pp. 135–142, 2007.

[166] A. Pantelopoulos and N. G. Bourbakis, "A Survey on Wearable Sensor-Based Systems for Health Monitoring and Prognosis," *IEEE Trans. Syst., Man, Cybern. C*, vol. 40, no. 1, pp. 1–12, 2010.

[167] H. Cho, "Personal Environmental Monitoring System and network platform," in *2015 9th International Conference on Sensing Technology (ICST): Date*, Auckland, New Zealand, 2015, pp. 751–756.

[168] A. Darwish and A. E. Hassanien, "Wearable and implantable wireless sensor network solutions for healthcare monitoring," (eng), *Sensors (Basel, Switzerland)*, vol. 11, no. 6, pp. 5561–5595, 2011.

[169] E. Bakker and M. Telting-Diaz, "Electrochemical Sensors," *Anal. Chem.*, vol. 74, no. 12, pp. 2781–2800, 2002.
[170] S. Das and V. Jayaraman, "SnO2: A comprehensive review on structures and gas sensors," *Progress in Materials Science*, vol. 66, pp. 112–255, 2014.
[171] C. Wang, L. Yin, L. Zhang, D. Xiang, and R. Gao, "Metal oxide gas sensors: Sensitivity and influencing factors," (eng), *Sensors (Basel, Switzerland)*, vol. 10, no. 3, pp. 2088–2106, 2010.
[172] G. Eranna, B. C. Joshi, D. P. Runthala, and R. P. Gupta, "Oxide Materials for Development of Integrated Gas Sensors—A Comprehensive Review," *Critical Reviews in Solid State and Materials Sciences*, vol. 29, no. 3-4, pp. 111–188, 2010.
[173] S. Gupta Chatterjee, S. Chatterjee, A. K. Ray, and A. K. Chakraborty, "Graphene–metal oxide nanohybrids for toxic gas sensor: A review," *Sensors and Actuators B: Chemical*, vol. 221, pp. 1170–1181, 2015.
[174] A. J. Bandodkar and J. Wang, "Non-invasive wearable electrochemical sensors: A review," (eng), *Trends in biotechnology*, vol. 32, no. 7, pp. 363–371, 2014.
[175] M. Magno *et al.,* "Low-Power Gas Sensing using Carbon Nanotubes in Wearable Devices," *IEEE Sensors J.*, p. 1, 2016.
[176] H. Li, X. Mu, Y. Yang, and A. J. Mason, "Low Power Multimode Electrochemical Gas Sensor Array System for Wearable Health and Safety Monitoring," *IEEE Sensors J.*, vol. 14, no. 10, pp. 3391–3399, 2014.
[177] J. Yang, B. Chen, J. Zhou, and Z. Lv, "A Low-Power and Portable Biomedical Device for Respiratory Monitoring with a Stable Power Source," (eng), *Sensors (Basel, Switzerland)*, vol. 15, no. 8, pp. 19618–19632, 2015.
[178] J. Dieffenderfer *et al.,* "Low-Power Wearable Systems for Continuous Monitoring of Environment and Health for Chronic Respiratory Disease," (eng), *IEEE journal of biomedical and health informatics*, vol. 20, no. 5, pp. 1251–1264, 2016.
[179] IEEE Symposium on Electromagnetic Compatibility and Signal Integrity; EMC & SI; EMCSI, *IEEE Symposium on Electromagnetic Compatibility and Signal Integrity, 2015: EMC & SI 2015 ; 15 - 21 March 2015, Silicon Valley, Santa Clara, CA, USA ; proceedings*. Piscataway, NJ, Piscataway, NJ: IEEE, 2015.
[180] S. Sojuyigbe and K. Daniel, "Wearables/IOT devices: Challenges and solutions to integration of miniature antennas in close proximity to the human body," in *IEEE Symposium on Electromagnetic Compatibility and Signal Integrity, 2015: EMC & SI 2015 ; 15 - 21 March 2015, Silicon Valley, Santa Clara, CA, USA ; proceedings*, Santa Clara, CA, USA, 2015, pp. 75–78.
[181] J. Yao, R. Schmitz, and S. Warren, "A Wearable Point-of-Care System for Home Use That Incorporates Plug-and-Play and Wireless Standards," *IEEE Trans. Inform. Technol. Biomed.*, vol. 9, no. 3, pp. 363–371, 2005.
[182] A. Takeda *et al.,* "A novel energy-efficient data acquisition method for wearable devices," in *Proceedings notebook for COOL Chips XVIII: Yokohama Joho Bunka Center, (Yokohama Media & Communications Center), April 13-15, 2015*, Yokohama, Japan, 2015, pp. 1–3.
[183] N. Oliver and F. Flores-Mangas, "HealthGear: A Real-time Wearable System for Monitoring and Analyzing Physiological Signals," in *BSN 2006: International Workshop on Wearable and Implantable Body Sensor Networks 2006*, Cambridge, MA, USA, 2006, pp. 61–64.
[184] stbe, "nRF51x22 PS.book,"
[185] STMICROELECTRONICS, "ARM®-based 32-bit MCU, 150DMIPs, up to 1 MB Flash/128+4KB RAM, USB OTG HS/FS, Ethernet, 17 TIMs, 3 ADCs, 15 comm. interfaces & camera,"
[186] Texas Instruments, Incorporated [SLAS735, and J], "MSP430G2x53, MSP430G2x13 Mixed Signal Microcontroller datasheet (Rev. J),"
[187] *nRF51822 Bluetooth Smart Beacon Kit.* [Online] Available: https://www.nordicsemi.com/Software-and-Tools/Reference-Designs/nRF51822-Beacon-Kit. Accessed on: Dec. 20 2018.
[188] A. Industries, *Adafruit WICED WiFi Feather - STM32F205 with Cypress WICED WiFi.* [Online] Available: https://www.adafruit.com/product/3056. Accessed on: Dec. 20 2018.
[189] *US $42.0 |ARM Cortex M3 Development Board STM32F103VET6 + 2.4 inch TFT LCD Touch Screen 320*240 on Aliexpress.com | Alibaba Group.* [Online] Available: https://www.aliexpress.com/item/ARM-Cortex-M3-STM32F103VET6-STM32-development-board-2-4-TFT-touch-screen/1017498789.html. Accessed on: Dec. 20 2018.
[190] *Aistin Blue - iProtoXi.* [Online] Available: https://iprotoxi.fi/index.php/services/iprotoxi-aistin-blue. Accessed on: Feb. 26 2018.
[191] "BTL3H3_Application_note_rev102,"
[192] *Gas Sensors for the Internet of Things.* [Online] Available: https://www.spec-sensors.com/. Accessed on: Feb. 27 2018.
[193] *undefined.* [Online] Available: undefined. Accessed on: Dec. 20 2018.
[194] *Small Sound Detection Sensor Module for Arduino - White + Blue.* [Online] Available: https://www.dx.com/p/ldtr-0003-small-sound-detection-sensor-module-for-arduino-white-blue-2048642#.XBrdiVxKjDc. Accessed on: Dec. 20 2018.
[195] *LM393 Sound Detection Voice Sound Sensor Module Electret Transducer Module for Arduino.* [Online] Available: http://www.icstation.com/lm393-sound-detection-voice-sound-sensor-module-electret-transducer-module-arduino-intelligent-vehicle-p-1513.html. Accessed on: Dec. 20 2018.
[196] *Sound Detection Sensor Module LM393 - SparkPCB.com.* [Online] Available: https://www.sparkpcb.com/sensors/sound-detection-sensor-module-lm393.html. Accessed on: Dec. 20 2018.
[197] *GY-MAX9814 Sound Sensor Module Electret Microphone Amplifier - MAX9814 - Raspberry Pi, Arduino, Robote, Motor etc. beim Eckstein Komponente, 3,85 €.* [Online] Available: https://eckstein-shop.de/GY-MAX9814-Sound-Sensor-Module-Electret-Microphone-Amplifier-MAX9814?curr=EUR&gclid=CjwKCAiA9efgBRAYEiwAUT-jtCabq0lMqHVU21tZQ2Zy87uH1MHsVzTiYnKAemqlw4K7chbqktBzHxoCzywQAvD_BwE. Accessed on: Dec. 20 2018.
[198] *undefined.* [Online] Available: undefined. Accessed on: Feb. 27 2018.
[199] S. J. Pawar, Y.-D. Jong, H. C. Her, and J. H. Huang, "Electrostatic Polarization Process Control: A Case Study on Electret Condenser Microphone Production Line," *J. Audio Eng. Soc.*, vol. 65, no. 4, pp. 321–332, 2017.
[200] P. R. Scheeper, A.G.H. van der Donk, W. Olthuis, and P. Bergveld, "A review of silicon microphones," *Sensors and Actuators A: Physical*, vol. 44, no. 1, pp. 1–11, 1994.
[201] B. com, *0,91 Zoll 128x32 IIC I2C Blau OLED LCD Display DIY Oled Modul SSD1306 Treiber IC DC 3.3V 5V Für Arduino PIC.* [Online] Available: https://www.banggood.com/de/0_91-Inch-128x32-IIC-I2C-Blue-OLED-LCD-Display-DIY-Oled-Module-SSD1306-Driver-IC-DC-3_3V-5V-p-1140506.html?gmcCountry=DE&currency=EUR&createTmp=1&utm_source=googleshopping&utm_medium=cpc_elc&utm_content=zouzou&utm_campaign=pla-de-elc2-brand-pc&gclid=Cj0KCQiAw9nUBRCTARIsAG11eif-Lg7mOOYU6iM1K3t3HZzyFv_-ExFGXgq9A_N9YQlIIKLljbEhDi4aAkvFEALw_wcB&cur_warehouse=CN. Accessed on: Feb. 28 2018.

[202] ivanl, "SSD1780," https://cdn-shop.adafruit.com/datasheets/SSD1306.pdf.
[203] *MICS-4514, Gas Sensor - MetalOxide, SGX Sensortech Limited (formerly e2v).* [Online] Available: https://sgx.cdistore.com/ProductDetail/MICS4514-SGX-Sensortech-Limited-formerly-e2v/333417/. Accessed on: Feb. 27 2018.
[204] G. Korotcenkov, "The role of morphology and crystallographic structure of metal oxides in response of conductometric-type gas sensors," *Materials Science and Engineering: R: Reports*, vol. 61, no. 1-6, pp. 1–39, 2008.
[205] *LMP91000 Configurable AFE Potentiostat for Low-Power Chemical Sensing Applications | TI.com.* [Online] Available: http://www.ti.com/product/LMP91000. Accessed on: Feb. 27 2018.
[206] *Electrical and Electronic Connectors - HIROSE Electric Group.* [Online] Available: https://www.hirose.com/. Accessed on: Feb. 27 2018.
[207] Renesas, "ISL60002 Datasheet,"
[208] Microchip Technology Inc., "MCP6041/MCP6042/MCP6043/MCP6044 Data Sheet,"
[209] Wikipedia, *Rostock - Wikipedia.* [Online] Available: https://en.wikipedia.org/w/index.php?oldid=827233344. Accessed on: Feb. 27 2018.
[210] Norris, "SPEC-AN-104-Environmental-Effects," https://www.spec-sensors.com/wp-content/uploads/2016/06/SPEC-AN-104-Environmental-Effects.pdf.
[211] D. R. Baselt *et al.,* "Design and performance of a microcantilever-based hydrogen sensor," *Sensors and Actuators B: Chemical*, vol. 88, no. 2, pp. 120–131, 2003.
[212] N. Yamazoe, "Toward innovations of gas sensor technology," *Sensors and Actuators B: Chemical*, vol. 108, no. 1-2, pp. 2–14, 2005.
[213] *celisca.* [Online] Available: http://celisca.de/. Accessed on: Feb. 27 2018.
[214] *BW Clip, Eingaswarngerät für CO, Laufzeit: 2 Jahre, 0 - 300 ppm, A1=35/A2=200 ppm - Gasmesstechnik.de - Ein- und Mehrgasmessgeräte von Dräger, BW, MSA, Crowcon von ACE im Onlineshop.* [Online] Available: https://www.gasmesstechnik.de/product/bw-clip-eingaswarngeraet-fuer-co-laufzeit-2-jahre-0-300-ppm-a1-35-a2-200-ppm.6846435.html?p=16&gclid=CjwKCAiAoNTUBRBUEiwAWje2lrxYTjIB-3-sOob9XC44lWaQymyYeZSFZyMbh4s2a7vfZAPmyWOZ-RoCqoAQAvD_BwE. Accessed on: Feb. 27 2018.
[215] *Home - Brüel & Kjær Sound & Vibration.* [Online] Available: https://bksv.com/en. Accessed on: Feb. 27 2018.
[216] S. Björklund and J. Sundberg, "Relationship Between Subglottal Pressure and Sound Pressure Level in Untrained Voices," (eng), *Journal of voice : official journal of the Voice Foundation*, vol. 30, no. 1, pp. 15–20, 2016.
[217] D. Davis and E. Patronis, *Sound system engineering,* 3rd ed. Oxford: Focal, 2006.
[218] A. Selamtzis and S. Ternström, "Investigation of the relationship between electroglottogram waveform, fundamental frequency, and sound pressure level using clustering," (eng), *Journal of voice : official journal of the Voice Foundation*, vol. 31, no. 4, pp. 393–400, 2017.

DECLARATION

This dissertation '**Personalized ambient parameters monitoring: design and implementing of a wrist-worn for hazardous gases and sound level detection**' is a presentation of my original research work. Wherever contributions of others are involved, every effort is made to indicate this clearly, with due reference to the literature, and acknowledgement of collaborative research and discussions. The work of this dissertation has been done by myself at the University of Rostock, Germany. Also, the dissertation has not been accepted for any degree and is not concurrently submitted in candidature of any other degree.

Rostock, 12 April, 2019
Mostafa Haghi

List of Publications

Journals:

1) **Pervasive and Personalized Ambient Parameters Monitoring: A Configurable, Prolonged and Independent watch**

IEEE Access, vol. 7, **Feb. 2019**, doi: 10.1109/ACCESS.2019.2897845

Mostafa Haghi, Regina Stoll and Kerstin Thurow,

2) **A Ubiquitous and Configurable Wrist-Worn Sensor Node in Hazardous Gases Detection**

Advances in Science, Technology and Engineering Systems Journal (ASTESJ), Oct. **2018**, DOI: 10.25046/aj030530
Mostafa Haghi, Regina Stoll, Kerstin Thurow,

3) **A Low-Cost, Standalone, and Multi-Tasking Watch for Personalized Environmental Monitoring**

IEEE Transactions on Biomedical Circuits and Systems, vol. 12, no. 5, pp. 1144-1154, Oct. **2018**.doi: 10.1109/TBCAS.2018.2840347
Mostafa Haghi, Regina Stoll and Kerstin Thurow,

4) **Wearable devices in medical internet of things: scientific research and commercially available devices**

Healthcare informatics research. **2017 January**
1; 23 (1):4-15. Doi: https://doi.org/10.4258/hir.2017.23.1.4
Mostafa Haghi, Kerstin Thurow and Regina Stoll,

5) **A New Methodology in Study of Effective Parameters in Network-on-Chip Interconnection's (Wire/Wireless) Performance**

International journal of advanced computer science and applications, 7(10), pp.75-85, **2017**, DOI: 10.14569/IJACSA.2016.071010
Mostafa Haghi, Kerstin Thurow, Norbert Stoll, Saed Moradi,

Conferences:

1) **A Multi-Tasking, Multi-Layer and Replaceable Wrist-Worn Environmental Monitoring Sensor Node**

2018 5th International Conference on Control, Decision and Information Technologies (CoDIT), Thessaloniki, **2018**, pp.25-31.
doi: 10.1109/CoDIT.2018.8394781
Mostafa Haghi, Kerstin Thurow and Norbert Stoll,

2) **Four-layer wrist worn device for sound level and hazardous gases environmental monitoring**

2017 2nd International Conference on System Reliability and Safety (ICSRS), Milan, **2017**, pp. 270-276. doi: 10.1109/ICSRS.2017.8272833
Mostafa Haghi, Kerstin Thurow and Norbert Stoll,

3) **A three-layer multi-sensor wearable device for physical environmental parameters and NO_2 monitoring**

2017 International Conference on Smart Systems and Technologies (SST), Osijek, **2017**, pp. 149-154. doi: 10.1109/SST.2017.8188686
Mostafa Haghi, Kerstin Thurow and Norbert Stoll,

4) **A multi-layer multi-sensor wearable device for physical and chemical environmental parameters monitoring (CO & NO_2)**

2017 International Conference on Information and Digital Technologies (IDT), Zilina, **2017**, pp. 137-141. doi: 10.1109/DT.2017.8024285
Mostafa Haghi, Kerstin Thurow and Norbert Stoll,

Auto-commentary

1) **Toward A New Approach in Wearable Devices in Safety Monitoring: Miniaturization and 3D Space Utilization**

Has been accepted for publication in SLAS Technology (April 2019).

Dissertation Theses

1- World Health Organization (WHO) has announced of one out of seven death due to individual's exposure to ambient parameters and in particular ambient air pollutants. In addition, patients who are suffering from heart disease, asthma and children are more vulnerable and influenced by ambient parameters. Therefore, individual's protection against ambient pollutants is necessary.

2- Methodologies of medicine are gradually shifting from traditional (treatment after diagnosis) to predictive and preventive (p2Health) which is achieved by a comprehensive and data fusion from different area of interests in healthcare. Ambient parameters monitoring also is one of important area.

3- After two promising experiences with m-health and e-health, now the medical internet of things (mIoT) is at the center of concentration. Personalized healthcare monitoring through measurement of different parameters is playing an important role in p2Health and mIoT.

4- Wearable devices in personalized monitoring are heavily concentrated due to portability and supporting individual's data record.

5- Wearable devices in ambient monitoring are getting more attention in recent years due to insufficient, inefficient, sparse, expensive and complicated stations of ambient monitoring.

6- Majority of the devices/prototypes in ambient monitoring are focused on air pollutants observation. Furthermore, these devices are more often single-task, in inconvenient mode of wearability, does not satisfy prolonged monitoring, and suffering from an inadequate data protection and transmission. Multi-tasking and expandability are of serious challenges and bottlenecks.

7- A prototype based on a tight strategy, careful hardware design and software development is proposed for a multi-parameters, multi-gas-monitoring and wrist-worn prototype.

8- The prototype is designed and implemented based on 3D space utilization and multi-physical-layer which each layer is dedicated to a task.

9- Gas sensor node consist of gas sensor and gas sensor driver, host platform, notification system driver, hardware interface for linking display, noise module, and gas sensor node to host platform are the physical layers of this prototype stuck on top of each other in "Z" direction.

10- Toxic and hazardous gases are generally categorized in active (e.g. CO) and reactive (e.g. NO_x). To detect each gas, specific configuration and set up is required. In this prototype gas sensor driver is designed universally to be compatible with 2/3 lead gas sensors and active/reactive gases. To support this features, LMP91000 from TI has been used due to its configurability.

11- The gas sensor (one at each time) is activated via user by sending command from the smartphone. In this approach, the user decides for the sensor(s) which are required to be on operation. This feature, bring the multi-gas-detection feature to the prototype.

12- Noise detection and gas sensors are strictly calibrated. Data sampling, data collection, conversion, pattern creation, data validation and data transmission are the sequences from receiving data (sensor) to observation on the smartphone/display.

13- The prototype protects data whether by data transmission to a smartphone or storage on an external memory and later these data are transmitted to smartphone once BLE is resumed.

14- A bidirectional data communication between the prototype and smartphone is established. Data are transmitted to smartphone in separated packets. In BLE connected mode, noise, gas sensors and display are configurable and may be activated/deactivated via sending commands from the smartphone.

15- When BLE is disconnected, the prototype is operating in standalone mode, which exhibits the data in real-time on display and stores the data in an external memory.

16- The sampling rate of gas and noise sensors is adjustable according to battery level. As the battery level is reduced, the sampling rate also is decreased. This feature, along with sensor(s)/display configuration can significantly contribute in prolonged monitoring.

17- This solution is expandable to add more number of sensors for a pervasive ambient parameters monitoring.

Abstract

Due to rapid urbanization and industrialization, individual's exposure to air pollutants and in larger scale, ambient parameters monitoring is a concern in safety and reliability of working conditions and in healthcare as well. In recent years, and after promising experiences with m-health, e-health and in general remote health monitoring (RHM), methodology of medicine in healthcare and occupational is shifting gradually from the traditional (treatment after diagnosis) to preventive and predictive (p2Health). Therefore, in the new era of remote

healthcare, medical internet of things (mIoT) is at the center of concentration. In mIoT and p2Health, the personalized monitoring, including different area of effective parameters in healthcare is seriously considered (physiological, motion and ambient parameters).

Wearable devices/prototypes are the means of personalized monitoring. In particular, wearables in ambient parameters monitoring are in need, where the numbers of stations in ambient monitoring are restricted due to expense, complexity, and high maintenances. Furthermore, these stations only provide an overview on the surrounding that does not necessarily indicate an individual exposure.

Commercial devices and prototypes have been widely provided but still there is a serious lack of efficient wearables in ambient parameters monitoring in terms of multi-parameters/comprehensive monitoring, mode of wearability, prolonged monitoring, and data protection.

To tackle the aforementioned disadvantages, and introducing a new generation of wearable in ambient parameters monitoring, in this work, a prototype has been designed and implemented in multi-physical-layer based on "3D space utilization" and "multi-layer" approach. In this approach, "X-Y" plane is remained constant and different physical layers are stuck one on top of another in "Z" direction.

Ubiqsense (the proposed prototype) measures numbers of gases (multi-gas-monitoring) from different categories (active/reactive), noise and also physical ambient parameters (temperature, humidity and air pressure).

In Ubiqsense, gas sensor with the gas sensor driver is located at the top layer (first layer). This forms the gas sensor node which is replaceable. The gas sensor node can be substituted with the other gas sensor nodes. The activation, calibration and measurement is completed through sending command from smartphone to the prototype. Gas sensor driver is universal and compatible with 2/3 gas sensors and to support gases from active and reactive types, which each has its own configuration, LMP91000 as an AFE is utilized. This AFE is configurable in different ranges of internal zero, 7 level internal resistors, and also load resistors to support different configurations.

Main platform, hosts the integrated sensors for ambient pressure, temperature and humidity monitoring. The external memory also is placed on the main platform (second layer).

The notification driver for early user warning in abnormal statuses is located at the bottom of host platform. The notification driver activates vibrating motor and beeper which are used as the means of notification. Notification system is activated in two low and high risks depending on the degree of risk in each parameter (third layer).

Hardware interface is designed as the heart of Ubiqsense to link noise sensor and display to the host platform. This layer is located between host platform and gas sensor node from bottom and top respectively. Display and noise are linked to the main platform through the tail of hardware interface (fourth layer).

To protect the data acquisition, the general strategy of operation in this prototype is according to BLE status. If BLE is connected, the data are transmitted to the smartphone in real-time and gas sensor node, display and noise module are activated/deactivated through sending command from the smartphone.

In BLE disconnected mode, the prototype switch to standalone operation. In this mode, all sensors are on operation and data are logged in the external memory and observable on the display. These data are re-transmitted to the smartphone based on the user decision via sending command from the smartphone once BLE is resumed.

A strict calibration is considered for gas sensor according to temperature that is the most significant parameter in gas sensor performance.

Furthermore, sampling rates of sensors in Ubiqsense is adjusted according to the level of battery. As the level is reduced, the sampling rate is decreased too (although the rate for each sensor is different). This feature along with sensor/display configuration (activated/deactivated) significantly contribute to prolonged monitoring.

As an important feature, this prototype has been designed in modular way and is expandable in hardware to significantly extend the covering range of parameters in ambient parameters monitoring.

Ubiqsense with the unique “3D space utilization” strategy based on multi-physical-layer, smartphone configurability, modular, hardware expandability and covering wide range of parameters might be an opening to the new generation of wearables in ambient parameters monitoring.

Zusammenfassung

Aufgrund der raschen Urbanisierung und Industrialisierung, der Exposition des Einzelnen gegenüber Luftschadstoffen und der Überwachung von Umgebungsparametern in einem größeren Maßstab, ist dies ein Problem hinsichtlich der Sicherheit und Zuverlässigkeit der Arbeitsbedingungen sowie im Gesundheitswesen. In den letzten Jahren und nach vielversprechenden Erfahrungen mit M-Health, E-Health sowie allgemeinem Remote Health Monitoring (RHM), verlagert sich die Methodik der Medizin im Gesundheits what do you mean by the stroke) und Beschäftigungsbereich schrittweise von der traditionellen (Behandlung nach der Diagnose) hin zur präventiven und

prädiktiven ((p2Health) Therapie). Daher steht das medizinische Internet der Dinge (mIoT) im neuen Zeitalter der Remote Gesundheitsfürsorge im Mittelpunkt der Konzentration. In mIoT und p2Health wird das personalisierte Monitoring und einschließlich verschiedener Bereiche wirksamer Parameter im Gesundheitswesen ernsthaft in Betracht gezogen (physiologische, Bewegungs- und Umgebungsparameter).

Wearable Devices / Prototypen sind das Mittel zur personalisierten Überwachung. Insbesondere bei der Überwachung von Umgebungsparametern sind Wearables erforderlich, bei denen die Anzahl der Stationen bei der Umgebungsüberwachung aufgrund von Kosten, Komplexität und hohen Wartungskosten beschränkt ist. Darüber hinaus geben diese Stationen nur einen Überblick über die Umgebung, der nicht unbedingt auf eine individuelle Exposition hinweist.

Kommerzielle Geräte und Prototypen wurden weithin bereitgestellt, aber es gibt immer noch einen Mangel an effizienten Wearables bei der Überwachung von Umgebungsparametern im Hinblick auf Multiparameter / umfassende Überwachung, Tragbarkeitsart, verlängerte Überwachung und Datenschutz.

Um den oben genannten Nachteilen zu begegnen und eine neue Generation von Wearable für die Überwachung von Umgebungsparametern einzuführen, wurde in dieser Arbeit ein Prototyp entworfen und auf Multi-Physical-Layer basierend auf dem Ansatz der „3D-Raumnutzung“ und „Multi-Layer“ implementiert. Bei diesem Ansatz bleibt die "X-Y" -Ebene konstant und verschiedene physikalische Schichten und werden in "Z" -Richtung aufeinander gesteckt.

Ubiqsense (der vorgeschlagene Prototyp) misst die Anzahl der Gase (Multi-Gas-Monitoring) aus verschiedenen Kategorien (aktiv / reaktiv), Lärm sowie physikalische Umgebungsparameter (Temperatur, Feuchtigkeit und Luftdruck).

In Ubiqsense befindet sich der Gassensor mit dem Gassensortreiber in der obersten Schicht (erste Schicht). Dies bildet den Gassensorknoten, der austauschbar ist. Der Gassensorknoten kann durch die anderen Gassensorknoten ersetzt werden. Die Aktivierung, Kalibrierung und Messung werden durch Senden eines Befehls vom Smartphone an den Prototyp abgeschlossen. Der Gassensortreiber ist universell und mit 2/3 Gassensoren kompatibel. Zur Unterstützung von Gasen aus aktiven und reaktiven Typen, die jeweils eine eigene Konfiguration haben, wird LMP91000 als AFE verwendet. Dieses AFE ist in verschiedenen Bereichen von internen Nullwiderständen mit sieben Widerständen sowie Lastwiderständen für unterschiedliche Konfigurationen konfigurierbar.

Hauptplattform beherbergt die integrierten Sensoren zur Überwachung von Umgebungsdruck, Temperatur und Feuchtigkeit. Der externe Speicher befindet sich auch auf der Hauptplattform (zweite Schicht).

Der Benachrichtigungstreiber für frühe Benutzerwarnungen in anormalen Status befindet sich am unteren Rand der Hostplattform. Der Benachrichtigungstreiber aktiviert den Vibrationsmotor und den Piepser, die als Benachrichtigungsmittel verwendet werden. Das Benachrichtigungssystem wird in zwei niedrigen und hohen Risiken abhängig vom Risikograd in jedem Parameter (dritte Schicht). Aktiviert.

Die Hardware-Schnittstelle ist als Herzstück von Ubiqsense konzipiert, um den Rauschsensor und die Anzeige mit der Host-Plattform zu verbinden. Diese Schicht befindet sich zwischen Host-Plattform und Gassensorknoten von unten bzw. oben. Anzeige und Rauschen sind über die Hardware-Schnittstelle (vierte Schicht) mit der Hauptplattform verbunden.

Um die Datenerfassung zu schützen, richtet sich die allgemeine Betriebsstrategie in diesem Prototyp nach dem BLE-Status. Wenn BLE angeschlossen ist, werden die Daten in Echtzeit an das Smartphone und den Gassensorknoten übertragen. Das Display und das Noise-Modul werden durch das Senden eines Befehls vom Smartphone aktiviert / deaktiviert.

Im BLE-Modus ohne Verbindung wechselt der Prototyp in den Standalone-Betrieb. In diesem Modus sind alle Sensoren in Betrieb und die Daten werden im externen Speicher aufgezeichnet und auf dem Display angezeigt. Diese Daten werden auf der Grundlage der Benutzerentscheidung durch Senden eines Befehls vom Smartphone erneut an das Smartphone übertragen, sobald BLE wieder aufgenommen wird.

Bei Gassensoren wird eine strikte Kalibrierung in Abhängigkeit von der Temperatur in Betracht gezogen, die der wichtigste Parameter für die Gassensorenleistung ist.

Darüber hinaus werden die Abtastraten von Sensoren in Ubiqsense entsprechend dem Batteriezustand angepasst. Wenn der Pegel verringert wird, verringert sich auch die Abtastrate, obwohl die Rate für jeden Sensor unterschiedlich ist. Zusammen mit der Sensor- / Display-Konfiguration (aktiviert / deaktiviert) trägt diese Funktion wesentlich zu einer längeren Überwachung bei.

Dieser Prototyp wurde als modulares System entwickelt und kann in Hardware erweitert werden, um den Parameterbereich bei der Überwachung der Umgebungsparameter erheblich zu erweitern.

Ubiqsense mit der einzigartigen Strategie der „3D-Raumnutzung“, die auf Smartphon für mehrere physische Schichten Konfigurierbarkeit basiert, Modularität, Erweiterbarkeit der Hardware und Abdeckung eines breiten Spektrums an Parametern könnte der neuen Generation von Wearables bei der Überwachung von Umgebungsparametern öffnen.

Resume

Academic CV:

Mostafa Haghi,

DoB: 12.April.1986 in Iran

July, 2016 – October, 2019
Status: M. Tech. in Embedded systems, Ph.D. candidate at the center for life science automation in Rostock University.

Fields: Wearable device in ambient parameters monitoring, Electronics sensor driver designer, Embedded hardware and software design

Jan. 2016 - June 2016
Technical member in Omid Pars Co. (Ilam-Iran)

2015
Lecturer University of Azad (Ilam-Iran)

2011 - 2014
Graduated as M.Tech. Embedded Systems University of JNTUH, India
Master Thesis: Evaluation of wire/wireless communication in network on chip with the concentration of system on chip (SoC).
Grade of thesis: A
Grade of master: First class with distinction

2005 - 2009
Bachelor of Electronics Eng. University of Urmia, Iran
Bachelor thesis: mine detector robot.
Grade of thesis: A